1.12 — metody numeryczne
i komputerowe, elementy
skończone, probabilistyka

Tran Duong Hien

DETERMINISTIC AND STOCHASTIC SENSITIVITY IN COMPUTATIONAL STRUCTURAL MECHANICS

Praca habilitacyjna

46/1990

WARSZAWA 1990

ISSN 0208-5658

Praca wpłynęła do Redakcji dnia 24 października 1990 r.

P r a c a h a b i l i t a c y j n a

recenzent - prof.dr hab.inż. Witold Gutkowski

Instytut Podstawowych Problemów Techniki PAN
Nakład 100 egz. Ark.wyd.9,0 Ark.druk.11,25
Oddano do drukarni w grudniu 1990 r.
Nr zamówienia 6/91

Warszawska Drukarnia Naukowa, Warszawa,
ul.Śniadeckich 8

The author wishes to acknowledge the help of his colleagues at the Institute of Fundamental Technological Research, Polish Academy of Sciences and at the Institute of Mechanics, National Center for Scientific Research of Vietnam.
Especially, he wishes to thank Professor Michal Kleiber, his teacher of computational mechanics, for the friendly guidance in writing of this text.

TRAN DUONG HIEN
Department of Computational Engineering

DETERMINISTIC AND STOCHASTIC SENSITIVITY IN COMPUTATIONAL STRUCTURAL MECHANICS

Abstract

In structural mechanics sensitivity problems concern the relationship between changes in structural response and variations in design variables. For a deterministic system the gradient of the response functional with respect to design variables is evaluated, whereas the subject of stochastic structural sensitivity is to estimate probabilistic distributions of this gradient.

The purpose of the text is to provide a theory and computational methods for deterministic and stochastic sensitivity analysis of time-independent and time-varying systems. Discussions are restricted to multi-degrees of freedom linear-elastic 3D structures with fixed global configuration. On the basis of the displacement finite element modelling and a stochastic Hamilton's variational principle proposed two new problems of computational mechanics are formulated for static and dynamic response sensitivity. A new form of response functionals is introduced in terms of a convolution of a time signal sequence enabling to deal with the dynamic sensitivity response at any particular time instant. To eliminate the secularity appearing in the perturbation solutions time-varying forcing functions are assembled into complex-valued series and the fast Fourier transform is employed to remove the resonant parts. To handle at acceptable computation cost large finite element systems, the two-fold superposition technique involving modal analysis and transformation from a correlated space to a uncorrelated space of random variables is presented. A complete algorithm has been worked out and implemented into the microcomputer program POLSAP, a finite element code for deterministic and stochastic analysis of statics, minimum-weight optimization, buckling load, eigenpair, forced-vibration, eigenvalue sensitivity, static and dynamic response sensitivity of truss-beam-shell structures. A number of numerical results illustrates the paper.

Introduction

The mathematical theory of sensitivity is concerned with changes in the system behaviour due to parameter variations. The objective of the theory is to define a sensitivity function which relates a set of parameter deviations to a set of parameter-induces errors of the behaviour functional. If the parameters are assumed to belong to a random set, then the functional is stochastic and the sensitivity function is referred to as the stochastic sensitivity function. In engineering mechanics structural sensitivity concerns the relationship between design parameters (or design variables) and structural response (or response functional) which is determined by the laws of continuum mechanics. Namely, for a deterministic system the gradient of the response functional with respect to design variables is evaluated, whereas the subject of stochastic structural sensitivity is to estimate probabilistic distributions of this gradient. Since the sensitivity gradient presents a trend for the structural performance, the typical method of structural design based on experience and intuition can be significantly enhanced if the designer is supported with the sensitivity database that explains, without requiring trial-and-error: 1) what the influence of design changes will be, 2) how to assess the effects of randomness in the mathematical model and to establish admissible tolerances on structural components, 3) how to choose a search direction to a new design.

Taking the above viewpoint the computer solution for deterministic and/or stochastic sensitivity problems stands for a key step in most automated structural design approaches. Among various computation techniques the one based on the finite element modelling is the most efficient tool for the solution of complex, large problems. The finite element approach was pioneered by Argyris and Kelsey [2], Przemieniecki [117], Szmelter [126], Zienkiewicz [144], Martin and Carey [100] and Oden [108]. It is based on a piecewise polynomial interpolation of the displacement field (or/and stress field) and application of an energy method to obtain approximated equations of boundary-initial problems. Studies in applied mathematics, see Oden and Reddy [109] and Ciarlet [20], have resulted in an increased confidence in treating the solutions. The variational approach to continuum mechanics developed by Goldstein [43], Lanczos [86], Prager [115], Lippmann [92] and Washizu [139] enables to incorporate into variational statements various aspects such as constitutive relations, compatibility and boundary conditions, etc. in a consistent way. Consequently, the variational finite element formulations introduced by Washizu [139], Bathe and Wilson [11], Cook [25], Gallagher [41], Tong and Rossettos [134] Hinton and Owen [64], Irons and Ahmad [70], Argyris, Kleiber and Doltsinis [3,4] and Kleiber [75,76,79] have proved to have definitive advantages over other energy formulations. As a result of this a series of the finite element solutions which are practically important and numerically interesting was obtained, for instance, those by Kleiber and Hien [54]–[59], [67], [80]–[82]. Recently by using the perturbation

technique, see Cole [23], Kato [72], Meirowitch [102] and Kleiber [78], randomness in structural parameters and loading can be incorporated into the finite element formulations. Using the concept of discretized random fields stochastic finite element models were developed by Vanmarcke et al [135]–[138], Hisada and Nakagiri [65,66], Liu, Belytschko and Mani [94,95], Ibrahim [69], Collins and Thomson [24] and Fox and Kapoor [38]. Some variational principles were extended to deal with probabilistic problems, such as the stochastic minimum potential principle and stochastic Hu-Washizu principle developed by Liu, Belytschko and Besterfield [93,96,97] and the stochastic Hamilton's principle introduced by Hien and Kleiber [61]. The main advantage of the stochastic finite element modelling is that only the first two moments of random variables are required, whereas the statistical approach is based on numerical simulations, see Crammer [27] and Davenport and Root [30], and requires a large number of samples generated from a given joint probability distribution, which is unavailable in most cases. Instead, it is usually assumed that input random data are mutually independent and Gaussian or can be transformed to be Gaussian, see Crandall and Mark [28], Lin et al [90,91], Ang and Tang [1], Augusti, Baratta and Casciati [9] and Hung, Khiem and Hien [68].

With the simplicity in concept and potency in software, the finite element modelling has been applied to structural sensitivity problems as the most effective approach. Generally, formulations for sensitivity analysis can be divided into three groups. The simplest technique is finite difference calculation of sensitivities based on successive perturbations of design variables followed by re-analysis of the system. This may be ineffective since the accuracy problem often arises; and in such a case analytical methods turn out to be more appropriate. The direct method is based on differentiation of system equations with respect to design variables to obtain sensitivity equations. The adjoint approach defines an adjoint system whose solution permits evaluation of sensitivities. As an extension of the general sensitivity theory, see Frank [40], the development of structural design sensitivity was initiated by Zienkiewicz and Campbell [145] for a 2D stress problem. Further, the adjoint and direct approaches were generalized to both the distributed- and discretized-parameter systems by Haug, Arora, Choi and Komkov [51]–[53], Ryu et al [121], Yang and Botkin [143] and Raju et al [119]. Dems and Mroz [32,33], Haftka and Mroz [47,49] and Haug [51] presented the variational approaches based on the initial load method to 1st- and 2nd-order sensitivities of linear and nonlinear systems. Using the fuzzy set theory Kleiber [77] estimated nonlinear response structural sensitivity to imperfections in terms of natural language expressions. Some computer codes have been supported with design sensitivity options, see Arora, Cardoso and Haririan [5,19,50], Santos et al [122] and Stone et al [125]. In free vibration and dynamic response sensitivity problems, beside the method based on Green function the direct and adjoint techniques are usually employed, out of which the adjoint technique is shown to be most efficient, see Haug, Choi and Komkov [53], Haftka et al [48], Jankovic [71], Meric [103], Wu and Arora [142], Arora and Tseng [6,7] and Livne [98]. Green and Haftka [44] used the differentiation method for a critical point constraint formulation of the transient loading problem. A comprehensive discussion on the finite element formulations and computational aspects for struc-

tural sensitivity problems in statics, free vibration and dynamics was presented by Hien and Kleiber [60]. The design sensitivity concept is employed in reliability analysis through a sensitivity index, see Franglopol [39], Thoft-Christensen [131], Madsen [99], Kwak and Lee [84], or through a reliability index, see Borkowski and Sikorski [17,124], Feng and Moses [35] and Khoi and Hien [73]. Since reliability analysis is a probabilistic problem whose main objective is to determine the probability distribution function, the use of statistical techniques is generally more preferably. In fact, the sensitivity index is assumed to be a deterministic quantity evaluated at averages of design parameters. An analytical formulation for the stochastic sensitivity function of dynamic control systems was developed by Szopa [127,128] and a computational formulation for stochastic sensitivity problems in structural statics and dynamics was proposed by Hien and Kleiber [62,63]. Comprehensive presentation and extension of the latter formulation and its computer performance are the main objectives of this text.

The purpose of the text is thus to provide a theory and computational methods for deterministic and stochastic sensitivity analysis of time-independent and time-varying systems. The formal treatment is restricted to multi-degrees of freedom linear 3D systems with fixed global configuration, small deformation and linear-elastic material. Since random and design properties appear in the behaviour of linear operators of discretized-parameter systems, the systems are nonlinear as functions of random and design variables. To treat the probabilistic-nonlinear problem with the deterministic computation techniques that take the advantage of mathematical features of linear operators is the aim of the text. The essential contents of this text are organized into six chapters which are assembled in two parts devoted to deterministic systems (Part 1) and stochastic systems (Part 2). In each part the chapters are arranged in the same order: 1) variational formulation for finite element equations of motion in which static problem is treated as a special case, 2) structural sensitivity of static response, 3) structural sensitivity of dynamic response. Contents of each chapter is also ordered in a similar manner: introductory remarks and chapter's scope are followed by the problem statement and methodology, computational aspects, numerical algorithms and their implementation into the finite element code POLSAP, which is used to solve a number of illustrative examples. Each chapter is completed with summarizing remarks.

Basic concepts of the finite element modelling are reviewed in Chapter 1 which includes the variational formulation of equations of motion based on the Hamilton's principle. These basic ideas are used in all the following chapters. Discussion is focused on the techniques to solve large algebraic equations, to implicitly integrate and to decouple equations of motion of damped systems. Chapter 2 provides a deterministic formulation for static sensitivity problems. Both the direct and adjoint approaches are described in the context of the computer performance for a system with the large number of load conditions, various constraints and design variables. The minimum-weight optimization problem is briefly outlined as an extension of the adjoint method; and an algorithm which is numerically similar to the tangent stiffness procedure is presented. Examples concern truss, beam, plate and complex truss-beam-shell structures. In Chapter 3, two problems of dynamic

response sensitivity followed by eigenvalue sensitivity analysis are considered and a parallel integration technique is introduced. The first problem is related to response functionals defined over a time domain. The second contains a simulation of the functionals via a signal sequence, which enables to evaluate response sensitivities at particular time instants. The relevance of the mode superposition methodology to the solution is emphasized, particularly in the case of sensitivity analysis at any particular time instant leading the adjoint equations to a uncoupled system excited by a unit impulse or unit terminal velocity. Beside an example of eigenvalue sensitivity of a cantilever beam to its cross-sectional area, numerical results are concerned with time-varying response sensitivity of the same structures solved in Chapter 2.

All the subjects outlined in Part 1 are considered once more in Part 2, but in a more general framework of stochastic systems. In Chapter 4 a stochastic form of the Hamilton's principle is developed through the 2nd-order perturbations and a stochastic finite element model of equations of motion is introduced. As a result, the first two moments of the nodal displacements, element strains and stresses are evaluated. The distinguishing features of the stochastic finite element approach are discussed in detail. A two-fold superposition technique which consists of the modal analysis and the transformation of random variables is introduced. A description of the base-two fast Fourier transform and a presentation of the secularity elimination procedure are given. Numerical results of static and forced-vibration response of a spring-mass system, bars and plates illustrate the accuracy of the solutions. In Chapter 5 a new problem of computational mechanics is formulated for static stochastic sensitivity. Since both the random and design variables are expressed in a discretized-parameter space, the stochastic sensitivity function can be modelled in a parallel way and evaluated by using a conventional deterministic finite element technique; and the computer procedures can be carried out in parallel for dual systems and sequentially for their 0th-, 1th- and 2nd-order equations. Different types of random design variables are assumed in examples concerning beam and cylindrical shell structures. Chapter 6 deals with stochastic sensitivity in structural dynamics. A combination of the adjoint variable method and second moment analysis is employed to estimate the time response of the first two moments of the sensitivity gradient. From a discussion on the computational aspects of the problem it can be seen that the effects of density of the finite element mesh, period elongation, amplitude decay and secularity can not be disregarded. Numerical results show that a good coincidence of the solutions is obtained using the Newmark and Wilson-θ integration schemes; more interesting, probabilistic distributions for the sensitivity response converge to stationary values more rapidly than that for displacement response, even when the latter response exhibits a chaotic tendency.

Conclusions and proposed future work are followed by a comprehensive list of references. The text is completed with an Appendix which introduces the main features and analysis options supported by the microcomputer code POLSAP, a considerably extended version of package SAP-IV [12], for deterministic and stochastic problems of statics, minimum-weight optimization, buckling load, free and forced vibration, and static and dynamic sensitivity of medium- and large-scale structures.

Part 1

DETERMINISTIC SYSTEMS

1 Hamilton's Variational Principle and Finite Element Model

1.1 Introductory Remarks

The equations of motion of dynamic systems can be formulated by any one of three distinct approaches, which are equivalent and lead to identical results. The simplest procedure is to establish the dynamic equilibrium of all forces acting in the system. taking account of inertial effects by means of the d'Alembert principle. However, in more complex systems, particularly those involving mass and stiffness distributed over finite regions, establishing a direct vectorial equilibration is not straightforward. The virtual-work and energy formulations which involve only scalar quantities can be more effective. The former is based on the principle of virtual displacements and the equations of motion are obtained by considering the work done during the virtual displacements. The latter is based on the Hamilton's principle and the variations of the kinetic and potential energy of the system lead to the equations of motion. The energy formulation has the advantage of dealing only with purely scalar energy quantities, whereas the forces and displacements used to represent corresponding effects in the virtual-work formulation are all vectorial in character even though the work terms are scalar. Another disadvantage of the virtual-work derivation is that the inertial and conservative forces acting on the system must be expressed and evaluated explicitly; and the problem may not directly derived if these forces are nonconservative. Moreover, the energy approach is much more efficient if design characteristics and randomness in geometry, material and loading parameters are accounted in analysis, since the mass, damping and stiffness are functions of random and/or design variables and the displacements are themselves implicit functions of these variables. That is why all the developments in this work are based on the Hamilton's principle. The treatment is restricted in this chapter to linear-elastic 3D systems. The formulation for the displacement finite element model of equations of motion is described and the computational aspects of the problem are discussed.

1.2 Hamilton's Variational Principle

Consider a linear continuum taking up in the 3D space a region Ω with a boundary $\partial\Omega$. We shall construct a displacement finite element model of the continuum as a function of space variables x, $x \in \Omega$, referred to a global system of coordinates $\{x\} = \{x_1, x_2, x_3\}$ and time variable t, $t \in [0, T]$. Suppose that the continuum Ω is

divided into a finite number of open disjoint subregions Ω_e called finite elements, $e = 1, \ldots, E$. Each of them is referred to separate local coordinates $\{x^e\}$. The admissible displacement field u_i, $i = 1, 2, 3$ is defined as function of x and t. Assume that δu_i is a virtual variation of u_i at the given time instant t and the values of u_i at t_1 and t_2 are prescribed, so that $\delta u_i(x, t_1) = \delta u_i(x, t_2) = 0$. Further, assume that the body forces f_i and boundary tractions $\hat{t}_i$ are independent of u_i so that their variations vanish. The Hamilton's variational principle states that among all the admissible displacements which satisfy the prescribed geometrical boundary conditions on $\partial\Omega$ and the prescribed conditions at the time limits $t = t_1$ and $t = t_2$, the actual solution renders stationary the functional

$$\int_{t_1}^{t_2} (\mathcal{T} - \mathcal{J})\, dt \ , \tag{1.1}$$

where

$$\mathcal{T} = \frac{1}{2} \int_\Omega \varrho \dot{u}_i \dot{u}_i \, d\Omega \ , \tag{1.2}$$

$$\mathcal{J} = \frac{1}{2} \int_\Omega C_{ijkl} u_{i,j} u_{k,l} \, d\Omega - \int_\Omega \varrho f_i u_i \, d\Omega - \int_{\partial\Omega} \hat{t}_i u_i \, d(\partial\Omega) \tag{1.3}$$

are the kinetic energy and the potential energy of the system. Symbols ϱ and C_{ijkl}, $i, j, k, l = 1, 2, 3$, represent mass density and components of the constitutive tensor. Comma and dot indicate spatial and time differentiation; repeated indices denote summation. Carrying out explicitly the variation in Eq. (1.1), with respect to displacement, through integration by parts with respect to time and modifying it to include viscous damping effect we obtain

$$\int_\Omega \delta u_i \varrho \ddot{u}_i \, d\Omega + \int_\Omega \delta u_i \zeta \dot{u}_i \, d\Omega + \int_\Omega \delta u_{i,j} C_{ijkl} u_{k,l} \, d\Omega = \\ = \int_\Omega \delta u_i \varrho f_i \, d\Omega + \int_{\partial\Omega} \delta u_i \hat{t}_i \, d(\partial\Omega) \ , \tag{1.4}$$

where symbol ζ in the second term of the left hand side of Eq. (1.4) represents the damping components appearing when the viscous damping effect is included. Eq. (1.4) is known as the d'Alembert principle. We note that the Hamilton's principle is an extension of the principle of stationary potential energy to the dynamic problems of the linear continuum. To be applied to static problems, the kinetic energy and damping terms vanish, and the only remaining term in the integrand of Eq. (1.1) is invariant with time. Thus the Hamilton's principle reduces to the principle of minimum potential energy

$$\delta \mathcal{J} = 0 \ . \tag{1.5}$$

Assume that displacement vector at any point of the continuum $u_i(x,t)$ can be expressed in terms of a finite number of generalized coordinates $q_\beta(t)$, $\beta = 1,\ldots,N$

$$u_i = u_i[x, q_\beta(t), t] = 0 \ . \tag{1.6}$$

The functions are chosen so as to satisfy the prescribed geometrical boundary conditions on $\partial\Omega$, irrespective of the values of the generalized coordinates. If the damping forces can be assumed to be proportional to the generalized velocities in the form of the Rayleigh's dissipation function

$$\mathcal{D} = \frac{1}{2}\zeta\, \dot{u}_i\dot{u}_i = \frac{1}{2}D_{\alpha\beta}\dot{q}_\alpha\dot{q}_\beta \ , \tag{1.7}$$

we obtain Lagrange's equations of motion in general form

$$\frac{d}{dt}\left(\frac{\partial\mathcal{L}}{\partial\dot{q}_\alpha}\right) - \frac{\partial\mathcal{L}}{\partial q_\alpha} + \frac{\partial\mathcal{D}}{\partial\dot{q}_\alpha} = f_\alpha \ , \tag{1.8}$$

where

$$\mathcal{L} = \frac{1}{2}\left(\int_\Omega \varrho\dot{u}_i\dot{u}_i\, d\Omega - \int_\Omega C_{ijkl}\varepsilon_{ij}\varepsilon_{kl}\, d\Omega\right) \ , \tag{1.9}$$

$$f_\alpha = \int_\Omega \varrho f_i\frac{\partial u_i}{\partial q_\alpha}\, d\Omega + \int_{\partial\Omega} \hat{t}_i\frac{\partial u_i}{\partial q_\alpha}\, d(\partial\Omega) \ , \tag{1.10}$$

with

$$\varepsilon_{ij} = \frac{1}{2}(u_{i,j} + u_{j,i}) \tag{1.11}$$

is the strain tensor. As a direct result of applying Hamilton's variational principle under the specific conditions that the energy and work can be expressed in terms of the generalized coordinates and of their time derivatives and variations, Lagrange's equations are applicable to all linear as well as nonlinear systems. In many problems there are no nonconservative forces involved, Lagrange's equations (1.8) reduce to

$$\frac{d}{dt}\left(\frac{\partial\mathcal{L}}{\partial\dot{q}_\alpha}\right) - \frac{\partial\mathcal{L}}{\partial q_\alpha} = 0 \ . \tag{1.12}$$

Lagrange's approach is very efficient for deriving the system of equations of motion, especially when the number of degrees of freedom of the system is large. The generalized coordinates and generalized forces can be given a convenient interpretation in the finite element context.

1.3 Displacement Finite Element Model

In the displacement finite element model the generalized coordinates $q_\alpha(t)$ are defined so that Eq. (1.6) takes the form

$$u_i(x,t) = \psi_{i\xi}(x)u_\xi^{(n)}(t) = \varphi_{i\alpha}(x)q_\alpha(t) , \tag{1.13}$$

$$\varphi_{i\alpha}(x) = \psi_{i\xi}(x)a_{\xi\alpha} , \tag{1.14}$$

$$i = 1,2,3 , \qquad \xi = 1,\ldots,N^{(e)} , \qquad \alpha = 1,\ldots,N ,$$

where symbol $u_\xi^{(n)}$ denotes vector of generalized nodal displacements in the local system of coordinates, $\psi_{i\xi}$ and $\varphi_{i\alpha}$ – the shape function matrices in the local and global system of coordinates, $a_{\xi\alpha}$ – the transformation matrix and $N^{(e)}$ is the number of degrees of freedom of an element. The strain tensor now can be rewritten as

$$\varepsilon_{ij}(x,t) = B_{ij\xi}(x)u_\xi^{(n)}(t) = B_{ij\alpha}(x)q_\alpha(t) , \tag{1.15}$$

$$B_{ij\alpha}(x) = B_{ij\xi}(x)a_{\xi\alpha} . \tag{1.16}$$

Introducing Eqs. (1.13),(1.15) into Lagrange's equations (1.8) the finite element version of the equations of motion reads

$$M_{\alpha\beta}\ddot{q}_\beta(t) + D_{\alpha\beta}\dot{q}_\beta(t) + K_{\alpha\beta}q_\beta(t) = f_\alpha(t) , \tag{1.17}$$

where

$$M_{\alpha\beta} = \sum_{e=1}^{E}\int_\Omega \varrho\psi_{i\xi}\psi_{i\eta}a_{\xi\alpha}a_{\eta\beta}\,d\Omega = \int_\Omega \varrho\varphi_{i\alpha}\varphi_{i\beta}\,d\Omega , \tag{1.18}$$

$$D_{\alpha\beta} = \sum_{e=1}^{E}\int_\Omega \zeta\psi_{i\xi}\psi_{i\eta}a_{\xi\alpha}a_{\eta\beta}\,d\Omega = \int_\Omega \zeta\varphi_{i\alpha}\varphi_{i\beta}\,d\Omega , \tag{1.19}$$

$$K_{\alpha\beta} = \sum_{e=1}^{E}\int_\Omega C_{ijkl}B_{ij\xi}B_{kl\eta}a_{\xi\alpha}a_{\eta\beta}\,d\Omega = \int_\Omega C_{ijkl}B_{ij\alpha}B_{kl\beta}\,d\Omega , \tag{1.20}$$

are the mass, damping and stiffness matrices of the system. In the compatible displacement model, Eq. (1.17) is satisfied a priori by the stress boundary conditions. In what follows, we will consider the boundary-initial problem for which the displacement boundary conditions have been already imposed in Eq (1.17). When the time-varying load and damping terms are ignored the free-vibration problem (or eigenproblem) reads

$$M_{\alpha\beta}\ddot{q}_\beta(t) + K_{\alpha\beta}q_\beta(t) = 0_\alpha \ . \tag{1.21}$$

If the inertial and damping terms are negligible, Eq. (1.17) reduces to (cf. Eq. (1.5))

$$K_{\alpha\beta}q_\beta = f_\alpha \ , \tag{1.22}$$

which is the equilibrium equation for static problems.

1.4 Computational Implementation

1.4.1 Solution of Linear Algebraic Equations

In the finite element implementation we have frequently to deal with solving a large set of simultaneous, linear algebraic equations. The effectiveness of the analysis depends to a large degree on the numerical procedures used for solution of the equations. Since Eq. (1.22) is a special case of Eq. (1.17), the relationship between the solution of the equilibrium equations and a dynamic analysis suggests that the algorithms used for the evaluation of q_β may also be employed as the basis of the algorithms employed for eigensolution and direct step-by-step integration of equations of motion. Therefore we shall discuss in detail some computational aspects of the problem.

In general, there are two different techniques for the solution of Eq. (1.22). In a direct procedure, an a priori calculation of the number of arithmetic operations can be made, whereas in indirect or iteration solution no such an a priori estimate can be made. The main advantages of the iteration technique such as Gauss-Seidel iteration are the reduced operating memory storage demands and the elimination of the triangular decomposition which is the most costly part of the direct solution. The disadvantages are the lack of general knowledge on how many iterations are necessary to achieve an acceptable tolerance and the value of the over-relaxation factor can change significantly the convergence. The technique also fails on indefinite coefficient matrices or in case of many right hand sides involved; no advantage can be taken of a previous solution step as the whole iteration process must be repeated. In the direct solution a resolution is relatively cheap once the triangular decomposition is carried out. Therefore, almost all state-of-the-art finite element solvers for linear algebraic equations use the direct techniques.

Assume now that in the direct solution, the stiffness matrix K in Eq. (1.22) is symmetric and positive definite (this has not to be the case when a finite element formulation is based on a mixed variational principle or some other weighted residual methods). One of the most effective techniques currently used is based on Gauss elimination [37,85,107], where N coefficient matrices of order $N, \ldots, 1$, corresponding to the $(N-n)$ last degrees of freedom, $n = 0, \ldots, N-1$, are formed. That is, the basic procedure of the Gauss elimination solution is to reduce the stiffness matrix K to an upper triangular matrix S from which the unknown displacement q can be obained by a back substitution. We have

$$K = LS = LDL^T \ , \tag{1.23}$$

where L is a lower triangular matrix with unit diagonal elements and D is a diagonal matrix. Having the LDL^T decomposition of K Eq. (1.22) can be solved for q by the forward-reduction and backward-substitution processes

$$Lr = f \ , \qquad DL^T q = r \ . \tag{1.24}$$

To reduce the required high-speed memory and computational effort for large systems. an effective storage scheme for the global stiffness matrix is to save only the nonzero part of the upper triangular portion including diagonal elements in a multi-block form. For each block, the active columns below the skyline of the matrix profile are saved in a one-dimensional array in compact form by columns in from-the-diagonals mode [10] or to-the-diagonals mode [144,146]. These storage techniques have definite advantages over the banded-storage method, since:

1) it always requires less operating memory,

2) it not severely affected (no node renumbering required) by a few very long columns; and rather the *mean*-bandwidth of the system matrix is of interest than the *max*-bandwidth in the banded-storage case,

3) the fact that only dot product routines are used to perform the factorization and forward reduction is important to modern machines which are vector oriented.

In addition to the LDL^T decomposition described above, there are various other decomposition procedures that are based on the Gauss elimination and are closely related. By the Cholesky factorization technique [37,107] the coefficient matrix is triangularized as follows

$$K = \tilde{L}\tilde{L}^T \ , \qquad with \qquad \tilde{L} = LD^{1/2} \ . \tag{1.25}$$

The elements of $\tilde{L}$ can be calculated directly or from the matrices L and D. When compared against the LDL^T decomposition, which can be used on nonpositive definite systems, the disadvantage of the Cholesky factorization is that it is only suitable for the positive definite systems for which all the diagonal elements of D are positive, since otherwise complex arithmetic operations would be required. The Cholesky decomposition, however, is efficiently used in the transformation of a generalized eigenproblem to the standard form. In the stochastic finite element context, as will be shown below, it is effectively applied to the transformation of correlated random variables to a set of uncorrelated random variables. In some cases an algorithm which can be efficiently employed to solve Eq. (1.22) is so called 'static condensation' [21,140,141], which is used to perform part of the solution of the total finite element equations prior to assembling the global stiffness matrix and loading vectors. Since the global stiffness matrix is established by direct addition of the element stiffness matrices, part of the total Gauss solution is already performed on the element level when condensing out internal element degrees of freedom. Consequently, the order of the system equations is reduced. This is an advantage of the technique, particularly if subsequent elements or parts of structure are identical. An application

of this concept is employed in substructure analysis, in which the total structure is considered as an assemblage of substructures [116,117]. The substructures, in turn, are considered as individual finite elements; and the total stiffness matrix is assembled by the condensed substructure stiffness matrices. In effect, input data are required only for each substructure in the library and information on the assemblage of substructures. The disadvantage of the procedure is that the order of the system matrix is changed during solution process; and it is difficult to adapt this procedure to fit into a standard numerical code available to solve problems included different types of finite elements.

It is important to use back-up storage effectively, since a great deal of reading and writing can be expensive and may limit the system size that can be solved. Sometimes instead of first assembling the complete global stiffness matrix, we may assemble and reduce the equations at the same time; and back-up storage for the total unreduced stiffness matrix is not required. In this case the frontal solution approach can be applied effectively: only those equations (in fact, element stiffness matrices) that are actually required for the elimination of a specific degree of freedom are assembled. Since the equations are assembled in the element order, the wave front (the elements that are related to the static condensation of the equations corresponding to one specific degree of freedom) and the bandwidth are determined by the element numbering. In principle, the frontal solution is Gauss elimination with this specific computation aspect. An advantage of the frontal technique is that elements can be easily added, since no node renumbering is required to preserve a small bandwidth. The technique is specially effective for problems of long-shape structures constructed from similar blocks. The disadvantage is that if the wave front is large, the total high-speed memory required may be too large; and using back-up storage decreases the effectiveness of the technique by a great amount. Also, a frontal solver may require more indexing in the solution when compared against that for active-column or banded-storage solvers.

1.4.2 Solution of Equations of Motion

Equation (1.17) represents a system of linear differential equations of second order. Mathematically, the equations with constant coefficients can be integrated over the time domain or frequency domain by standard procedures, the Laplace transform or the Fourier transform. In practice, the procedures developed for the solution of general systems can be quite laborious if the order of the systems is large, unless specific advantage is taken of the special characteristics of the coefficient matrices. In finite element context, we shall therefore concentrate in two approaches: direct integration and mode superposition. Although the two techniques are seemingly quite different they are closely related. Assume that Eq. (1.17) is to be integrated with respect to time variable t from 0 to T and the time domain $[0, T]$ is divided into n equal time interval Δt. Further, assume that the solutions of Eq. (1.17) at any time interval from 0 to t are known and that the solution at time $t + \Delta t$ is to be found. Under these assumptions we shall consider some computational aspects of the two integration techniques.

Direct Step-by-Step Integration

In direct integration schemes no transformation of Eq. (1.17) into a different form is performed and the equations are solved using a numerical step-by-step procedure. There are two basic assumptions for the direct integration approach: 1) Eq. (1.17) is satisfied only at separate time intervals Δt; and need not be satisfied at any other time instant, 2) the acceleration, velocity and consequently, displacement functions are prescribed within each time interval. Thus, at each separated time interval the solution of equations of motion can be treated as a static solution, i.e. the system of the linear differential equations can be converted to a corresponding system of linear algebraic equations, which include the effective stiffness matrix, inertia and damping forces and time-varying load.

Theoretically, a large number of finite difference expressions can be used to approximate the accelerations and velocities in terms of the displacements. Using an explicit integration procedure, the central difference method [34] solves for displacement q at time $t + \Delta t$ using the equilibrium conditions at time t; and the accelerations and velocities evaluated at time t are approximated by second-order central difference functions of the displacements at times $t - \Delta t$, t and $t + \Delta t$ with errors of order $0(\Delta t)^2$. For a undamped system with the diagonal mass matrix, this integration technique does not require a decomposition of the effective stiffness matrix and only vector multiplications are required to form the effective loads. Consequently, it is also not necessary to assemble the global mass and stiffness matrices; since the right hand side can be computed at the element level by summing the contributions from each element to the load vector. Thus, the main advantage of the central difference method is that relatively little operating memory is required for large scale systems. The shortcomings of the technique are that it depends on the modelling the diagonal mass matrix and on the neglecting velocity-dependent damping. Moreover, in order to obtain acceptable solution the value of the time interval Δt must be selected much smaller when compared against other integration techniques. The central difference method is conditionally stable. Another integration scheme frequently used is the Houbolt method [10]. This technique is related to the method discussed above in that the standard finite difference functions are also used to approximate the accelerations and velocities. Basing on backward-difference formulas the acceleration and velocity evaluated at time $t + \Delta t$ are approximated by a function of the displacements at times $t - 2\Delta t$, $t - \Delta t$, t and $t + \Delta t$ with errors of order $0(\Delta t)^2$. The technique differs from the central difference strategy by using an implicit integration scheme, i.e. equilibrium condition is considered at time $t + \Delta t$. In terms of the computational implementation, this means that the effective stiffness matrix appears on the left hand side and the factorization is required during solution of the algebraic equations. On the other hand, Houbolt method does not require a critical time-interval limit and Δt can be chosen much larger than that for the central difference technique.

In the following we shall concentrate on some computational aspects of two implicit integration techniques which are most efficiently used in finite element implementation. The techniques are known as the Wilson-θ method and Newmark

method. The both methods are essentially extension of the linear acceleration strategy [21,76], in which the acceleration function is assumed to be linear from time t to time $t+\Delta t$. On this basis, the changes in acceleration and velocity can be expressed in terms of the displacements which may be evaluated through any standard linear algebraic equation procedure discussed in the preceding paragraph. In the Wilson-θ method the acceleration is assumed to be a linear function at the time interval from t to $t+\theta\Delta t$ with $\theta \geq 1$ [10]

$$\ddot{q}^{t+\tau} = \ddot{q}^t + \frac{\tau}{\theta\Delta t}(\ddot{q}^{t+\theta\Delta t} - \ddot{q}^t) , \qquad 0 \leq \tau \leq \theta\Delta t . \tag{1.26}$$

The approximate velocities and displacements are then obtained by integrating Eq. (1.26) with respect to time from 0 to τ. Under these assumptions $\ddot{q}^{t+\theta\Delta t}$ and $\dot{q}^{t+\theta\Delta t}$ can be expressed in terms of $q^{t+\theta\Delta t}$

$$\ddot{q}^{t+\theta\Delta t} = \frac{6}{\theta^2\Delta t^2}(q^{t+\theta\Delta t} - q^t) - \frac{6}{\theta\Delta t}\dot{q}^t - 2\ddot{q}^t , \tag{1.27}$$

$$\dot{q}^{t+\theta\Delta t} = \frac{3}{\theta\Delta t}(q^{t+\theta\Delta t} - q^t) - 2\dot{q}^t - \frac{\theta\Delta t}{2}\ddot{q}^t . \tag{1.28}$$

Substituting Eqs. (1.27),(1.28) into the equations of motion at time $t+\theta\Delta t$

$$M\ddot{q}^{t+\theta\Delta t} + D\dot{q}^{t+\theta\Delta t} + Kq^{t+\theta\Delta t} = f^{t+\theta\Delta t} \tag{1.29}$$

where

$$f^{t+\theta\Delta t} = f^t + \theta(f^{t+\Delta t} - f^t) , \tag{1.30}$$

we obtain a linear algebraic system for $q^{t+\theta\Delta t}$. Having solved for $\ddot{q}^{t+\theta\Delta t}$ from Eq. (1.27) and consequently for $\ddot{q}^{t+\Delta t}$ evaluated at $\tau = \Delta t$ from Eq. (1.26), $\dot{q}^{t+\Delta t}$ and $q^{t+\Delta t}$ can be computed and the solution is completed.

In the Newmark integration the equilibrium condition is considered at time $t+\Delta t$. The velocities and displacements are approximated by

$$\ddot{q}^{t+\Delta t} = \frac{1}{\alpha\Delta t^2}(q^{t+\Delta t} - q^t) - \frac{1}{\alpha\Delta t}\dot{q}^t - (\frac{1}{2\alpha} - 1)\ddot{q}^t , \tag{1.31}$$

$$\dot{q}^{t+\Delta t} = \dot{q}^t + \Delta t[(1-\delta)\ddot{q}^t + \delta\ddot{q}^{t+\Delta t}] , \tag{1.32}$$

where α and δ are constants that can be selected to obtain integration accuracy and stability. If $\alpha = 0.25$ and $\delta = 0.5$ the acceleration function is constant at each time interval Δt. The solution proceeds similarly to the case of Wilson-θ

integration. Using $\alpha = 0.25$, $\delta = 0.5$ and $\theta = 1$ the same approximation is obtained in both methods. Note that with $\delta \geq 0.5$, $\alpha \geq 0.25(\delta + 0.5)^2$ and $\theta \geq 1.37$ the Newmark and Wilson-θ methods are unconditionally stable. The close relationship between the computer implementation of the Newmark and Wilson-θ integration makes it possible to conveniently use both integration schemes in one finite element routine. The techniques are simple and can be directly used for solution of nonlinear-continuum systems with no limiting the Rayleigh's form of the damping effects. The shortcomings of the Newmark and Wilson-θ methods, and of the direct integration techniques as a whole, are:

1) they have always to deal with all the degrees of freedom of the system equations during solution,

2) the computation efforts depend on the bandwidth of the coefficient matrices and it will be more costly for a large system with the consistent mass and damping coefficients,

3) the number of operations required is directly proportional to the number of time intervals used in the analysis; and the techniques is expected to be efficient when the response may be accurately approximated for a small number (say, a few hundreds) of time intervals.

Mode Superposition

The considerations in the preceding paragraph show that the computation cost of the direct integration strategy would be unacceptable high for the response analysis of large systems with a relatively long duration (a large number of time intervals) required. It may be more effective to first transform the equations of motion into a form in which the step-by-step solution is less costly. The objective of the transformation is to obtain new system mass, damping and stiffness matrices, which have a smaller bandwidth than the original ones. Mathematically, there can be many different orthogonal transformations [10,21,102], which would reduce the bandwidth of the system matrices. In structural dynamics, however, one of the most effective transformations is based on a change of basis from the finite element coordinates to modal (normalized) coordinates. The basic idea behind modal analysis is to transform the simultaneous set of coupled equation represented by Eq. (1.17) into a uncoupled set of equations, where the transformation matrix is the mode shape matrix. These uncoupled equations can be integrated independently for the modal displacements, which are then superposed to obtain the finite element displacements. Let us write the solution of Eq. (1.17) as the superposition

$$q_s(x,t) = Q_{sz}(x)y_z(t) \ , \qquad z = 1,\ldots,Z \leq N \ , \tag{1.33}$$

where $q_s(x,t)$ is the vector of finite element coordinates, symbol $y_z(t)$ denotes the vector of modal coordinates. The mode shape matrix $Q_{sz}(x)$ is nonsingular and determined through the eigensolution of the undamped free vibration equations of the dynamic system (1.17)

$$K_{\alpha\beta}Q_{\beta z} = \Omega_{(z)}M_{\alpha\beta}Q_{\beta z} \ , \tag{1.34}$$

with $\Omega_{(z)}$ is the diagonal matrix of the natural frequencies squared. Inserting Eq. 1.33) into Eq. (1.17), premultipling the result by $Q^T_{\beta z}$, using the orthonormality conditions

$$M_{\alpha\beta}Q_{\alpha u}Q_{\beta z} = \delta_{uz} \ , \qquad K_{\alpha\beta}Q_{\alpha u}Q_{\beta z} = \Omega_{(z)} \ , \tag{1.35}$$

$$u, z = 1, \ldots, Z \ , \qquad \delta_{uz} - \textit{Kronecker delta} \ ,$$

as well as assuming that

$$D_{\alpha\beta}Q_{\alpha u}Q_{\beta z} = 2\xi_u\omega_z\delta_{uz} \ , \qquad \textit{(no sum on } u, z) \tag{1.36}$$

we obtain the set of Z uncoupled equations for the normalized coordinates $y_z(t)$

$$\ddot{y}_z(t) + 2\xi_z\omega_z\dot{y}_z(t) + \omega_z^2 y_z(t) = f_z(t) \ , \tag{1.37}$$

$$z = 1, \ldots, Z \ , \qquad \textit{(no sum on } z)$$

where ξ_z is a damping factor associated with the z-th mode, ω_z is the z-th frequency of the undamped system and the z-th normalized force is defined as

$$f_z(t) = Q_{\alpha z}f_\alpha(t) \ . \tag{1.38}$$

Each equation in system (1.37) can be solved independently for the modal coordinate $y_z(t)$ by using a standard procedure or by the Duhamel's convolution

$$y_z(t) = \frac{1}{\tilde{\omega}_z}\int_0^t f_z(\tau)\exp[-\xi_z\omega_z(t-\tau)]\sin\tilde{\omega}_z(t-\tau)\,d\tau + \\ + \exp(-\xi_z\omega_z t)\{a_z\sin\tilde{\omega}_z t + b_z\cos\tilde{\omega}_z t\} \ , \tag{1.39}$$

$$\tilde{\omega}_z = \omega_z(1-\xi_z^2)^{1/2} \ , \qquad \textit{(no sum on } z) \tag{1.40}$$

where a_z and b_z are integration constants, which are determined from the initial conditions expressed in normalized coordinates. In finite element analysis, each equaion in system (1.37) can be solved more effectively by the direct integration schenes mentioned above. Similarly to the derivations described in the preceding paragraph for coupled systems, for the specific direct step-by-step integration scheme considered we can establish a recursive relationship of the form [10]

$$\hat{y}_z^{t+\Delta t} = A_z \hat{y}_z^t + p_z f_z^{t+\nu} \ , \qquad \textit{(no sum on } z\textit{)} \tag{1.41}$$

where $\hat{y}_z^{t+\Delta t}$ and $\hat{y}_z^t$ are vectors involving the solution quantities, e.g. the displacements, velocities and accelerations. The matrix A_z and vector p_z are the integration approximation and load operators. Each quantity in Eq. (1.41), as well as index ν which may be 0, Δt, or $\theta \Delta t$, depends on the specific integration technique employed in analysis. For example, the simulation of the unit impulse excitation (or Dirac delta distribution, which plays an important role in dynamic response sensitivity at any time instant) in terms of a discrete-time forcing sequence in the Newmark's and Wilson-θ integration schemes can be shown to have the forms given in Fig. 1.1.

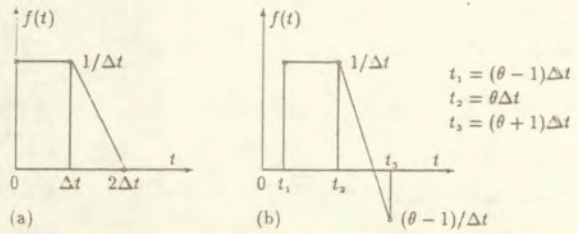

Figure 1.1: Simulation of the unit impulse in Newmark's (a) and Wilson-θ's (b) schemes.

In the mode superposition context, the response of a general damped system represents a much more difficult problem, since relation (1.36) is not valid; and the classical modal analysis does not lead to an independent system of differential equations, unless the overall energy dissipation during the time response can be appropriately approximated. This is a disadvantage of the modal analysis. Our considerations are restricted to the cases when the damping effects can be expressed approximately as a linear combination of the mass and stiffness, i.e.

$$D = \alpha M + \beta K \ , \tag{1.42}$$

where α and β are constants to be determined. Hence, the damping matrix becomes diagonal

$$2\xi_z \omega_z = \alpha + \beta \omega_z^2 \ , \qquad \textit{(no sum on } z\textit{)} \ . \tag{1.43}$$

The parameters α and β can be determined from two given damping factors that correspond to two unequal natural frequencies. In practice it may be that the damping factors are known for many more than two frequencies. In that case two pairs of average values of the damping factors and corresponding frequencies can be selected considering the spacing of the natural frequency sequence [10]. The two pairs of averaged frequencies $\bar{\omega}_1, \bar{\omega}_2$ and averaged damping factors $\bar{\xi}_1, \bar{\xi}_2$ then can be used as the coefficients and the components of the right hand side vector of second-order algebraic equations resulting from Eq. (1.43) for α and β as follows

$$\alpha + \bar{\omega}_1^2 \beta = 2\bar{\omega}_1 \bar{\xi}_1 \ , \qquad \alpha + \bar{\omega}_2^2 \beta = 2\bar{\omega}_2 \bar{\xi}_2 \ . \tag{1.44}$$

Also, the practical observations in some cases [80] show that for any given pair of α_z and β_z the frequency ω_z, which renders ξ_z minimum, can be expressed as

$$\omega_z = \left(\frac{\alpha_z}{\beta_z} \right)^{1/2} \ , \qquad \textit{(no sum on } z\textit{)} \tag{1.45}$$

and the coefficients α_z and β_z for each mode can be determined as

$$\alpha_z = \xi_z \omega_z \ , \qquad \beta_z = \frac{\xi_z}{\omega_z} \ , \qquad \textit{(no sum on } z\textit{)} \ . \tag{1.46}$$

It is observed that the mode superposition differs from the direct integration only by changing of generalized coordinate basis prior to the time integration. Mathematically, the same space is spanned by the N eigenvectors as by the N finite element degrees of freedom; and the solution obtained in both analyses are identical within the numerical errors of the eigenpairs and time integration routines and the round-off errors in the computer used. As shown in practice, only a fraction of the total number of uncoupled equations need be considered to obtain a good approximation to the system response, i.e. we need to solve only for Z ($Z \ll N$) lowest eigenpairs from Eq. (1.34) and to superpose only the first Z modes in Eq. (1.33).

Summarizing Remarks

*In the foregoing chapter the state-of-the-art finite element modelling in structural dynamics, wherein static and free-vibration problems are treated as special cases, was summarized. When compared against the vectorial-equilibrium and virtual-work approaches, the variational formulation based on Hamilton's principle is shown to be the most efficient. It will be subsequently used as a basis to derive problems of the deterministic structural sensitivity in statics, free and forced vibrations (*Chapter 2 *and* Chapter 3*), to develop a stochastic Hamilton's principle and the corresponding stochastic finite element model of equations of motion (*Chapter 4*), which is used to formulate the stochastic sensitivity problems for the static and dynamic response (*Chapter 5 *and* Chapter 6*).*

The computer performance in finite element analysis was described. The computational aspects of the Gauss and Cholesky decomposition schemes used in linear algebraic equation solvers, the Wilson-θ and Newmark methods for integration of equations of motion and the mode superposition strategy for damped systems are discussed in more detail, since 1) their definite advantages are shown in case of out-of-core dynamic systems and a large number of time intervals required, 2) in combination with the 2nd-order perturbation method, the adjoint variable approach and the fast Fourier transform, the techniques mentioned above enable us to work out a set of parallel algorithms applicable to large-scale stochastic sensitivity problems with low computation cost.

2 Structural Sensitivity Problem for Static Response

2.1 Scope of the Chapter

The objective of structural design sensitivity (SDS) analysis is to consider the dependence of state variables on design variables. For deterministic systems this means to evaluate the change of the response functional with variations in geometry, material and loading parameters. Generally the dependence of structural response such as the displacement and stress fields, support reactions, etc. on design parameters such as cross-sectional area, length, thickness, Young modulus or mass density of structural members is implicitly defined through the laws of continuum mechanics. The gradients of a structural response functional and constraints, which represent and characterize the trend of the structural response variation when design variables are changed, provide valuable database for choosing a search direction to obtain an improved new design.

Since design variables appear in the coefficients of linear operators, the system equations are generally nonlinear as functions of state and design variables. This is why analytical applications of SDS are restricted to simple, distributed parameter 1D or 2D systems and are generally imbedded in papers devoted to optimization by the gradient approach. In one of the first works on SDS [145], a formulation for the stress sensitivity analysis and a discussion restricted to a 2D problem was presented. Developments in [49,51,52,120] provided the theoretical foundation of SDS for general distributed parameter systems. In some finite element codes a version of SDS has been incorporated, but a lot of essential work remains to be done. Attention is restricted in this chapter and in the entire work to linear structural mechanics, i.e. to structures whose equilibrium equations are linear in the state variables, once the design variables are fixed. The state variables are considered as a finite-dimensional vector of displacements and stresses, and the design variables form finite-dimensional vector of design parameters. In the finite element context the state equations are matrix equations for static response, with design variables appearing in the coefficient matrix. This chapter is concerned with numerical analysis and computer implementation of structural design sensitivity for static problems. Both the direct differentiation and adjoint variable approaches [53] for SDS analysis are summarized. The computational aspects of both the methods are discussed in some detail. A version of the static sensitivity analysis incorporated into the microcomputer finite element code POLSAP is described. Examples include SDS analysis of trusses, frames, plates and a truss-beam-plate structure.

MODEL PROBLEM OF CHAPTER 2

Given ◁ vector of design variables $h(x)$, x – spatial coordinates
(for example: cross-sectional area, thickness, length, Young modulus)
◁ response functional $\phi(x, h)$
(for example: cost function, displacement or stress constraint function)
◁ displacement-expressed finite element equilibrium equations $F(x, h) = 0$

Find ▷ gradient of response functional ϕ with respect to design variables h

2.2 Finite Element Formulation

Consider structural response of the linear-elastic system of N degrees of freedom defined by the functional

$$\phi = G[q(h), h] \ , \tag{2.1}$$

where $h = \{h^e\}$, $e = 1, \ldots, E$ is the vector of design variables, $q(h) = \{q_\beta(h)\}$, $\beta = 1, \ldots, N$, describes the vector of nodal displacements. The displacement vector satisfies the equilibrium equations

$$K_{\alpha\beta}(h) q_\beta(h) = f_\alpha(h) \ , \tag{2.2}$$

where symbols $K_{\alpha\beta}(h)$ and $f_\alpha(h)$, $\alpha = 1, \ldots, N$, denote the system stiffness matrix and load vector. Since the stiffness and load are functions of design variables, the displacements are implicit functions of these variables. The objective of the deterministic analysis of SDS is to determine changes in the structural response functional with variations of design parameters, i.e. to find $\partial\phi/\partial h^e$ – the sensitivity gradient of functional ϕ. Using the chain rule of differentiation leads to

$$\phi^{,e} = G^{,e} + G_{,\beta} q_\beta^{,e} \ , \qquad e=1,\ldots,E \ , \tag{2.3}$$

where symbols $(.)^{,e}$ and $(.)_{,\beta}$ describe the first partial derivatives with respect to the e-th design variable and the β-th nodal displacement, respectively. Since G is an explicit function of design variables and displacements, $G^{,e}$ and $G_{,\beta}$ are known while $q_\beta^{,e}$ remains to be calculated. Suppose that $K_{\alpha\beta}(h)$, $f_\alpha(h)$ and consequently $q_\beta(h)$ (according to the implicit function theorem, [42,22]) are S times continuously differentiable with respect to the design variables h. Differentiating both sides of Eq. (2.2) with respect to h^e leads to

$$K_{\alpha\beta}(h) q_\beta^{,e}(h) = f_\alpha^{,e}(h) - K_{\alpha\beta}^{,e}(h) q_\beta(h) \ . \tag{2.4}$$

Since the stiffness matrix $K_{\alpha\beta}(h)$ is nonsingular, Eq. (2.4) can be solved for $q_\beta^{,e}$ which substituted into Eq. (2.3) results in

$$\dot{o}^{\epsilon} = G^{\epsilon} + G_{,\beta} K^{-1}_{\alpha\beta} (f^{\epsilon}_{\alpha} - K^{\epsilon}_{\alpha\beta} q_{\beta}) \ . \tag{2.5}$$

This procedure is referred to as the direct differentiation method, which has been used extensively in structural optimization. The second strategy can be described by defining an adjoint variable vector $\lambda = \{\lambda_{\alpha}\}$ as follows

$$\lambda_{\alpha} = G_{,\beta} K^{-1}_{\alpha\beta} \ . \tag{2.6}$$

Since the stiffness matrix $K_{\alpha\beta}(h)$ is symmetric the adjoint equations for λ can be defined as

$$K_{\alpha\beta} \lambda_{\beta} = G_{,\alpha} \ , \tag{2.7}$$

Having solved Eq. (2.7) for the adjoint variables the coefficients of the sensitivity gradient of the structural response functional can be obtained

$$\dot{o}^{\epsilon} = G^{\epsilon} + \lambda_{\alpha} (f^{\epsilon}_{\alpha} - K^{\epsilon}_{\alpha\beta} q_{\beta}) \ . \tag{2.8}$$

2.3 Computational Implementation

Formally, the direct differentiation method (DDM) and adjoint variable method (AVM) seem to be identical in formulation and solution, even in terms of the computational implementation. However, for realistic design problems, their computer performance are considerably different. In the design process the designer must frequently evaluate response of systems with large number of degrees of freedom and account for numerous loading conditions and numerous performance constraints at some trial design. Let us assume that instead of a single load vector and a single constraint considered in Section 2.2, L load cases and C active constraints are accounted for in the design sensitivity analysis of a static problem and assume that some constraint is active for each load condition. We shall consider the formulation in which the reduced stiffness matrix approach is employed , i.e. the boundary conditions associated with the structure are assumed to have been imposed before the solution phase. Further, suppose that the derivatives of the element stiffness matrix and load vectors with respect to E design variables have been computed and expressed in terms of the global coordinates, and the global stiffness matrix has been triangularized. Because of the linearity of the problem under consideration these data are constant and assumed to have been saved on a back-up storage memory.

To compute the sensitivity gradient coefficients for each of C constraints using DDM. Eq.(2.2) must be solved for L load conditions. Next each of the L vectors of calculated nodal displacements is used to determine the E right hand sides of Eq. (2.4). Having obtained solution for dq/dh the sensitivity gradient coefficients may be directly evaluated for C constraints. It is seen that there are $L \times E$ equations to be solved. More precisely, the forward-reduction and backward-substitution

processes in the Gauss elimination procedure must be carried out $L \times E$ times. On the other hand, assuming in AVM that each of the C constraints is active for the L loading cases, there are $L + C$ equations (2.7) to be solved for the displacements and adjoint variables. Design sensitivity coefficients of C constraints for L loads are then calculated directly from Eq. (2.8) for E design variables. It is seen that if $L \times E < L + C$ then DDM is preferred. This may likely occur for preliminary design problems, when a small number of design variables and a large number of constraints are accounted in the analysis. For structural optimization problems, for which usually $C < E$, AVM is more efficient, even for a single loading condition. With multiple load cases C is frequently much smaller than $L \times E$, leading to the fact that in most structural optimization analyses AVM is more effective. Besides, the equation solution phase of AVM is generally less costly since $L + C$ systems of algebraic equations may be solved simultaneously (when the structural response functional is linear with respect to the displacements which is usually assumed in design practice), whereas applying DDM the process always contains two separate steps and between them an additional procedure must be inserted to calculate the right hand sides of Eq. (2.4). Taking these advantages into account AVM has been chosen to develop a version of structural sensitivity analysis for statics problems in the conputer code POLSAP for L, C and S being arbitrarily large.

Similarly to the assemblage of the global stiffness matrix, the system matrix of derivatives of the total stiffness with respect to design variables is assembled simply by addition over the derivatives of element matrices in the global coordinate system. It should not be overlooked that in contrast to the global stiffness matrix profile almost all terms in the matrices of their derivatives with respect to design are equal to zero. This simplifies the algorithms of procedures for the sensitivity gradient calculation, since almost all operations can be carried out at the element level. Another consideration that is to be taken into account involves computing the derivatives of stiffness functions with respect to design variables when the element stiffnes matrices are implicitly generated in the finite element program, [41,83,144]. To generate the matrices, some modern finite element formulations carry out numerical integration rather than use closed form expressions in terms of design variables, such as those described in Section 2.2. For implicitly generated element matrices, differentiation with respect to design variables can be performed through the sequenceof computations used to generate these matrices, leading to implicit design derivatve procedures. The element matrices of design derivatives can be alternatively approximated by using the perturbation technique and finite differences. For instance,

$$\frac{\partial k_{ee}}{\partial h_m^{(e)}} \approx \frac{1}{\theta}[k_{ee}(h^{(e)} + 1_m\theta) - k_{ee}(h^{(e)})] \,, \tag{2.9}$$

where symbol k_{ee} denotes the element stiffness matrix, $h^{(e)} = \{h_m^{(e)}\}$ indices the m-dimensonal vector of design variables of the element, θ represents a small perturbation n the m-th component of the element design variable vector and 1_m is an m-dimesional identification vector, which has *one* at the m-th position and *zeros* elsewhee.

The computer program POLSAP which provides capabilities for analysis of static and dynamic responses and stability of deterministic and stochastic structural systems, has been extended to include the sensitivity calculation options. The extended version provides a new tool for design sensitivity analysis of complex structures such as truss-beam-plate-shell systems. All modules developed in the program are functionally independent and interact with the global database by means of a database control system. In the input phase the control parameters monitor the macro process, set up storage and open files required for the sensitivity calculations. The right hand side vectors of the equilibrium and adjoint equations are generated and assembled simultaneously. At the element level the derivatives of the mass, damping and stiffness matrices with respect to design are evaluated, transformed to the global coordinates and saved in the peripheral memory for any element groups concerned with the sensitivity analysis. The structural response functionals may be defined in terms of displacements and stresses. Four types of the design variables can be simultaneously considered – cross-sectional area and length of the 3D truss and 3D beam elements, thickness of the plate and shell elements and Young modulus for all the element groups. For the case of beam-type elements the effects of cross-section geometry are assumed to be proportional to square of the cross-sectional area by a constant, [53]. In the solution phase, the state equations of the structure and adjoint systems are solved simultaneously. The last phase of the analysis is the evaluation of the design sensitivity gradient coefficients, whose values are output in tabular mode in separate for each element group, load condition, displacement and/or stress constraints and design variables.

2.4 Sensitivity Analysis and Minimum-Weight Optimization

In the context of sensitivity analysis let us now consider the minimum-weight optimization problem as an application of the adjoint variable technique. For the linear system of N-degrees of freedom and E design variables we consider the cost function

$$\mathcal{W} = h^T l = h_e l_e \ , \tag{2.10}$$

and a set of constraints

$$K_{\alpha\beta}(h) q_\beta(h) = f_\alpha \ , \tag{2.11}$$

$$q_\beta^A - q_\beta \geq 0 \ , \tag{2.12}$$

$$\sigma_e^A - Z_{e\beta} q_\beta \geq 0 \ , \tag{2.13}$$

$$h_e - h_e^{MIN} \geq 0 \ , \tag{2.14}$$

$$e = 1, \ldots, E \ , \qquad \alpha, \beta = 1, \ldots, N \ ,$$

where $h = \{h_e\}$ and $l = \{l_e\}$ are the vector of design variables which are assumed as cross-sectional areas and the vector of member lengths for the case of truss-beam systems or thickness and area of structural members for the case of sheet-plate-shell systems, correspondingly. As defined above Eq. (2.11) represents the equilibrium equations with the boundary conditions imposed, q_β^A and σ_e^A denote the admissible values of the nodal displacements and element stresses, $Z_{e\beta}$ describes the displacement-stress relating matrix in the finite element model. The objective of the minimum-weight optimization problem is to determine minimum value of the cost function expressed by Eq. (2.10) satisfying the constraints mentioned in Eqs. (2.11)–(2.14).

Up to now there exist two main approaches developed to deal with this problem. One is based on the mathematical programming techniques, [36,113,123] and the other is based on the concept of optimality criteria, [15,36,74,89]. In terms of the computational implementation the disadvantages of both the methods is that it is difficult to establish unique algorithms for various classes of large-scale systems; and in some cases the computation cost would be unacceptable high. Recently, a method based on the Kuhn-Tucker necessary conditions for optimization problem has been developed, [45,46]. According to the method proposed, a set of linear algebraic equations is obtained by the Lagrange's multiplier technique through the direct stiffness approach used for problems of the linear-elastic continuum. As a result a nonlinear discretized-parameter problem can be treated with techniques that take advantages of linear operators. When compared against the methods based on the mathematical programming and optimality criteria, another advantage of the method is that the algorithms worked out for the problem would be much more efficiently used for large-scale systems with relatively low computation cost and could be readily adapted to fit into existing finite element codes. In what follows the computer implementation is described as an application of the adjoint variable method in sensitivity analysis to the minimum-weight problem.

The main idea behind the method proposed in [45] is quite simple. By introducing Lagrange's multipliers the problem expressed by Eqs. (2.10)–(2.14) can be rewritten in the scalar form

$$\mathcal{S} = -\mathcal{W} + \lambda_\alpha^{(1)}(K_{\alpha\beta}q_\beta - f_\alpha) + \lambda_\alpha^{(2)}(q_\alpha^A - q_\alpha) + \\ + \lambda_e^{(3)}(\sigma_e^A - Z_{e\beta}q_\beta) + \lambda_e^{(4)}(h_e - h_e^{MIN}) \,, \tag{2.15}$$

where symbols $\lambda_\alpha^{(1)}$, $\lambda_\alpha^{(2)}$, $\lambda_e^{(3)}$ and $\lambda_e^{(4)}$ describe the vectors included Lagrange's multipliers associated with the equilibrium conditions, displacement constraints, stress constraints and cross-sectional area limitations, respectively. Since the stiffness matrix is assumed to be positive definite and symmetric, if a unique solution of the problem represented by Eq. (2.15) can be obtained, then according to the Kuhn-Tucker and Fritz-John theorems there exist non-negative values of the Lagrange's multipliers $\lambda_\alpha^{(1)}$, $\lambda_\alpha^{(2)}$, $\lambda_e^{(3)}$ and $\lambda_e^{(4)}$, such that the necessary conditions for the minimum-weight problem are given by expressions

$$K_{\alpha\beta}q_\beta = f_\alpha \ , \tag{2.16}$$

$$K_{\alpha\beta}\lambda_\beta^{(1)} = \lambda_\alpha^{(2)} + \lambda_e^{(3)}Z_{e\alpha} \ , \tag{2.17}$$

$$l_e - \lambda_\alpha^{(1)}K_{\alpha\beta}^{,e}q_\beta + \lambda_d^{(3)}Z_{d\beta}^{,e}q_\beta - \lambda_e^{(4)} = 0_e \ , \tag{2.18}$$

$$q_\beta^\wedge - q_\beta = 0 \ , \tag{2.19}$$

$$\sigma_e^\wedge - Z_{e\beta}q_\beta = 0 \ , \tag{2.20}$$

$$h_e - h_e^{MIN} = 0 \ , \tag{2.21}$$

$$e,d = 1,\ldots,E \ , \qquad \alpha,\beta = 1,\ldots,N \ ,$$

where $K_{\alpha\beta}^{,e}$ and $Z_{d\beta}^{,e}$ are derivatives of the stiffness matrix and the displacement-stress relating matrix with respect to design variables.

It is seen that both the formulations of the static sensitivity problem (in the adjoint variable context, Section 2.2) as well as the minimum-weight problem are themselves applications of the Lagrange's multiplier technique. Also, we observe that formally Eqs. (2.16), (2.17) of the optimization analysis can be interpreted as the equilibrium conditions of the structural and adjoint systems represented by Eqs. (2.2), (2.7) in the sensitivity analysis. The only difference of the two pairs of equations is that loads acting on the adjoint structure in sensitivity analysis are derivatives of the state function with respect to design variables, whereas in optimization analysis the right hand sides are expressed in terms of the Lagrange's multipliers associated with the displacement and stress constraints and the displacement-stress relating matrix. Further, the second term involved in Eq. (2.18) is the expression used to evaluate the sensitivity gradient coefficients by the adjoint variable approach (cf. Eq. (2.8)), when the response functional is defined implicitly in terms of design variables and structure load is independent of these variables. Hence, Eq. (2.18) can be interpreted as a sensitivity residual measure of the discretized model in consideration and is chosen in [45] to check for convergence of the solution process. With the observations mentioned above, it is easy to see that the optimization problem can be directly solved for the design variables which render the cost function minimum by using a successive approximation technique and, namely by using the main routines for sensitivity analysis. Thus, given an arbitrary set of initial design variables the successive solution for each iteration proceeds as follows:

1) form and solve equilibrium equations for the nodal displacements and consequently, for the element stresses,

2) calculate the scale factor by using the expression

$$s^{(1)} = \max\left(\max\frac{|\,q_\beta\,|}{q_\beta^\wedge}, \max\frac{|\,\sigma_e\,|}{\sigma_e^\wedge}\right) \ , \qquad \textit{(no sum on } \beta, e) \tag{2.22}$$

scale design variables and displacements with the factor $s^{(1)}$

$$h_e := h_e \times s^{(1)} \ , \qquad q_\beta := q_\beta / s^{(1)} \ , \tag{2.23}$$

and check if the cross-section conditions are satisfied

$$h_e := h_e^{MIN} \qquad if \qquad h_e < h_e^{MIN} , \tag{2.24}$$

3) select $\lambda_\alpha^{(2)} \geq 0$, $\lambda_e^{(3)} \geq 0$ and $\lambda_e^{(4)} \geq 0$ by the trial-and-error technique [45] to fulfill equation

$$W = \lambda_\alpha^{(2)} q_\alpha^A + \lambda_e^{(3)} \sigma_e^A + \lambda_e^{(4)} h_e^{MIN} , \tag{2.25}$$

and check for convergence: the convergence norm is assumed to be relative difference of the cost function between the two successive iterations; the solution is terminated at this step if convergence is achieved, otherwise go to the next step,

4) calculate the right hand side, modify system stiffness matrix (if required) and solve Eq. (2.17) for the adjoint variables $\lambda_\beta^{(1)}$,

5) calculate the sensitivity residual vector from Eq. (2.18)

$$r_e = l_e - \lambda_\alpha^{(1)} K_{\alpha\beta}^e q_\beta + \lambda_d^{(3)} Z_{d\beta}^e q_\beta - \lambda_e^{(4)} , \tag{2.26}$$

and modify the design variables once more

$$a = (r_e^2 h_e^2)^{1/2} , \tag{2.27}$$

$$s_e^{(2)} := s_e^{(2)} (1_e + a r_e) , \qquad \textit{(no sum on e)} \tag{2.28}$$

$$h_e := h_e \gamma s_e^{(2)} , \qquad \textit{(no sum on e)} \tag{2.29}$$

where γ is the accelerating coefficient for iterations. The inherent disadvantage of the approach is that except for the adjoint variables $\lambda_\beta^{(1)}$ which can be determined by adjoint equations (2.17), it is difficult to select appropriate relations for $\lambda_\alpha^{(2)}$, $\lambda_e^{(3)}$ and $\lambda_e^{(4)}$. Note that the algorithm described above differs from the algorithm presented in [45] by assuming another convergence norm. By using the relative difference of the object function between two iterations (rather than the sensitivity residual norm) the iteration solution would be more stable and converge to a tolerance more rapidly. Numerically, the method is similar to the tangent stiffness method used in nonlinear continuum mechanics; and generally the global stiffness matrix must be modified twice at each solution step. However, in some cases the same system stiffness matrix generated at step 1) can be used for the structure system (Eq. (2.16)) as well as the adjoint system (Eq. (2.17)) to obtain acceptable results. Using the algorithms described above a new option based on the sensitivity analysis has been incorporated into the numerical code POLSAP to deal with problems of minimum-weight optimization design of trusses under the displacement, stress and cross-section constraints.

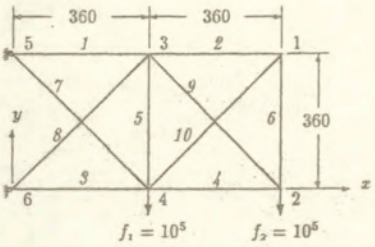

Figure 2.1: 10-element cantilever truss.

2.5 Numerical Results

In order to illustrate the preceding formulation and computer implementation consider some examples, which have been calculated on the IBM PC/AT microcomputer with 640KB of RAM and 80287-coprocessor.

Example 1 Fig. 2.1 shows the geometry and dimensions of a 10-element cantilever truss. This example is known as a well-known program-test in optimization analysis. Young modulus $E = 10^7$. The problem is to choose the most appropriate cross-section of each member of the truss considering the displacement response sensitivity with respect to the cross-sectional areas. The response functionals are assumed as the displacement limits at various degrees of freedom and stress limits at various elements and can be expressed as

$$\phi^{(q)} = \frac{|\, q_\alpha \,|}{q_\alpha^A} - 1 \le 0 \;, \qquad \phi^{(\sigma)} = \frac{|\, \sigma_{(\epsilon)} \,|}{\sigma_{(\epsilon)}^A} - 1 \le 0 \;,$$

where q_α and q_α^A, $q_\alpha^A > 0$, are the calculated and allowable values of the α-th displacement component, $\sigma_{(\epsilon)}$ and $\sigma_{(\epsilon)}^A$ are the calculated and allowable values of the ϵ-th element stress, respectively. Thus, the adjoint load vectors for the cases of displacement constraints and stress constraints take the form

$$\phi_{,\alpha}^{(q)} = \mathrm{sign}(q_\alpha)[\; 0 \ldots 0 \quad \frac{1}{q_\alpha^A} \quad 0 \ldots 0 \;] \;, \qquad \phi_{,\alpha}^{(\sigma)} = \frac{E_{(\epsilon)}}{l_{(\epsilon)}\sigma_{(\epsilon)}^A} \frac{dq_\alpha}{dh_{(\epsilon)}} \;,$$

where $E_{(\epsilon)}$ and $l_{(\epsilon)}$ are Young modulus and length of the ϵ-th element. With the displacement functional defined at node 2 in y-direction, $q_\alpha^A = 2.0$ and the stress functional defined at elements 5,7, $\sigma_{(\epsilon)}^A = 2.5 \times 10^4$ the computed values of coefficients of the sensitivity gradients are given in Table 2.1, and compared with results of [53]. It is seen that for the case of the displacement constraint a unit change in cross-sectional area of the element 5 has largest effect on the vertical displacement at node 2. To decrease the displacement most effectively, the cross-sectional area of the elements 2, 5, 6, 10 should be decreased and of the elements 1, 3, 4, 7, 8, 9 increased. The computation time was about 12 sec. for each case.

		Displacement Analysis		Stress Analysis	
El.	Area	Haug	POLSAP	Haug	POLSAP
1	28.6	-0.0093	-9.28360248d-03	0.0082	8.19707762d-03
2	0.2	0.0109	1.08976076d-02	-0.0696	- 6.95800321d-02
3	23.6	-0.0062	-6.20279631d-03	-0.0104	- 1.04232459d-02
4	15.4	-0.0076	-7.63222800d-03	-0.0006	- 6.58796546d-04
5	0.2	0.1402	1.40233017d-01	-2.3520	- 2.35206279d-00
6	0.2	0.0109	1.08976076d-02	-0.0696	- 6.69574935d-02
7	3.0	-0.0177	-1.77427793d-02	-0.8369	- 8.36972324d-01
8	21.0	-0.0128	-1.27751763d-02	0.0231	2.30863275d-02
9	21.8	-0.0108	-1.07727054d-02	-0.0009	- 8.99234187d-04
10	0.2	0.0308	3.08230891d-02	-0.1968	- 1.96789653d-01

Table 2.1: Displacement and stress sensitivity of 10-element truss.

Example 2 Consider the displacement and rotation responses of the clamped-clamped beam of unit length under load $(f + wh)$, where the following data were adopted: uniformly distributed load $f = 49.61$ per unit length, cross-sectional area $h = 0.005$, weight density $w = 77.126$ per unit volume, Young modulus $E = 2.0 \times 10^5$, Poisson ratio $\nu = 0.3$, moments of inertia $I_x = I_y = \alpha h^2$ with $\alpha = 1/6$, cf. Fig. 2.2a. As the design variable we take the cross-section whereas the response functional is defined as follows

$$\phi = \int_0^1 \delta(x - x^*) y(x)\, dx \ ,$$

where δ is the Dirac delta function. Interpreting the function as a unit load applied at $x = 0.5$, the adjoint beam is subjected to a positive unit concentrated load at x^* for the case of the displacement response analysis and to a positive unit moment at x^* for the case of the rotation response analysis. The two cases are computed simultaneously using a model including 100 finite elements. The computation time was 81 sec. The POLSAP's result given in Table 2.2 is compared with analytical solution [53] and shown in Fig. 2.2. Fig. 2.2b indicates how material should be preferably added or removed to decrease the vertical displacement at the mid-point. Material should be added near $x = 0.0$ and $x = 1.0$ and deleted at $x = 0.22$ and $x = 0.78$ to decrease displacement at the center most effectively. For the rotation function Fig. 2.2c shows that if material is added or removed symmetrically with respect to $x = 0.5$ then the slope remains zero. Removing the material to the left of $x = 0.5$ decreases the slope, while removing it to the right has the reverse effect.

Example 3 To account for the effect of variation of plate thickness on the displacement response at a discrete point of plates, consider a clamped square plate of unit dimension and of uniform thickness $h = 0.05$, with $E = 2.0 \times 10^5$, $\nu = 0.3$ and uniformly distributed load $(f + wh)$, $f = 22.2$ per unit area, weight density $w = 77.1$ per unit volume. A quarter of the plate is considered with a model including 100

X	Displ. Analysis	Rot. Analysis
0.0	-2.39934037d-01	4.75022437d-01
0.1	-7.57817895d-02	1.05182598d-01
0.2	-3.26120603d-03	-4.90013489d-03
0.3	-1.12741956d-02	9.63420713d-02
0.4	-6.34898231d-02	2.99916411d-01
0.5	-1.23577153d-01	4.96830080d-01
0.6	-6.34898231d-02	-2.99916411d-01
0.7	-1.12741956d-02	-9.63420713d-02
0.8	-3.26120603d-03	4.90013489d-03
0.9	-7.57817895d-02	-1.05182598d-01
1.0	-2.39934037d-01	-4.75022437d-01

Table 2.2: Displacement and rotation sensitivity of 100-element beam.

finite elements and 460 degrees of freedom. If displacement response at the center of the plate is considered, that is if

$$\phi = \int_\Omega \delta(x - x^*) z(x)\, d\Omega \ ,$$

then the adjoint load is just a unit concentrated load at the center. The computed result (see Fig. 2.3) shows that the local extrema of the sensitivity gradient occur at the center elements and the elements near the middle of the four edges. The minimum value of $\partial\phi/\partial h$ is -1.173×10^{-3} (vs. -1.167×10^{-3} in [53]) at the corner elements, the maximum of $\partial\phi/\partial h$ is -4.278×10^{-6} (vs. -3.164×10^{-6} in [53]). It may be noticed that to decrease the deflection at the center of the plate most effectively, material should be removed near the four corners and added at the center. The computation time was 467 sec.

Example 4 Consider the truss-beam-plate structure shown in Fig. 2.4. Thin flat plates are stiffened by longitudinal and transverse beams and the entire structure is supported by four of four-bar trusses. A uniformly distributed vertical load is applied to the plates. The structural response functionals are given similarly to the above example. The design variables for this complex structure are thickness for the plates and cross-sectional area for beams and trusses. Input data are: $E = 3.0 \times 10^7$, $\nu = 0.3$, $L_x \times L_y = 15 \times 15$, beam spacing is 3, truss cross-sectional area $A = 0.1$ and length $l = 5.346$, beam cross-sectional area $b \times h = 0.15 \times 0.5$, plate uniform thickness $t = 0.1$, distributed load $f = 1.0$ per unit area. Due to symmetry only one quarter of the structure is considered. The finite element mesh includes 100 rectangular plate elements, 40 beam elements and 4 truss elements and total number of degrees of freedom is 561. Table 2.3 gives the sensitivity gradient values for the analysis. The computation time was 497 sec.

Example 5 Consider minimum-weight optimization design of the 10-element cantilever truss whose dimensions and finite element model are given in Fig. 2.1. The

Truss							
1	-7.45131d-05	2	-7.45131d-05	3	-7.45131d-05	4	-7.45131d-05
Beam							
1	-1.19435d-02	11	-9.09208d-03	21	-6.86874d-06	31	-4.39387d-07
2	-1.11915d-02	12	-6.38932d-03	23	-5.06162d-05	33	-3.93060d-05
4	-2.65098d-03	14	-1.04476d-03	25	2.00890d-04	35	8.58583d-04
6	8.58583d-04	16	2.00890d-04	27	-1.04476d-03	37	-2.65098d-03
8	-3.93060d-05	18	-5.06162d-05	29	-6.38932d-03	39	-1.11915d-02
10	-4.39387d-07	20	-6.86874d-06	30	-9.09208d-03	40	-1.19435d-02
Plate							
1	1.27987d-01	21	2.75473d-00	52	7.88902d-00	81	15.8486d-00
2	-6.38389d-02	23	1.44330d-00	54	4.49230d-00	83	12.5180d-00
3	-3.08105d-01	25	2.38565d-01	56	1.36198d-00	85	7.88902d-00
4	-2.76982d-01	27	1.00636d-00	58	2.38565d-01	87	3.76016d-00
5	2.80716d-01	29	2.69089d-00	60	2.80716d-01	89	9.90840d-01
6	1.44309d-00	32	3.76016d-00	61	11.2312d-00	91	19.3150d-00
7	2.74439d-00	34	1.46938d-00	63	8.54175d-00	92	15.8486d-00
8	3.79016d-00	36	2.64045d-01	65	4.49230d-00	93	13.4615d-00
9	4.83372d-00	38	1.00636d-00	67	1.46938d-00	94	11.2312d-00
10	6.00905d-00	40	2.74439d-00	69	8.36124d-02	95	8.80431d-00
12	9.90840d-01	41	6.42468d-00	72	12.5180d-00	96	6.42468d-00
14	8.36124d-02	43	4.29904d-00	74	8.54175d-00	97	4.38064d-00
16	8.14239d-01	45	1.36198d-00	76	4.29904d-00	98	2.75473d-00
18	2.69089d-00	47	2.64045d-01	78	1.44329d-00	99	1.34394d-00
20	4.83372d-00	49	8.14239d-01	80	-3.08105d-01	100	1.27988d-01

Table 2.3: Truss-beam-plate structure. Displacement sensitivity.

displacement constraints are the same for all degrees of freedom with the limit equal to 2.0. The stress constraints are also the same for all members and the allowable value is 2.5×10^4. None of cross-sectional areas can be smaller than 0.1. Young modulus $E = 10^7$. Initial cross-sectional areas are arbitrarily assumed as 31.0, 0.15, 22.0, 14.15, 0.15, 0.98, 8.59, 22.0, 22.9, 0.15, respectively. Fig. 2.5 shows the dependence of the minimum-weight versus the number of iterations corresponding to five different values of the accelerating coefficient γ. The computation time was 12 sec. The minimum-weight (5024) converged within the tolerance of 10^{-3} after 11 iterations. In terms of computed minimum-weight value as well as number of iterations the solution obtained by POLSAP is better than the solutions presented in [36,45,52]. It is noted that the iteration process would be unstable when $\gamma \geq 0.36$ for the problem.

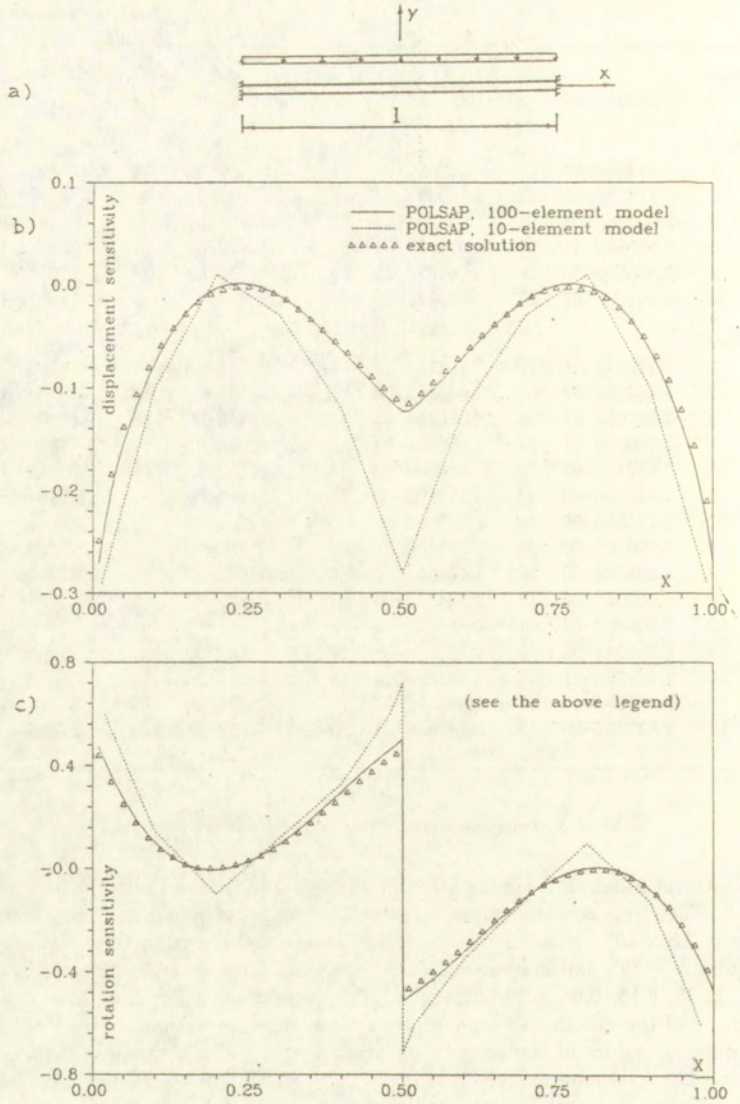

Figure 2.2: Clamped beam. Displacement and rotation sensitivity.

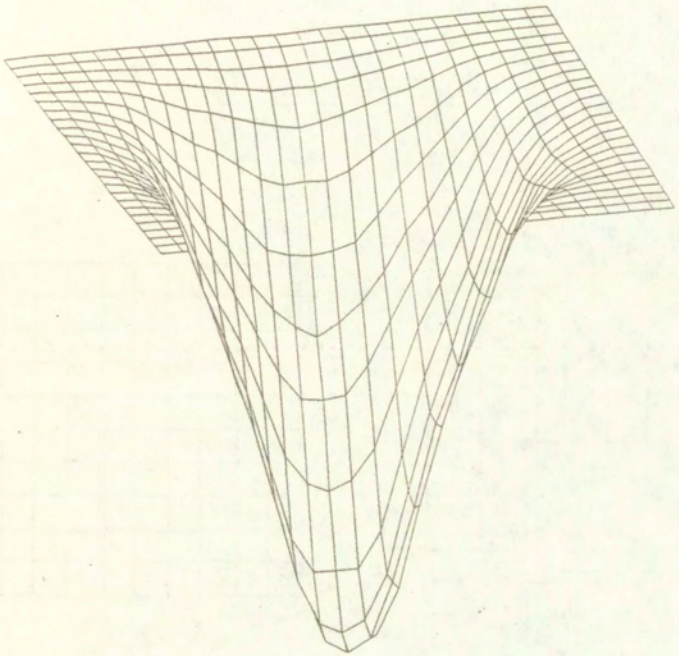

Figure 2.3: Static sensitivity of clamped square plate.

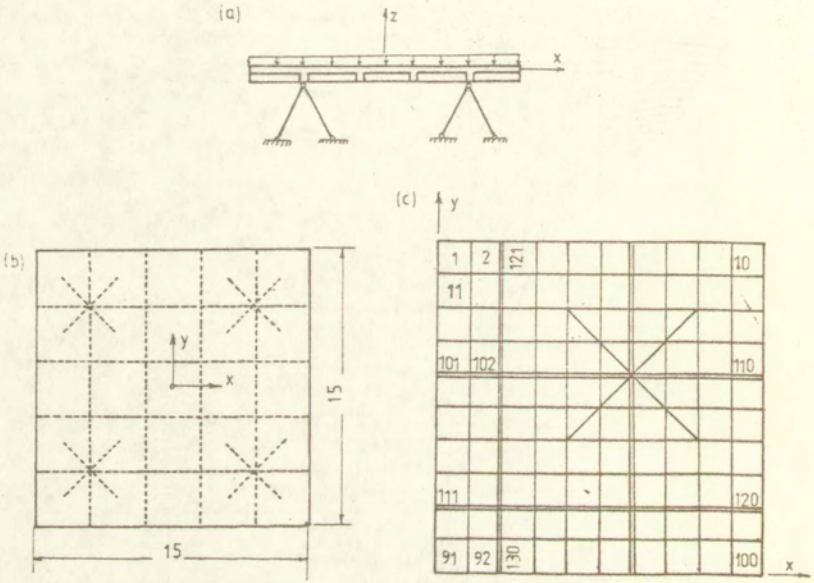

Figure 2.4: Truss-beam-plate structure. a) Side view. b) Top view. c) Finite element model.

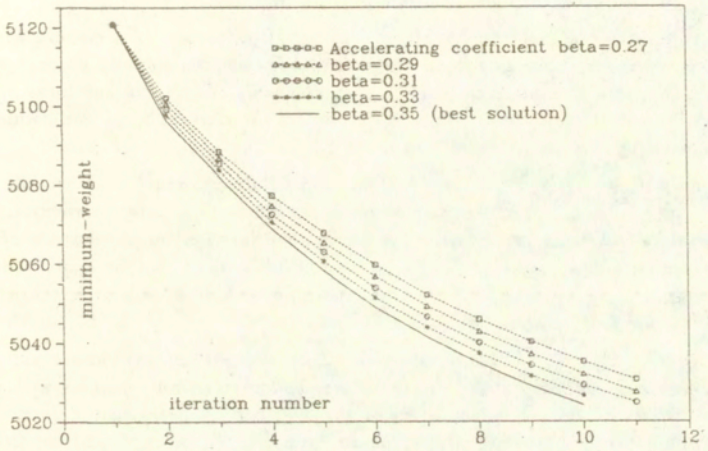

Figure 2.5: 10-element truss. Minimum-weight optimization.

Summarizing Remarks

In the foregoing chapter the finite element formulation for structural design sensitivity problems in statics was described. The computational aspects of both the direct differentiation and adjoint variable approaches were compared and discussed in detail. It can be shown that in the preliminary design problems the direct differentiation method is preferred. However, in general the adjoint variable method should be much more efficient.

Depending on the existing finite element code the design derivative matrices can be generated alternatively explicitly or implicitly. Computational methods with implicitly generated finite elements, however, have not yet been fully investigated and require future work due to increasing use of such elements.

The computational cost can be reduced significantly since only the global stiffness matrix has to be assembled and factorized and both the equilibrium and adjoint equations can be solved simultaneously. Moreover, because almost all calculations of the sensitivity gradient coefficients can be performed at the element level, the computation time spent for sensitivity analysis is only a fraction of the total cost.

It should be emphasized that the sensitivity computation is much more sensitive to finite element mesh than that for displacement-stress analysis, since mathematically the sensitivity gradients are bilinear functions of generalized displacements of the original and adjoint structures. That is, a good finite element grid for displacement-stress analysis may become too coarse for sensitivity analysis. In design sensitivity analysis a finer finite element mesh is required.

An effective algorithm based on standard finite element software and sensitivity analysis has been worked out for minimum-weight optimization problems with various constraints of displacements, stresses and member geometry parameters. The disadvantages of the approach used in the analysis are: 1) the sufficient conditions for the minimum weight are not verified; 2) appropriate selection of the Lagrange's multipliers is not easy; and 3) iteration stability depends to a large degree on the accelerating coefficient which is problem-dependent.

The numerical algorithms developed for sensitivity analysis and minimum-weight optimization problems can readily be adapted to existing finite element programs with no considerable modifications required. The numerical results obtained with the code POLSAP show that its static sensitivity and minimum-weight optimization options seem to offer reliable and cost-effective alternatives in research and application environments.

3 Structural Sensitivity Problem for Dynamic Response

3.1 Scope of the Chapter

In the preceding chapter the finite element formulation and computational implementation of structural design sensitivity problems have been considered for deterministic problems of statics response, i.e. for systems whose inertial and damping effects are negligible. If initial conditions are to be imposed, loads are time-varying and damping terms must be included the response is time-dependent and the structural sensitivity problem must be treated in the context of dynamic systems. In contrast to the massive literature on sensitivity and optimization of dynamic control systems, dynamic sensitivity applications to deformable bodies have had little attention and essentially focused on distributed parameter systems, [51,53]. Some recent developments [32,88,120] provided the preliminary mathematical basis for dynamic sensitivity analysis of structures. In terms of the computational implementation the state-of-the-art structural sensitivity analysis and effective numerical codes available to deal with this class of problems are scarce, [53,60]. In general, the considerations are restricted to analyze the sensitivity response over a time domain; and a numerical formulation for problems of the sensitivity response at any time instant in which the constraint functional must hold for all times up to the time instant of interes seems to be non-existent. This chapter is thus concerned with the finite element formulation and computational aspects of structural design sensitivity for dynamic systems. Similarly to the static sensitivity analysis considerations are restricted in this chapter to the deterministic, linear-elastic systems. The state variable is assumed as a finite-dimensional vector of nodal displacements or element stresses, and the design variable is a finite-dimensional vector of design parameters, such as cross-sectional area, length, thickness, Young modulus or mass density of structural members. In the finite element context the state equations are matrix differential equations with design variables involved in the mass, damping and stiffness matrices and time-varying load vector. The problem is formulated by using the adjoint variable approach, which is shown to be preferable over the direct differentiation method for dynamic sensitivity problems, particularly when the deterministic system is treated as a special case of stochastic systems considered in Part 2. Computational aspects of both the direct step-by-step integration and mode superposition are discussed. An alternative form of the constraint functional that holds for all times is proposed to consider the time response of dynamic sensitivity. The problem of sensitivity response at any time instant is formulated by using the mode superposition technique leading to the analysis of the time response

of an adjoint system excited by a unit impulse or a unit terminal velocity. Basing on the solution of free vibrations of a conservative system the problem of eigenvalue sensitivity is considered. A version of the deterministic analysis of the dynamic sensitivity has been worked out and adapted to the microcomputer finite element code POLSAP. Examples include dynamic sensitivity analysis of a frame and of a truss-beam-plate structure.

MODEL PROBLEM OF CHAPTER 3

Given
- vector of design variables $h(x)$, x - spatial coordinates (for example: cross-sectional area, thickness, length, Young modulus)
- response functional $\phi(x,h,t)$ (for example: object function, displacement or stress constraint function)
- displacement-expressed finite element equations of motion $F(x,h,t)=0$
- terminal time condition $T(h)=0$

Find
- time-dependent gradient of response functional ϕ with respect to design variables h

3.2 Finite Element Formulation

3.2.1 Dynamic Sensitivity over Time Domain (o.t.d.)

Consider structural response of the linear-elastic system with N degrees of freedom described by an integral functional

$$\phi = \int_0^{T(h)} G[q(h,t),h]\,dt \ , \tag{3.1}$$

where the vector of nodal displacements $q = \{q_\beta(h,t)\}$, $\beta = 1,\dots,N$ is an implicit function of design variables $h = \{h^e\}$, $e = 1,\dots,E$. Symbol t, $t \in [0,T(h)]$, denotes time variable and $T(h)$ represents the terminal time determined uniquely by so called the terminal-time condition, [53]

$$\mathcal{T}[q(T),\dot{q}(T),h] = 0 \ . \tag{3.2}$$

The system satisfies the equations of motion expressed in the finite element model (cf. Eq. (1.17))

$$M_{\alpha\beta}(h)\ddot{q}_\beta(h,t) + D_{\alpha\beta}(h)\dot{q}_\beta(h,t) + K_{\alpha\beta}(h)q_\beta(h,t) = f_\alpha(h,t) \ , \tag{3.3}$$

$$q_\beta(h,0) = , \qquad \dot{q}_\beta(h,0) = 0 \ , \qquad \alpha,\beta = 1,\dots,N \ , \tag{3.4}$$

where $M_{\alpha\beta}(h)$, $D_{\alpha\beta}(h)$, $K_{\alpha\beta}(h)$ and $f_\alpha(h,t)$, $\alpha,\beta = 1,\dots,N$, are the mass, damping, stiffness matrices and the nodal load vector, respectively. The objective of dynamic analysis of deterministic design sensitivity is to evaluate the change in the structural response functional of Eq. (3.1) with the constraints of Eqs. (3.2),(3.3),(3.4) to

design variations, i.e. to determine the time-dependent sensitivity gradient of this functional with respect to design variables.

It is shown [47] that if the functions of the mass, damping, stiffness matrices and load vector are S times continuously differentiable with respect to h^ϵ and if the mass matrix is nonsingular, then the displacement, velocity and acceleration functions are S times continuously differentiable with respect to h^ϵ, [22]. This guarantees the dynamic response of the structural system to be as smooth as the dependence on design variables in the equations of motion. Differentiation of Eq. (3.1) with respect to design variables using Leibnitz's rule [130] reads

$$\phi^{,\epsilon} = G(T)T^{,\epsilon} + \int_0^T [G^{,\epsilon}(t) + G_{,\beta}(t)q_\beta^{,\epsilon}(t)]\,dt \ , \tag{3.5}$$

where symbols $(.)^{,\epsilon}$ and $(.)_{,\beta}$, as defined above in Section 2.2, are the first partial derivatives with respect to design variables and nodal displacements. The first term appearing on the right hand side of Eq. (3.5) involves the derivative of T with respect to design variables, since the terminal-time condition expressed by Eq. (3.2) used to evaluate T is design-dependent. In order to express $\phi^{,\epsilon}$ implicitly in terms of the derivative term, taking the derivative of Eq. (3.2) with respect to design variables h^ϵ by the chain rule leads to

$$\mathcal{T}^{,\epsilon} + \mathcal{T}_{,\beta}[q_\beta^{,\epsilon}(T) + \dot{q}_\beta(T)T^{,\epsilon}] + \frac{\partial \mathcal{T}}{\partial \dot{q}_\beta}[\dot{q}_\beta^{,\epsilon}(T) + \ddot{q}_\beta(T)T^{,\epsilon}] = 0^\epsilon. \tag{3.6}$$

Note that by the definition of the terminal-time condition T is determined uniquely if the following condition is satisfied

$$\dot{\mathcal{T}} \equiv \mathcal{T}_{,\beta}\dot{q}_\beta(T) + \frac{\partial \mathcal{T}}{\partial \dot{q}_\beta}\ddot{q}_\beta(T) \neq 0 \ . \tag{3.7}$$

Hence Eq. (3.6) can be rewritten in terms of $T^{,\epsilon}$ as

$$T^{,\epsilon} = -\frac{1}{\dot{\mathcal{T}}}[\mathcal{T}^{,\epsilon} + \mathcal{T}_{,\beta}q_\beta^{,\epsilon}(T) + \frac{\partial \mathcal{T}}{\partial \dot{q}_\beta}\dot{q}_\beta^{,\epsilon}(T)] \ , \tag{3.8}$$

and consequently, Eq. (3.5) takes the form

$$\phi^{,\epsilon} = -\frac{G}{\dot{\mathcal{T}}}(T)[\mathcal{T}^{,\epsilon} + \mathcal{T}_{,\beta}q_\beta^{,\epsilon}(T) + \frac{\partial \mathcal{T}}{\partial \dot{q}_\beta}\dot{q}_\beta^{,\epsilon}(T)] + \int_0^T [G^{,\epsilon}(t) + G_{,\beta}(t)q_\beta^{,\epsilon}(t)]\,dt \ . \tag{3.9}$$

To express the foregoing equation explicitly in terms of variations in design variables, i.e. to eliminate the terms involving $q_\beta^{,\epsilon}$ and $\dot{q}_\beta^{,\epsilon}$ the adjoint variable technique can be used. We define an adjoint vector $\lambda = \{\lambda_\alpha(t)\}$, $\alpha = 1, \ldots, N$, which is taken to be independent of design variables. Differentiating both sides of Eq.(3.3) with respect to design variables, premultiplying all terms of the resulting equation by the adjoint vector λ_α, integrating over the time domain from 0 to T and integrating by

parts with respect to time variable t the first two terms involving $\dot{q}_\beta^s$ and $\tilde{q}_\beta^s$ and noting that the mass, damping and stiffness matrices are symmetric, yields

$$M_{\alpha\beta}\lambda_\alpha \dot{q}_\beta^s(T) - (M_{\alpha\beta}\dot{\lambda}_\alpha - D_{\alpha\beta}\lambda_\alpha)q_\beta^s(T) + \int_0^T (M_{\alpha\beta}\ddot{\lambda}_\alpha - D_{\alpha\beta}\dot{\lambda}_\alpha + K_{\alpha\beta}\lambda_\alpha)q_\beta^s\, dt = \\ = \int_0^T \lambda_\alpha (f_\alpha^s - M_{\alpha\beta}^s \tilde{q}_\beta - D_{\alpha\beta}^s \dot{q}_\beta - K_{\alpha\beta}^s q_\beta)\, dt \ . \qquad (3.10)$$

Because Eq. (3.10) must hold for arbitrary λ_α, the adjoint variables can be chosen so that the coefficients of terms involving q_β^s and $\dot{q}_\beta^s$ in Eq. (3.9) and Eq. (3.10) are equal, leading to the differential equations of motion of the adjoint system (cf. Eq. (3.3))

$$M_{\alpha\beta}(h)\ddot{\lambda}_\beta(t) - D_{\alpha\beta}(h)\dot{\lambda}_\beta(t) + K_{\alpha\beta}(h)\lambda_\beta(t) = G_\alpha(h,t)\,, \qquad t \in [0,T]\,, \qquad (3.11)$$

with the terminal conditions for the adjoint displacements and velocities at time T

$$M_{\alpha\beta}(h)\lambda_\beta(T) = -\frac{G(T,h)}{\dot{T}}\frac{\partial T}{\partial \dot{q}_\alpha}\,, \qquad (3.12)$$

$$M_{\alpha\beta}(h)\dot{\lambda}_\beta(T) = D_{\alpha\beta}(h)\lambda_\beta(T) + \frac{G(T,h)}{\dot{T}}T_{,\alpha}\ . \qquad (3.13)$$

Equations (3.11)–(3.13) are known as the terminal problem. The system of Eqs. (3.3),(3.4) and Eqs. (3.11)–(3.13) form the initial-terminal problem that gives a unique solution for the state and design variables of dynamic response sensitivity analysis in the time domain form 0 to T. Finally, introducing Eqs. (3.11)–(3.13) into Eq. (3.10) and substituting the result in Eq. (3.9) yields the sensitivity gradient coefficients for the general dynamic problem as

$$\phi^{,s} = -\frac{G(T)}{\dot{T}}T^{,s} + \int_0^T G^{,s}(t)\, dt + \\ + \int_0^T \lambda_\alpha (f_\alpha^s - M_{\alpha\beta}^s \tilde{q}_\beta - D_{\alpha\beta}^s \dot{q}_\beta - K_{\alpha\beta}^s q_\beta)\, dt \ . \qquad (3.14)$$

3.2.2 Dynamic Sensitivity at Particular Time Instants (a.t.i.)

In preceding paragraph the sensitivity problem has been formulated for the o.t.d. case; and the sensitivity gradient coefficients could not be evaluated at any time instant in the time domain. In order to consider the structural response functional that must hold for all times, i.e. to consider the time response of sensitivity, assuming that the terminal-time condition of Eq. (3.2) can be expressed in an explicit form with respect to the terminal time T the structural response functional given by Eq. (3.1) can be redefined in terms of a convolution of a signal sequence such as

$$\phi = \int_0^\infty G[q(h,t^*),h]\delta(t-t^*)\, dt^* = \int_0^t G[q(h,t-t^*),h]\delta(t^*)\, dt^*\,, \qquad (3.15)$$

$$t^* \in [0,t], \qquad t \in [0,T]\,,$$

where the symbols t^* and t denote a dummy variable of integration and the running terminal time, and $\delta(t^*)$ is a Dirac delta measure. Note that $\delta(t^*)$ is an even distribution. The function $G(t^*)$ is assumed to be continuous in the entire time domain $[0,T]$. Eq. (3.15) can be interpreted as a linear combination of shifted unit impulses, wherein the weight on the unit impulse $\delta(t-t^*)$ is $G(t^*)dt^*$. Observing that

$$G(t-t^*)\delta(t^*) = G(t)\delta(t^*) \ , \tag{3.16}$$

since $\delta(t^*)$ is the limit as $\Delta \to 0$ of $\delta_\Delta(t^*)$ (Δ - Dirac time interval) and using the similar derivation as above in Section 3.2.1 the terminal problem can be written as

$$M_{\alpha\beta}\ddot{\lambda}_\beta(\tau) - D_{\alpha\beta}\dot{\lambda}_\beta(\tau) + K_{\alpha\beta}\lambda_\beta(\tau) = G_{.\alpha}(t)\delta(\tau) \ , \tag{3.17}$$

with the running terminal conditions

$$\lambda_\beta(\tau = t) = 0 \ , \qquad \dot{\lambda}_\beta(\tau = t) = 0 \ , \tag{3.18}$$

$$\tau \in [t,0] \ , \qquad \alpha,\beta = 1,\ldots,N \ .$$

Having solved Eqs. (3.3),(3.17) we may obtain

$$\phi^*(t) = G^*(t) + \int_0^t \lambda_\alpha(t^*)[f_\alpha^*(t^*) - M_{\alpha\beta}^*\ddot{q}_\beta(t^*) - D_{\alpha\beta}^*\dot{q}_\beta(t^*) - K_{\alpha\beta}^*q_\beta(t^*)]\,dt^* \ , \tag{3.19}$$

$$t^* \in [0,t] \ , \qquad t \in [0,T] \ .$$

3.2.3 Eigenvalue Sensitivity

It is known that the natural frequencies of free vibrations and buckling loads can be treated as eigenvalues of some generalized eigenproblems. Since the structural mass and stiffness are design-dependent the eigenvalues and associated eigenvectors are functions of design variables. This paragraph is devoted to this problem under the assumptions that the structural system considered is conservative and the mass and stiffness matrices are well-conditioned in the finite element context so that no repeated eigenvalues occur. Let us consider the structural design sensitivity problem of natural frequencies (or buckling load factors in structural stability analysis) as a special case of the dynamic system described in Eqs. (3.1)-(3.4), when the damping terms, nodal load vector and initial-terminal time conditions are neglected. The general response functional given by Eq. (3.1) reduces to

$$\phi = \Omega_{(\alpha)}(h) \ , \tag{3.20}$$

with the constraint in terms of free vibration equations of the dynamic problem

$$K_{\alpha\eta}(h)Q_{\eta\beta}(h) = \Omega_{(\alpha)}(h)M_{\alpha\eta}(h)Q_{\eta\beta}(h) \ , \qquad \alpha,\beta,\eta = 1,\ldots,N \ . \tag{3.21}$$

Eigenvalues $\Omega_{(\alpha)}$ and eigenvectors $Q_{\eta\beta}$ are thus sought such that the nodal displacements q_β are harmonic. For the buckling problems $M_{\alpha\eta}(h)$ represents the geometric (initial stress) stiffness matrix.

It can be shown [53] that if the mass (geometric stiffness) and stiffness matrices are positive definite, symmetric and continuously differentiable with respect to design variables and if an eigenvalue $\Omega_{(\alpha)}$ is not repeated, then the eigenvalue and corresponding eigenvector of Eq. (3.21) are continuously differentiable with respect to the design variables. Taking differentiation of Eq. (3.21) with respect to design variables and premultiplying the resulting equation by the transposed eigenvector matrix $Q_{\beta\eta}$ we obtain

$$\Omega^{,e}_{(\alpha)} M_{\alpha\eta} Q_{\eta\mu} Q_{\mu\beta} = (K^{,e}_{\alpha\eta} - \Omega_{(\alpha)} M^{,e}_{\alpha\eta}) Q_{\eta\mu} Q_{\mu\beta} + (K_{\alpha\eta} Q_{\eta\mu} - \Omega_{(\alpha)} M_{\alpha\eta} Q_{\eta\mu}) Q_{\mu\beta} \ . \quad (3.22)$$

Note that the second term of the right hand side of Eq. (3.22) is zero according to the definition of the free vibration problem of Eq. (3.21). Using the orthonormalization condition (cf. Eq. $(1.35)_1$, Section 1.4.2) for eigenvectors the expression for sensitivity of the α-th eigenvalue reads

$$\Omega^{,e}_{(\alpha)} = (K^{,e}_{\alpha\eta} - \Omega_{(\alpha)} M^{,e}_{\alpha\eta}) Q_{\eta\mu} Q_{\mu\beta} \ . \quad (3.23)$$

3.3 Computational Implementation

For the case of the o.t.d. sensitivity the computation process proceeds as follows:

1) given a vector of design variables Eq. (3.3) is integrated forward with respect to time t to monitor the value of $\mathcal{T}[q(T), \dot{q}(T), h]$. The instant at which Eq. (3.2) satisfied is defined as the terminal time T; and the quantities q_β, $\dot{q}_\beta$, $\partial\mathcal{T}/\partial q_\beta$ and $\partial\mathcal{T}/\partial\dot{q}_\beta$ can be calculated,

2) Eqs. (3.12),(3.13) are used to evaluate the terminal conditions for the adjoint displacements $\lambda_\alpha(T)$ and adjoint velocities $\dot{\lambda}_\alpha(T)$. Thus, the adjoint terminal problem given by Eqs. (3.11)–(3.13) is in a closed form and can be integrated backward with respect to time from T to 0, yielding a unique solution for $\lambda_\alpha(t)$

3) once the initial-terminal problem is alternatively solved by a step-by-step direct integration method or the mode superposition, the design sensitivity gradient coefficients expressed by Eq. (3.14) can be computed by a numerical integration formula, [8].

Note that above procedures are applicable to the most general case. In many situations the structural damping effects are negligible or can be approximated as a linear combination of the mass and stiffness coefficients (cf. Section 1.4.2). Moreover, the terminal conditions are frequently given explicitly with respect to the final time T and then an essential computational advantage arises when using the mode superposition method for sensitivity analysis.

In principle, for the case of the a.t.i. sensitivity the following calculation steps must be carried out:

1) integrate Eq. (3.3) forward with respect to time from 0 to t,

2) calculate the terminal conditions at running time t by Eq. (3-17), form the right hand side of Eq. (3.17) and integrate these equations backward with respect to time from t to 0,

3) evaluate the design sensitivity gradients at t by Eq. (3.19),

4) the process 1)–3) has to be repeated for all time instants t, $t \in [0, T]$.

The computation cost would be unacceptable high (especially by using the direct integration technique, which has to deal with all the degrees of freedom of the system under consideration), since Eqs. (3.3),(3.17),(3.19) are generally integrated numerically by the step-by-step techniques, and integration of Eqs. (3.17),(3.18) must be performed over $n(n+1)/2$ time increments $\Delta\tau$, $n = T/\Delta\tau$. However, we observe that the state operators involved in the initial-terminal system of Eqs. (3.3),(3.17) are linear operators, the initial conditions of the structural equations are zero and the running terminal conditions of the adjoint equations are also zero at any time t. This observation enables us to develop an effective procedure such that the adjoint system of Eqs. (3.17) can be integrated backward only once from T to 0 over n time increments. As will be shown below, the response of the adjoint system can be treated through the unit impulse response of a normalized structural system whose state operators being functions of the structural mass, damping and stiffness are independent of $G(t)$ and t.

In general, the multi-degree-of-freedom system (3.17) cannot be solved in a straightforward manner. This is so because the right hand side is not an ordinary function of time τ in the sense that the Dirac delta function is defined in terms of its properties rather than its values, and the generalized coordinates on the left hand side are coupled. To overcome these difficulties let us first use in Eq. (3.17) (and similarly in Eq. (3.3)) a transformation from the generalized coordinates $\lambda_\beta(\tau)$ to the normalized coordinates $\vartheta_z(\tau)$, $z = 1, \ldots, Z \ll N$, through the normalized mode shapes $Q_{z\beta}$, frequencies ω_z and damping factors ξ_z of Rayleigh's type in order to get the system of Z uncoupled equations of the form

$$\ddot{\vartheta}_z(\tau) - 2\xi_z\omega_z\dot{\vartheta}_z(\tau) + \omega_z^2\vartheta_z(\tau) = Q_{z\beta}G_{\beta}(t)\delta(\tau) \ , \qquad \textit{(no sum on } z\textit{)} \tag{3.24}$$

$$\vartheta_z(t) = 0 \ , \qquad \dot{\vartheta}_z(t) = 0 \ ,$$

where

$$\vartheta_z(\tau) = Q_{z\beta}\lambda_\beta(\tau) \ , \qquad z = 1, \ldots, Z \ , \qquad \beta = 1, \ldots, N \ , \tag{3.25}$$

Interpreting the z-th independent adjoint equation of Eq. (3.24) as a linear system excited by an impulse of fixed magnitude $Q_{z\beta}G_\beta$ at time t let us now consider the response of the system to the unit impulse excitation $\delta(\tau)$ in the adjoint time domain $[t, 0]$ that is

$$\ddot{\vartheta}_z(\tau) - 2\xi_z\omega_z\dot{\vartheta}_z(\tau) + \omega_z^2\vartheta_z(\tau) = \delta(\tau) \ , \qquad \textit{(no sum on } z\textit{)} \tag{3.26}$$

$$\vartheta_z(t) = 0 \ , \qquad \dot{\vartheta}_z(t) = 0 \ .$$

Recognizing that the terminal conditions $(3.26)_2$ are zero, both sides of the Eq. $(3.26)_1$ can be integrated with respect to time over the interval $\Delta\tau = \varepsilon$ to obtain

$$\lim_{\varepsilon\to 0}\int_t^{t-\varepsilon}[\ddot{\vartheta}_z(\tau) - 2\xi_z\omega_z\dot{\vartheta}_z(\tau) + \omega_z^2\vartheta_z(\tau)]\,d\tau = \lim_{\varepsilon\to 0}\int_t^{t-\varepsilon}\delta(\tau)\,d\tau = 1\ , \tag{3.27}$$

where

$$\lim_{\varepsilon\to 0}\int_t^{t-\varepsilon}\ddot{\vartheta}_z(\tau)\,d\tau = \lim_{\varepsilon\to 0}[\dot{\vartheta}_z(t-\varepsilon) - \dot{\vartheta}_z(t)] = \dot{\vartheta}_z(t-)\ , \tag{3.28}$$

$$\lim_{\varepsilon\to 0}\int_t^{t-\varepsilon}\dot{\vartheta}_z(\tau)\,d\tau = \lim_{\varepsilon\to 0}[\vartheta_z(t-\varepsilon) - \vartheta_z(t)] = 0\ , \tag{3.29}$$

$$\lim_{\varepsilon\to 0}\int_t^{t-\varepsilon}\vartheta_z(\tau)\,d\tau = 0\ , \tag{3.30}$$

and consequently

$$\dot{\vartheta}_z(t-) = 1\ . \tag{3.31}$$

The notation $\dot{\vartheta}_z(t-)$ is referred to as a change in velocity at the end of the time increment $\Delta\tau = \varepsilon$. Noting that τ is the backward time variable the foregoing identity can be given the following interpretation. Immediately after a unit impulse excitation the unit mass gains a momentum of unit magnitude, but there is still no time for an instantaneous change in the normalized displacement; thereafter the system is left without excitation. Since the normalized system is at rest immediately prior to the excitation, an instantaneous increment in the normalized velocity appears so that the unit impulse excitation applied at t can be regarded as the equivalent of the unit terminal velocity. In fact this is the way in which initial velocities are imparted to systems possessing inertia [90,112]. In view of this interpretation the response to a unit impulse excitation described by Eq. (3.26) can be expressed as

$$\ddot{\vartheta}_z(\tau) - 2\xi_z\omega_z\dot{\vartheta}_z(\tau) + \omega_z^2\vartheta_z(\tau) = 0\ , \qquad \textit{(no sum on } z\textit{)} \tag{3.32}$$

$$\vartheta_z(t) = 0\ , \qquad \dot{\vartheta}_z(t) = 1\ .$$

Due to the linearity of the system the normalized adjoint response described by Eq. (3.24) is proportional to the unit impulse response described by Eq. (3.32) by the amplitude $Q_{z\alpha}G_\alpha$ evaluated at time t. Finally, the adjoint response described by Eq. (3.17) can be obtained by superposition of the modal responses

$$\lambda_\beta(\tau) = \sum_{z=1}^{Z} Q_{z\beta}Q_{z\alpha}G_\alpha(t)\vartheta_z(\tau)\ , \tag{3.33}$$

$$\tau\in[t,0]\,, \qquad t\in[0,T]\,, \qquad \alpha,\beta = 1,\ldots,N\ .$$

Since the left hand sides of the adjoint equations (3.11),(3.17) differ from the structural system (3.3) only by the algebraic sign of the damping terms, the terminal problem described by Eqs. (3.11)–(3.13) or Eqs. (3.17),(3.18) can be rewritten in a form similar to that of the initial problem described by Eqs. (3.3),(3.4) by defining a forward time variable $t = T - \tau$, so that

$$\frac{\partial(.)}{\partial \tau} = -\frac{\partial(.)}{\partial t} \ . \tag{3.34}$$

Thus the terminal conditions of the adjoint equations expressed in terms of the backward time variable τ become the initial conditions with respect to the forward time variable t; and the adjoint system assumes exactly the same form as that of the structural system. This observation is very useful: 1) the eigenproblem has to be solved only once and the same eigenpairs are used for either the structural or adjoint system; 2) the structural and adjoint equations can be solved in parallel and by the same algorithm for integrating equations of motion. The uncoupled equations of structural and adjoint systems can be in turn solved alternatively by a step-by-step direct integration technique, or, having solved Eqs. (3.26),(3.32) for unit impulse response, by the Duhamel's convolution. The techniques are described in Section 1.4.2. Similarly to the static case we observe that, in contrast to the global mass, damping and stiffness matrices, most terms in the matrices of their derivatives with respect to design variables are equal to zero; and almost all operations required to compute the right hand sides and sensitivity gradient coefficients can be carried out by vector multiplications and at the element level. Note that the right hand side of the adjoint equations (3.17) involves a Dirac delta distribution evaluated at time τ and a force function of the running terminal time t. Employing the superposition principle for linear systems the adjoint response described by Eq. (3.17) can be treated as the solution of a system excited by an terminal velocity or unit impulse, cf. Eqs. (3.26),(3.32).

The nonhomogeneous initial conditions of Eq. (3.4) do not obscure the computer implementation. To obtain a homogeneous initial problem from the nonhomogeneous system (3.3),(3.4) we define a particular solution

$$q^*_\beta(h,t) = q^o_\beta(h) - \dot{q}^o_\beta(h)\, t \ , \tag{3.35}$$

use a new variable

$$z_\beta(h,t) = q_\beta(h,t) - q^*_\beta(h,t)\, t \ , \tag{3.36}$$

and substitute Eq. (3.36) into Eqs. (3.3),(3.4) to get

$$M_{\alpha\beta}(h)\ddot{z}_\beta(h,t) + D_{\alpha\beta}(h)\dot{z}_\beta(h,t) + K_{\alpha\beta}(h)z_\beta(h,t) =$$

$$= f_\alpha(h,t) - D_{\alpha\beta}(h)\dot{q}^*_\beta(h,t) - K_{\alpha\beta}(h)q^*_\beta(h,t) \ , \tag{3.37}$$

with the homogeneous initial conditions

$$z_\rho(h,0) = 0\,, \qquad \dot{z}_\rho(h,0) = 0\,, \qquad \alpha,\beta = 1,\ldots,N\,. \tag{3.38}$$

The eigenvalue sensitivity problem differs from the problems of static or forced-vibration sensitivity in that the derivatives of the eigenvalues with respect to design variables can be determined without the solution of an adjoint structures or derivatives of the eigenvectors with respect to design variables. This feature of the eigenvalue sensitivity allows direct computation of the sensitivity values once the eigenproblem has been solved. Recall that the problem is formulated assuming that the system is conservative; for nonconservative systems the situation is different [104]. In free vibration and buckling analysis it can be shown that if repeated eigenvalues arise some computational difficulties can appear leading to singular or non-differentiable problems. For example, the initial stress matrix may be nonpositive definite in buckling analysis, the boundary conditions may not be imposed in the mass and stiffness matrices in some sensitivity problems, the mass or stiffness matrix may be ill-conditioned, etc. Formulations for the sensitivity analysis with the repeated eigenvalues go beyond the framework of this text and can be found in [53,101,110,114,129,132].

The computer program POLSAP has been extended to include the dynamic sensitivity calculation options. In the modified version sensitivity analysis for eigenvalues and dynamic response of any truss-beam-plate-shell structures has been supported. Five types of the design variables can be considered: cross-sectional area and length of the 3D truss-beam elements, thickness of the plate-shell elements and Young modulus and mass density for all the element groups. In the solution phase, once the structural equations of motion are integrated forward in time and the values of displacements, velocities and accelerations are saved in a scratch file at each time step, and the terminal conditions are determined, the adjoint equations of motion can be integrated backward in time to obtain the adjoint displacement response. The solution process can be carried out by the direct integration (Wilson-θ) or mode superposition. For the latter uncoupled equations can be integrated alternatively by Wilson-θ and Newmark methods, using an integration approximation and load operator in the recursive relations given by Eq. (1.41), Section 1.4.2.

3.4 Numerical Results

Example 6 Consider sensitivity of the smallest eigenvalue of a cantilever beam of unit length. The input data for geometry and material properties are: cross-sectional area $h = 0.005$, moments of inertia $I_1 = I_2 = 0.5I_0 = 4.175 \times 10^{-5}$, mass density $\varrho = 7.87 \times 10^{-4}$, Young modulus $E = 2.0 \times 10^5$, Poisson ratio $\nu = 0.3$. As the design variable we take the cross-sectional area. The computation time for the 100-element model was 36 sec. The result given in Fig. 3.1 is compared with the analytical solution. The design sensitivity values indicate understandally that a unit change in cross-section area at the free end of the beam has substantially smaller effect on the first eigenvalue than a unit change at the clamped end.

Example 7 Fig. 3.2a shows the geometry, dimensions and loading of a portal frame. Input data are: cross-sectional area $h = 2 \times 5$, moments of inertia $I_z = 3.3333$,

$I_y = 20.8333$, $I_z = I_x + I_y$, mass density $\varrho = 0.02$, Young modulus $E = 2.0 \times 10^5$, Poisson ratio $\nu = 0.2$ and the finite element mesh includes 200 elements with 597 degrees of freedom. The cross section areas are assumed as design variables (200-dimensional vector) whereas the response functional is defined as

$$\phi = \int_0^l \delta(x - x^*) q(x)\, dx \ ,$$

where δ is the Dirac delta function. For dynamic analysis the functional is defined as the mean over time of square of displacement at a given point, that is

$$\phi = \frac{1}{T} \int_0^T \int_\Omega \delta(x - x^*) q^2(x,t)\, d\Omega dt \ ,$$

where Ω is the structure volume; and the terminal-time condition is given explicitly with respect to the terminal time T as $\mathcal{T} = T - T^{END} = 0$, with $T^{END} = 4$ sec. is the terminal instant. Thus the terminal conditions of the adjoint system are $\lambda(T) = \dot{\lambda}(T) = 0$. The structural and adjoint equations are integrated forward and backward by the step-by-step direct method with 100 time intervals with $\Delta t = 0.04$ sec. Assume that the time-varying load function is of the Heaviside's form, $f(t) = 50$. Table 3.1 gives the values of the gradients for the static and dynamics analyses as well as the first two eigenvalues for the left-hand-side elements of the structure (the results are symmetric). Fig. 3.2b gives the so called sensitivity curves for the first two eigenvalues and sensitivity gradient coefficients for the static and dynamic cases are shown in Fig. 3.2c. The computation times were 165 sec. for statics, 188 sec. for eigenvalue analysis and 1605 sec. for dynamics. In the latter 151 sec. was needed for forward integration and 1309 sec. for backward integration. It is emphasized that the sensitivity calculation is much more sensitive to finite element mesh than displacement-force calculation, i.e. a good grid model for the latter may become too coarse for the former. For example, the maximum value of displacement occurred at $t = 1.8$ sec. is 1.572 and 1.538 using correspondingly 40-element and 200-element meshes, whereas the sensitivity coefficient of the center element is -3.644×10^{-2} and -0.829×10^{-2}, respectively. In design sensitivity analysis a finer mesh is recommended.

Example 8 Consider the truss-beam-plate structure of Example 4, Section 2.5 in the dynamic response context. Distributed vertical load applied to the plate has the form of the Heaviside's function with amplitude equal to value of the static load acting on structure in static analysis. The structural response functional are given in the form similar to the case of the portal frame, above. The design variables for this complex structure are thickness for the plates and cross section area for beams and trusses. Mass density for the entire structure $\varrho = 0.1$. The forward and backward integrations are carried out by Wilson-θ technique over 100 time steps with the time interval $\Delta t = 8 \times 10^{-4}$sec. implying $T^{END} = 0.08$sec. Table 3.2 gives the sensitivity gradient values for the dynamic analysis. The computation times were 497 sec. and 6810 sec., respectively.

El.	Statics	Eigenvalue 1	Eigenvalue 2	Dynamics
1	−4.50964d−04	6.12914d−03	2.80544d−03	−1.10495d−03
5	−2.55802d−04	4.56086d−03	1.56409d−03	−6.24188d−04
10	−8.94544d−05	2.92415d−03	5.20416d−04	−2.15517d−04
15	−9.33459d−06	1.64181d−03	3.47256d−05	−1.97038d−05
20	−1.54424d−05	7.03429d−04	8.93372d−05	−3.50918d−05
25	−1.07778d−04	9.29604d−05	6.53202d−04	−2.59032d−04
30	−2.86341d−04	−2.11620d−04	1.68311d−03	−6.88211d−04
35	−5.51131d−04	−2.38132d−04	3.12795d−03	−1.31947d−03
40	−9.02149d−04	−1.95842d−05	4.93534d−03	−2.15060d−03
45	−1.33940d−03	4.06851d−04	7.05985d−03	−3.18046d−03
50	−1.86287d−03	1.00119d−03	9.47232d−03	−4.40836d−03
51	−1.82465d−03	1.03628d−03	9.14184d−03	−4.31188d−03
55	−1.15294d−03	7.81238d−04	5.11016d−03	−2.68908d−03
60	−5.29295d−04	4.80999d−04	1.60711d−03	−1.17885d−03
65	−1.45654d−04	2.04476d−04	−2.95455d−04	−2.43151d−04
70	−2.01341d−06	−4.49316d−05	−8.08933d−04	1.22512d−04
75	−9.83732d−05	−2.63834d−04	−2.39119d−04	−7.00800d−05
80	−4.34733d−04	−4.48993d−04	1.03849d−03	−7.98896d−04
85	−1.01109d−03	−5.97459d−04	2.61731d−03	−2.03146d−03
90	−1.82745d−03	−7.06717d−04	4.10651d−03	−3.72638d−03
95	−2.88382d−03	−7.74828d−04	5.17903d−03	−5.83387d−03
100	−4.18018d−03	−8.00545d−04	5.61324d−03	−8.29400d−03

Table 3.1: Sensitivity of statics, eigenvalues and dynamics of 200-element portal frame

Truss							
1	-7.53822d-07	2	-7.53822d-07	3	-7.53822d-07	4	-7.53822d-07
Beam							
1	-1.48074d-04	11	-1.07113d-04	21	9.59047d-09	31	-2.57930d-07
2	-1.38723d-04	12	-7.63456d-05	23	4.28135d-07	33	3.41623d-06
4	-3.40757d-05	14	-1.32839d-05	25	4.89779d-06	35	1.85860d-05
6	1.85860d-05	16	4.89779d-06	27	-1.32839d-05	37	-3.40757d-05
8	3.41623d-06	18	4.28135d-07	29	-7.63456d-05	39	-1.38723d-04
10	-2.57930d-07	20	9.59046d-09	30	-1.07113d-04	40	-1.48074d-04
Plate							
1	4.89874d-03	21	3.58900d-02	52	9.86408d-02	81	1.95730d-01
2	2.03808d-03	23	1.89811d-02	54	5.65106d-02	83	1.55429d-01
3	-1.51512d-03	25	3.20904d-03	56	1.73136d-02	85	9.86408d-02
4	-1.96293d-03	27	1.28758d-02	58	3.20904d-03	87	4.77659d-02
5	4.42245d-03	29	3.32269d-02	60	4.42245d-03	89	1.43196d-02
6	1.87295d-02	32	4.77659d-02	61	1.39743d-01	91	2.35911d-01
7	3.49388d-02	34	1.87505d-02	63	1.06647d-01	92	1.95730d-01
8	4.58743d-02	36	3.39230d-03	65	5.65106d-02	93	1.66983d-01
9	5.47205d-02	38	1.28758d-02	67	1.87505d-02	94	1.39743d-01
10	6.35900d-02	40	3.49388d-02	69	1.92529d-03	95	1.09997d-01
12	1.43196d-02	41	8.07836d-02	72	1.55429d-01	96	8.07836d-02
14	1.92529d-03	43	5.41840d-02	74	1.06647d-01	97	5.55876d-02
16	1.05878d-02	45	1.73136d-02	76	5.41840d-02	98	3.58900d-02
18	3.32269d-02	47	3.39230d-03	78	1.89811d-02	99	1.90808d-02
20	5.47205d-02	49	1.05878d-02	80	-1.51511d-03	100	4.89874d-03

Table 3.2: Dynamic sensitivity of truss-beam-plate structure

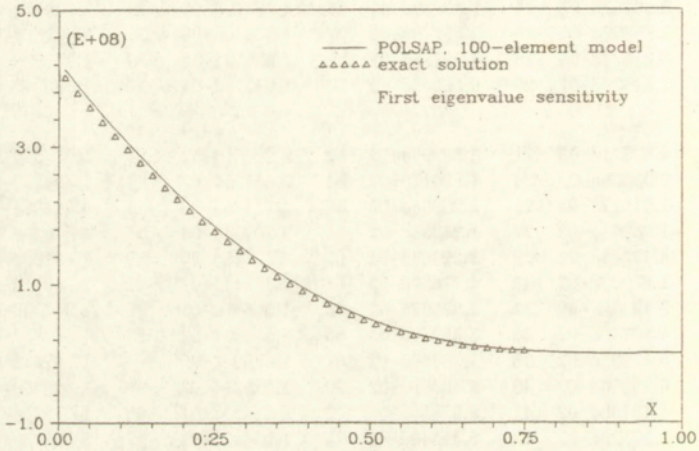

Figure 3.1: 100-element cantilever beam. Eigenvalue sensitivity.

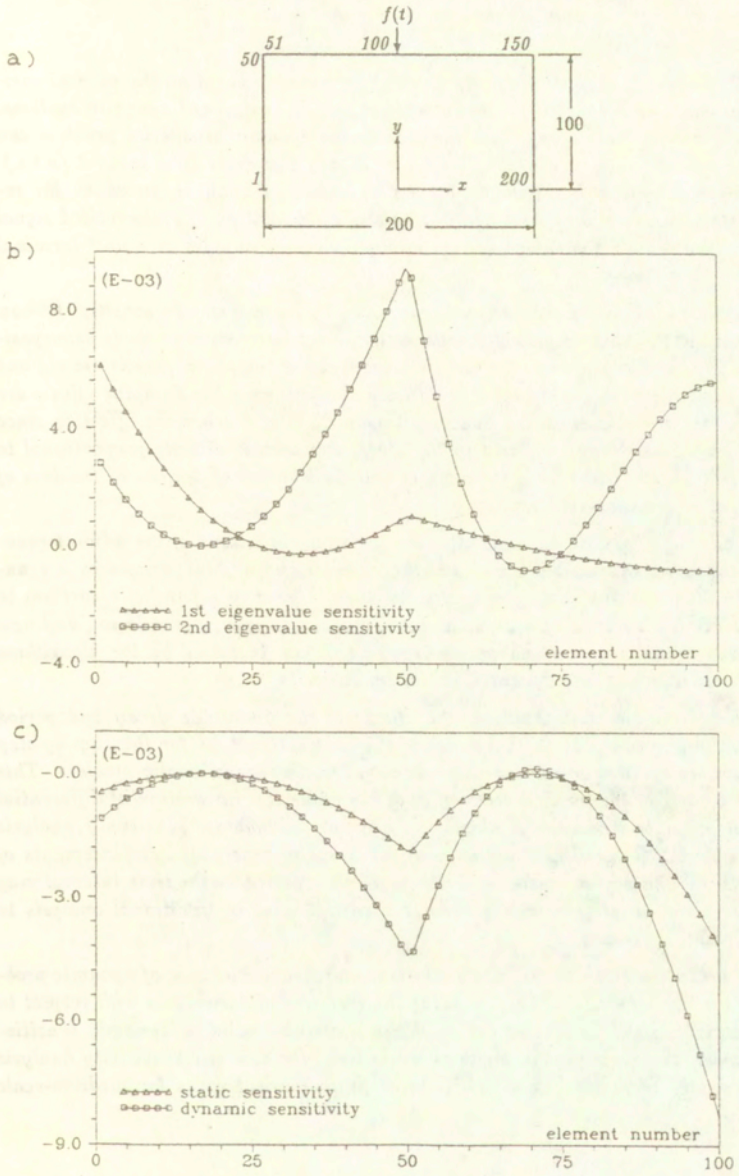

Figure 3.2: 200-element portal frame. Static, eigenvalue and dynamic sensitivity

Summarizing Remarks

In the foregoing chapter the finite element formulation based on the adjoint variable approach was presented for structural sensitivity analysis of dynamic systems. Depending on the class of response functionals the dynamic sensitivity problem can be considered over a time domain (o.t.d.) or at any particular time instant (a.t.i.). An original numerical treatment of the a.t.i. sensitivity analysis, in which the response functionals are approximated in terms of a convolution of a discretized signal sequence leading to a uncoupled system excited by a unit impulse or a unit terminal velocity, was proposed.

Discussions on the computational aspects of dynamic response sensitivity show that in case of the o.t.d. sensitivity analysis the direct integration or mode superposition can be alternatively used; the selection between the two techniques is merely one of numerical effectiveness. In a.t.i. sensitivity analysis, once the damping effects are appropriately approximated, the superposition method is much more effective since the number of operations required in the direct approach is directly proportional to the number of time steps used in analysis and the number of degrees of freedom of the system under consideration.

By defining a forward time variable the terminal conditions of the adjoint equations become the initial conditions and the original and adjoint structures are numerically identical; the same eigenpairs can then be used in a parallel algorithm to integrate the two systems of equations. Further, using a particular solution and new generalized coordinates a nonhomogeneous system can be solved by the algorithms used for systems with homogeneous initial conditions.

In the forced-vibration analysis the effects of the amplitude decay and period elongation may occur due to the choice of the time interval Δt for the step-by-step integration procedures (even for those known to be unconditionally stable). This inherent feature of the implicit techniques of the numerical integration of differential equations must be necessarily taken into account in dynamic sensitivity analysis since the sensitivity gradients are bilinear functions of generalized displacements of the structural and adjoint systems. From author's experiences the time interval may be chosen to be about three times smaller than that used in traditional analysis to obtain acceptable results.

Note that since static sensitivity analysis is merely a special case of dynamic problems all the remarks related to generating the matrices of derivatives with respect to design variables, the finite element mesh, etc. are also valid in dynamic sensitivity analysis. The numerical algorithms worked out for dynamic sensitivity analysis can be adapted to fit into existing PC-based finite element codes for medium-scale systems.

Part 2

STOCHASTIC SYSTEMS

4 Stochastic Hamilton's Principle and Stochastic Finite Element Model

4.1 Scope of the Chapter

The finite element method has been weak in dealing with variations of structural parameters due to uncertainties of these parameters. In this context, the concept of a random field [136] cannot be ignored. An analytical way enabling the stochastic finite element method to cope with uncertain parameter systems has been devised on the basis of the 2nd-order perturbation method [66,95,136,138]. This nonstatistical approach is numerically much more efficient than a statistical approach, such as the Monte Carlo simulations [133]. A major advantage of the stochastic finite element approach is that only the first two moments need to be known; and not the multivariate distribution function and a large number of samples required in the statistical approach. However, since the problems are formulated in the framework of the direct stiffness approach it is difficult to consistently handle problems with different types of randomness. To incorporate a number of classes of uncertainties into structural statics some variational formulations have been developed using the minimum potential energy principle [93], and the three-field Hu-Washizu principle [97]. The resulting probabilistic characters of these aspects are translated entirely into nodal forces in the form of variational statements. Similar variational descriptions for structural dynamic problems seem to be non-existent. Applications of probability and perturbation concepts to standard finite element analysis can be numerically costly. In [96], a numerical formulation for stochastic finite elements was introduced and a methodology for secularity elimination in multi-degrees of freedom systems was developed. In this chapter a stochastic version of Hamilton's variational principle applied to linear dynamic systems is proposed. The stochastic Hamilton's principle and consequently a stochastic finite element displacement model of equations of motion are formulated on the basis of the 2nd-order perturbation technique. A transformation from a general system with correlated random variables to the system with uncorrelated random variables through the standard eigenproblem and a two-fold application of mode superposition technique to integrate the stochastic equations of motion and evaluate the spatial probabilistic distributions of discretized displacement, strain and stress fields are described. An alternative technique based on the methodology discussed in [96] to eliminate secularities appearing during the perturbation solution is introduced. Numerical algorithms has been worked out and an option for stochastic analysis of forced vibrations has been implemented into the computer code POLSAP. Numerical results illustrate the chapter.

MODEL PROBLEM OF CHAPTER 4

Given ◁ expectations and covariances of random variables $b(x)$, x – spatial coordinates
(for example: cross-sectional area, thickness, length, Young modulus)

Find ▷ displacement-expressed finite element equations of motion $F(x, h, t) = 0$ or equilibrium equations $F(x, h) = 0$
▷ time-dependent or time-invariant expectations and covariances of nodal displacements, element strains and stresses

4.2 Stochastic Hamilton's Principle

According to the Hamilton's principle (Chapter 1, Eq. (1.1)), during any time interval the variation of the kinetic and potential energy is equal to the change of the work done by the external forces; and the application of the principle leads directly to the equations of motion for any given system. Assume that spatial uncertainties are involved in geometry, material parameters of a linear-elastic system and in external loads. Since the parameters are random variables the kinetic and potential energy and the external work are random quantities. In Eqs. (1.2),(1.3),(1.7) the components of constitutive tensor $C_{ijkl}(x)$, mass density $\varrho(x)$, damping factor $\zeta(x)$, body forces $f_i(x)$ and boundary tractions $\hat{t}_i(x)$ are explicit functions of random variables, whereas the displacements $u_i(x, t)$ and their spatial and time derivatives are implicit functions. The stochastic Hamilton's principle, which is an extended version of the Hamilton's principle on the basis of the 2nd-order perturbation technique, embeds the probabilistic distributions in terms of the first two moments of the random variables to obtain the first two moments in the variational statements. In this formulation the vector of random variables $b(x) = \{b^r(x)\}$, $r = 1, \ldots, R$, can represent randomness in cross-sectional area, length, thickness, Young modulus, mass density, damping component, etc. of structural members and uncertainties in external loads. The random variables can be defined by their first two moments as

$$E(b^r) \equiv b_o^r = \int_{-\infty}^{+\infty} b^r g(b^r)\, db^r \ , \tag{4.1}$$

$$Cov(b^r, b^s) = \int_{-\infty}^{+\infty}\int_{-\infty}^{+\infty} (b^r - b_o^r)(b^s - b_o^s) g(b^r, b^s)\, db^r db^s \ . \tag{4.2}$$

The latter equation can be replaced by

$$Cov(b^r, b^s) = R(b^r, b^s)[Var(b^r) Var(b^s)]^{1/2} \ , \qquad \textit{(no sum on } r, s\textit{)} \tag{4.3}$$

with

$$R(b^r, b^s) = \int_{-\infty}^{+\infty}\int_{-\infty}^{+\infty} b^r b^s g(b^r, b^s)\, db^r db^s \ , \tag{4.4}$$

$$Var(b^r) = \alpha^2 E^2(b^r) \ , \qquad \textit{(no sum on } r\textit{)} \tag{4.5}$$

where $E(b^r)$, $Cov(b^r, b^s)$, $R(b^r, b^s)$, $Var(b^r)$, $g(b^r, b^s)$ and α denote the spatial expectation, covariance, correlation, variance, joint probability density functions and the coefficient of variation, respectively. Employing second moment analysis the main idea behind the formulation of the stochastic Hamilton's principle involves expanding all the random functions C_{ijkl}, ϱ, ζ, f_i, $\hat{t}_i$ and u_i about the spatial expectations of the random variables b^r, denoted by $b^r_\circ$, via Taylor series with a given small perturbation θ and retaining up to second order terms. We write

$$C_{ijkl} = C^\circ_{ijkl} + \theta C^{,r}_{ijkl}\Delta b^r + \frac{1}{2}\theta^2 C^{,rs}_{ijkl}\Delta b^r \Delta b^s \ , \tag{4.6}$$

$$\varrho = \varrho^\circ + \theta \varrho^{,r}\Delta b^r + \frac{1}{2}\theta^2 \varrho^{,rs}\Delta b^r \Delta b^s \ , \tag{4.7}$$

$$\zeta = \zeta^\circ + \theta \zeta^{,r}\Delta b^r + \frac{1}{2}\theta^2 \zeta^{,rs}\Delta b^r \Delta b^s \ , \tag{4.8}$$

$$f_i = f^\circ_i + \theta f^{,r}_i \Delta b^r + \frac{1}{2}\theta^2 f^{,rs}_i \Delta b^r \Delta b^s \ , \tag{4.9}$$

$$\hat{t}_i = \hat{t}^\circ_i + \theta \hat{t}^{,r}_i \Delta b^r + \frac{1}{2}\theta^2 \hat{t}^{,rs}_i \Delta b^r \Delta b^s \ , \tag{4.10}$$

$$u_i = u^\circ_i + \theta u^{,r}_i \Delta b^r + \frac{1}{2}\theta^2 u^{,rs}_i \Delta b^r \Delta b^s \ , \tag{4.11}$$

$$i, j = 1, \ldots, 3 \ , \qquad r, s = 1, \ldots, R \ ,$$

where $\theta\Delta b^r \equiv \delta b^r$ denotes the first order variation of b^r about $b^r_\circ$; $(.)^\circ$, $(.)^{,r}$ and $(.)^{,rs}$ represent the expectation, first and second (mixed) partial derivatives with respect to the random variables evaluated at their expectations, respectively. Substituting the expanded functions of C_{ijkl}, ϱ, ζ, f_i, $\hat{t}_i$, and u_i into Eq. (1-4) equating coefficients of like powers of θ the 0th-, 1st- and 2nd-order expressions for the stochastic Hamilton's principle can be shown to be:

one 0th-order equation

$$\int_\Omega \delta u_i \varrho^\circ \ddot{u}^\circ_i \, d\Omega + \int_\Omega \delta u_i \zeta^\circ \dot{u}^\circ_i \, d\Omega + \int_\Omega \delta u_{i,j} C^\circ_{ijkl} u^\circ_{k,l} \, d\Omega =$$
$$= \int_\Omega \delta u_i \varrho^\circ f^\circ_i \, d\Omega + \int_{\partial\Omega} \delta u_i \hat{t}^\circ_i \, d(\partial\Omega) \ , \tag{4.12}$$

R 1st-order equations $(r = 1, \ldots, R)$

$$\int_\Omega \delta u_i \varrho^\circ \ddot{u}^{,r}_i \, d\Omega + \int_\Omega \delta u_i \zeta^\circ \dot{u}^{,r}_i \, d\Omega + \int_\Omega \delta u_{i,j} C^\circ_{ijkl} u^{,r}_{k,l} \, d\Omega =$$
$$= \int_\Omega \delta u_i \varrho^\circ f^{,r}_i \, d\Omega + \int_{\partial\Omega} \delta u_i \hat{t}^{,r}_i \, d(\partial\Omega) -$$
$$- \int_\Omega \delta u_i \varrho^{,r} \ddot{u}^\circ_i \, d\Omega + \int_\Omega \delta u_i \zeta^{,r} \dot{u}^\circ_i \, d\Omega + \int_\Omega \delta u_{i,j} C^{,r}_{ijkl} u^\circ_{k,l} \, d\Omega \ , \tag{4.13}$$

one 2nd-order equation

$$\left(\int_\Omega \delta u_i \varrho^o \ddot{u}_i^{rs}\, d\Omega + \int_\Omega \delta u_i \zeta^o \dot{u}_i^{rs}\, d\Omega + \int_\Omega \delta u_{i,j} C^o_{ijkl} u^{rs}_{k,l}\, d\Omega\right) Cov(b^r, b^s) =$$

$$= \left[\int_\Omega \delta u_i (\varrho^o f_i^{rs} + 2\varrho^r f_i^s + \varrho^{rs} f_i^o)\, d\Omega + \int_{\partial\Omega} \delta u_i \hat{t}_i^{rs}\, d(\partial\Omega) - \right.$$

$$- \int_\Omega \delta u_i (2\varrho^r \ddot{u}_i^s + \varrho^{rs} \ddot{u}_i^o)\, d\Omega - \int_\Omega \delta u_i (2\zeta^r \dot{u}_i^s + \zeta^{rs} \dot{u}_i^o)\, d\Omega -$$

$$\left. - \int_\Omega \delta u_{i,j} (2C^r_{ijkl} u^s_{k,l} + C^{rs}_{ijkl} u^o_{k,l})\, d\Omega\right] Cov(b^r, b^s) \ . \qquad (4.14)$$

Note that according to the definition of the covariance function the 2nd-order equation is obtained by multiplying the joint probability density function by the 2nd-order terms and integrating over the domain of the random field $b^r(x)$. In Eqs. (4.12)–(4.14) all the functions with superscript 'o' are deterministic functions evaluated at the averages b^r_o; and the 0th-order equation (4.12) is the standard deterministic variational statement of the Hamilton's principle applied to deterministic systems, c.f. Eq. (1.1). The functions with superscripts '$,r$', '$,s$' and '$,rs$' are random functions characterized by the random field $b^r(x)$. In general the random functions ϱ^r, ζ^r, f_i^r, $\hat{t}_i^r$, C^r_{ijkl} and ϱ^{rs}, ζ^{rs}, f_i^{rs}, $\hat{t}_i^{rs}$, C^{rs}_{ijkl} can be described explicitly in terms of random variables through their first two moments, i.e. the spatial expectations and correlations. Except for the displacements functions and their time and spatial derivatives, all terms involved on the left hand sides of Eqs. (4.12)–(4.14) are identical. The resulting probabilistic characteristics of the problem are translated entirely into the effective forces on the right hand sides. Once the 0th-order displacements are solved from Eq. (4.12) the random functions of 1st- and 2nd-order displacements can be evaluated by using Eqs. (4.13),(4.14). Having solved probabilistic distribution of the 0th-, 1st- and 2nd-order displacements, the probabilistic description of the strains and stresses can be determined.

Similarly to the case of deterministic systems, if the inertial and damping effects are negligible the stochastic Hamilton's principle expressed by Eqs. (4.12)–(4.14) reduces to a stochastic version of the principle of minimum potential energy, cf. Eqs. (1.1),(1.5). We obtain

one 0th-order equation

$$\int_\Omega \delta u_{i,j} C^o_{ijkl} u^o_{k,l}\, d\Omega = \int_\Omega \delta u_i \varrho^o f_i^o\, d\Omega + \int_{\partial\Omega} \delta u_i \hat{t}_i^o\, d(\partial\Omega) \ , \qquad (4.15)$$

R 1st-order equations ($r = 1, \ldots, R$)

$$\int_\Omega \delta u_{i,j} C^o_{ijkl} u^r_{k,l}\, d\Omega =$$

$$= \int_\Omega \delta u_i \varrho^o f_i^r\, d\Omega + \int_{\partial\Omega} \delta u_i \hat{t}_i^r\, d(\partial\Omega) - \int_\Omega \delta u_{i,j} C^r_{ijkl} u^o_{k,l}\, d\Omega \ , \qquad (4.16)$$

one 2nd-order equation

$$\left(\int_\Omega \delta u_{i,j} C^o_{ijkl} u^{rs}_{k,l}\, d\Omega\right) Cov(b^r, b^s) =$$

$$= \left[\int_\Omega \delta u_i (\varrho^o f_i^{rs} + 2\varrho^r f_i^s + \varrho^{rs} f_i^o)\, d\Omega + \int_{\partial\Omega} \delta u_i \hat{t}_i^{rs}\, d(\partial\Omega) - \right.$$

$$\left. - \int_\Omega \delta u_{i,j} (2C^r_{ijkl} u^s_{k,l} + C^{rs}_{ijkl} u^o_{k,l})\, d\Omega\right] Cov(b^r, b^s) \ . \qquad (4.17)$$

4.3 Stochastic Finite Element Equations of Motion

Since in Eqs. (4.12)–(4.14) all the functions with superscript 'o' are deterministic, Eq. (4.12) is Hamilton's principle applied to deterministic systems and the standard finite element technique can be employed directly. To be consistent with the finite element approximation and to maintain the compatibility with the discretized random feld b^r, the displacement field and the forcing functions are discretized by N shape functions, cf. Eq. (1.13). We have

$$u_i^o(x,t) = \psi_{i\xi}(x) u_\xi^{o(n)}(t) = \varphi_{i\alpha}(x) q_\alpha^o(t) \ , \qquad (4.18)$$

$$u_i^r(x,t) = \psi_{i\xi}(x) u_\xi^{r(n)}(t) = \varphi_{i\alpha}(x) q_\alpha^r(t) \ , \qquad (4.19)$$

$$u_i^{rs}(x,t) = \psi_{i\xi}(x) u_\xi^{rs(n)}(t) = \varphi_{i\alpha}(x) q_\alpha^{rs}(t) \ , \qquad (4.20)$$

$$i = 1,\ldots,3 \ , \qquad r,s = 1,\ldots,R \ , \qquad \alpha = 1,\ldots,N \ ,$$

$$x \in \Omega \ , \qquad t \in [0,T] \ ,$$

where symbols $u_\xi^{o(n)}$, $u_\xi^{r(n)}$, $u_\xi^{rs(n)}$ and q_α^o, q_α^r, q_α^{rs} denote the vectors of the 0th-, 1st-, 2nd-order generalized nodal displacements in the local and global coordinate systems. Recall that $\psi_{i\xi}$ and $\varphi_{i\alpha}$ are the shape function matrices in the local and global coordinate systems and $a_{i\alpha}$ is the transformation matrix. By the same shape functions and in a similar manner the 0th-, 1st-, 2nd-order body forces and boundary tractions are interpolated. The approximations of strain tensors expressed by Eq. (1.11),(1.15) for deterministic systems now can be rewritten as

$$\varepsilon_{ij}^o(x,t) = B_{ij\xi}(x) u_\xi^{o(n)}(t) = B_{ij\alpha}(x) q_\alpha^o(t) \ , \qquad (4.21)$$

$$\varepsilon_{ij}^r(x,t) = B_{ij\xi}(x) u_\xi^{r(n)}(t) = B_{ij\alpha}(x) q_\alpha^r(t) \ , \qquad (4.22)$$

$$\varepsilon_{ij}^{rs}(x,t) = B_{ij\xi}(x) u_\xi^{rs(n)}(t) = B_{ij\alpha}(x) q_\alpha^{rs}(t) \ , \qquad (4.23)$$

Substituting the above interpolations into the 0th-, 1st- and 2nd-order variational statements of Eqs. (4.12)–(4.14), the finite element model of equations of motion for stochastic systems can be obtained as:

one system of the 0th-order differential equations

$$M^{\circ}_{\alpha\beta}\ddot{q}^{\circ}_{\beta}(t) + D^{\circ}_{\alpha\beta}\dot{q}^{\circ}_{\beta}(t) + K^{\circ}_{\alpha\beta}q^{\circ}_{\beta}(t) = f^{\circ}_{\alpha}(t) \ , \tag{4.24}$$

R systems of the 1st-order differential equations ($r = 1, \ldots, R$)

$$M^{\circ}_{\alpha\beta}\ddot{q}^{r}_{\beta}(t) + D^{\circ}_{\alpha\beta}\dot{q}^{r}_{\beta}(t) + K^{\circ}_{\alpha\beta}q^{r}_{\beta}(t) =$$

$$= f^{r}_{\alpha}(t) - [M^{r}_{\alpha\beta}\ddot{q}^{\circ}_{\beta}(t) + D^{r}_{\alpha\beta}\dot{q}^{\circ}_{\beta}(t) + K^{r}_{\alpha\beta}q^{\circ}_{\beta}(t)] \ , \tag{4.25}$$

one system of the 2nd-order differential equations

$$M^{\circ}_{\alpha\beta}\ddot{q}^{(2)}_{\beta}(t) + D^{\circ}_{\alpha\beta}\dot{q}^{(2)}_{\beta}(t) + K^{\circ}_{\alpha\beta}q^{(2)}_{\beta}(t) =$$

$$= \left\{\frac{1}{2}f^{rs}_{\alpha}(t) - [M^{r}_{\alpha\beta}\ddot{q}^{s}_{\beta}(t) + D^{r}_{\alpha\beta}\dot{q}^{s}_{\beta}(t) + K^{r}_{\alpha\beta}q^{s}_{\beta}(t)] - \right.$$

$$\left. - \frac{1}{2}\,[M^{rs}_{\alpha\beta}\ddot{q}^{\circ}_{\beta}(t) + D^{rs}_{\alpha\beta}\dot{q}^{\circ}_{\beta}(t) + K^{rs}_{\alpha\beta}q^{\circ}_{\beta}(t)]\right\} Cov(b^{r}, b^{s}) \ , \tag{4.26}$$

where

$$q^{(2)}_{\beta}(t) = \frac{1}{2}q^{rs}_{\beta}(t)Cov(b^{r}, b^{s}) \ . \tag{4.27}$$

Similarly, from the variational statements of Eqs. (4.15)–(4.17) wherein the displacements are time-independent, the finite element model of equilibrium equations for stochastic systems reads:

one system of the 0th-order equilibrium equations

$$K^{\circ}_{\alpha\beta}q^{\circ}_{\beta} = f^{\circ}_{\alpha} \ , \tag{4.28}$$

R systems of the 1st-order equilibrium equations ($r = 1, \ldots, R$)

$$K^{\circ}_{\alpha\beta}q^{r}_{\beta} = f^{r}_{\alpha} - K^{r}_{\alpha\beta}q^{\circ}_{\beta} \ , \tag{4.29}$$

one system of the 2nd-order equilibrium equations

$$K^{\circ}_{\alpha\beta}q^{(2)}_{\beta} = \frac{1}{2}\left(f^{rs}_{\alpha} - 2K^{r}_{\alpha\beta}q^{s}_{\beta} - K^{rs}_{\alpha\beta}q^{\circ}_{\beta}\right) Cov(b^{r}, b^{s}) \ , \tag{4.30}$$

In Eqs. (4.24)–(4.26) and Eqs. (4.18)–(4.20) the expectations and the first, second partial derivatives of the mass, damping, stiffness matrices with respect to random variables can be shown to be (cf. Eqs. (1-18)–(1-20) and Eqs. (4.6)–(4.8)):

the expectations

$$M^{o}_{\alpha\beta} = \sum_{e=1}^{E} \int_{\Omega} \varrho^{o} \psi_{i\xi} \psi_{i\eta} a_{\xi\alpha} a_{\eta\beta} \, d\Omega = \int_{\Omega} \varrho^{o} \varphi_{i\alpha} \varphi_{i\beta} \, d\Omega \ , \tag{4.31}$$

$$D^{o}_{\alpha\beta} = \sum_{e=1}^{E} \int_{\Omega} \zeta^{o} \psi_{i\xi} \psi_{i\eta} a_{\xi\alpha} a_{\eta\beta} \, d\Omega = \int_{\Omega} \zeta^{o} \varphi_{i\alpha} \varphi_{i\beta} \, d\Omega \ , \tag{4.32}$$

$$K^{o}_{\alpha\beta} = \sum_{e=1}^{E} \int_{\Omega} C^{o}_{ijkl} B_{ij\xi} B_{kl\eta} a_{\xi\alpha} a_{\eta\beta} \, d\Omega = \int_{\Omega} C^{o}_{ijkl} B_{ij\alpha} B_{kl\beta} \, d\Omega \ , \tag{4.33}$$

the first partial derivatives

$$M^{r}_{\alpha\beta} = \sum_{e=1}^{E} \int_{\Omega} \varrho^{r} \psi_{i\xi} \psi_{i\eta} a_{\xi\alpha} a_{\eta\beta} \, d\Omega = \int_{\Omega} \varrho^{r} \varphi_{i\alpha} \varphi_{i\beta} \, d\Omega \ , \tag{4.34}$$

$$D^{r}_{\alpha\beta} = \sum_{e=1}^{E} \int_{\Omega} \zeta^{r} \psi_{i\xi} \psi_{i\eta} a_{\xi\alpha} a_{\eta\beta} \, d\Omega = \int_{\Omega} \zeta^{r} \varphi_{i\alpha} \varphi_{i\beta} \, d\Omega \ , \tag{4.35}$$

$$K^{r}_{\alpha\beta} = \sum_{e=1}^{E} \int_{\Omega} C^{r}_{ijkl} B_{ij\xi} B_{kl\eta} a_{\xi\alpha} a_{\eta\beta} \, d\Omega = \int_{\Omega} C^{r}_{ijkl} B_{ij\alpha} B_{kl\beta} \, d\Omega \ , \tag{4.36}$$

the second partial derivatives

$$M^{rs}_{\alpha\beta} = \sum_{e=1}^{E} \int_{\Omega} \varrho^{rs} \psi_{i\xi} \psi_{i\eta} a_{\xi\alpha} a_{\eta\beta} \, d\Omega = \int_{\Omega} \varrho^{rs} \varphi_{i\alpha} \varphi_{i\beta} \, d\Omega \ , \tag{4.37}$$

$$D^{rs}_{\alpha\beta} = \sum_{e=1}^{E} \int_{\Omega} \zeta^{rs} \psi_{i\xi} \psi_{i\eta} a_{\xi\alpha} a_{\eta\beta} \, d\Omega = \int_{\Omega} \zeta^{rs} \varphi_{i\alpha} \varphi_{i\beta} \, d\Omega \ , \tag{4.38}$$

$$K^{rs}_{\alpha\beta} = \sum_{e=1}^{E} \int_{\Omega} C^{rs}_{ijkl} B_{ij\xi} B_{kl\eta} a_{\xi\alpha} a_{\eta\beta} \, d\Omega = \int_{\Omega} C^{rs}_{ijkl} B_{ij\alpha} B_{kl\beta} \, d\Omega \ , \tag{4.39}$$

Sinilarly to the case of deterministic systems it is assumed that in the compatible displacement modelling presented above the displacement boundary conditions have been inposed in the boundary-initial problem.

4.4 Probabilistic Distribution Output

Having solved for q^{o}_{β}, q^{r}_{β}, $q^{(2)}_{\beta}$ and their time derivatives, the probabilistic distributions for the nodal displacements, velocities, accelerations, element strains and stresses can be determined. From Eqs. (4.18)–(4.20) the random displacement functions can be expressed as

$$q_\beta(t) = q^o_\beta(t) + \theta q^r_\beta(t)\Delta b^r + \frac{1}{2}\theta^2 q^{rs}_\beta(t)\Delta b^r \Delta b^s \ . \tag{4.40}$$

By the definition of the spatial expectations and covariances for the nodal displacements (and similarly for the velocities and accelerations) we have

$$E[q_\beta(t)] = \int_{-\infty}^{+\infty} q_\beta(t) g(b^r)\, db^r \ , \tag{4.41}$$

$$Cov[q_\alpha(t), q_\beta(t)] = \int_{-\infty}^{+\infty}\int_{-\infty}^{+\infty} \{q_\alpha(t) - E[q_\alpha(t)]\} \{q_\beta(t) - E[q_\beta(t)]\} g(b^r, b^s)\, db^r db^s \ . \tag{4.42}$$

Substituting Eq. (4.40) into Eq. (4.41), using Eq. (4.27) and observing that the terms including the first variation of Δb^r vanish by definition, yields the 2nd-order accurate expectations of the nodal displacements as

$$E[q_\beta(t)] = q^o_\beta(t) + \frac{1}{2} q^{rs}_\beta(t) Cov(b^r, b^s) = q^o_\beta(t) + q^{(2)}_\beta(t) \ . \tag{4.43}$$

The 2nd-order accurate covariances of the nodal displacements are obtained by employing Eq. (4.40) in Eq. (4.42) to give

$$Cov[q_\alpha(t), q_\beta(t)] = q^r_\alpha(t) q^s_\beta(t) Cov(b^r, b^s) + \frac{1}{2}[q^r_\alpha(t) q^{st}_\beta(t) + q^{rs}_\alpha(t) q^t_\beta(t)] C(b^r, b^s, b^t) + \frac{1}{4} q^{rs}_\alpha(t) q^{tu}_\beta(t) C(b^r, b^s, b^t, b^u) \ . \tag{4.44}$$

where $C(b^r, b^s, b^t)$ and $C(b^r, b^s, b^t, b^u)$ denote the 3rd- and 4th-order center moments. If the 1st-order estimate of the spatial covariances of the nodal displacements is of interest, Eq. (4.44) reduces to

$$Cov[q_\alpha(t), q_\beta(t)] = q^r_\alpha(t) q^s_\beta(t) Cov(b^r, b^s) \ . \tag{4.45}$$

By using Eqs. (4.21)– (4.23) and Eq. (4.40) the strain tensor for the e-th finite element can be written as

$$\varepsilon^e_{ij}(t) = B^{(e)}_{ij\alpha}(x)[q^o_{\alpha(e)}(t) + \theta q^r_{\alpha(e)}(t)\Delta b^r + \frac{1}{2}\theta^2 q^{rs}_{\alpha(e)}(t)\Delta b^r \Delta b^s] \ . \tag{4.46}$$

Since the shapes $B^{(e)}_{ij\alpha}(x)$ are deterministic functions, substitution of Eq. (4.46) into equations similar to Eqs. (4.41),(4.42) for strain yields the 2nd-order accurate expectations, the 1st-order accurate covariances of the strain tensor components

$$E[\varepsilon^e_{ij}(t)] = B^{(e)}_{ijo}(x)[q^o_{\alpha(e)}(t) + q^{(2)}_{\alpha(e)}(t)] \ , \tag{4.47}$$

$$Cov[\varepsilon^e_{ij}(t), \varepsilon^l_{kl}(t)] = B^{(e)}_{ijo}(x) B^{(f)}_{kl\beta}(x) q^r_{\alpha(e)}(t) q^s_{\beta(f)}(t) Cov(b^r, b^s) \ , \tag{4.48}$$

From Eq. (4.46), the stress tensor for the e-th element can be written as

$$\sigma^e_{ij}(t) = C^{(e)}_{ijkl} B^{(e)}_{kl\alpha}(x)[q^o_{\alpha(e)}(t) + \theta q^r_{\alpha(e)}(t)\Delta b^r + \frac{1}{2}\theta^2 q^{rs}_{\alpha(e)}(t)\Delta b^r \Delta b^s] \ . \tag{4.49}$$

Employing Eqs. (4.6),(4.49) in equations similar to Eqs. (4.41),(4.42) for stress the 2nd-order accurate expectations and the 1st-order accurate covariances of the stress tensor components can be shown to be

$$\begin{aligned} E[\sigma^e_{ij}(t)] &= \Big\{ C^{\alpha(e)}_{ijkl} q^o_{\alpha(e)}(t) + \frac{1}{2}\Big[C^{\alpha(e)}_{ijkl} q^{rs}_{\alpha(e)}(t) + \\ &\quad + 2C^{r(e)}_{ijkl} q^s_{\alpha(e)}(t) + C^{rs(e)}_{ijkl} q^o_{\alpha(e)}(t)\Big]\Big\} B^{(e)}_{kl\alpha}(x) Cov(b^r, b^s) = \\ &= C^{\alpha(e)}_{ijkl} E[\varepsilon^e_{kl}(t)] + \frac{1}{2}\Big[2C^{r(e)}_{ijkl} q^s_{\alpha(e)}(t) + C^{rs(e)}_{ijkl} q^o_{\alpha(e)}(t)\Big] B^{(e)}_{kl\alpha}(x) Cov(b^r, b^s) \ , \end{aligned} \tag{4.50}$$

$$\begin{aligned} Cov[\sigma^e_{ij}(t), \sigma^f_{kl}(t)] &= \Big[C^{\alpha(e)}_{ijmn} C^{\alpha(f)}_{klgh} q^r_{\alpha(e)}(t) q^s_{\beta(f)}(t) + \\ &\quad + C^{r(e)}_{ijmn} C^{s(f)}_{klgh} q^o_{\alpha(e)}(t) q^o_{\beta(f)}(t) + C^{r(e)}_{ijmn} C^{\alpha(f)}_{klgh} q^s_{\alpha(e)}(t) q^o_{\beta(f)}(t) + \\ &\quad + C^{\alpha(e)}_{ijmn} C^{s(f)}_{klgh} q^o_{\alpha(e)}(t) q^s_{\beta(f)}(t)\Big] B^{(e)}_{mn\alpha}(x) B^{(f)}_{gh\beta}(x) Cov(b^r, b^s) \ . \end{aligned} \tag{4.51}$$

Note that the probabilistic distributions of displacement, strain and stress for static problems can be also obtained by Eqs. (4.40)–(4.51) provided Eqs. (4.28)–(4.30) have been solved. The only difference is that the nodal displacements and their derivatives with respect to random variables are time-invariant.

4.5 Computational Implementation

As shown in the preceding section, the functions with superscript 'o' are deterministic whereas the functions with superscripts '$,r$' and '$,rs$' are random. The latter functions involving first and second partial derivatives of the mass, damping, stiffness matrices and load vector with respect to random variables are generally given in explicit form in terms of random variables and can be generated exactly by partial differentiation, by finite difference techniques or by the least square fit method, [105]. These quantities are evaluated at the expectations of random variables. Once $\bar{q}^o_\beta(t)$, $\dot{q}^o_\beta(t)$ and $q^o_\beta(t)$ are solved for by Eq. (4.24), the random functions $\bar{q}^r_\beta(t)$, $\dot{q}^r_\beta(t)$, $q^r_\beta(t)$ and $\bar{q}^{(2)}_\beta(t)$, $\dot{q}^{(2)}_\beta(t)$, $q^{(2)}_\beta(t)$ can be determined by Eqs. (4.25),(4.26),

sequentially. In other words, there are $R+2$ systems of linear ordinary differential equations to be integrated. In fact, the solution process can be performed in parallel for $q_s^o(t)$, $q_s^r(t)$ and $q_s^{(2)}(t)$ since the global mass, damping and stiffness matrices involved on the left hand sides of Eqs. (4.24)–(4.26) and consequently the effective coefficient matrix have to be formed only once and almost all operations required to calculate right hand sides can be carried out by vector multiplications and at the element level. Nonetheless, the amount of computations required to solve Eqs. (4.24)–(4.26) and to compute the first two moments of the nodal accelerations, velocities, displacements, strains and stresses can be quite expensive due to the double summation in Eqs. (4.26), (4.43), (4.45), (4.47), (4.48), (4.50), (4.51). In particular, by using the direct step-by-step integration techniques in analysis of medium- or large-scale systems with a large number of time intervals required the computation cost could be unacceptable high. In order to solve the problem much more efficiently an approach termed two-fold superposition technique may be used. The main ideas behind the technique are:

1) transformation of the system with correlated random variables to a system with uncorrelated random variables through the standard eigenproblem,

2) transformation of the coupled equations of motion to uncoupled equations by the generalized eigenproblem,

3) superposition of resulting uncorrelated and modal responses to have complete solution.

Another aspect of the problem which should not be overlooked is that the application of the 2nd-order perturbation technique can produce invalid solutions due to the appearance of secular terms which grow indefinitely with time. The secularity effects can be eliminated effectively by using the fast Fourier transform of a complex-valued sequence of large length. In this section the aspects mentioned above are considered.

4.5.1 Two-Fold Superposition Technique

As shown above the total solution requires integrating $R+2$ systems of differential equations and evaluating probabilistic distributions of displacement, strain and stress. The number of matrix operations is proportional to $R(R+1)/2$ due to the double summations. To reduce the double summation to single summation so that the number of matrix multiplications is proportional to R, a transformation from a set of correlated random variables b^r to a set of uncorrelated random variables c^r, $r = 1, \ldots, R$, can be applied, [95]. This involves solution of the standard eigenproblem

$$Cov(b^r, b^s)\, U = \Theta U \ , \tag{4.52}$$

where the covariance matrix $Cov(b^r, b^s)$, $r, s = 1, \ldots, R$, is assumed to be positive definite, U is an orthonormal RxR-dimensional fundamental matrix and Θ is a R-dimensional diagonal matrix. In contrast to the modal structural problem, wherein the *lowest* natural frequencies are used, only V ($V \ll R$) *highest* values of Θ are required to simulate the major characteristics of many probabilistic distributions, [95].

If the random vector b^r is composed of three uncorrelated parts of random load, geometry and material, the highest modes for each of the three parts of $Cov(b^r, b^s)$ are extracted and combined to obtain $Var(c^v)$. Once the matrix of the eigenvectors U is determined from the solution of Eq. (4.52) the uncorrelated random variables c^v, their derivatives, expectations and variances are obtained from the correlated random variables b^r as

$$c^v = U_{rv} b^r \,, \quad \frac{\partial(.)}{\partial c^v} = U_{rv} \frac{\partial(.)}{\partial b^r} \,, \quad E(c^v) = U_{rv} b^r_o \,, \quad Var(c^v) = \Theta_v \,, \tag{4.53}$$

$$r = 1, \ldots, R \,; \qquad v = 1, \ldots, V.$$

Substituting Eqs. (4.52),(4.53) in Eqs. (4.24)–(4.26) the mixed partial derivatives $(.)^{,rs}$ reduce to the second derivatives $(.)^{,rr}$ (no sum on r); and the double summation over r, s $(r, s = 1, \ldots, R)$ reduces to the single summation over v $(v = 1, \ldots, V)$. Thus, by employing uncorrelated random variables c^v, Eqs. (4.24)–(4.26) read:

one system of the uncorrelated 0th-order equations

$$M^o_{\alpha\beta} \ddot{q}^o_\beta(t) + D^o_{\alpha\beta} \dot{q}^o_\beta(t) + K^o_{\alpha\beta} q^o_\beta(t) = f^o_\alpha(t) \,, \tag{4.54}$$

V systems of the uncorrelated 1st-order equations $(v = 1, \ldots, V)$

$$M^o_{\alpha\beta} \ddot{q}^v_\beta(t) - D^o_{\alpha\beta} \dot{q}^v_\beta(t) + K^o_{\alpha\beta} q^v_\beta(t) = p^v_\alpha(t) \,, \tag{4.55}$$

one system of the uncorrelated 2nd-order equations

$$M^o_{\alpha\beta} \ddot{q}^{(2)}_\beta(t) + D^o_{\alpha\beta} \dot{q}^{(2)}_\beta(t) + K^o_{\alpha\beta} q^{(2)}_\beta(t) = p^{(2)}_\alpha(t) \,, \tag{4.56}$$

with

$$q^{(2)}_\beta(t) = \frac{1}{2} \sum_{v=1}^{V} q^{vv}_\beta Var(c^v) \,, \tag{4.57}$$

$$p^v_\alpha(t) = f^v_\alpha(t) - [M^v_{\alpha\beta} \ddot{q}^o_\beta(t) + D^v_{\alpha\beta} \dot{q}^o_\beta(t) + K^v_{\alpha\beta} q^o_\beta(t)] \,, \tag{4.58}$$

$$p^{(2)}_\alpha(t) = \frac{1}{2} \sum_{v=1}^{V} \Big\{ f^{vv}_\alpha(t) - 2[M^v_{\alpha\beta} \ddot{q}^v_\beta(t) + D^v_{\alpha\beta} \dot{q}^v_\beta(t) + K^v_{\alpha\beta} q^v_\beta(t)] - $$
$$- [M^{vv}_{\alpha\beta} \ddot{q}^o_\beta(t) + D^{vv}_{\alpha\beta} \dot{q}^o_\beta(t) + K^{vv}_{\alpha\beta} q^o_\beta(t)] \Big\} Var(c^v) \,, \tag{4.59}$$

In the above equations $(.)^v$ and $(.)^{vv}$ denote the first and second derivatives with respect to the uncorrelated random variables c^v. Note that the solution of Eqs. (4.54)–(4.56) requires only $V + 2$ $(V \ll R)$ integrations of equations of motion.

For the case of time-independent systems of Eqs. (4.28)–(4.30), the finite element model of the equilibrium equations for stochastic systems expressed in terms of the uncorrelated random variables c^v reads:

one system of the uncorrelated 0th-order equilibrium equations

$$K^{\circ}_{\alpha\beta} q^{\circ}_{\beta} = f^{\circ}_{\alpha} \ , \tag{4.60}$$

R systems of the uncorrelated 1st-order equilibrium equations ($r = 1, \ldots, R$)

$$K^{\circ}_{\alpha\beta} q^{:r}_{\beta} = f^{:r}_{\alpha} - K^{:r}_{\alpha\beta} q^{\circ}_{\beta} \ , \tag{4.61}$$

one system of the uncorrelated 2nd-order equilibrium equations

$$K^{\circ}_{\alpha\beta} q^{(2)}_{\beta} = \frac{1}{2} \sum_{v=1}^{V} \left(f^{:vv}_{\alpha} - 2K^{:v}_{\alpha\beta} q^{:v}_{\beta} - K^{:vv}_{\alpha\beta} q^{\circ}_{\beta} \right) Var(c^v) \ , \tag{4.62}$$

Next, let us transform the equations of motion expressed in terms of the uncorrelated random variables c^v to a form in which the step-by-step integration is less costly. To do this, the transformation of Eq. (1.33) is carried out to change basis from the finite element coordinates $q_\beta(t)$ to the normalized coordinates $y_s(t)$ through the mode shape matrix $Q_{\beta s}$. As a result, a system of uncoupled differential equations which can be integrated independently is obtained and solved for the modal coordinates. From Eqs. (4.54)–(4.56) we have then:

Z systems of the uncoupled 0th-order equations

$$\tilde{y}^{\circ}_{s}(t) + 2\xi_s \omega_s \dot{y}^{\circ}_{s}(t) + \omega_s^2 y^{\circ}_{s}(t) = p^{\circ}_{s}(t) \ , \tag{4.63}$$

$Z \times V$ systems of the uncoupled 1st-order equations ($v = 1, \ldots, V$)

$$\tilde{y}^{:v}_{s}(t) + 2\xi_s \omega_s \dot{y}^{:v}_{s}(t) + \omega_s^2 y^{:v}_{s}(t) = p^{:v}_{s}(t) \ , \tag{4.64}$$

Z systems of the uncoupled 2nd-order equations

$$\tilde{y}^{(2)}_{s}(t) - 2\xi_s \omega_s \dot{y}^{(2)}_{s}(t) + \omega_s^2 y^{(2)}_{s}(t) = p^{(2)}_{s}(t) \ , \tag{4.65}$$

Summation over index z is not implied in Eqs. (4.63)–(4.65); the following notation is used

$$y^{\circ}_{s}(t) = Q_{s\beta} q^{\circ}_{\beta}(t), \qquad y^{:r}_{s}(t) = Q_{s\beta} q^{:r}_{\beta}(t), \qquad y^{(2)}_{s}(t) = Q_{s\beta} q^{(2)}_{\beta}(t), \tag{4.66}$$

$$p^{\circ}_{s}(t) = Q_{s\alpha} f^{\circ}_{\alpha}(t), \qquad p^{:v}_{s}(t) = Q_{s\alpha} p^{:v}_{\alpha}(t), \qquad p^{(2)}_{s}(t) = Q_{s\alpha} p^{(2)}_{\alpha}(t), \tag{4.67}$$

Similarly to the case of the coupled systems with correlated random variables expressed by Eqs. (4.24)–(4.26), having solved uncorrelated systems of Eqs. (4.54)–(4.56) the 2nd-order accurate expectations and the 1st-order accurate covariances for the nodal displacements and for the components of the element strain and stress tensors can be obtained respectively as:

for displacement

$$E(q_\alpha) = q^o_\beta(t) + q^{(2)}_\beta(t) \ , \tag{4.68}$$

$$Cov(q_\alpha, q_\beta) = \sum_{v=1}^{V} q^v_\alpha q^v_\beta Var(c^v) \ , \tag{4.69}$$

for strain

$$E(\varepsilon^e_{ij}) = B^{(e)}_{ij\alpha}(q^o_{\alpha(e)} + q^{(2)}_{\alpha(e)}) \ , \tag{4.70}$$

$$Cov(\varepsilon^e_{ij}, \varepsilon^f_{kl}) = \sum_{v=1}^{V} B^{(e)}_{ij\alpha} B^{(f)}_{kl\beta} q^v_{\alpha(e)} q^v_{\beta(f)} Var(c^v) \ , \tag{4.71}$$

for stress

$$E(\sigma^e_{ij}) = C^{\alpha(e)}_{ijkl} E(\varepsilon^e_{kl}) + \frac{1}{2} \sum_{v=1}^{V} \left(2C^{,v(e)}_{ijkl} q^v_{\alpha(e)} + C^{,vv(e)}_{ijkl} q^o_{\alpha(e)} \right) B^{(e)}_{kl\alpha} Var(c^v) \ , \tag{4.72}$$

$$Cov(\sigma^e_{ij}, \sigma^f_{kl}) = \sum_{v=1}^{V} \left(C^{\alpha(e)}_{ijmn} C^{\alpha(f)}_{klgh} q^v_{\alpha(e)} q^v_{\beta(f)} + C^{,v(e)}_{ijmn} C^{,v(f)}_{klgh} q^o_{\alpha(e)} q^o_{\beta(f)} + \right.$$

$$\left. + C^{,v(e)}_{ijmn} C^{\alpha(f)}_{klgh} q^v_{\alpha(e)} q^o_{\beta(f)} + C^{\alpha(e)}_{ijmn} C^{,v(f)}_{klgh} q^o_{\alpha(e)} q^v_{\beta(f)} \right) B^{(e)}_{mn\alpha} B^{(f)}_{gh\beta} Var(c^v) \ . \tag{4.73}$$

4.5.2 Fast Fourier Transform and Secularity Elimination

The 2nd-order expansion of random functions can produce invalid solutions due to the appearance of secular terms which grow indefinitely with time. Such unbounded solution may occur even for systems that are known to possess bounded solution, such as conservative systems. It is seen that the natural frequencies are the same for the 0th-, 1st- and 2nd-order equations. This is also the case for the transformed or/and uncoupled equations. The 0th-order equations are only excited by external forces so generally no resonance occurs. But the 1st- and 2nd-order forcing sequences are functions of 0th-order response that ensure resonant excitation until the transient part of the 0th-order solution is damped away. Hence, a simple application of the 2nd-order perturbation method whereby only the amplitude is altered may not always be satisfactory; and the resonant part involved on the right hand sides of the 1st- and 2nd-order equations has to be removed or weighted to maintain validity of the solution. In other words, a modification to prevent the formation of

the secular terms must alter both the amplitude and the period of vibration. Some theoretical methodologies have been developed in [16,106,111,118]. However, little work has been done on the numerical elimination of secularities for multi-degrees of freedom systems. An efficient technique developed has been [96], in which the sine and cosine transform pair have been used. The numerical algorithm presented below is an alternative form of the above: the forcing sequence is composed and treated as a complex-valued sequence of half length, and the fast Fourier transform (FFT) [26] is carried out on the complex-valued sequence. Since FFT is one of the most important tools to probabilistic problems it is worth to summarize the main ideas and distinguishing advantages of the modern computational technique. In what follows in this section the notation of summation over repeated indices is not implied.

Base-2 Fast Fourier Transform

It is known that the Fourier transform is a universally accepted tool of modern analysis. Generally the Fourier transform pair is defined as

$$P(\omega) = a_1 \int_{-\infty}^{+\infty} p(t) \exp(-\mathrm{i}\omega t)\, dt \ , \tag{4.74}$$

$$p(t) = a_2 \int_{-\infty}^{+\infty} P(\omega) \exp(\mathrm{i}\omega t)\, d\omega \ , \tag{4.75}$$

where $a_1 a_2 = 1/2\pi$. The coefficients are assumed depending on the user. Some set $a_1 = 1$, $a_2 = 1/2\pi$, [21]; others set $a_1 = a_2 = (1/2\pi)^{1/2}$, or set $a_1 = 1/2\pi$, $a_2 = 1$, [102]. To be consistent with the definition of the Laplace transform the Fourier transform pair can be defined as, [14,18]

$$P(f) = \int_{-\infty}^{+\infty} p(t) \exp(-\mathrm{i}\, 2\pi f t)\, dt \ , \tag{4.76}$$

$$p(t) = \int_{-\infty}^{+\infty} P(f) \exp(\mathrm{i}\, 2\pi f t)\, df \ , \tag{4.77}$$

where $f = \omega/2\pi$. It is more convenient to use the foregoing equations for description of the FFT procedures but it would be confusing in physical interpretation and application. For this reason Eqs. (4.76),(4.77) are chosen in this paragraph and Eqs. (4.74),(4.75) will be used for discussions related to the secularity elimination in the next paragraph. Theoretically the infinite-range transform $P(f)$ of Eq. (4.76) will not exist for any $p(t)$ which represents a random quantity when the infinite limits are used. By restricting the limit to a finite time interval $[0, T]$ the finite-range Fourier transform will exist as defined by

$$P(f,T) = \int_0^T p(t) \exp(-\mathrm{i}\, 2\pi f t)\, dt \ . \tag{4.78}$$

Assume that $p(t)$ is recorded at L equally points a distance Δt apart, i.e.

$$p(t) = p_j(t) = p(j\Delta t) \ , \qquad j = 0, 1, \ldots, L-1 \ . \tag{4.79}$$

For arbitrary f Eq. (4.78) can then be expressed in the discretized form as

$$P(f,T) = \Delta t \sum_{j=0}^{L-1} p_j \exp(-\mathrm{i}\, 2\pi j f \Delta t) \ . \tag{4.80}$$

Selecting discrete frequency values for the approximation of $P(f,T)$

$$f_k = kf = \frac{k}{T} = \frac{k}{L\Delta t} \ , \qquad k = 0, 1, \ldots, L-1 \ , \tag{4.81}$$

the transformed values of the Fourier transform can be written as

$$P_k = \frac{1}{\Delta t} P(f_k, T) = \sum_{j=0}^{L-1} p_j \exp(-\mathrm{i}\, 2\pi j k / L) \ . \tag{4.82}$$

The fast Fourier transform is designed to determine the quantities P_k (Fourier analysis); and can also be used to calculate the coefficients p_j by an inverse transform of Eq. (4.82) (Fourier synthesis). Let

$$W(u) = \exp(-\mathrm{i}\, 2\pi u / L) \ , \tag{4.83}$$

and note that

$$W(L) = 1 \ , \qquad W(u+v) = W(u)\, W(v) \ , \tag{4.84}$$

then Eq. (4.82) becomes

$$P_k = \sum_{j=0}^{L-1} p_j \, W(jk) \ , \qquad k = 0, 1, \ldots, L-1 \ . \tag{4.85}$$

Eq. (4.82),(4.85) can be treated as the Fourier transform of p_j when p_j is described by a sequence of length L. Thus the computations require a total of L^2 complex multiply-add operations. Note that one complex multiply-add is equivalent to four real multiply-adds. We shall consider the case when the sequence p_j is of length of power two since with $L = 2^\beta$, β integer valued, FFT is shown to be most efficient.

Let us observe that when $L = 2^\beta$ every integer (index) j, $0 \le j \le L-1$, has a unique representation of the binary form

$$j \equiv (j_{\beta-1}, j_{\beta-2}, \cdots, j_0) = \sum_{\alpha=0}^{\beta-1} 2^\alpha j_\alpha \ , \tag{4.86}$$

where j_α is the remainder in the successive division of j by 2. In Fortran, for instance, we can write the expression of j_α as

$$j_\alpha = \mathrm{mod}\,(\underbrace{j/2/2\ldots/2}_{(\alpha+1)\text{ times}})\,, \tag{4.87}$$

Note that j_α has only the value 0 or 1. As an example, with $L = 16 = 2^4$ and $j = 13$ we get

$$13_{\text{decimal}} = 2^3 . 1 + 2^2 . 1 + 2^1 . 0 + 2^0 . 1 = 1101_{\text{binary}} \equiv (1,1,0,1)\,. \tag{4.88}$$

Using Eq. (4.86), Eq. (4.82) can be expressed in the binary form

$$P(j_{\beta-1}, j_{\beta-2}, \ldots, j_0) = \sum_{k_0=0}^{1}\sum_{k_1=0}^{1}\cdots\sum_{k_{\beta-1}=0}^{1} p(k_{\beta-1}, k_{\beta-2}, \ldots, k_0)\times$$

$$\times\, W\left(\sum_{\alpha=0}^{\beta-1} 2^\alpha j_\alpha \sum_{\alpha=0}^{\beta-1} 2^\alpha k_\alpha\right) \tag{4.89}$$

From Eq. $(4.84)_2$ W(.) involved in Eq. (4.89) can be rewritten as

$$W\left(\sum_{\alpha=0}^{\beta-1} 2^\alpha j_\alpha \sum_{\alpha=0}^{\beta-1} 2^\alpha k_\alpha\right) = W\left(2^{\beta-1} k_{\beta-1} \sum_{\alpha=0}^{\beta-1} 2^\alpha j_\alpha\right) \times$$

$$\times\, W\left(2^{\beta-2} k_{\beta-2} \sum_{\alpha=0}^{\beta-1} 2^\alpha j_\alpha\right) \ldots W\left(k_0 \sum_{\alpha=0}^{\beta-1} 2^\alpha j_\alpha\right)\,. \tag{4.90}$$

Remembering Eq. $(4.84)_1$ and the assumption that $L = 2^\beta$ the first term of Eq. (4.90) can be decomposed to give

$$W\left(2^{\beta-1} k_{\beta-1} \sum_{\alpha=0}^{\beta-1} 2^\alpha j_\alpha\right) = W(2^\beta 2^{\beta-2} j_{\beta-1} k_{\beta-1}) W(2^\beta 2^{\beta-3} j_{\beta-2} k_{\beta-1}) \ldots$$

$$\ldots\, W(2^\beta j_1 k_{\beta-1})\, W(2^{\beta-1} j_0 k_{\beta-1}) = W(2^{\beta-1} j_0 k_{\beta-1})\,, \tag{4.91}$$

since $2^{\beta-2} j_{\beta-1} k_{\beta-1}$, $2^{\beta-3} j_{\beta-2} k_{\beta-1}$ and $j_1 k_{\beta-1}$ are integer-valued expressions. This equation represents the main idea behind FFT and not only the case with $L = 2^\beta$. Similarly, decomposition of the second term of Eq. (4.90) leads to

$$W\left(2^{\beta-2}k_{\beta-2}\sum_{\alpha=0}^{\beta-1}2^{\alpha}j_{\alpha}\right) = W(2^{\beta}2^{\beta-3}j_{\beta-1}k_{\beta-2})\,W(2^{\beta}2^{\beta-4}j_{\beta-2}k_{\beta-2})\dots$$

$$\dots\, W(2^{\beta-1}j_1k_{\beta-2})\,W(2^{\beta-2}j_0k_{\beta-2}) = W\left((2j_1+j_0)2^{\beta-1}k_{\beta-2}\right)\,, \qquad (4.92)$$

As the procedure proceeds over the terms (except for the last one) of Eq. (4.90), at each step a new term which does not vanish by the condition of Eq. (4.84), is added. This decomposition process continues until the last term is reached so that Eq. (4.89) takes the form

$$P(j_{\beta-1},j_{\beta-2},\dots,j_0) = \sum_{k_0=0}^{1}\sum_{k_1=0}^{1}\dots\sum_{k_{\beta-1}=0}^{1} p_0(k_{\beta-1},k_{\beta-2},\dots,k_0)\,W(2^{\beta-1}j_0k_{\beta-1})\times$$

$$\times\, W\left((2j_1+j_0)2^{\beta-2}k_{\beta-2}\right)\dots\, W\left((2^{\beta-1}j_{\beta-1}+2^{\beta-2}j_{\beta-2}+\dots+j_0)k_0\right)\,. \qquad (4.93)$$

Carrying out each of the summations in Eq. (4.93) corresponding to the indices $k_{\beta-1}$, $k_{\beta-2},\dots,k_0$ of Eq. (4.93) separately and labeling the intermediate results leads to the recursive equations

$$p_1(j_0,k_{\beta-2},\dots,k_0) = \sum_{k_{\beta-1}=0}^{1} p_0(k_{\beta-1},k_{\beta-2},\dots,k_0)\,W(2^{\beta-1}j_0k_{\beta-1})\,,$$

$$p_2(j_0,j_1,k_{\beta-3},\dots,k_0) = \sum_{k_{\beta-2}=0}^{1} p_1(j_0,k_{\beta-2},\dots,k_0)\,W\left((2j_1+j_0)2^{\beta-2}k_{\beta-2}\right)\,,$$

$$\dots \qquad \dots \qquad \dots$$

$$p_{\beta}(j_0,j_1,\dots,j_{\beta-1}) = \sum_{k_0=0}^{1} p_{\beta-1}(j_0,j_1,\dots,k_0)\,W\left(k_0\sum_{\alpha=0}^{\beta-1}2^{\alpha}j_{\alpha}\right)\,,$$

$$P(j_{\beta-1},j_{\beta-2},\dots,j_0) = p_{\beta}(j_0,j_1,\dots,j_{\beta-1})\,. \qquad (4.94)$$

These equations are referred to as the Cooley-Tukey algorithm of the base-2 FFT, [26]. The extensions to the case for L chosen according to other criteria than $L = 2^{\beta}$ can be found in [14,18,31,29]. It is seen that the summation in the i-th equation of Eqs. (4.94) contains only one complex multiply-add operation with the summation index $k_{\beta-i} = 1$, since if $k_{\beta-i} = 0$ then $W(uk_{\beta-i}) = 1$. Further, since it can be shown in discrete Fourier transform that there exist the relation $W(u) = -W(u + L/2)$. The total number of complex multiply-add operations is then $L\beta/2$. Recall that $\beta = \ln L$ and the total number of complex multiply-add operations required in the traditional Fourier transform is equal to L^2, the

base-2 FFT reduces the computation cost $0(L/\ln L)$ times. In general case when $L = u_1 u_2 \dots u_j \neq 2^s$ this relation is equal to $0[L/(u_1 + u_2 + \dots + u_j)]$, [29]. That is why in many areas of application such as time-series and spectral analysis, telecommunication, etc. these algorithms have caused a complete change of attitude toward what can be done by using Fourier or Laplace methods on a computer.

Elimination of Secular Terms

Let us now consider a time-varying force function $f(t)$, $t \in [0, T]$, approximated by a discretized time sequence

$$f(t) \approx f_n(t) \equiv f(t_n) = f(n\Delta t) \ , \tag{4.95}$$

$$n = 0.1, \dots, 2L \ , \qquad 2L\Delta t = T \ .$$

To remove the resonant part from the time sequence, a complex-valued sequence $p(t)$ is generated from the real-valued sequence f_n

$$p(t) \approx p_k(t) \equiv p(t_k) = f(t_{2k}) + \mathrm{i}\, f(t_{2k+1}) \ , \qquad k = 0, 1, \dots, L \ , \tag{4.96}$$

where L is the number of the Fourier's degrees of the transform (the complex sequence length). The fast Fourier analysis on a complex-valued sequence can then be performed to determine the discretized, one-sided Fourier spectrum $P(\omega)$ of the time sequence $p_k(t)$ in the form of a discretized frequency sequence

$$P(\omega) \approx P_j(\omega) \equiv P(\omega_j) =$$

$$= \frac{T}{L} \sum_{k=0}^{L-1} p(t_k) \exp(-\mathrm{i}\,\omega_j t_k) = \frac{T}{L} \sum_{k=0}^{L-1} p_k \exp(-\mathrm{i}\, 2\pi jk/L) \ , \tag{4.97}$$

with

$$\omega_j = j\Delta\omega \ , \qquad 0 \leq \omega_j \leq \omega_{nyq} \ , \qquad j, k = 0, 1, \dots, L \ . \tag{4.98}$$

In the foregoing expressions ω_{nyq} is the highest frequency that appears in the record data. It is referred to as the Nyquist cutoff or folding frequency, [14], and given by

$$\omega_{nyq} = \frac{2\pi L}{T} = \frac{\pi}{\Delta t} \ . \tag{4.99}$$

Symbol $\Delta\omega$ denotes frequency increment, which must be appropriately chosen to avoid the possibility of serious errors due to aliasing or folding effects that may occur in simulation of spectrum records [13]. It is important that these data have no significant mean square value in the frequency range above Nyquist cutoff frequency prior to digital conversion. Thus the allowable value of the frequency increment used to simulate a frequency sequence reads

$$\Delta\omega \leq \frac{\omega_{nyq}}{L} \ . \tag{4.100}$$

It is observed that since the modal forcing records in Eqs. (4.64),(4.65) are already uncoupled, only the corresponding j-th natural frequency will produce secularity. To remove the secular terms the coefficients $P_j(\omega)$ of the frequency sequence which lie within a specified range of the modal system are eliminated or weighted accordingly, thereby removing the resonant part from Fourier spectra. In other words, the coefficients corresponding to the Fourier analysis frequencies ω_a that are very close to the j-th natural frequency ω_a are almost entirely eliminated (modified), whereas the coefficients separated from this frequency are unaffected. Therefore, with the Fourier analysis the transform coefficients of a frequency sequence are assumed to cause secularities when the following condition is met

$$(\omega_a - r) \leq \omega_j \leq (\omega_a + r) \ , \tag{4.101}$$

where r is a specified range. Applicable frequency weighting functions are given below, [111,118]

triangular

$$P_j := P_j \mid \omega_a - \omega_j \mid /r \ , \tag{4.102}$$

cosine

$$P_j := P_j\{1 - \cos[\pi(\omega_a - \omega_j)/2r]\} \ , \tag{4.103}$$

cosine-2

$$P_j := P_j\{1 - \cos[\pi(\omega_a - \omega_j)/r]\} \ , \tag{4.104}$$

Once the frequency sequence is weighted, the inverse Fourier transform (Fourier synthesis) is carried out to recover the time sequence, i.e. the complex-valued forcing record with no resonant part

$$p_k(t) = \frac{1}{T}\sum_{j=0}^{L-1} P(\omega_j)\exp(\mathrm{i}\omega_j t_k) = \frac{1}{T}\sum_{j=0}^{L-1} P_j \exp(\mathrm{i}\,2\pi jk/L) \ , \tag{4.105}$$

and consequently, the real-valued forcing sequences in which the secular terms have been eliminated can be recovered from the real and imagine parts of the complex-valued forcing sequence

$$f_{2k}(t) = \mathrm{Re}\, p_k(t)\,, \qquad f_{2k+1}(t) = \mathrm{Im}\, p_k(t)\,, \qquad k = 0, 1, \ldots, L\,. \tag{4.106}$$

As will be shown below in the numerical examples, the secular terms are eliminated using FFT on the sequences of length $L = 2^{10}$, that is the computer time would be reduced about 100 times. A minor drawback of the stochastic finite element applications in dynamics is that its accuracy deteriorates for large times even with slight structural damping. To ensure that all statistical results are valid for long response time and to save acceptable computation cost, there is a substantial need to incorporate an effective algorithm for secularity elimination in any stochastic finite element code. In this regard, use of FFT is most suitable.

4.6 Numerical Results

The procedures described above have been employed in the finite element code POLSAP to include new options for stochastic analysis. The extended version would be a new tool for static and dynamic analysis of medium-scale systems such as truss-beam-plate-shell structures with uncertainties in material, geometry and loading parameters. The structural eigenproblem and the standard eigen-orthogonalization problem for the correlated random variables are solved simultaneously and can be saved in back-up storage to restart subsequent computations. At the element level the first and second derivatives of the mass, damping, stiffness and load with respect to the random variables are evaluated, transformed into the uncorrelated space and assembled in the global coordinates. Five types of the random variables can be considered: cross-sectional area or length of the 3D-truss and 3D-beam elements, thickness of the plate and shell elements, Young modulus and mass density for all the element groups. In the equation solution phase, the 0th-, 1st- and 2nd-order systems are parallelly integrated by the two-fold superposition technique. The right hand sides of these equations are calculated at element level and elimination of the secular terms, if any, is performed by FFT pairs. Having solved 0th-, 1st- and 2nd-order nodal displacements, the 2nd-order accurate expectations and 1st-order accurate covariances of the nodal displacements, element strains and stresses are evaluated and output in the tabular form as discretized-time sequences of dynamic response.

Example 9 Let us first consider the static response of a two-element cantilever bar subjected to axial loads, Fig. 4.1. Deterministic input data given for two members of the bar, respectively, are as follows. Cross-sectional area: $a_1 = 4$, $a_2 = 2$; length $l_1 = 15$, $l_2 = 10$; load $f_1 = 200$, $f_2 = 250$. Randomness in Young modulus is assumed with the expectations $e_1 = 3000$, $e_2 = 2500$ and the covariance matrix of the random variables is given by

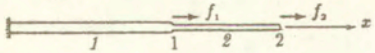

Figure 4.1: 2-element bar.

$$Cov(e_1, e_2) = \begin{bmatrix} 2.5 \times 10^5 & 2.0 \times 10^5 \\ symm. & 1.6 \times 10^5 \end{bmatrix} .$$

The computed expectations and covariances of displacements at the nodes 1 and 2 are obtained as

$$E(q_1) = 0.561187 , \qquad E(q_2) = 1.060723 ,$$

$$Cov(q_1, q_2) = \begin{bmatrix} 8.789162 \times 10^{-3} & 1.628906 \times 10^{-3} \\ symm. & 3.018906 \times 10^5 \end{bmatrix} .$$

It is easy to check that almost identical result can be obtained by an analytical approach.

Example 10 In this example the deflections of a simply supported square plate and a clamped square plate with random thickness subjected to a concentrated center load are examined. Deterministic input data are: side lengths $l = 100$, Young modulus $e = 1.0 \times 10^7$, Poisson ratio $\nu = 0.3$, load $f = 100$. The expectation of the thickness $E[t(x,z)]$ is equal to 1.0 and the homogeneous autocovariance function of the thickness is assumed to be

$$Cov\,[t(x_r, z_r), t(x_s, z_s)] = \sigma^2 \exp\left(\frac{x_r - x_s}{d_x}\right)^2 \exp\left(\frac{z_r - z_s}{d_z}\right)^2 ,$$

where the standard deviation $\sigma = 0.1$, d_x and d_z are the decay factors in the x and z directions and determined from the end-point correlations $R[t(x_o, z), t(x_1, z)]$ and $R[t(x, z_o), t(x, z_1)]$ (see [87] for detail). In each problem the thicknesses at various points are perfectly correlated and the deflections at the center of the plates are calculated. Because of symmetry only a quarter of the plates is considered and discretized by a 8×8-element mesh. The POLSAP's solutions are compared with the solutions based on the basic random variable technique (BRV) [87], Tab. 4.1. Since with the stochastic finite element model the thickness of each element is modeled as a random variable, the finite element mesh controls the accuracy of the thickness approximation and the accuracy of the displacement interpolation. This can be less efficient than the BRV because the displacement field is usually more complex than the covariances of the thickness. On the other hand, in the BRV more difficult integrals must be evaluated due to the higher order polynomials. Moreover, the accuracy of the covariances depends on the number of Legendre functions used in the approximation and adaptation of the procedures to existing deterministic finite

	POLSAP	BRV
Simple plate		
Expectation	0.013112	0.013386
Std. deviation	0.003473	0.003894
Fixed plate		
Expectation	0.006205	0.006467
Std. deviation	0.001592	0.001877

Table 4.1: Square plate. Stochastic statics.

element codes is not straightforward, particularly if a large class of different random variables are simultaneously required.

Example 11 The statement of the example is depicted in Fig. 4.2a. The two degrees of freedom spring-mass system is modeled through a two-element cantilever bar with concentrated masses. Deterministic input data are: structural masses $m_1 = 0.372$, $m_2 = 0.248$; stiffness-proportional damping factor $\xi = 0.03$, sinusoidal forcing function $f(t) = 25.0 \times 10^6 \sin(2000t)$. The random spring constants are normally distributed with expectations $k_1 = 24.0 \times 10^6$, $k_2 = 12.0 \times 10^6$; the coefficient of variation α is equal to 0.1. The system of eight equations is solved by the combination of the mode superposition method and the Wilson-θ algorithm ($\theta = 1.4$) for each of the uncoupled modal equations. The number of time intervals is equal to 1024, with the time increment $\Delta t = 1.2 \times 10^5$. The elimination of secularities is performed on sequences of 1024 Fourier's degrees and the frequency range r is equal to 0.15 of the first natural frequency. The expectation and standard deviation of the displacement at the free end of the system are plotted in Figs. 4.2b,4.2c, in comparison with the results obtained by the Monte Carlo simulation (MCS). It is seen that the expectation computed by POLSAP compares well with the MCS [94], whereas difference in the variance is more significant due to the different frequency ranges used for eliminating secularities.

Example 12 Consider effects of the secularity elimination on the solution in the problem of wave propagation in an 1D bar,Fig. 4.3a. Deterministic input data are: cross-sectional area $a_r = 6$, length $l = 1000$, mass density $\varrho = 0.00776$, Heaviside's forcing function $f(t) = 25.0 \times 10^4$. The expectation, correlation function and coefficient of variation of the Young modulus e_r of the bar are assumed as follows:

$$E(e_r) = e_o + (1 + \vartheta x_r / l)\,, \qquad e_o = 3.0 \times 10^7\,, \qquad \vartheta = 0.1\,,$$

$$R(e_r, e_s) = \exp(0.1 \mid x_r - x_s \mid / l)\,, \qquad \alpha = 0.1\,.$$

Bar is approximated by 32-element system, i.e. $r, s = 1, \ldots, 32$. Eight lowest structural modes are used. The number of time intervals is equal to 1024, with the time

increment $\Delta t = 1.0 \times 10^{-3}$ for the expectation solution and $\Delta t = 2.8 \times 10^{-4}$ for the covariance solution. The elimination of secularities is performed on sequences of 1024 Fourier's degrees. The effect of the elimination of the secular terms on the computed expectations and variances at the free end of the bar is shown in Figs. 4.3b,4.3c and Fig. 4.4. The results are obtained for the cases of undamped and damped systems (different values of the damping factor equal to 0.0, 0.2, 0.4) and different values of the frequency range ($r = 0.0, 0.17, 0.30$) to eliminating the secular terms. It is observed that only eight highest modes, which correspond to the eight largest variances from the set of 32-uncorrelated random modes, are sufficient to approximate the random field with an error less than 1.5 per cent. The total computer time for the problem was 430 sec., out of which 43 sec. were spent on solving the structural eigenproblem, 50 sec. on the transformation from the correlated random variables to the uncorrelated random variables and 56 sec. on eliminating secularities. By using the Monte Carlo simulation method 800 randomly generated realizations would be required to obtain results of the same order accuracy; and it would take about 12 hours of the computation time when the problem were solved by the direct step-by-step integration technique.

The distinguishing feature of the stochastic finite element analysis is that it involves the discretization of the parameter space of random fields. With local average across each element (random variable) it is easy to incorporate any specified mean, variance and correlation structure into existing deterministic finite element codes, because the stochastic finite element procedures essentially involve solution of a set of deterministic problems. Since the same system matrices such as mass, damping and stiffness (and consequently, the effective stiffness matrix) corresponding to the expectations of random variables appear on all the left hand sides of the 0th-, 1st- and 2nd-order equations, their assemblage and decomposition need to be performed only once and the computations are thereby much more reduced. Further, it is well known in dynamic analysis of deterministic systems that the application of the mode superposition method has definitive advantage by using several lowest modes to describe the system response. This is more important in stochastic analysis, especially for medium- or large-scale structures since the direct approaches seem to be unavailable in the context of the computational cost. Also, the reduction from the double summation to single summation in calculations of the right hand sides of the 1st- and 2nd-order equations through the transformation of random variables from the correlated field to a uncorrelated field enables us to deal only with diagonal matrix operations instead of full matrix multiplications. In terms of the computational implementation the fact that only a few highest modes (normalized variances and shapes) can accurately approximate almost all probabilistic properties of discretized random variables has in practice the same significance as that of the mode superposition in dynamic analysis.

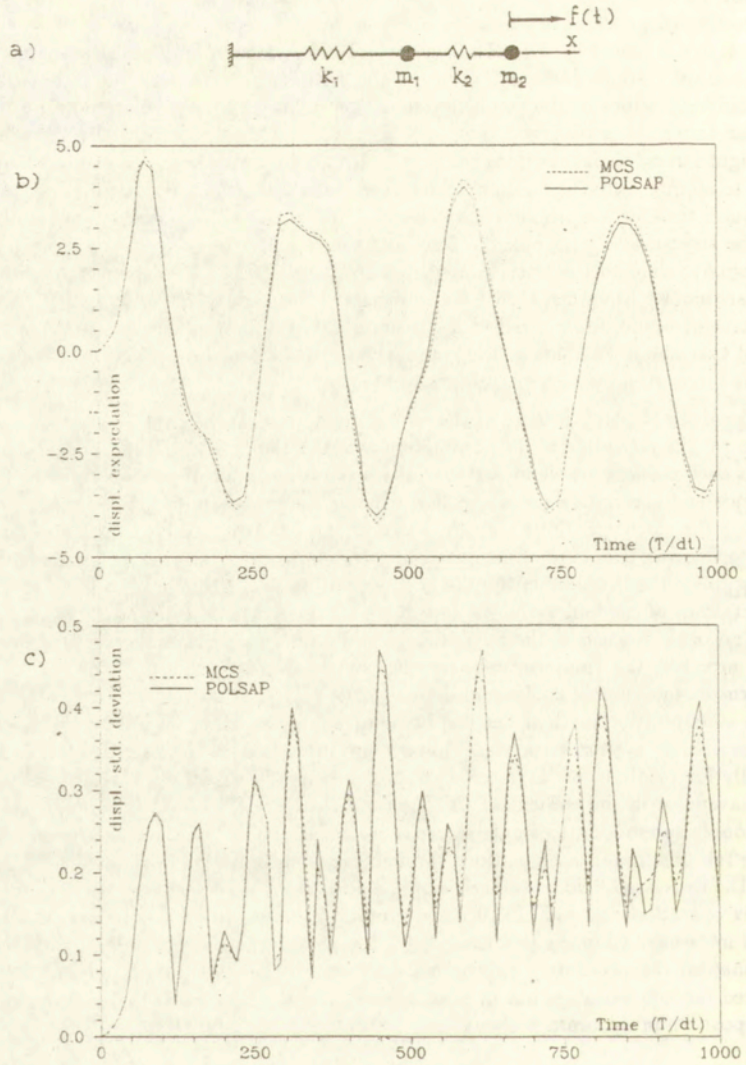

Figure 4.2: Spring-mass system. Stochastic dynamic response

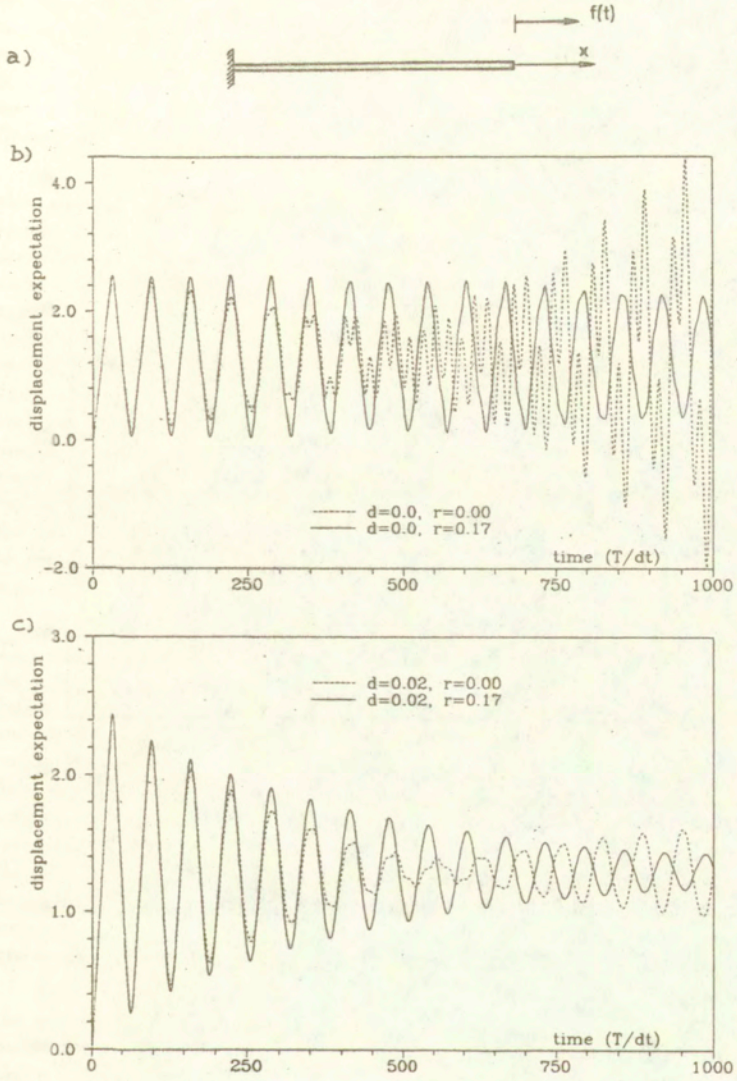

Figure 4.3: 32-element beam. Stochastic dynamic response.

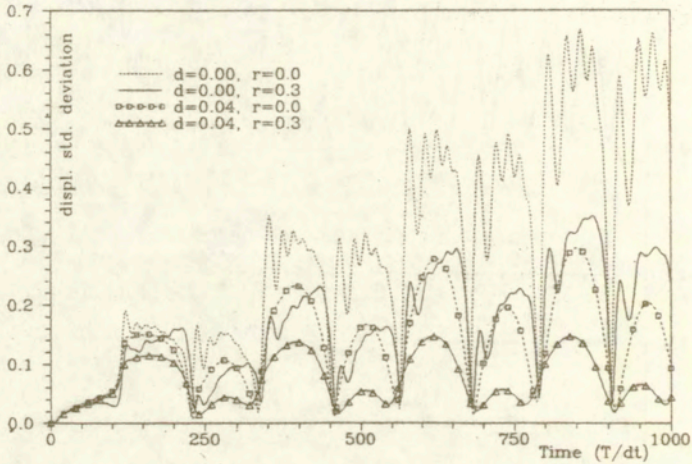

Figure 4.4: 32-element beam. Secularity elimination effects.

Summarizing Remarks

The fact that variational formulations based on the Hamilton's principle have the advantage of dealing only with purely scalar energy quantities and the application of this principle leads directly to the equations of motion for any given system enable us to treat structural uncertainties in many aspects. The probabilistic features can be incorporated in a concise way and consequently easily implemented into existing deterministic finite element codes. This is the main advantage of the stochastic Hamilton's principle proposed in this chapter.

In stochastic finite element analysis only the first two moments of random variables are need to be known, whereas the statistical techniques such as the Monte Carlo simulation or Hermite-Gauss quadrature generally require knowledge of probability density functions that are usually not available in practice. The Monte Carlo technique requires a large number of samples randomly generated from a suitable normal approximation of the probabilistic distribution. With the Hermite-Gauss method the number of simulations grows exponentially with respect to the numbers of random variables and integration points. The number of solutions required in the stochastic finite element processing is equal only to the number of random variables plus two; and it is applicable to both the homogeneous and inhomogeneous random fields. Although this nonstatistical technique is most effectively used when the variances are small, it performs quite well when the response shows a large coefficient of variation (up to 0.15). With the transformation from the correlated space to the uncorrelated space of random variables and the change of basis from the finite element coordinates to the modal coordinates the stochastic finite element technique seems to offer the most efficient tool for stochastic analysis of structures.

The randomness discussed here is described by discretized random variables. The structure and load parameters are often continuous functions in space. When there exists randomness associated with these parameters we have discretized random fields; and the 1st- and 2nd-order solutions of the stochastic finite element equations are themselves the 1st- and 2nd-order response sensitivities. In this context, the computer performance of random field problems are similar to that of discretized design field problems considered in Chapter 2 *and* Chapter 3. *Therefore: 1) the computational aspects in sensitivity problems such as generating the derivative matrices, formation of the right hand sides of equations, finite element mesh, computations at the element level, etc. remain valid and can be directly accounted to work out effective algorithms for random analysis, 2) the above enables us to treat in a consistent way a new class of problems of computational mechanics in which design parameters are random. This will be presented in* Chapter 5 *and* Chapter 6.

The above procedures are more conveniently applied to problems related directly to the probabilistic distributions of the nodal displacements rather than to the first two moments of the element strains or stresses. This direct method would be expensive if the number of random variables was greater than the number of the first two moments of strain or stress requested. For this case an alternative technique similar to the adjoint variable approach used in sensitivity analysis could be developed.

5 Stochastic Structural Sensitivity of Static Response

5.1 Scope of the Chapter

In the preceding chapters the structural design sensitivity of deterministic systems and the structural response of stochastic systems were formulated as separate areas of structural mechanics in the finite element context. If a system is stochastic then its sensitivity functions are referred to as stochastic sensitivity functions. It seems interesting and practically important to estimate structural response sensitivity with respect to probabilistic variations in design parameters. Such a formulation seems to be non-existent in the available literature in contrast to a substantial literature on structural sensitivity of deterministic systems and displacement-stress response of stochastic systems. As shown in Chapter 2 and Chapter 3 the structural sensitivity in deterministic analysis deals with the change in the system behaviour due to design-parameter variations, namely it determines values of the coefficients of the structural response gradient with respect to design variables; the adjoint variable approach rather than the direct variable approach can be effectively used for this class of problems. On the other hand, to incorporate randomness into traditional structural analysis the second moment method is employed in deterministic finite elements and the stochastic finite element technique turns out to be numerically much more efficient than the statistical techniques such as Monte Carlo simulations or Hermite-Gauss quadrature schemes, Chapter 4. In fact, both the adjoint variable and second moment techniques are based on the perturbation approach; this enables us to treat problems of structural sensitivity for stochastic systems in a natural manner. The stochastic sensitivity problems developed in this and next chapter are thus concerned with the change of structural parameters due to uncertainties in these parameters, i.e. to evaluate probabilistic distributions of the sensitivity gradient coefficients. In this chapter we shall consider the structural sensitivity problem of stochastic systems under static loads. The follow-up Chapter 6 deals with the dynamic case. As we shall see, structural sensitivity and stochastic analyses are both similar in terms of the methodology and computer implementation which greatly facilitates the combined analysis. The computations are much more less costly when based on the transformation from the correlated space of random variables to a uncorrelated space. Numerical algorithms have been worked out and shown to be readily adapted to existing deterministic finite element codes. A new option for sensitivity analysis in structural statics has been supported by the computer code POLSAP and used to solve a number of illustrative examples.

MODEL PROBLEM OF CHAPTER 5

Given ◁ vector of design variables $h(x)$, x – spatial coordinates
(for example: cross-sectional area, thickness, length, Young modulus)
◁ expectations and covariances of random variables $b(x)$,
(for example: cross-sectional area, thickness, length, Young modulus)
◁ displacement-expressed finite element equilibrium equations $F(x, h, b) = 0$

Find ▷ expectations and covariances of design sensitivity gradient coefficients

5.2 Finite Element Formulation

Consider structural response of the linear-elastic system with N degrees of freedom described by the functional

$$\phi = G[q(h,b),h] \ . \tag{5.1}$$

and the system equilibrium equations

$$K_{\alpha\beta}(h,b)q_\beta(h,b) = f_\alpha(h,b) \ , \qquad \alpha,\beta = 1,\ldots,N \ , \tag{5.2}$$

where $h = \{h^e\}$, $e = 1,\ldots,E$ and $b = \{b^r\}$, $r = 1,\ldots,R$, are the vectors of design variables and random variables. Some or all components in the vectors h and b can coincide. Symbols $K_{\alpha\beta}(h,b)$, $f_\alpha(h,b)$ and $q = \{q_\beta\} = q_\beta(h,b)$ represent the system stiffness matrix, the vectors of external loads and nodal displacements, respectively. Since uncertainties in geometry and material properties of the system members are taken on account, the stiffness, load and displacement are random functions; $K_{\alpha\beta}(h,b)$and $f_\alpha(h,b)$ are generally explicit functions of random and design variables, whereas $q = \{q_\beta\} = q_\beta(h,b)$ is implicit function of these variables. The objective of stochastic analysis of structural sensitivity is to evaluate the probabilistic distributions of the change in the structural response functional of Eq. (5.1) with the equilibrium condition of Eq. (5.2) to design variations, i.e. to find the spatial expectations and covariances of the sensitivity gradient coefficients of this functional.

Since the design variables and random variables appear in the coefficients of the linear operator the system equations are generally nonlinear as random functions of state and design. Suppose that the functions $K_{\alpha\beta}(h,b)$, $f_\alpha(h,b)$ (and consequently $q(h,b)$) are continuously differentiable with respect to h^e and b^r. This guarantees the system response to be as smooth as the dependence on random and design variables in the equilibrium equations. Similarly to the deterministic case differentiation of Eq. (5.1) by the Leibnitz's rule with respect to the design variables h^e leads to

$$\phi^{,e} = G^{,e} + G_{,\beta}q^{,e}_\beta \ . \tag{5.3}$$

Recall that symbols $(.)^{,e}$ and $(.)_{,\beta}$ denote the first partial derivatives with respect to the $e-$th design variable and the β-th nodal displacement, respectively. In order to write Eq. (5.3) explicitly in terms of variations in design variables the adjoint technique is employed. Defining an adjoint vector $\lambda = \{\lambda_\beta(b)\}$, $\beta = 1,\ldots,N$, which is taken to be independent of design variables, and noting that the stiffness matrix is assumed to be positive definite and symmetric, the adjoint system equations take the form, (cf.Eq. (2.7))

$$K_{\alpha\beta}\lambda_\beta = G_{,\alpha} \ , \tag{5.4}$$

From Eq. (5.4) it is obvious that the adjoint variables $\lambda_\beta(b)$ are implicit random function of random variables b^r. The coefficients of the sensitivity gradient of the structural response functional can then be obtained as

$$o^e = G^{,e} + \lambda_\alpha(f^{,e}_\alpha - K^{,e}_{\alpha\beta}q_\beta) \ . \tag{5.5}$$

It is observed that so far the derivation of the stochastic sensitivity problem and the deterministic sensitivity problem are formally identical. We have two similar pairs of structural and adjoint systems of the equations which represent the equilibrium conditions and design constraints. The only difference between Eqs. (5.2),(5.4) and Eqs. (2.2),(2.7) is that all the quantities involved in the former are random functions whereas the functions included in the latter are deterministic. To incorporate into the analysis uncertainties of structural material, geometry and load the stochastic finite element technique described in Chapter 4 now can be employed. From the equilibrium conditions of Eq. (5.2) we then obtain a system of the 0th-, 1st- and 2nd-order equations similar to Eqs. (4.28)–(4.30). To ensure the compatibility with the discretized random field b^r, the vector of adjoint variables $\lambda_\alpha(b)$ is also approximated by the 2nd-order perturbation technique using an expansion similar to Eq. (4.40) for the adjoint vector. To be consistent with the finite element displacements q_β, the resulting terms that represent the 0th-, 1st- and 2nd-order adjoint coordinates can then be interpolated by the same shape functions used to discretize the displacement field. Further, for the random functions $G_{,\beta}$, $G^{,e}$, $K^{,e}_{\alpha\beta}$, $f^{,e}_\alpha$, the Taylor expansion is done via the 2nd-order perturbation about the spatial expectations b^r_o of the random variables b^r with the small parameter θ to get

$$G_{,\beta}(h,b) = G^o_{,\beta}(h) + \theta G^{,r}_{,\beta}(h)\Delta b^r + \frac{1}{2}\theta^2 G^{,rs}_{,\beta}(h)\Delta b^r\Delta b^s \ , \tag{5.6}$$

$$G^{,e}(h,b) = G^{o,e}(h) + \theta G^{,e,r}(h)\Delta b^r + \frac{1}{2}\theta^2 G^{,e,rs}(h)\Delta b^r\Delta b^s \ , \tag{5.7}$$

$$K^{,e}_{\alpha\beta}(h,b) = K^{o,e}_{\alpha\beta}(h) + \theta K^{,e,r}_{\alpha\beta}(h)\Delta b^r + \frac{1}{2}\theta^2 K^{,e,rs}_{\alpha\beta}(h)\Delta b^r\Delta b^s \ , \tag{5.8}$$

$$f^{,e}_\alpha(h,b) = f^{o,e}_\alpha(h) + \theta f^{,e,r}_\alpha(h)\Delta b^r + \frac{1}{2}\theta^2 f^{,e,rs}_\alpha(h)\Delta b^r\Delta b^s \ , \tag{5.9}$$

$$i,j = 1,\ldots,N \ , \quad e = 1,\ldots,E \ , \quad r,s = 1,\ldots,R \ ,$$

where symbols $(.)^{o,e}$, $(.)^{e,r}$ and $(.)^{e,rs}$ represent the expectation, first and second partial derivatives of functions $(.)^e$ with respect to random variables and evaluated at their expectations, respectively. Recall that $(.)^e$ denotes the first partial derivative with respect to design variables and that functions with superscript 'o' are deterministic, whereas functions with superscripts '$,r$' and '$,rs$' are random. These random functions can be expressed through the probabilistic characteristics of random variables defined by Eq. (4.1)–(4.5). The functions including the partial derivatives of stiffness and loading with respect to random variables can be calculated exactly by partial differentiation, by the finite difference technique or by the least square fit method, as mentioned in Chapter 4. The partial derivatives $G^o_{,\beta}$, $G^r_{,\beta}$, $G^{rs}_{,\beta}$, $G^{o,e}$, $G^{e,r}$ and $G^{e,rs}$ can be generally calculated by the finite differences or the least square fits, since they are implicit functions of random variables. In view of the above considerations, by collecting terms of order 0, θ and θ^2, the 0th-, 1st- and 2nd-order equilibrium equations of the structure and adjoint systems can be respectively obtained as:

one pair of the 0th-order equilibrium equations

$$K^o_{\alpha\beta} q^o_\beta = f^o_\alpha \ , \tag{5.10}$$

$$K^o_{\alpha\beta} \lambda^o_\beta = G^o_{,\alpha} \ , \tag{5.11}$$

R pairs of the 1st-order equilibrium equations ($r = 1, \ldots, R$)

$$K^o_{\alpha\beta} q^r_\beta = f^r_\alpha - K^r_{\alpha\beta} q^o_\beta \ , \tag{5.12}$$

$$K^o_{\alpha\beta} \lambda^r_\beta = G^r_{,\alpha} - K^r_{\alpha\beta} \lambda^o_\beta \ , \tag{5.13}$$

one pair of the 2nd-order equilibrium equations

$$K^o_{\alpha\beta} q^{(2)}_\beta = \frac{1}{2} \left(f^{rs}_\alpha - 2K^r_{\alpha\beta} q^s_\beta - K^{rs}_{\alpha\beta} q^o_\beta \right) Cov(b^r, b^s) \ , \tag{5.14}$$

$$K^o_{\alpha\beta} \lambda^{(2)}_\beta = \frac{1}{2} \left(G^{rs}_{,\alpha} - 2K^r_{\alpha\beta} \lambda^s_\beta - K^{rs}_{\alpha\beta} \lambda^o_\beta \right) Cov(b^r, b^s) \ , \tag{5.15}$$

with $r, s = 1, \ldots, R$, $\alpha, \beta = 1, \ldots, N$; $q^{(2)}_\beta$ and $K^o_{\alpha\beta}$, $K^r_{\alpha\beta}$, $K^{rs}_{\alpha\beta}$ are given in Eq.(4.27) and Eqs.(4.33),(4.36),(4.39); and

$$\lambda^{(2)}_\beta = \frac{1}{2} \lambda^{rs}_\beta Cov(b^r, b^s) \ . \tag{5.16}$$

Having solved systems of Eqs. (5.10)–(5.15) the probabilistic distributions for the sensitivity gradient coefficients of structural response can be evaluated. By definition the spatial expectations and covariances of the sensitivity gradient coefficients are written as

$$E(\phi^{,e}) = \int_{-\infty}^{+\infty} \phi^{,e} g(b^r)\, db^r \ , \tag{5.17}$$

$$Cov(\phi^{,e}, \phi^{,f}) = \int_{-\infty}^{+\infty}\int_{-\infty}^{+\infty} [\phi^{,e} - E(\phi^{,e})][\phi^{,f} - E(\phi^{,f})] g(b^r, b^s)\, db^r\, db^s \ . \tag{5.18}$$

Substituting Eq. (5.5) into Eqs. (5.17), (5.18) leads to

$$E(\phi^{,e}) = E(G^{,e}) + E(f_\alpha^{,e}\lambda_\beta) - E(K_{\alpha\beta}^{,e} q_\beta \lambda_\alpha) \ , \tag{5.19}$$

$$Cov(\phi^{,e}, \phi^{,f}) = \int_{-\infty}^{+\infty}\int_{-\infty}^{+\infty} [G^{,e} + (f_\alpha^{,e} - K_{\alpha\beta}^{,e} q_\beta)\lambda_\alpha - E(\phi^{,e})]$$
$$[G^{,f} + (f_\zeta^{,f} - K_{\zeta\zeta}^{,f} q_\zeta)\lambda_\zeta - E(\phi^{,f})] g(b^r, b^s)\, db^r\, db^s \ . \tag{5.20}$$

Employing the expansion equations for the random functions q_β, λ_β, $K_{\alpha\beta}^{,e}$, $f_\alpha^{,e}$ and $G^{,e}$ into Eqs. (5.19),(5.20), retaining variations of b^r up to the 2nd-order terms yields the 2nd-order accurate expectations and the 1st-order accurate covariances of the sensitivity gradient coefficients as follows

$$E(\phi^{,e}) = G^{o,e} + \frac{1}{2} G^{,e,rs} Cov(b^r, b^s) + \mathcal{A}_\alpha^e(\lambda_\alpha^o + \lambda_\alpha^{(2)}) -$$
$$- K_{\alpha\beta}^{o,e} q_\beta^{(2)} \lambda_\alpha^o + (\mathcal{B}_\alpha^{er}\lambda_\alpha^{,r} + \mathcal{C}_\alpha^{ers}\lambda_\alpha^o) Cov(b^r, b^s) \ , \tag{5.21}$$

$$Cov(\phi^{,e}, \phi^{,f}) = [G^{,e,r} G^{,f,s} + (G^{,e,r}\mathcal{A}_\alpha^f + G^{,f,r}\mathcal{A}_\alpha^e)\lambda_\alpha^{,s} +$$
$$+ (G^{,e,r}\mathcal{B}_\alpha^{fs} + G^{,f,r}\mathcal{B}_\alpha^{es})\lambda_\alpha^o + \mathcal{A}_\alpha^e\mathcal{A}_\beta^f\lambda_\alpha^{,r}\lambda_\beta^{,s} +$$
$$+ (\mathcal{A}_\alpha^e\mathcal{B}_\beta^{fr} + \mathcal{A}_\beta^f\mathcal{B}_\alpha^{er})\lambda_\alpha^{,s}\lambda_\beta^o + \mathcal{B}_\alpha^{er}\mathcal{B}_\beta^{fs}\lambda_\alpha^o\lambda_\beta^o] Cov(b^r, b^s) \ , \tag{5.22}$$

where the following notation is used

$$\mathcal{A}_\alpha^e = f_\alpha^{o,e} - K_{\alpha\beta}^{o,e} q_\beta^o \ , \tag{5.23}$$

$$\mathcal{B}_\alpha^{er} = f_\alpha^{,e,r} - K_{\alpha\beta}^{o,e} q_\beta^{,r} - K_{\alpha\beta}^{,e,r} q_\beta^o \ , \tag{5.24}$$

$$\mathcal{C}_\alpha^{ers} = \frac{1}{2}(f_\alpha^{,e,rs} - 2K_{\alpha\beta}^{,e,r} q_\beta^{,s} - K_{\alpha\beta}^{,e,rs} q_\beta^o) \ , \tag{5.25}$$

$$e, f = 1, \ldots, E \ , \qquad r, s = 1, \ldots, R \ , \qquad \alpha, \beta = 1, \ldots, N \ .$$

Note that the second moment function of the sensitivity gradient coefficients can be expressed in the form of Eq. (5.22) if only we observe that: 1) the terms involving the first variation vanish by the definition of the first two moments, 2) the covariance matrix $Cov(b^r, b^s)$ of random variables is symmetric, and, 3) repeated indices are dummy. The system of Eqs. (5.10)–(5.15) and Eqs. (5.21),(5.22) gives a closed form of the stochastic structural sensitivity problem in the finite element context. This model requires only $2(R+2)$ solutions of algebraic equation systems while the number of sampled systems need to be solved in a statistical scheme would be about 2×1.000 or more to obtain the same order accurate results.

5.3 Computational Implementation

It is seen from Eqs. (5.10)–(5.15) that once the 0th-order nodal displacements and adjoint variables q°_{β} and λ°_{β} are known, the 1st- and 2nd-order displacement and adjoint vectors q^{r}_{β}, λ^{r}_{β} and $q^{(2)}_{\beta}$, $\lambda^{(2)}_{\beta}$ can be found in a sequential manner. In fact, the solution process can be performed in parallel for these 0th-, 1st- and 2nd-order unknowns since the coefficient matrices on the left hand sides of Eqs. (5.10)–(5.15) are identical. Thus, the solution of the structure and adjoint equations involves one decomposition given by Eq. (1.23) and $2(R+2)$ forward reductions and backward substitutions, Eq. (1.24). The latter computations include two solutions for q°_{β} and λ°_{β}, 2R solutions for q^{r}_{β} and λ^{r}_{β} and two solutions for $q^{(2)}_{\beta}$ and $\lambda^{(2)}_{\beta}$. Although the above procedures are compatible with the finite element software and even almost all operations required to calculate right hand sides of the 2nd-order equations can be carried out by vector multiplications and at the element level, the computation cost would remain unacceptably high since the matrix multiplications are equal to $0[2(R+2)]$ due to the double summations in establishing the right hand sides of the 2nd-order equations (5.14),(5.15) and evaluating the probabilistic distributions of sensitivity gradients, Eq. (5.21),(5.22).

To overcome this situation, reducing the double summations to single summations so that the number of the multiplications are equal to $0(R)$, the correlated covariance matrix $Cov(b^{r}, b^{s})$ can be transformed to a diagonal (uncorrelated) variance $Var(c^{v})$ through a standard eigensolution. This technique of transformation from a set of correlated random variables to a uncorrelated set is numerically similar to the modal analysis widely used in structural dynamics and is described in Section 4.5.1. Recall that in case of various groups of uncertainties involved in the system vector of correlated variables, uncorrelation of these types must be assumed; and each dominant part taken from every group is used to assemble the system vector of uncorrelated variables. Employing this transformation in Eqs. (5.10)–(5.15) the mixed derivatives reduce to the second derivatives whereas the double summation from 1 to R reduce to the single summation from 1 to V. Thus, by the implementation of the uncorrelated random variables c^{v}, the 0th-, 1th- and 2nd-order correlated systems of the structure and adjoint equations reduce to corresponding uncorrelated systems. We have:

one pair of the uncorrelated 0th-order equilibrium equations

$$K^{\circ}_{\alpha\beta} q^{\circ}_{\beta} = f^{\circ}_{\alpha} \,, \tag{5.26}$$

$$K^{\circ}_{\alpha\beta} \lambda^{\circ}_{\beta} = G^{\circ}_{\cdot\alpha} \,, \tag{5.27}$$

V pairs of the uncorrelated 1st-order equilibrium equations ($v = 1, \ldots, V$)

$$K^{\circ}_{\alpha\beta} q^{v}_{\beta} = f^{v}_{\alpha} - K^{v}_{\alpha\beta} q^{\circ}_{\beta} \,, \tag{5.28}$$

$$K^{\circ}_{\alpha\beta} \lambda^{v}_{\beta} = G^{v}_{\cdot\alpha} - K^{v}_{\alpha\beta} \lambda^{\circ}_{\beta} \,, \tag{5.29}$$

one pair of the uncorrelated 2nd-order equilibrium equations

$$K^{o}_{\alpha\beta} q^{(2)}_{\beta} = \frac{1}{2} \sum_{v=1}^{V} \left(f^{,vv}_{\alpha} - 2K^{,v}_{\alpha\beta} q^{,v}_{\beta} - K^{,vv}_{\alpha\beta} q^{o}_{\beta} \right) Var(c^{v}) \ , \tag{5.30}$$

$$K^{o}_{\alpha\beta} \lambda^{(2)}_{\beta} = \frac{1}{2} \sum_{v=1}^{V} \left(G^{,vv}_{\alpha} - 2K^{,v}_{\alpha\beta} \lambda^{,v}_{\beta} - K^{,vv}_{\alpha\beta} \lambda^{o}_{\beta} \right) Var(c^{v}) \ , \tag{5.31}$$

where $\alpha, \beta = 1, \ldots, N$; symbols $(.)^{,v}$, $(.)^{,vv}$ denote the first and second derivatives with respect to the uncorrelated random variables c^{v}, $q^{(2)}_{\beta}$ is given in Eq.(4.57), $K^{o}_{\alpha\beta}$, $K^{,v}_{\alpha\beta}$ and $K^{,vv}_{\alpha\beta}$ are determined form Eqs.(4.33),(4.36),(4.39) and Eqs.$(4.53)_2$, $Var(c^{v})$ from Eqs.$(4.53)_4$; and

$$\lambda^{(2)}_{\beta} = \frac{1}{2} \sum_{v=1}^{V} \lambda^{,vv}_{\beta} Var(c^{v}) \ , \tag{5.32}$$

Having solved systems of Eqs. (5.26)–(5.31) the first two moments of the sensitivity gradient coefficients given by Eqs. (5.21),(5.22) can now be rewritten as

$$E(\phi^{,\epsilon}) = G^{o,\epsilon} + \frac{1}{2} G^{,\epsilon,vv} Var(c^{v}) + \mathcal{A}^{\epsilon}_{\alpha} (\lambda^{o}_{\alpha} + \lambda^{(2)}_{\alpha}) - $$

$$- K^{o,\epsilon}_{\alpha\beta} q^{(2)}_{\beta} \lambda^{o}_{\alpha} + \sum_{v=1}^{V} (\mathcal{B}^{\epsilon v}_{\alpha} \lambda^{,v}_{\alpha} + \mathcal{C}^{\epsilon vv}_{\alpha} \lambda^{o}_{\alpha}) Var(c^{v}) \ , \tag{5.33}$$

$$Cov(\phi^{,\epsilon}, \phi^{,f}) = \sum_{v=1}^{V} [G^{,\epsilon,v} G^{,f,v} + (G^{,\epsilon,v} \mathcal{A}^{f}_{\alpha} + G^{,f,v} \mathcal{A}^{\epsilon}_{\alpha}) \lambda^{,v}_{\alpha} +$$

$$+ (G^{,\epsilon,v} \mathcal{B}^{fv}_{\alpha} + G^{,f,v} \mathcal{B}^{\epsilon v}_{\alpha}) \lambda^{o}_{\alpha} + \mathcal{A}^{\epsilon}_{\alpha} \mathcal{A}^{f}_{\beta} \lambda^{,v}_{\alpha} \lambda^{,v}_{\beta} +$$

$$+ (\mathcal{A}^{\epsilon}_{\alpha} \mathcal{B}^{fv}_{\beta} + \mathcal{A}^{f}_{\beta} \mathcal{B}^{\epsilon v}_{\alpha}) \lambda^{,v}_{\alpha} \lambda^{o}_{\beta} + \mathcal{B}^{\epsilon v}_{\alpha} \mathcal{B}^{fv}_{\beta} \lambda^{o}_{\alpha} \lambda^{o}_{\beta}] Var(c^{v}) \ , \tag{5.34}$$

where

$$\mathcal{B}^{\epsilon v}_{\alpha} = f^{,\epsilon,v}_{\alpha} - K^{o,\epsilon}_{\alpha\beta} q^{,v}_{\beta} - K^{,\epsilon,v}_{\alpha\beta} q^{o}_{\beta} \ , \tag{5.35}$$

$$\mathcal{C}^{\epsilon vv}_{\alpha} = \frac{1}{2} (f^{,\epsilon,vv}_{\alpha} - 2K^{,\epsilon,v}_{\alpha\beta} q^{,v}_{\beta} - K^{,\epsilon,vv}_{\alpha\beta} q^{o}_{\beta}) \ , \qquad \textit{(no sum on } v\textit{)} \tag{5.36}$$

$$\epsilon, f = 1, \ldots, E \ , \qquad v = 1, \ldots, V \ , \qquad \alpha, \beta = 1, \ldots, N \ .$$

Similar to the solution of Eq. (5.10)–(5.15) only one stiffness matrix is assembled and factorized for Eq. (5.26)–(5.31) and parallel computations can also be used. The system of Eq. (5.26)–(5.31), however, requires only $2(V+2)$ solutions of algebraic equations. Since only a few highest modes of $Var(c^{v})$, $v = 1, \ldots, V \ll R$, are required to accurately approximate the main properties of many random quantities, the computation effort is significantly reduced.

5.4 Numerical Results

As describedin Chapter 2 and Chapter 4, the options for structural design sensitivity analysis of deterministic systems and for displacement-stress analysis of stochastic systems are supported by the finite element code POLSAP. On the basis of these two versions and of the computational formulation discussed above in this chapter, a combined numerical algorithm has been worked out and incorporated in POLSAP to deal with stochastic analysis of static sensitivity of truss-beam-shell structures. Four groups of random design variables can be considered: cross-sectional area and length of the 3D truss or 3D beam elements, thickness of the plate or shell elements, and Young modulus for all the three element types. To illustrate the preceding formulation we consider below some numerical examples.

Example 13 Consider the displacement and slope responses of a 100-element clamped-clamped beam of unit length $l = 1.0$, Fig. 5.1. As design variables we take element cross-sectional areas, wherein randomness is assumed. We have then a set of 100 random design variables a_r, $r = 1,\ldots,100$. The expectation, correlation function and coefficient of variation of the cross-sectional areas are given, respectively, as follows:

$$E(a_r) = a_o(1.0 + \vartheta x_r/l) \ , \qquad E(a_{100-r+1}) = E(a_r) \ ,$$

$$a_o = 5.0 \times 10^{-3} \ , \qquad \vartheta = 0.3 \ , \qquad r = 1,\ldots,50 \ ,$$

$$R(a_r, a_s) = \exp(- \mid x_r - x_s \mid /\lambda) \ , \qquad \lambda = 0.1 \ , \qquad r,s = 1,\ldots,100 \ ,$$

$$\alpha = 0.07 \ ,$$

where ordinates x_r are defined at mid-point of r-th element. The following deterministic data are adopted: distributed load $(f + \gamma a_o)$, with uniformly distributed load $f = 49.61$ per unit length, weight density $\gamma = 7.7126$; Young modulus $e = 2.0 \times 10^5$; Poisson ratio $\nu = 0.3$; moments of inertia $I_y = I_z = \beta E^2(a_r)$, $I_x = I_y + I_z$, $\beta = 1/6$. The response functional is defined as

$$\phi = \int_0^1 \delta(x - x^*) y(x)\, dx \ .$$

With the unit values of given allowable displacement and slope at the mid-point of the beam, interpreting the Dirac delta function as a unit load applied at $x = x^* = 0.5$, the adjoint beam is subjected to a unit concentrated force at x^* for the case of the displacement analysis and to a unit moment at x^* for the case of the slope analysis. With the expectations of the vertical displacement and the slope at the mid-point of the beam -1.411097×10^{-2} and 2.076255×10^{-3} (compared against the values of -1.390371×10^{-2} and 2.044906×10^{-3} of the deterministic case) the expectations and standard deviation of the sensitivity coefficients of the both cases are given in Fig. 5.1, in which they are compared against deterministic results for the cases of varying and constant cross-sectional areas and against the exact solution, [53]. It is noted that relative differences in the expected and deterministic values of the

sensitivities are several times bigger than the differences of the displacements. The computation time was about 420 sec. for each case (compared against 35 sec. for the deterministic solution).

Example 14 This example concerns the displacement and slope responses of the clamped beam given in Fig. 5.2. The beam is of unit length $l = 1.0$ and of constant cross-sectional area $a = 0.005$; it is subjected to uniformly distributed load $(f + \gamma a)$, with $f = 49.61$, $\gamma = 7.7126$; Poisson ratio $\nu = 0.3$; moments of inertia $I_y = I_z = \beta a^2$, $I_x = I_y + I_z$, $\beta = 1/6$. The response functional has the form similar to that of the above example. The admissible displacement and slope at the mid-point of the beam are given as 0.02 and 0.02. As random design variables we take element Young moduli e_r, $r = 1, \ldots, 100$. The expectation, correlation function and coefficient of variation of the Young moduli are given, respectively, as follows:

$$E(e_r) = e_o(1.0 + \vartheta x_r/l) \ , \qquad E(e_{100-r+1}) = E(e_r) \ ,$$

$$e_o = 2.0 \times 10^5 \ , \qquad \vartheta = 0.3 \ , \qquad r = 1, \ldots 50 \ ,$$

$$R(e_r, e_s) = \exp(- \mid x_r - x_s \mid /\lambda) \ , \qquad \lambda = 0.1 \ , \qquad r, s = 1, \ldots, 100 \ ,$$

$$\alpha = 0.09 \ ,$$

The numerical results are shown in Fig. 5.2. In both the preceding examples it can be observed that some perturbations in probabilistic distributions appear at $0.20 < x < 0.26$ and $0.74 < x < 0.80$. The sensitivity gradients decrease to zero, whereas the values of the coefficient of variation considerably increase. The stochastic finite element technique can be less efficient in this case, since the approximate displacement field is more complex than the discretized random field, the random design variables being modeled by taking local averages over each element.

Example 15 In this example the response of a thin shell structure is considered. Fig. 5.3 shows the half of a cylindrical shell clamped at boundaries under uniformly distributed pressure $f = 100.0$. The remaining input data are: radius $r = 4.0$, length $l = 9.6$, Young modulus $e = 1.0 \times 10^7$, Poisson ratio $\nu = 0.3$, allowable translation in z-direction $r_z = 0.01$. The response functional of the form similar to the that of Example 13 for two-dimensional case is defined and considered at the mid-point of the shell. Uncertainty in shell thickness t_r is assumed as:

$$E(t) = t_o = 0.1 \ ,$$

$$R(t_r, t_s) = \vartheta \exp[- \mid x_r - x_s \mid /\lambda] \exp[- \mid y_r - y_s \mid /\lambda] \ ,$$

$$\vartheta = 1.5/rl \ , \qquad \lambda = 2.5rl \ , \qquad \alpha = 0.1 \ .$$

Due to symmetry only one-quarter of the shell is considered. The finite element mesh includes 60 rectangular elements (60 random design variables), and the total number of degrees of freedom is 313. Tab. 5.1 and Fig. 5.3 give the computed values of the expectations and standard deviations of the sensitivity coefficients. The computation time was 611 sec.

El.	(1)	(2)	(3)	El.	(1)	(2)	(3)
1	.002852	.002882	.000339	36	-.083495	-.084376	.009899
2	-.005441	-.005498	.000649	37	-.131804	-.133194	.015627
3	-.029982	-.030298	.003556	38	-.035087	-.035457	.004150
4	-.055090	-.055671	.006533	39	.194803	.196857	.023098
5	-.066496	-.067197	.007886	40	.365612	.369468	.043354
6	-.061529	-.062178	.007298	51	.035007	.035375	.004152
7	-.032914	-.033262	.003906	52	.092122	..093093	.010921
8	.029378	.029688	.003485	53	.076855	.077665	.009112
9	.112316	.113500	.013318	54	.091088	.092048	.010801
10	.174356	.176194	.020673	55	.114183	.115387	.013542
31	.041778	.042218	.004953	56	.042881	.043333	.005093
32	.075451	.076247	.008945	57	-.237742	-.240249	.028193
33	.053064	.053623	.006291	58	-.781013	-.789250	.092616
34	.044044	.044508	.005222	59	-1.510115	-1.526042	.179078
35	.002877	.002908	.000331	60	-2.053181	-2.074836	.243493

Table 5.1: (1) Deterministic solution, (2) Expectation, (3) Standard deviation.

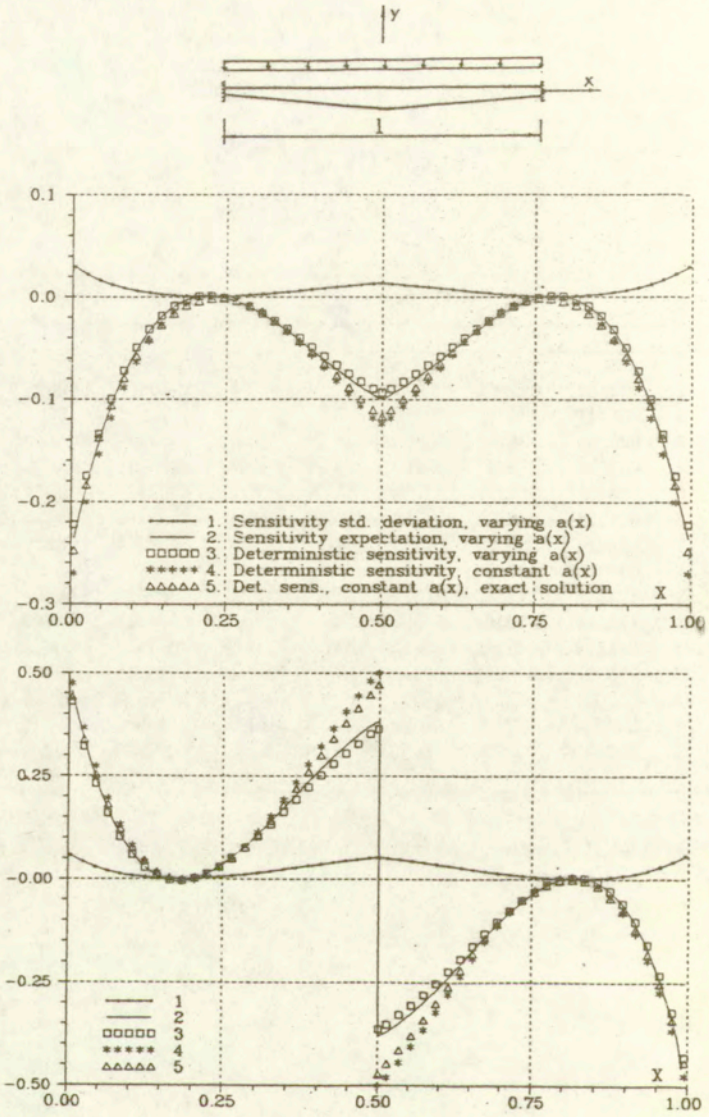

Figure 5.1: 100-element clamped beam. Cross-section as random design variable

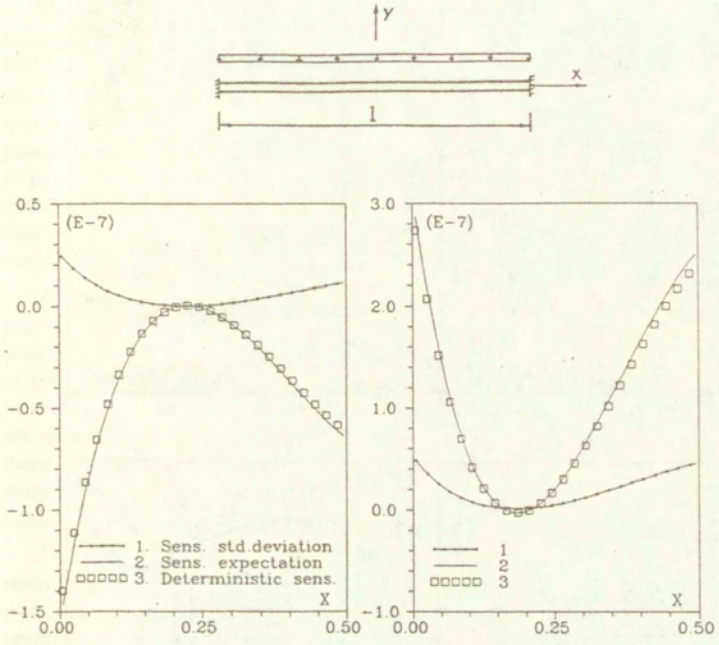

Figure 5.2: 100-element clamped beam. Young modulus as random design variable

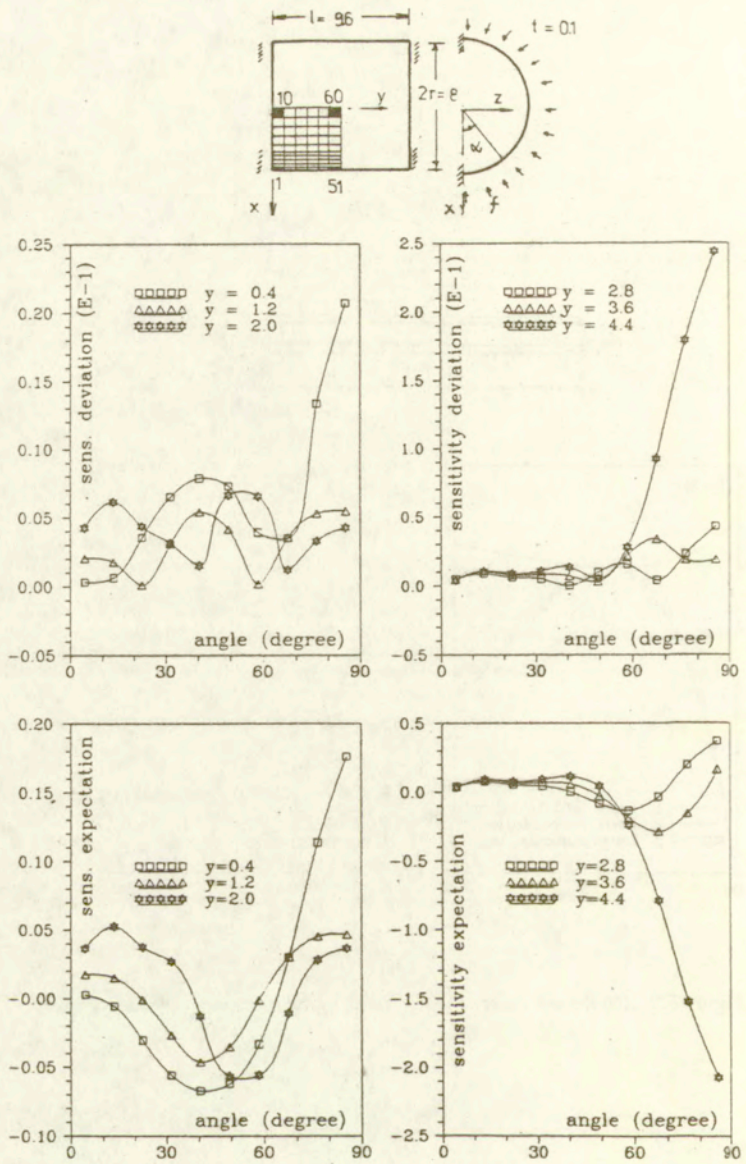

Figure 5.3: 60-element shell. Variations of sensitivity versus coordinates.

Summarizing Remarks

In this chapter a new important problem of computational mechanics was formulated. Structural design sensitivity (SDS) of the static response to stochastically described variations in design parameters seems to be an important subject which can be studied using current finite element technology. Since SDS and the stochastic finite elements (SFE) are closely related in problem statement, modelling and computer implementation, the stochastic sensitivity problem can be formulated and solved in a natural and consistent way.

Mathematically, both the formulations for SDS and SFE are based on the perturbation approach. If the first order perturbation is assumed, the models of SDS and SFE are almost identical, especially if the direct differentiation technique is used in SDS. Another common feature is that involving the discretization of the parameter spaces (of a design field for SDS and of a random field for SFE). This enables us to approximate both the two fields by the same (or compatible) interpolation functions. In particular, if a design variable and a random variable are both defined by the same quantity, the derivatives of the element stiffness and loads need to be generated only once and can be used simultaneously as the derivatives with respect to the design variable as well as to the random variable.

A disadvantage of the proposed model of SDS in the stochastic finite element context is that with local averages of random variables and design variables across each element, the finite element mesh controls the accuracy of the approximations of the random and design fields and therefore, of the displacement field. This can be inefficient, since the discretized displacement field is usually more complex than the discretized random and design fields; and SDS requires a finer finite element mesh than a typical displacement-stress problem does. To test the accuracy of the computed results it is essential and interesting to investigate the sensitivity of the density of finite element grids to the solutions.

The probabilistic features of SFE (for both the homogeneous and inhomogeneous random fields) and the design characteristics of SDS are translated entirely onto the right hand sides of the systems of the 0th-, 1st- and 2nd-order structure and adjoint equations. Thus the global stiffness matrix need to be assembled and factorized only once and both the structure and adjoint systems can be solved simultaneously and in parallel. Moreover, almost all calculations of the right hand sides and evaluations of the probabilistic distributions of the sensitivity gradient coefficients can be performed by vector multiplications at the element level.

With the transformation from correlated random variables to uncorrelated variables and by using only dominant parts of the transformed set, the algorithms worked out are effective even for PC-based stochastic sensitivity analysis of large-scale systems with the acceptable computation cost. Since almost all operations related to random quantities can be carried out by the procedures for deterministic calculations the algorithms developed can be immediately adapted to existing deterministic finite element programs.

6 Stochastic Structural Sensitivity of Dynamic Response

6.1 Scope of the Chapter

In Chapter 5 the problem of stochastic structural sensitivity was formulated for static case, i.e. for time-invariant systems. If loading is time-varying and the inertial and damping effects need to be taken on account in the formulation, the stochastic sensitivity functions are time-dependent and must be considered in the dynamic context. This chapter is thus devoted to the general case of stochastic response sensitivity analysis, i.e. to assessment of the change of spatial probabilistic distributions for time response sensitivity with respect to spatial probabilistic variations in design parameters. Such a methodology and a formulation for dynamic structural systems seem to be non-existent in the available literature, especially for multi-degrees of freedom systems and through the nonstatistical approach.

Before we start a brief discussion on the relationship between the sensitivity and reliability analysis seems to be in place. In reliability problems the design sensitivity concept is closely related to the so-called reliability index [99,131], which is defined as the smallest distance from the origin to the failure surface in a standard normal system. The index can be estimated for any failure mode of a structural member if the corresponding failure functions is given but it is much more complicated to estimate the probability of failure for the complete structure, since usually multivariate probability distributions can not be known. In the 1st-order reliability considerations the omission sensitivity factor was introduced [99] and applied to reduce the number of random design (basic) variables in the search for the most likely failure point. Instead of use of the mean values, the values based on the calculated asymptotic omission sensitivity factors are employed. For the class of reliability problems where the 1st-order reliability index is sufficiently accurate, the sensitivity factors can be used without reservation to evaluate the importance of uncertainties on design variables. However, the factors are not appropriate to omit variables for the 2nd-order reliability computations since they depend only on the location of the most likely failure point and not on the curvatures of the failure surface at this point. In the two papers devoted to structural sensitivity of stochastic systems [128,127], equations for the stochastic sensitivity function were established and the influence of changes in the initial conditions were discussed. In an analytical way the problem is formulated through a statistical scheme for the response sensitivity of a dynamic control system. As a result, a chaotic system is obtained for a limit cycle in the form of the Duffing's equation with a harmonic excitation, whose amplitude and

phase angle are random variables with uniform distribution sampled by a random number generator. The disadvantage of the formulation is that 1) the probability density function needs to be known, 2) the application to structural systems is not straightforward, 3) it could be developed for simple distributed-parameter systems and not for discretized-parameter systems of a large number of degrees of freedom.

This chapter is concerned with the structural response sensitivity of multi-degrees of freedom dynamic systems. Both the cases of sensitivity response over a time domain and at particular time instants presented in Chapter 3 for deterministic systems are considered here in the context of stochastic systems. The formal treatment is restricted in this chapter to the case of the terminal time condition given explicitly in terms of the terminal time; the formulation can be easily applied to the case of the terminal time condition given implicitly. The computational aspects of the problem are discussed in detail. Combined numerical algorithms based on the procedures developed for dynamic sensitivity analysis of deterministic systems (Chapter 3) and for forced-vibration analysis of stochastic systems (Chapter 4) have been worked out and shown to be readily adapted to existing deterministic finite element codes. A new option for sensitivity analysis in structural dynamics has been incorporated into the computer code POLSAP. A number of numerical examples illustrates the formulation and effectiveness of the algorithms.

MODEL PROBLEM OF CHAPTER 6

Given ◁ vector of design variables $h(x)$, x – spatial coordinates
(for example: cross-sectional area, thickness, length, Young modulus)
◁ expectations and covariances of random variables $b(x)$
(for example: cross-sectional area, thickness, length, Young modulus)
◁ displacement-expressed finite element equations of motion $F(x, h, b, t) = 0$

Find ▷ time-dependent expectations and covariances of design sensitivity gradient coefficients

6.2 Finite Element Formulation

Given a linear-elastic system with N degrees of freedom, consider the system response over a time domain $[0, T]$ described by the integral functional

$$\phi = \int_0^T G[q(h, b, t), h]\, dt \ , \tag{6.1}$$

and the system response at any time instant t, expressed in terms of a convolution of a time series of shifted impulses, (cf. Eq. (3.15))

$$\phi = \int_0^\infty G[q(h, b, t^*), h]\delta(t - t^*)\, dt^* = \int_0^t G[q(h, b, t - t^*), h]\delta(t^*)\, dt^* \ , \tag{6.2}$$

$$t^* \in [0.t] \ , \qquad t \in [0, T] \ ,$$

where $h = \{h^\epsilon\}$, $\epsilon = 1, \ldots, E$, and $b = \{b^r\}$, $r = 1, \ldots, R$, denote the vector of design variables and the vector of random variables; some or all components in the vectors h and b can coincide. The even function $\delta(.)$ is the Dirac distribution. The general forms of the structural response functionals of Eqs.(6.1),(6.2) can be used to represent or approximate most the cost or constraint quantities that measure structural response in practice. The nodal displacements $q = \{q_\beta\} = q_\beta(h, b, t)$ are implicit function of random and design variables and satisfy the equations of motion

$$M_{\alpha\beta}(h,b)\ddot{q}_\beta(h,b,t) + D_{\alpha\beta}(h,b)\dot{q}_\beta(h,b,t) + K_{\alpha\beta}(h,b)q_\beta(h,b,t) = f_\alpha(h,b,t)\,, \tag{6.3}$$

$$q_\beta(h,b,0) = 0\,, \qquad \dot{q}_\beta(h,b,0) = 0\,, \qquad \alpha,\beta = 1,\ldots,N\,,$$

where mass, damping, stiffness matrices and load vector, $M_{\alpha\beta}(h,b)$, $D_{\alpha\beta}(h,b)$, $K_{\alpha\beta}(h,b)$ and $f_\alpha(h,b,t)$ are generally explicit functions of random and design variables. The objective of dynamic analysis of stochastic design sensitivity is to determine the probabilistic distributions of the change in the structural response functionals of Eq. (6.1) or Eq. (6.2) with the constraint of Eq. (6.3) to design variations, i.e. to evaluate the time response of the spatial expectations and covariances of the sensitivity gradients of this functional.

Assume that the function $G(t^*)$ is continuous in the entire time domain $[0,T]$. Further, suppose that the functions $M_{\alpha\beta}(h,b)$, $D_{\alpha\beta}(h,b)$, $K_{\alpha\beta}(h,b)$, $f_\alpha(h,b,t)$ and consequently the solution of the dynamic problem $q_\beta(h,b,t)$ are continuously differentiable with respect to design variables h^ϵ and random variables b^r. Differentiation of Eqs. (6.1),(6.2) with respect to the design variables leads to

$$o^\epsilon = \int_0^T [G^\epsilon(h,b,t) + G_{,\beta}(h,b,t)q^\epsilon_\beta(h,b,t)]\,dt\,, \tag{6.4}$$

and

$$o^\epsilon = \int_0^T [G^\epsilon(h,b,t-t^*) + G_{,\beta}(h,b,t-t^*)q^\epsilon_\beta(h,b,t-t^*)]\delta(t^*)\,dt\,, \tag{6.5}$$

where symbols $(.)^\epsilon$ and $(.)_{,\beta}$ denote the first partial derivatives with respect to the ϵ−th design variable and the i-th nodal displacement, respectively. In order to write Eq. (6.3) explicitly in terms of variations in design variables, the adjoint approach is used. By defining an adjoint vector $\lambda = \{\lambda_\beta(b,t)\}$, $\beta = 1,\ldots,N$, which is taken to be independent of design, and with the derivations corresponding to that for Eqs. (3.11),(3.17) the adjoint systems are obtained leading to the terminal problems for the functionals of Eqs. (6.1),(6.2), respectively as

$$M_{\alpha\beta}(h,b)\ddot{\lambda}_\beta(b,\tau) - D_{\alpha\beta}(h,b)\dot{\lambda}_\beta(b,\tau) + K_{\alpha\beta}(h,b)\lambda_\beta(b,\tau) = G_\alpha(h,b,\tau)\,, \tag{6.6}$$

$$\lambda_\beta(b,T) = 0\,, \qquad \dot{\lambda}_\beta(b,T) = 0\,,$$

$$\tau \in [T,0]\,. \qquad \alpha,\beta = 1,\ldots,N\,.$$

and

$$M_{\alpha\beta}(h,b)\ddot{\lambda}_\beta(b,\tau) - D_{\alpha\beta}(h,b)\dot{\lambda}_\beta(b,\tau) + K_{\alpha\beta}(h,b)\lambda_\beta(b,\tau) = G_\alpha(h,b,t)\delta(\tau)\,, \quad (6.7)$$

$$\lambda_\beta(b,t) = 0\,, \qquad \dot{\lambda}_\beta(b,t) = 0\,,$$

$$\tau \in [t,0]\,, \qquad t \in [0,T]\,, \qquad \alpha,\beta = 1,\ldots,N\,.$$

The initial-terminal problem of the stochastic dynamic response sensitivity is formed by the original system of Eq. (6.3) and the adjoint system of Eq. (6.6) when a constraint functional is defined over a time domain (o.t.d. sensitivity) and by Eqs. (6.3),(6.7) for the case of a constraint on response and design parameters that must hold for all times (a.t.i. sensitivity). Eqs. (6.3),(6.6) or Eqs. (6.3),(6.7) give a unique solution for the probabilistic distributions of the states variables as well as random and design variables. The homogeneous initial conditions of Eq. (6.3) and terminal conditions of Eqs. (6.6),(6.7) are not restrictive, since nonhomogeneous initial (terminal) conditions can be treated by defining a new variable based on a particular solution that is a linear function of time to obtain an initial-terminal problem with homogeneous initial (terminal) conditions and with the right hand sides that involve two additional terms including the damping and stiffness matrices. This aspect has been discussed in Chapter 3 for deterministic systems and can be immediately employed in stochastic systems since the changed variables are defined in terms of design variables. Note that in Eq. (6.7) the time t is referred to as the running terminal time and the terminal conditions of this equation are evaluated at the running terminal instants. Therefore, for the case of dynamic response sensitivity at all time instants, we have a set of equations of motion of the adjoint system corresponding to the set of terminal time instants in the total time domain $[0,T]$. For convenience, here and below the notation $G(t)$ and $q(t)$ is used instead of $G[q(h,b,t),h]$ and $q(h,b,t)$.

Having solved Eqs. (6.3),(6.6) and Eqs. (6.3),(6.7), by the derivation similar to that for deterministic systems in Chapter 3, the expressions for the sensitivity gradient coefficients corresponding to the cost functionals of Eqs. (6.1),(6.2) can be written explicitly with respect to design variables as follows:

o.t.d. sensitivity gradient coefficients

$$\phi^{*} = \int_0^T \{G^{*}(t) + \lambda_\alpha(t)[f^{*}_\alpha(t) - M^{*}_{\alpha\beta}\ddot{q}_\beta(t) - D^{*}_{\alpha\beta}\dot{q}_\beta(t) - K^{*}_{\alpha\beta}q_\beta(t)]\}\,dt\,. \quad (6.8)$$

a.t.i. sensitivity gradient coefficients

$$\phi^{*}(t) = G^{*}(t) + \int_0^t \lambda_\alpha(t^{*})[f^{*}_\alpha(t^{*}) - M^{*}_{\alpha\beta}\ddot{q}_\beta(t^{*}) - D^{*}_{\alpha\beta}\dot{q}_\beta(t^{*}) - K^{*}_{\alpha\beta}q_\beta(t^{*})]\,dt\,, \quad (6.9)$$

$$t^{*} \in [0,t]\,, \qquad t \in [0,T]\,.$$

It is observed that Eq. (6.9) differs from Eq. (6.8) essentially by the appearance of the running terminal time t instead of the fixed terminal time T which is the last time instant of the time domain required in sensitivity analysis. That is, the solution of the a.t.i. sensitivity includes a set of convolution summations corresponding to the set of the running terminal time instants used to discretize the time domain $[0,T]$, whereas in the case of the o.t.d. sensitivity the solution requires only one integration to determine each sensitivity gradient coefficient. In addition, the adjoint variables $\lambda_\alpha(t^*)$ are unknowns of an adjoint system subjected to an impulse excitation in the form of the Dirac distribution and not to a time-varying forcing function in the normal sense as for the case of the original system of Eq. (6.6).

To incorporate into the formulation randomness in structural geometry, material and loading parameters, the Taylor series expansion truncated at the second order terms now can be used for the random functions in the stochastic finite element context. Similarly to the derivation presented in Chapter 4 for the linearized stochastic differential equations of motion, from Eq. (6.3) we get a system of 0th-, 1st- and 2nd-order equations. The resulting equations formally have similar form of Eqs. (4-24)–(4-27), since the same linear operator evaluated at the expectations of random variables appears on the left hand sides, and all the uncertainty properties of the system are translated to the right hand sides in terms of the 0th-, 1st- and 2nd-order nodal loads. The only difference between them is that in the former equations the mass, damping, stiffness matrices and the nodal accelerations, velocities, displacements and their first and second partial derivatives with respect to random variables are explicit or implicit functions of design variables. To be compatible with the random-parameter space b^r and to be consistent with the finite element coordinates $q_\beta(h,b,t)$, the vector of adjoint variables $\lambda_\beta(b,t)$ is also first expanded about the expectations $\lambda^o_\beta(b,t)$ with the small parameter θ retaining up to the 2nd-order perturbations, and then the resulting 0th-,1th- and 2nd-derivative terms are approximated by the same shape matrices used to interpolate the displacement field. Also, the 2nd-order perturbation is done correspondingly for the random functions G^*_β, G^*, $M^*_{\alpha\beta}$, $D^*_{\alpha\beta}$, $K^*_{\alpha\beta}$ and f^*_α in a way similar to that employed for Eq. (5.6)–(5.9). Substituting the above expansion equations into Eq. (6.6),(6.7) and equating equal order terms to obtain the 0th-, 1st- and 2nd-order systems of the structure equations and adjoint equations, leads to the initial-terminal problems of the o.t.d. sensitivity and a.t.i. sensitivity. We have:

• *initial problem, original system*

one system of the 0th-order equations

$$M^o_{\alpha\beta}\ddot{q}^o_\beta(t) + D^o_{\alpha\beta}\dot{q}^o_\beta(t) + K^o_{\alpha\beta}q^o_\beta(t) = f^o_\alpha(t)\ , \tag{6.10}$$

R systems of the 1st-order equations $(r = 1,\ldots,R)$

$$M^o_{\alpha\beta}\ddot{q}^r_\beta(t) + D^o_{\alpha\beta}\dot{q}^r_\beta(t) + K^o_{\alpha\beta}q^r_\beta(t) = \\ = f^r_\alpha(t) - [M^r_{\alpha\beta}\ddot{q}^o_\beta(t) + D^r_{\alpha\beta}\dot{q}^o_\beta(t) + K^r_{\alpha\beta}q^o_\beta(t)]\ , \tag{6.11}$$

one system of the 2nd-order equations

$$M^{\circ}_{\alpha\beta}\ddot{q}^{(2)}_{\beta}(t) + D^{\circ}_{\alpha\beta}\dot{q}^{(2)}_{\beta}(t) + K^{\circ}_{\alpha\beta}q^{(2)}_{\beta}(t) =$$
$$= \left\{\frac{1}{2}f^{rs}_{\alpha}(t) - [M^{r}_{\alpha\beta}\ddot{q}^{s}_{\beta}(t) + D^{r}_{\alpha\beta}\dot{q}^{s}_{\beta}(t) + K^{r}_{\alpha\beta}q^{s}_{\beta}(t)] - \right.$$
$$\left. - \frac{1}{2}[M^{rs}_{\alpha\beta}\ddot{q}^{\circ}_{\beta}(t) + D^{rs}_{\alpha\beta}\dot{q}^{\circ}_{\beta}(t) + K^{rs}_{\alpha\beta}q^{\circ}_{\beta}(t)]\right\} Cov(b^{r}, b^{s}) \ , \tag{6.12}$$

• *o.t.d. terminal problem, adjoint system:*

one system of the 0th-order equations

$$M^{\circ}_{\alpha\beta}\ddot{\lambda}^{\circ}_{\beta}(\tau) - D^{\circ}_{\alpha\beta}\dot{\lambda}^{\circ}_{\beta}(\tau) + K^{\circ}_{\alpha\beta}\lambda^{\circ}_{\beta}(\tau) = G^{\circ}_{\cdot\alpha}(\tau) \ , \tag{6.13}$$

R systems of the 1st-order equations ($r = 1, \ldots, R$)

$$M^{\circ}_{\alpha\beta}\ddot{\lambda}^{r}_{\beta}(\tau) - D^{\circ}_{\alpha\beta}\dot{\lambda}^{r}_{\beta}(\tau) + K^{\circ}_{\alpha\beta}\lambda^{r}_{\beta}(\tau) =$$
$$= G^{r}_{\cdot\alpha}(\tau) - [M^{r}_{\alpha\beta}\ddot{\lambda}^{\circ}_{\beta}(\tau) - D^{r}_{\alpha\beta}\dot{\lambda}^{\circ}_{\beta}(\tau) + K^{r}_{\alpha\beta}\lambda^{\circ}_{\beta}(\tau)] \ , \tag{6.14}$$

one system of the 2nd-order equations

$$M^{\circ}_{\alpha\beta}\ddot{\lambda}^{(2)}_{\beta}(\tau) - D^{\circ}_{\alpha\beta}\dot{\lambda}^{(2)}_{\beta}(\tau) + K^{\circ}_{\alpha\beta}\lambda^{(2)}_{\beta}(\tau) =$$
$$= \left\{\frac{1}{2}G^{rs}_{\cdot\alpha}(\tau) - [M^{r}_{\alpha\beta}\ddot{\lambda}^{s}_{\beta}(\tau) - D^{r}_{\alpha\beta}\dot{\lambda}^{s}_{\beta}(\tau) + K^{r}_{\alpha\beta}\lambda^{s}_{\beta}(\tau)] - \right.$$
$$\left. - \frac{1}{2}[M^{rs}_{\alpha\beta}\ddot{\lambda}^{\circ}_{\beta}(\tau) - D^{rs}_{\alpha\beta}\dot{\lambda}^{\circ}_{\beta}(\tau) + K^{rs}_{\alpha\beta}\lambda^{\circ}_{\beta}(\tau)]\right\} Cov(b^{r}, b^{s}) \ , \tag{6.15}$$

• *a.t.i. terminal problem, adjoint system:*

one system of the 0th-order equations

$$M^{\circ}_{\alpha\beta}\ddot{\lambda}^{\circ}_{\beta}(\tau) - D^{\circ}_{\alpha\beta}\dot{\lambda}^{\circ}_{\beta}(\tau) + K^{\circ}_{\alpha\beta}\lambda^{\circ}_{\beta}(\tau) = G^{\circ}_{\cdot\alpha}(t)\delta(\tau) \ , \tag{6.16}$$

R systems of the 1st-order equations ($r = 1, \ldots, R$)

$$M^{\circ}_{\alpha\beta}\ddot{\lambda}^{r}_{\beta}(\tau) - D^{\circ}_{\alpha\beta}\dot{\lambda}^{r}_{\beta}(\tau) + K^{\circ}_{\alpha\beta}\lambda^{r}_{\beta}(\tau) =$$
$$= G^{r}_{\cdot\alpha}(t)\delta(\tau) - [M^{r}_{\alpha\beta}\ddot{\lambda}^{\circ}_{\beta}(\tau) - D^{r}_{\alpha\beta}\dot{\lambda}^{\circ}_{\beta}(\tau) + K^{r}_{\alpha\beta}\lambda^{\circ}_{\beta}(\tau)] \ , \tag{6.17}$$

one system of the 2nd-order equations

$$M^{\circ}_{\alpha\beta}\ddot{\lambda}^{(2)}_{\beta}(\tau) - D^{\circ}_{\alpha\beta}\dot{\lambda}^{(2)}_{\beta}(\tau) + K^{\circ}_{\alpha\beta}\lambda^{(2)}_{\beta}(\tau) =$$
$$= \left\{\frac{1}{2}G^{rs}_{\cdot\alpha}(t)\delta(\tau) - [M^{r}_{\alpha\beta}\ddot{\lambda}^{s}_{\beta}(\tau) - D^{r}_{\alpha\beta}\dot{\lambda}^{s}_{\beta}(\tau) + K^{r}_{\alpha\beta}\lambda^{s}_{\beta}(\tau)] - \right.$$
$$\left. - \frac{1}{2}[M^{rs}_{\alpha\beta}\ddot{\lambda}^{\circ}_{\beta}(\tau) - D^{rs}_{\alpha\beta}\dot{\lambda}^{\circ}_{\beta}(\tau) + K^{rs}_{\alpha\beta}\lambda^{\circ}_{\beta}(\tau)]\right\} Cov(b^{r}, b^{s}) \ , \tag{6.18}$$

where the 2nd-order structural and adjoint unknowns are defined as

$$q_\beta^{(2)}(t) = \frac{1}{2} q_\beta^{rs}(t) Cov(b^r, b^s) \,, \tag{6.19}$$

$$\lambda_\beta^{(2)}(\tau) = \frac{1}{2} \lambda_\beta^{rs}(\tau) Cov(b^r, b^s) \,, \tag{6.20}$$

with $r, s = 1, \ldots, R\,; \alpha, \beta = 1, \ldots, N$.

Having solved Eqs. (6.10)–(6.18) the probabilistic distributions for the sensitivities of structural dynamic response can be determined. Substituting the expansion equations for q_β, λ_β, $G_{\cdot\beta}$, $G^{\cdot\epsilon}$, $M_{\alpha\beta}^{\cdot\epsilon}$, $D_{\alpha\beta}^{\cdot\epsilon}$, $K_{\alpha\beta}^{\cdot\epsilon}$ and $f_\alpha^{\cdot\epsilon}$ into the equations similar to Eqs. (5.17),(5.18) for dynamic case, retaining variations of b^r up to the second order and observing that the terms involving the first variation vanish, from Eqs.(6.8),(6.9) the 2nd-order accurate expectations and the 1st-order accurate covariances of the sensitivity gradient coefficients can be expressed explicitly in terms of the probabilistic distributions of random variations as follows:

o.t.d. response sensitivity

$$\begin{aligned} E(\phi^{\cdot\epsilon}) = \int_0^T [G^{\circ\cdot\epsilon}(\tau) + \frac{1}{2} G^{\cdot\epsilon,rs}(\tau) Cov(b^r, b^s)] \, d\tau + \\ + \int_0^T \{\mathcal{A}_\beta^{\epsilon}(\tau)[\lambda_\beta^{\circ}(\tau) + \lambda_\beta^{(2)}(\tau) +] - \mathcal{F}_\beta^{\epsilon 2} \lambda_\beta^{\circ}(\tau) + \\ + [\mathcal{B}_\beta^{\epsilon r}(\tau) \lambda_\beta^{\cdot r}(\tau) + \mathcal{C}_\beta^{\epsilon rs}(\tau) \lambda_\beta^{\circ}(\tau)] Cov(b^r, b^s)\} \, d\tau \,, \end{aligned} \tag{6.21}$$

$$\begin{aligned} Cov(\phi^{\cdot\epsilon}, \phi^{\cdot\jmath}) = \Big(\int_0^T \int_0^T G^{\cdot\epsilon,r}(\tau) G^{\cdot\jmath,s}(\nu) \, d\tau d\nu + \\ + \int_0^T \int_0^T G^{\epsilon,r}(\tau) [\mathcal{A}_\beta^{\jmath}(\nu) \lambda_\beta^{\cdot r}(\nu) + \mathcal{B}_\beta^{\jmath s}(\nu) \lambda_\beta^{\circ}(\nu)] \, d\tau d\nu + \\ + \int_0^T \int_0^T G^{\jmath,r}(\tau) [\mathcal{A}_\beta^{\epsilon}(\nu) \lambda_\beta^{\cdot r}(\nu) + \mathcal{B}_\beta^{\epsilon r}(\nu) \lambda_\beta^{\circ}(\nu)] \, d\tau d\nu + \\ + \int_0^T \int_0^T \{\mathcal{A}_\alpha^{\epsilon}(\tau) \mathcal{A}_\beta^{\jmath}(\nu) \lambda_\alpha^{\cdot r}(\tau) \lambda_\beta^{\cdot s}(\nu) + \mathcal{B}_\alpha^{\epsilon r}(\tau) \mathcal{B}_\beta^{\jmath s}(\nu) \lambda_\alpha^{\circ}(\tau) \lambda_\beta^{\circ}(\nu) + \\ + [\mathcal{A}_\alpha^{\epsilon}(\tau) \mathcal{B}_\beta^{\jmath r}(\nu) + \mathcal{A}_\beta^{\jmath}(\tau) \mathcal{B}_\alpha^{\epsilon r}(\nu)] \, \lambda_\alpha^{\cdot r}(\tau) \lambda_\beta^{\circ}(\nu)\} \, d\tau d\nu \Big) \, Cov(b^r, b^s) \,, \end{aligned} \tag{6.22}$$

a.t.i. response sensitivity

$$\begin{aligned} E[\phi^{\cdot\epsilon}(t)] = G^{\circ\cdot\epsilon}(t) + \frac{1}{2} G^{\cdot\epsilon,rs}(t) Cov(b^r, b^s) + \\ + \int_0^t \{\mathcal{A}_\beta^{\epsilon}(\tau)[\lambda_\beta^{\circ}(\tau) + \lambda_\beta^{(2)}(\tau)] - \mathcal{F}_\beta^{\epsilon 2}(\tau) \lambda_\beta^{\circ}(\tau) + \\ + [\mathcal{B}_\beta^{\epsilon r}(\tau) \lambda_\beta^{\cdot r}(\tau) + \mathcal{C}_\beta^{\epsilon rs}(\tau) \lambda_\beta^{\circ}(\tau)] Cov(b^r, b^s)\} \, d\tau \,, \end{aligned} \tag{6.23}$$

$$Cov[\phi^{e,r}(t), \phi^{f,s}(t)] = \Big(G^{e,r}(t)G^{f,s}(t) + G^{e,r}(t)\int_0^t [\mathcal{A}^f_\beta(\tau)\lambda^{s}_\beta(\tau) +$$

$$+ \mathcal{B}^{fs}_\beta(\tau)\lambda^{o}_\beta(\tau)]\,d\tau + G^{f,s}(t)\int_0^t [\mathcal{A}^e_\alpha(\tau)\lambda^{r}_\alpha(\tau) + \mathcal{B}^{er}_\alpha(\tau)\lambda^{o}_\alpha(\tau)]\,d\tau +$$

$$+ \int_0^t\int_0^t \{\mathcal{A}^e_\alpha(\nu)\mathcal{A}^f_\beta(\tau)\lambda^{r}_\alpha(\nu)\lambda^{s}_\beta(\tau) + \mathcal{B}^{er}_\alpha(\nu)\mathcal{B}^{fs}_\beta(\tau)\lambda^{o}_\alpha(\nu)\lambda^{o}_\beta(\tau) +$$

$$+ [\mathcal{A}^e_\alpha(\nu)\mathcal{B}^{fr}_\beta(\tau) + \mathcal{A}^f_\beta(\tau)\mathcal{B}^{er}_\alpha(\nu)]\,\lambda^{s}_\alpha(\nu)\lambda^{o}_\beta(\tau)\}\,d\nu\,d\tau\Big)\,Cov(b^r, b^s)\ , \qquad (6.24)$$

where τ, ν are dummy variables of integration; and the following notation is used

$$\mathcal{A}^e_\alpha = f^{o,e}_\alpha - \mathcal{D}^e_\alpha\ , \qquad (6.25)$$

$$\mathcal{B}^{er}_\alpha = f^{e,r}_\alpha - \mathcal{E}^{er}_\alpha - \mathcal{G}^{er}_\alpha\ , \qquad (6.26)$$

$$\mathcal{C}^{ers}_\alpha = 0.5 f^{e,r,s}_\alpha - \mathcal{H}^{ers}_\alpha - 0.5\mathcal{K}^{ers}_\alpha\ , \qquad (6.27)$$

$$\mathcal{D}^e_\alpha = M^{o,e}_{\alpha\beta}\ddot{q}^o_\beta(t) + D^{o,e}_{\alpha\beta}\dot{q}^o_\beta(t) + K^{o,e}_{\alpha\beta}q^o_\beta(t)\ , \qquad (6.28)$$

$$\mathcal{E}^{er}_\alpha = M^{o,e}_{\alpha\beta}\ddot{q}^r_\beta(t) + D^{o,e}_{\alpha\beta}\dot{q}^r_\beta(t) + K^{o,e}_{\alpha\beta}q^r_\beta(t)\ , \qquad (6.29)$$

$$\mathcal{F}^{e(2)}_\alpha = M^{o,e}_{\alpha\beta}\ddot{q}^{(2)}_\beta(t) + D^{o,e}_{\alpha\beta}\dot{q}^{(2)}_\beta(t) + K^{o,e}_{\alpha\beta}q^{(2)}_\beta(t)\ , \qquad (6.30)$$

$$\mathcal{G}^{er}_\alpha = M^{e,r}_{\alpha\beta}\ddot{q}^o_\beta(t) + D^{e,r}_{\alpha\beta}\dot{q}^o_\beta(t) + K^{e,r}_{\alpha\beta}q^o_\beta(t)\ , \qquad (6.31)$$

$$\mathcal{H}^{ers}_\alpha = M^{e,r}_{\alpha\beta}\ddot{q}^s_\beta(t) + D^{e,r}_{\alpha\beta}\dot{q}^s_\beta(t) + K^{e,r}_{\alpha\beta}q^s_\beta(t)\ , \qquad (6.32)$$

$$\mathcal{K}^{ers}_\alpha = M^{e,r,s}_{\alpha\beta}\ddot{q}^o_\beta(t) + D^{e,r,s}_{\alpha\beta}\dot{q}^o_\beta(t) + K^{e,r,s}_{\alpha\beta}q^o_\beta(t)\ , \qquad (6.33)$$

$$e, f = 1, \ldots, E; \qquad r, s = 1, \ldots, R; \qquad \alpha, \beta = 1, \ldots, N\ .$$

6.3 Computational Implementation

In general, the computation process for both the o.t.d. sensitivity and a.t.i. sensitivity proceeds as follows:

1) if the structure equations of motion are given with nonhomogeneous initial conditions, the nonhomogeneous initial-terminal problem is transformed to a corresponding homogeneous problem in the form of Eqs. (6.10)–(6.12) by using Eqs. (3.35)–(3.36),

2) Eqs. (6.10)–(6.12) are integrated forward with respect to time in sequence to determine the 0th-, 1st- and 2nd-order solutions for the nodal accelerations, velocities and displacements; the right hand side of the 0th-order adjoint equations are calculated,

3) by defining a new time variable $t = T - \tau$ (τ is the backward time variable) the 0th-, 1st- and 2nd-order adjoint systems of Eqs. (6.13)–(6.15) or Eqs. (6.16)–(6.18) expressed in terms of the forward time variable t are integrated sequentially

over the time domain $[0,T]$ by the same algorithm used for the initial problem of Eqs. (6.10)–(6.12), yielding a unique solution for the 0th-,1st- and 2nd-order adjoint displacements,

4) once the initial-terminal problems are solved the 2nd-order accurate expectations and 1st-order accurate covariances of the sensitivity gradient coefficients are evaluated by Eqs. (6.21), (6.22) for the case of the o.t.d. response or by Eqs. (6.23), (6.24) for the case of the a.t.i response. Note that for the latter case the above process needs to be repeated for all the running time instants t used to discretize the time domain $[0,T]$.

In order to reduce the double summation in Eqs. (6.11),(6.12), Eqs. (6.14),(6.15), Eqs. (6.17),(6.18), to the single summation, the correlated random variables b^v are transformed to a set of uncorrelated random variables c^v by Eqs. (4.52),(4.53). By employing uncorrelated random variables c^v Eqs. (6.10)-(6.18) now can be rewritten as follows:

one pair of the uncorrelated 0th-order equations

$$M^o_{\alpha\beta}\ddot{q}^o_\beta(t) + D^o_{\alpha\beta}\dot{q}^o_\beta(t) + K^o_{\alpha\beta}q^o_\beta(t) = f^o_\alpha(t) \ , \tag{6.34}$$

$$M^o_{\alpha\beta}\ddot{\lambda}^o_\beta(\tau) - D^o_{\alpha\beta}\dot{\lambda}^o_\beta(\tau) + K^o_{\alpha\beta}\lambda^o_\beta(\tau) = g^o_\alpha(\tau) \ , \tag{6.35}$$

V pairs of the uncorrelated 1st-order equations ($v = 1,\ldots,V$)

$$M^o_{\alpha\beta}\ddot{q}^v_\beta(t) + D^o_{\alpha\beta}\dot{q}^v_\beta(t) + K^o_{\alpha\beta}q^v_\beta(t) = p^v_\alpha(t) \ , \tag{6.36}$$

$$M^o_{\alpha\beta}\ddot{\lambda}^v_\beta(\tau) - D^o_{\alpha\beta}\dot{\lambda}^v_\beta(\tau) + K^o_{\alpha\beta}\lambda^v_\beta(\tau) = g^v_\alpha(\tau) \ , \tag{6.37}$$

one pair of the uncorrelated 2nd-order equations

$$M^o_{\alpha\beta}\ddot{q}^{(2)}_\beta(t) + D^o_{\alpha\beta}\dot{q}^{(2)}_\beta(t) + K^o_{\alpha\beta}q^{(2)}_\beta(t) = p^{(2)}_\alpha(t) \ , \tag{6.38}$$

$$M^o_{\alpha\beta}\ddot{\lambda}^{(2)}_\beta(\tau) - D^o_{\alpha\beta}\dot{\lambda}^{(2)}_\beta(\tau) + K^o_{\alpha\beta}\lambda^{(2)}_\beta(\tau) = g^{(2)}_\alpha(\tau) \ , \tag{6.39}$$

with

$$q^{(2)}_\beta(t) = \frac{1}{2}\sum_{v=1}^{V} q^{vv}_\beta(t) Var(c^v) \ , \tag{6.40}$$

$$\lambda^{(2)}_\beta(\tau) = \frac{1}{2}\sum_{v=1}^{V} \lambda^{vv}_\beta(\tau) Var(c^v) \ , \tag{6.41}$$

$$p^v_\alpha(t) = f^v_\alpha(t) - [M^v_{\alpha\beta}\ddot{q}^o_\beta(t) + D^v_{\alpha\beta}\dot{q}^o_\beta(t) + K^v_{\alpha\beta}q^o_\beta(t)] \ , \tag{6.42}$$

$$p^{(2)}_\alpha(t) = \sum_{v=1}^{V}\left\{\frac{1}{2}f^{vv}_\alpha(t) - [M^v_{\alpha\beta}\ddot{q}^v_\beta(t) + D^v_{\alpha\beta}\dot{q}^v_\beta(t) + K^v_{\alpha\beta}q^v_\beta(t)] - \right.$$
$$\left. - \frac{1}{2}[M^{vv}_{\alpha\beta}\ddot{q}^o_\beta(t) + D^{vv}_{\alpha\beta}\dot{q}^o_\beta(t) + K^{vv}_{\alpha\beta}q^o_\beta(t)]\right\} Var(c^v) \ . \tag{6.43}$$

The uncorrelated 0th-, 1st- and 2nd-order adjoint loads are defined for the case of the o.t.d. sensitivity as

$$g_\alpha^\circ(\tau) = G_{,\alpha}^\circ(\tau) , \tag{6.44}$$

$$g_\alpha^{,v}(\tau) = G_{,\alpha}^{,v}(\tau) - [M_{\alpha\beta}^{,v}\ddot{\lambda}_\beta^\circ(\tau) - D_{\alpha\beta}^{,v}\dot{\lambda}_\beta^\circ(\tau) + K_{\alpha\beta}^{,v}\lambda_\beta^\circ(\tau)] , \tag{6.45}$$

$$g_\alpha^{(2)}(\tau) = \sum_{v=1}^{V}\left\{\frac{1}{2}G_{,\alpha}^{,vv}(\tau) - [M_{\alpha\beta}^{,v}\ddot{\lambda}_\beta^v(\tau) - D_{\alpha\beta}^{,v}\dot{\lambda}_\beta^v(\tau) + K_{\alpha\beta}^{,v}\lambda_\beta^v(\tau)] - \right.$$
$$\left. - \frac{1}{2}[M_{\alpha\beta}^{,vv}\ddot{\lambda}_\beta^\circ(\tau) - D_{\alpha\beta}^{,vv}\dot{\lambda}_\beta^\circ(\tau) + K_{\alpha\beta}^{,vv}\lambda_\beta^\circ(\tau)]\right\} Var(c^v) . \tag{6.46}$$

and for the case of the a.t.i. sensitivity as

$$g_\alpha^\circ(\tau) = G_{,\alpha}^\circ(t)\delta(\tau) , \tag{6.47}$$

$$g_\alpha^{,v}(\tau) = G_{,\alpha}^{,v}(t)\delta(\tau) - [M_{\alpha\beta}^{,v}\ddot{\lambda}_\beta^\circ(\tau) - D_{\alpha\beta}^{,v}\dot{\lambda}_\beta^\circ(\tau) + K_{\alpha\beta}^{,v}\lambda_\beta^\circ(\tau)] , \tag{6.48}$$

$$g_\alpha^{(2)}(\tau) = \sum_{v=1}^{V}\left\{\frac{1}{2}G_{,\alpha}^{,vv}(t)\delta(\tau) - [M_{\alpha\beta}^{,v}\ddot{\lambda}_\beta^v(\tau) - D_{\alpha\beta}^{,v}\dot{\lambda}_\beta^v(\tau) + K_{\alpha\beta}^{,v}\lambda_\beta^v(\tau)] - \right.$$
$$\left. - \frac{1}{2}[M_{\alpha\beta}^{,vv}\ddot{\lambda}_\beta^\circ(\tau) - D_{\alpha\beta}^{,vv}\dot{\lambda}_\beta^\circ(\tau) + K_{\alpha\beta}^{,vv}\lambda_\beta^\circ(\tau)]\right\} Var(c^v) . \tag{6.49}$$

Recall that in the above equations $(.)^{,v}$ and $(.)^{,vv}$ denote the first and second derivatives with respect to c^v. Furthermore, the transformation of Eq. (1.33) from the generalized coordinates $q_\beta(t)$ and $\lambda_\beta(\tau)$ to the normalized coordinates $y_z(t)$ and $\vartheta_z(\tau)$ is used to decouple Eqs. (6.34)–(6.39). We have then:

Z pairs of the uncoupled 0th-order equations

$$\ddot{y}_z^\circ(t) + 2\xi_z\omega_z\dot{y}_z^\circ(t) + \omega_z^2 y_z^\circ(t) = p_z^\circ(t) , \tag{6.50}$$

$$\ddot{\vartheta}_z^\circ(\tau) - 2\xi_z\omega_z\dot{\vartheta}_z^\circ(\tau) + \omega_z^2\vartheta_z^\circ(\tau) = g_z^\circ(\tau) , \tag{6.51}$$

$Z \times V$ pairs of the uncoupled 1st-order equations $(v = 1, \ldots, V)$

$$\ddot{y}_z^{,v}(t) + 2\xi_z\omega_z\dot{y}_z^{,v}(t) + \omega_z^2 y_z^{,v}(t) = p_z^{,v}(t) , \tag{6.52}$$

$$\ddot{\vartheta}_z^{,v}(\tau) - 2\xi_z\omega_z\dot{\vartheta}_z^{,v}(\tau) + \omega_z^2\vartheta_z^{,v}(\tau) = g_z^{,v}(\tau) , \tag{6.53}$$

Z pairs of the uncoupled 2nd-order equations

$$\ddot{y}_z^{(2)}(t) - 2\xi_z\omega_z\dot{y}_z^{(2)}(t) + \omega_z^2 y_z^{(2)}(t) = p_z^{(2)}(t) , \tag{6.54}$$

$$\ddot{\vartheta}_z^{(2)}(\tau) - 2\xi_z\omega_z\dot{\vartheta}_z^{(2)}(\tau) + \omega_z^2\vartheta_z^{(2)}(\tau) = g_z^{(2)}(\tau) . \tag{6.55}$$

Summation over index z is not implied in Eqs. (6.50)–(6.55); and the following notation is used

$$y_z^\circ(t) = Q_{z\beta} q_\beta^\circ(t), \qquad y_z^*(t) = Q_{z\beta} q_\beta^*(t), \qquad y_z^{(2)}(t) = Q_{z\beta} q_\beta^{(2)}(t), \tag{6.56}$$

$$\vartheta_z^\circ(\tau) = Q_{z\beta} \lambda_\beta^\circ(\tau), \qquad \vartheta_z^*(\tau) = Q_{z\beta} \lambda_\beta^*(\tau), \qquad \vartheta_z^{(2)}(\tau) = Q_{z\beta} \lambda_\beta^{(2)}(\tau), \tag{6.57}$$

$$p_z^\circ(t) = Q_{z\alpha} f_\alpha^\circ(t), \qquad p_z^*(t) = Q_{z\alpha} p_\alpha^*(t), \qquad p_z^{(2)}(t) = Q_{z\alpha} p_\alpha^{(2)}(t), \tag{6.58}$$

$$g_z^\circ(\tau) = Q_{z\alpha} g_\alpha^\circ(\tau), \qquad g_z^*(\tau) = Q_{z\alpha} g_\alpha^*(\tau), \qquad g_z^{(2)}(\tau) = Q_{z\alpha} g_\alpha^{(2)}(\tau), \tag{6.59}$$

$$z = 1, \ldots, Z; \qquad \alpha, \beta = 1, \ldots, N .$$

Since the left hand sides of the normalized 0th-, 1st- and 2nd-order adjoint equations (6.51), (6.53), (6.55) differ from the structural system (6.50), (6.52), (6.54) only by the algebraic sign of the damping terms, the terminal problem described by Eqs. (6.51), (6.53), (6.55) can be rewritten in a form similar to that of the initial problem described by Eqs. (6.50),(6.52),(6.54) by defining a forward time variable $t = T - \tau$, as mentioned above at the beginning of this section. Thus the terminal conditions of the adjoint equations expressed in terms of the backward time variable τ become the initial conditions expressed in terms of the forward time variable t; and the adjoint system assumes exactly the same form as that of the structural system. In terms of the computer implementation this observation is very useful: 1) the eigenproblem has to be solved only once and the same eigenpairs are used for either the structural or adjoint system, 2) the 0th-, 1st-, 2nd-order structural and adjoint equations can be solved for $q_\beta^\circ(t)$, $\lambda_\beta^\circ(\tau)$, $q_\beta^*(t)$, $\lambda_\beta^*(\tau)$ and $q_\beta^{(2)}(t)$, $\lambda_\beta^{(2)}(\tau)$ in parallel and by the same algorithm for integrating equations of motion. The uncoupled equations (6.50)–(6.55) can be solved alternatively by the step-by-step direct integration techniques or by the Duhamel's convolution.

In view of the computational aspects discussed in Section 3.3 we observe that for the case of the a.t.i. sensitivity the computations of the adjoint systems and of the sensitivity coefficients require integrations over $n(n+1)$ time steps Δt, where $n = T/\Delta t$. Similar to deterministic systems, we also observe that the state operators involved in the initial-terminal systems are linear, the initial conditions of the structural equations are zero and the running terminal conditions of the adjoint equations are also zero at any time t. This observation enables us to develop a combined algorithms such that the 0th-, 1st- and 2nd-order adjoint systems can be integrated forward with respect to the forward time variable t only once in the time domain $[0, T]$ over n time increments. With a Dirac delta distribution appearing on the right hand sides, the response of the adjoint systems can be treated through the unit impulse response (or the response to a unit terminal velocity) of a normalized structural system whose state operators being functions of the structural mass, damping and stiffness are independent of $G(t)$ and t. Note that in this case the running time t is a stationary variable. The procedures for the a.t.i. sensitivity introduced in Section 3.3 can be directly applied to stochastic systems since all terms involved in Eqs. (6.50),(6.55) are expressed through deterministic quantities. Since

the right hand sides of the modal adjoint equations involve a Dirac delta distribution evaluated at the running time t and a force function of the backward time τ, employing the superposition principle for linear systems the adjoint response described by Eqs. (6.51), (6.53), (6.55) can be treated as a linear combination of the solution of a system excited by an terminal unit impulse and the solution of a system excited by a time-varying force.

As stressed in Chapter 4 while discussing stochastic forced-vibration problems, the application of the second moment analysis can give invalid solutions due to the appearance of secularity in the 1st- and 2nd-order forcing functions. The effects are much more significant in sensitivity analysis since the expectations of the sensitivity coefficients are bilinear functions of the nodal displacements of the structural and adjoint systems, and their covariances are square functions of the expectations. According to the procedures described in Section 4.5.2, to eliminate secular terms the modal 1st- and 2nd-order forcing sequences are composed and treated as complex valued sequences. The fast Fourier analysis is performed on each modal force sequence to obtain its discrete Fourier spectra. To remove the resonant part from the Fourier spectra the coefficients of each frequency series which lie within a specified range close to the natural frequency are weighted, and the fast Fourier synthesis is carried out on the weighted frequency series to recover the modal force sequence with no resonant excitation. In a typical algorithm for dynamic sensitivity analysis of stochastic systems procedures of the secularity elimination need necessarily to be incorporated.

Having solved the uncorrelated-uncoupled system of Eqs. (6.50)–(6.55) the 2nd-order accurate expectations and 1st-order accurate covariances of the sensitivity gradient coefficients for the case of the o.t.d. sensitivity can be obtained as

$$E(\phi^{\cdot s}) = \int_0^T [G^{o,s}(\tau) + \frac{1}{2}\sum_{v=1}^{\nu} G^{s,vv}(\tau) Var(c^v)]\, d\tau + \\ + \int_0^T \{\mathcal{A}^s_\beta(\tau)[\lambda^o_\beta(\tau) + \lambda^{(2)}_\beta(\tau) +] - \mathcal{F}^{o2}_\beta \lambda^o_\beta(\tau) + \\ + \sum_{v=1}^{\nu} [\mathcal{B}^{sv}_\beta(\tau)\lambda^{,v}_\beta(\tau) + \mathcal{C}^{svv}_\beta(\tau)\lambda^o_\beta(\tau)] Var(c^v)\}\, d\tau \,, \tag{6.60}$$

$$Cov(\phi^{\cdot s}, \phi^{\cdot l}) = \sum_{v=1}^{\nu} \Big(\int_0^T \int_0^T G^{s,o}(\tau) G^{l,v}(\nu)\, d\tau d\nu + \\ + \int_0^T \int_0^T G^{s,v}(\tau)[\mathcal{A}^l_\beta(\nu)\lambda^{,v}_\beta(\nu) + \mathcal{B}^{lv}_\beta(\nu)\lambda^o_\beta(\nu)]\, d\tau d\nu + \\ + \int_0^T \int_0^T G^{l,v}(\tau)[\mathcal{A}^s_\beta(\nu)\lambda^o_\beta(\nu) + \mathcal{B}^{sv}_\beta(\nu)\lambda^o_\beta(\nu)]\, d\tau d\nu + \\ + \int_0^T \int_0^T \{\mathcal{A}^s_\alpha(\tau)\mathcal{A}^l_\beta(\nu)\lambda^{,v}_\alpha(\tau)\lambda^{,v}_\beta(\nu) + \mathcal{B}^{sv}_\alpha(\tau)\mathcal{B}^{lv}_\beta(\nu)\lambda^o_\alpha(\tau)\lambda^o_\beta(\nu) + \\ + [\mathcal{A}^s_\alpha(\tau)\mathcal{B}^{lv}_\beta(\nu) + \mathcal{A}^l_\beta(\tau)\mathcal{B}^{sv}_\alpha(\nu)]\, \lambda^{,v}_\alpha(\tau)\lambda^o_\beta(\nu)\}\, d\tau d\nu \Big)\, Var(c^v) \,, \tag{6.61}$$

and for the case of the a.t.i. sensitivity as

$$E[\phi^{,e}(t)] = G^{o,e}(t) + \frac{1}{2}\sum_{v=1}^{V} G^{,e,vv}(t) Var(c^v) + \\ + \int_0^t \{\mathcal{A}^e_\beta(\tau)[\lambda^o_\beta(\tau) + \lambda^{(2)}_\beta(\tau)] - \mathcal{F}^{e2}_\beta(\tau)\lambda^o_\beta(\tau) + \\ + \sum_{v=1}^{V}[\mathcal{B}^{ev}_\beta(\tau)\lambda^v_\beta(\tau) + \mathcal{C}^{evv}_\beta(\tau)\lambda^o_\beta(\tau)] Var(c^v)\}\, d\tau \ , \tag{6.62}$$

$$Cov[\phi^{,e}(t), \phi^{,f}(t)] = \sum_{v=1}^{V}\Big(G^{,e,v}(t)G^{,f,v}(t) + G^{,e,v}(t)\int_0^t [\mathcal{A}^f_\beta(\tau)\lambda^v_\beta(\tau) + \\ + \mathcal{B}^{fv}_\beta(\tau)\lambda^o_\beta(\tau)]\, d\tau + G^{,f,v}(t)\int_0^t [\mathcal{A}^e_\beta(\tau)\lambda^v_\beta(\tau) + \mathcal{B}^{ev}_\beta(\tau)\lambda^o_\beta(\tau)]\, d\tau + \\ + \int_0^t\int_0^t \{\mathcal{A}^e_\alpha(\nu)\mathcal{A}^f_\beta(\tau)\lambda^v_\alpha(\nu)\lambda^v_\beta(\tau) + \mathcal{B}^{ev}_\alpha(\nu)\mathcal{B}^{fv}_\beta(\tau)\lambda^o_\alpha(\nu)\lambda^o_\beta(\tau) + \\ + [\mathcal{A}^e_\alpha(\nu)\mathcal{B}^{fv}_\beta(\tau) + \mathcal{A}^f_\beta(\tau)\mathcal{B}^{ev}_\alpha(\nu)]\, \lambda^v_\alpha(\nu)\lambda^o_\beta(\tau)\}\, d\nu\, d\tau\Big) Var(c^v) \ , \tag{6.63}$$

where $\mathcal{A}^e_\alpha$, $\mathcal{D}^e_\alpha$ are defined above in Eqs. (6.25),(6.28); and

$$\mathcal{B}^{ev}_\alpha = f^{,e,v}_\alpha - \mathcal{E}^{ev}_\alpha - \mathcal{G}^{ev}_\alpha \ , \tag{6.64}$$

$$\mathcal{C}^{evv}_\alpha = 0.5 f^{,e,vv}_\alpha - \mathcal{H}^{evv}_\alpha - 0.5\mathcal{K}^{evv}_\alpha \ , \qquad \textit{(no sum on } v\textit{)} \tag{6.65}$$

$$\mathcal{E}^{ev}_\alpha = M^{o,e}_{\alpha\beta}\ddot{q}^v_\beta(t) + D^{o,e}_{\alpha\beta}\dot{q}^v_\beta(t) + K^{o,e}_{\alpha\beta}q^v_\beta(t) \ , \tag{6.66}$$

$$\mathcal{F}^{e2}_\alpha = M^{o,e}_{\alpha\beta}\ddot{q}^{(2)}_\beta(t) + D^{o,e}_{\alpha\beta}\dot{q}^{(2)}_\beta(t) + K^{o,e}_{\alpha\beta}q^{(2)}_\beta(t) \ , \tag{6.67}$$

$$\mathcal{G}^{ev}_\alpha = M^{,e,v}_{\alpha\beta}\ddot{q}^o_\beta(t) + D^{,e,v}_{\alpha\beta}\dot{q}^o_\beta(t) + K^{,e,v}_{\alpha\beta}q^o_\beta(t) \ , \tag{6.68}$$

$$\mathcal{H}^{evv}_\alpha = M^{,e,v}_{\alpha\beta}\ddot{q}^v_\beta(t) + D^{,e,v}_{\alpha\beta}\dot{q}^v_\beta(t) + K^{,e,v}_{\alpha\beta}q^v_\beta(t) \ , \qquad \textit{(no sum on } v\textit{)} \tag{6.69}$$

$$\mathcal{K}^{evv}_\alpha = M^{,e,vv}_{\alpha\beta}\ddot{q}^o_\beta(t) + D^{,e,vv}_{\alpha\beta}\dot{q}^o_\beta(t) + K^{,e,vv}_{\alpha\beta}q^o_\beta(t) \ , \qquad \textit{(no sum on } v\textit{)} \tag{6.70}$$

$$e, f = 1, \ldots, E; \qquad v = 1, \ldots, V; \qquad \alpha, \beta = 1, \ldots, N,$$

6.4 Numerical Results

The numerical algorithms based on the formulation and computer implementations presented above in this chapter have been worked out and their procedures have been incorporated into the program POLSAP to deal with dynamic response sensitivity of stochastic systems. From 14 analysis types recently supported in the code, the option for stochastic sensitivity analysis of dynamic structural systems is the most complicated version and can be treated as the most general case.

The procedures used to analyze deterministic sensitivity in dynamics (introduced in Chapter 3), stochastic forced-vibration (Chapter 4) and stochastic static sensitivity (Chapter 5) have been modified, extended and combined to deal with both the o.t.d. senstivity and a.t.i. sensitivity analysis of medium-scale truss-beam-shell structures in the stochastic finite element context. Five types of random design variables can be considered: cross sectional area and length of the 3D truss or 3D beam elements, thickness of the plate and shell elements, Young modulus and mass density for all the three element groups. To illustrate the formulation we shall consider below a few numerical examples

Example 16 Consider response sensitivity of a portal beam subjected to a time-varying load, cf. Fig. 6.1. The response functional is assumed as

$$\phi = q_y^2 / q_0^2 - 1 \leq 0 \ ,$$

where q_y is the vertical displacement at the mid-point A of the beam and q_0 denotes an admissible value. The element cross-sectional areas are assumed as random variables: a_r, $r = 1, \ldots, 100$. The respective expectation, correlation function and coeficient of variation of the designs are assumed as follows:

$$E(a_r) = a_0 = 10.0 \ ,$$

$$R(a_r, a_s) = \exp(- \mid x_r - x_s \mid / \lambda) \ ,$$

$$\lambda = 0.5 \ , \qquad x_0 = 0.0, \ldots, x_{100} = 1.0 \ ,$$

$$\alpha = 0.05 \ .$$

The following deterministic data are assumed: length $l = 200.$, high $h = 100.$, $h_1 = 50.$, Young modulus $e = 2.0 \times 10^7$, Poisson ratio $\nu = 0.2$, mass density $\varrho = 0.001$, damping factor $\xi = 0.05$, allowable displacement $q_0 = 0.012$. To solve the inital-terminal problem the mode superposition technique is used with 10 lowest eigensystems. The set of 100 correlated random variables is transformed to a set of uncorrelated variables, out of which 10 highest modes are used in the calculation. The equations are integrated with respect to time for 512 time steps (time interval value $\Delta t = 0.001$). The secular terms are removed with the secularity elimination facor $r = 0.15$ and with 1024 Fourier terms. Fig. 6.1 shows the time response of expectations, variances and covariances of the vertical displacement at mid-point A and horizontal displacement at boundary point B when compared against the deterministic solution. The time responses of the spatial expectations, variances and covariance of the sensitivity gradient at A and at B are shown in Fig. 6.2. The conputation time was 1920 sec.

Example 17 This example is concerned with time response of the sensitivity of the hal of a cylindrical shell clamped at boundaries and subjected to a concentrated time-varying load at mid-point A (cf. Fig. 6.3). Because of the symmetry only one-quarter of the shell is considered. The finite element mesh includes 60 rectangular elenents (60 random design variables), and the total number of degrees of freedom is 313. The response functional is assumed as

$$\phi = q_z^2 / q_0^2 - 1 \leq 0 \ ,$$

where q_z is z-displacement at the mid-point A of the shell and q_0 denotes an allowable value. The element thicknesses are assumed as random variables t_r, $r = 1, \ldots, 60$. The expectation, correlation function and coefficient of variation of the design variables are given, respectively, as follow:

$$E(t_r) = t_0 = 0.05 \ ,$$

$$R(t_r, t_s) = \exp(- \mid x_r - x_s \mid / \lambda_x) \exp(- \mid y_r - y_s \mid / \lambda_y) \ ,$$

$$\lambda_x = \theta r \ , \qquad \lambda_y = \theta r / 2 \ , \qquad \theta = 0.4 \ ,$$

$$\alpha = 0.05 \ .$$

The following deterministic data are assumed: length $l = 9.6$, radius $r = 4.0$, Young modulus $e = 1.0 \times 10^5$, Poisson ratio $\nu = 0.3$, mass density $\varrho = 0.02$, damping factor $\xi = 0.05$, admissible displacement $q_0 = 1.0$. To solve the initial-terminal problem the mode superposition technique is used with 10 lowest eigensystems. The set of 60 correlated random variables is transformed to a set of uncorrelated variables, out of which 10 highest modes are used in the calculation. The equations are integrated with respect to time for 512 time steps (time interval value $\Delta t = 0.001$). The secular terms are removed with the secularity elimination factor $r = 0.15$ and with 1024 Fourier terms. The time response of expectations and standard deviation of the z-displacement at mid-point A (compared against the deterministic solution) are displayed in Fig. 6.3. The time response of the spatial probabilistic distributions for expectations, variances and covariance of the sensitivity gradient coefficients at the mid-point A and at the boundary point B are shown in Fig. 6.4. The computation time was 1380 sec. In Fig. 6.5 the solutions obtained by the Wilson-θ ($\theta = 1.4$) and Newmark ($\delta = 0.5$, $\alpha = 0.25$) integration schemes are compared. It is seen that the results are compare very well for both the integration techniques; the Newmark's scheme gives small perturbations at extrema in time response of the second moments of sensitivity gradient coefficients, though.

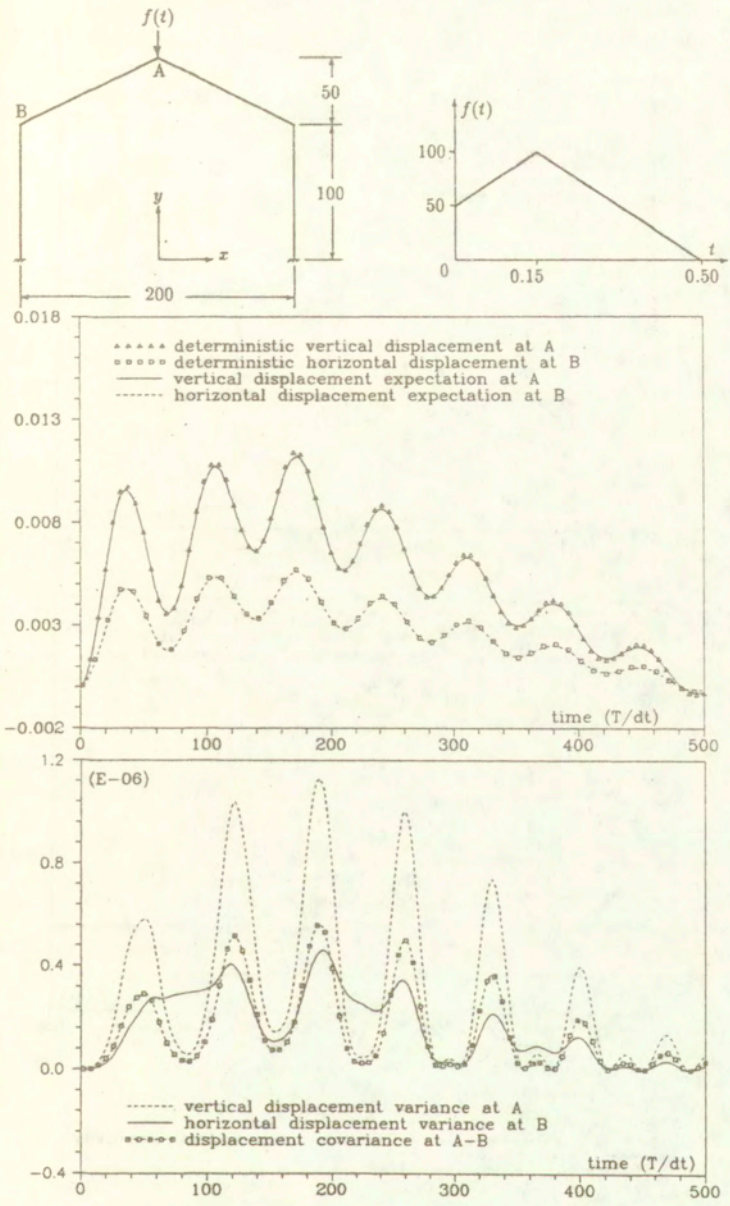

Figure 6.1: 100-element frame. Time response of stochastic displacements

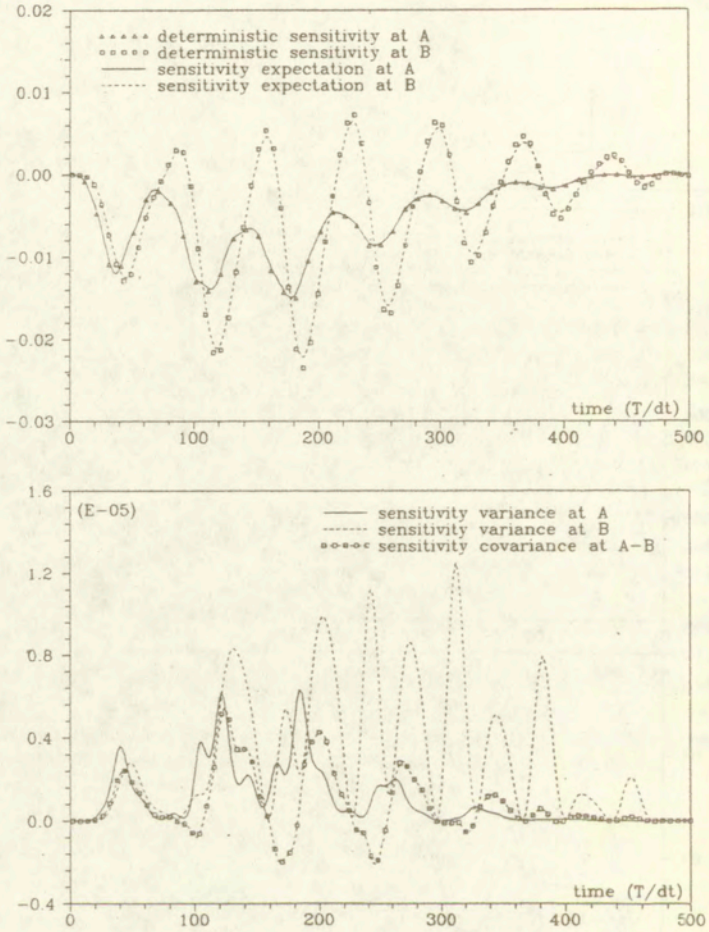

Figure 6.2: 100-element frame. Time response of stochastic sensitivity

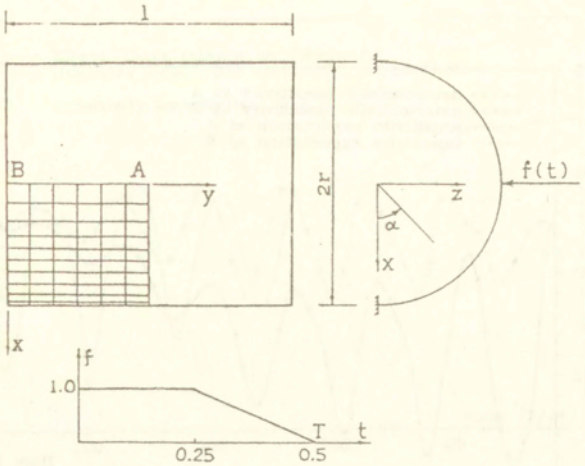

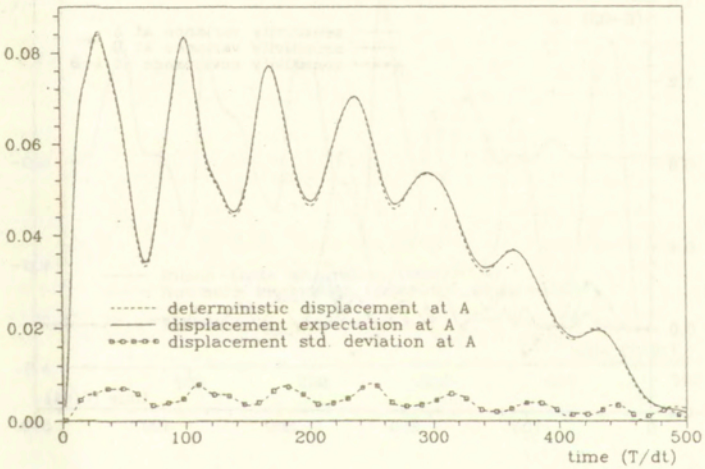

Figure 6.3: 60-element shell. Time response of stochastic displacements

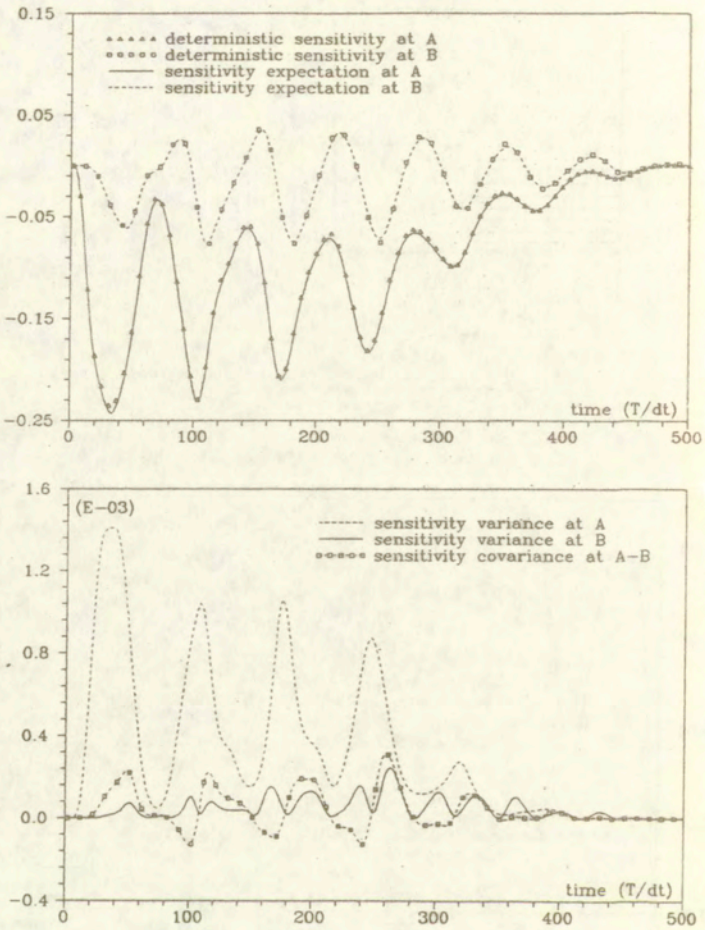

Figure 6.4: 60-element shell. Time response of stochastic sensitivity

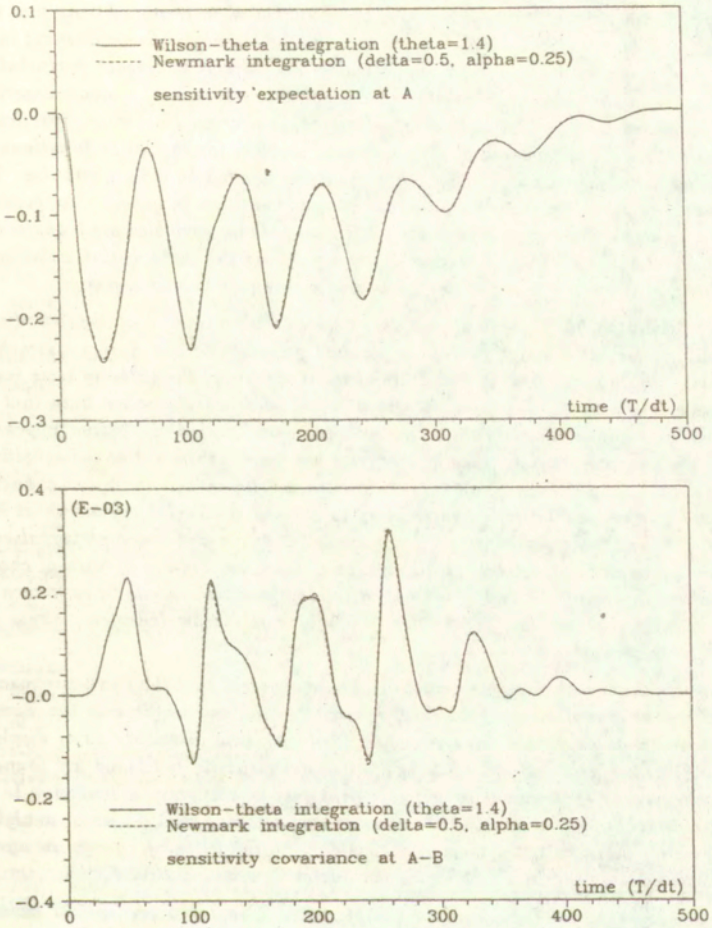

Figure 6.5: 60-element shell. Response computed by Wilson-θ and Newmark schemes

Summarizing Remarks

In this chapter a new problem of computational mechanics was formulated. The values of stochastic sensitivity functions can be evaluated in terms of their first two moments for dynamic structural systems through the stochastic finite element modelling. The combination of the adjoint variable method and 2nd-order perturbation technique is employed to consider stochastic sensitivity response of systems described by the state functionals that hold over a time domain as well as at any particular time instant in the time domain. The terminal problem for the latter functional is formulated using equivalent homogeneous equations excited by a unit impulse. The initial-terminal problem is solved by a two-fold superposition technique: the generalized coordinates are normalized and the correlated random variables are transformed to a uncorrelated set. The secularity appearing during the perturbation solution is eliminated by using the fast Fourier transform of complex valued sequences.

The stochastic finite element method involves discretization of the coordinate spaces of random and design fields; the required probabilistic and design characterization is strongly dependent on the finite element mesh and the value of time increment used in analysis. The time increment must be selected smaller than that for the classical analysis to avoid the amplitude decay and period elongation appearing in the numerical integration since these effects are more significant in the sensitivity computation. The local variation in a parameter usually causes nonlinear change of structural behaviour. Hence, it is necessary to employ the Taylor expansion at least up to the second order to cover such nonlinearity. If the 3rd-order perturbation is taken the computation cost will greatly increase, since the 3rd-order rates of change must be included; and the sixth moment of random variables needs to be known for the compatible computations of the first two moments for displacement, stress and sensitivity response.

From the computational experiences it can be observed that the time responses of spatial expectations and covariances of sensitivity gradient coefficients are damped away more rapidly than the time response of probabilistic distributions of displacements. Also, the first two moments of stochastic sensitivity functions are found to have finite values even when the displacement response appears a tendency to exhibit chaotic characteristics. The same result was obtained in [128] *in an analytical way by using the sensitivity theory to consider the influence of change in system parameters on solution of a distributed-parameter dynamic control system.*

Since the problems considered in Chapter 2 to Chapter 5 are special cases of the stochastic dynamic sensitivity problem discussed in this chapter, all the aspects discussed in the preceding chapters and related to physical interpretations and computational implementations are valid here as well. The numerical algorithms incorporated in the computer code POLSAP have been proven to be accurate and can be efficiently applied for medium-scale systems with the acceptable computation cost. Finally, the numerical formulation based on a combination of the two seemingly quite different topics (design sensitivity and stochastic finite elements) for structural dynamics seems to offer most effective tool to estimate the sensitivity of a structural system to variations of its randomly described parameters.

Conclusions and Proposed Future Work

The development of numerical methods and computation techniques enable us to deal with large, complex structural mechanics problems of great engineering significance, which were unsolvable a few years ago. In this context the problems discussed in this text form a typical example. The following aspects of the work seem to be original:

- The stochastic version of the Hamilton's variational principle proposed in Chapter 4 is applicable in a natural way to conventional finite element formulations, thereby enabling the modification of deterministic finite element codes to probabilistic problems of stochastic structural systems.

- On the basis of the stochastic Hamilton's principle two new problems of computational mechanics devoted to stochastic design sensitivity in structural statics and stochastic design sensitivity in structural dynamics were posed and solved in Chapter 5 and Chapter 6, respectively.

- Besides the class of the well-known sensitivity functionals conventionally used, a new form of response functionals was introduced in Chapter 3 in terms of a convolution of a time signal sequence. This enables us to determine the time-varying deterministic sensitivity functions (Chapter 3) or to estimate response of the stochastic sensitivity functions at any time instant in a given finite time domain (Chapter 6).

- To eliminate the secularity appearing in the perturbation solutions, an alternative treatment of forcing functions was developed. The time-varying functions are discretized and assembled into time complex-valued series of half length and the fast Fourier analysis and synthesis are employed to remove the resonant parts.

- To handle at acceptable computation cost large finite element systems, a combination of basis changes (structural modal analysis and transformation from a correlated space to a uncorrelated space of random variables) termed the two-fold superposition technique was presented.

- A complete algorithm was worked out and implemented into the personal computer program POLSAP, a finite element code for deterministic and stochastic analysis of statics, minimum-weight optimization, buckling load, eigenpair, forced-vibration, eigen-value sensitivity, static and dynamic response sensitivity of medium-scale truss-beam-shell structures.

Summing up the features of the formulation and its computational aspects it can be seen that:

1) sensitivity of the structural static and dynamic response to stochastically described variations in design parameters of structural members can be studied using current deterministic finite element technology,

2) structural design sensitivity and stochastic finite elements are closely related in problem statement, modelling and computer performance: the stochastic sensitivity problem can be formulated and in a parallel way and solved by the same algorithms used in deterministic calculations,

3) the algorithms developed have proven to be accurate and cost effective in analysis of medium- or large-scale systems; they can be immediately adapted to fit into existing deterministic finite element codes.

The variational formulation based on Hamilton's principle has definitive advantages when compared against the vectorial-equilibrium and virtual-work approaches, since the compatibility and constitutive relationships and boundary conditions are directly incorporated into the variational statements. Nonconservative loadings, geometrical and material nonlinearity, design properties and probabilistic distributions can be treated in a consistent manner; and all of them are translated into right hand sides of variational equations. In structural sensitivity analysis the adjoint variable approach is shown generally to be more efficient than the direct differentiation technique, leading to the parallel procedures and the systems with nonhomogeneous initial conditions which can be solved through corresponding homogeneous systems by a variable change. Also, by using the forward time variable instead of the backward time variable for integration of the adjoint equations, the structural and adjoint systems have identical form. In the case of the at-any-time-instant sensitivity, the adjoint response can be evaluated through the response of a uncoupled system to a unit terminal velocity or unit impulse excitation, reducing the computation cost from $0(n)^2$ to $0(n)$ vector operations in deterministic analysis and from $0(n)^4$ to $0(n)^2$ in stochastic analysis, where n is the number of time intervals used in analysis. The advantages of the stochastic finite element modelling over the statistical approach such as Monte Carlo simulations or Hermite-Gauss quadrature are that only the first two moments of random variables need to be known, and not the probability density function and a large number of realizations randomly generated. Furthermore, stochastic finite elements can be directly used for random fields that are homogeneous as well as nonhomogeneous, whereas the situation in the statistical techniques is not so straightforward. Also, the normal approximation of a given non-normal probability distribution and the selections of an appropriate random number generator, which affect significantly the accuracy of the solutions, are problem-dependent and one of the most difficult aspects of statistical methods. Such a difficulty is non-existent in the stochastic finite element approach. By using a combination of the 2nd-order perturbation and adjoint variable methods, all probabilistic characteristics are translated onto the right hand sides of equations of the structural and adjoint systems. The coefficient matrices involved on the left hand sides of these equations have identical form and are simply mass, damping and stiffness matrices of the linear systems. In other words, although the structural and adjoint equations

are nonlinear as functions of state and design variables due to the appearance of random and design variables in the state operators, equations of the discretized-parameter systems in the stochastic finite element modelling remain linear. Thus, the formulation enables us to treat nonlinear problems with the techniques that take advantages of mathematical properties of linear operators and to solve probabilistic problems by using the procedures for deterministic analysis. This seems to be the main advantage of the proposed formulation. Besides, with the applications of the two-fold superposition technique and the fast Fourier transform to eliminate secular terms the combined algorithms based on the formulation are available for large-scale problems of time response sensitivity with a relatively long duration required. In general, the state-of-the-art software for structural design sensitivity analysis is scarce, and a computer program for stochastic sensitivity analysis seems to be non-existent. In this regard, the numerical results obtained with POLSAP show that this finite element code would offer a reliable and cost-effective tool in research and applicable environments.

In the case of stochastic forced-vibration sensitivity analysis, the discretization and interpolation of the random and design fields depend on the finite element approximation of the displacement field. The shape functions used to describe displacements are frequently more complex than those for random and design quantities. With local-averaged values of random and design variables across each element, the finite element mesh controls the accuracy of the solutions. Moreover, the sensitivity gradients are bilinear functions of structural and adjoint displacements. Hence, the stochastic or sensitivity computations are much more sensitive to the finite element discretization than those for the conventional analysis. To obtain the same order of accuracy of the results these types of analysis require a finer element mesh. For the same reasons the effects of the period elongation and amplitude decay appeared during the numerical integration grow more rapidly than those of the conventional analysis; and the value of time interval must be selected several times smaller. In addition, the assumption of proportional damping enabling us to employ the modal analysis is also a matter of controversy. Another drawback of the stochastic finite element approach based on the second moment analysis is that the randomness can not be too large, i.e. the second moments of random variables must be relative small when compared against their expectations. According to the central limit theorem, this means that the probabilistic distribution of the input data for a stochastic finite element solution must be closely related (or exhibit a tendency) to normal distribution.

Even with these minor limitations, the computational efficiency of the approach presented far exceeds the others. The formulation for the problems of stochastic sensitivity analysis in statics and dynamics can easily be extended to deal with randomness in the domain and boundary conditions, which in turn are assumed to be design variables. In this case the surface and volume integrals can be expressed via parametric representation through their Jacobians and displacement gradient with respect to a reference configuration.

Nonlinearity in system geometry and material can be directly incorporated into

the formulation via the incremental approach by using the stochastic Hamilton's principle in the incremental form. Depending on the special class of problems and the numerical procedures preferred, the initial stress and initial displacement matrices and/or the matrix arising due to material nonlinearity and their derivatives with respect to random and design variables can be translated onto the right hand sides of equations in the form of initial loads (in terms of the initial strain or initial stress in the variational statements), or retained on the left hand sides, or both if a mixed scheme is preferred. The computational efficiency of such a formulation for static problems can be easily shown. In dynamic sensitivity analysis, however, the situation is not so straightforward. An explicit or implicit scheme of the step-by-step direct integration technique can be used. However, the computation cost would be too expensive due to dealing with all the system degrees of freedom, with all the time intervals and with the iteration solution of the effective nonlinear algebraic equations. In particular, for the at-any-time-instant sensitivity computation effort would be unacceptable high. One of the main advantages of the computer performance for these problems is that the two-fold superposition technique can be employed to decouple equations and to change basis of random variables. In geometrically and physically nonlinear systems difficulties would arise in decoupling equations of the structural and adjoint systems, since eigenpairs are not time-invariant functions and damping effects are inconveniently expressed in the Rayleigh's form. The transformation procedure from a correlated set to a uncorrelated set of random variables is also much more complicated, since the covariance matrix generally may not be positive definite. In addition, in nonlinear systems the randomness involved in natural frequencies strongly affects the wave phases of system response, leading in some cases to invalid perturbation solutions in the stochastic analysis.

Because of the shape functions used to approximate the displacement field and random and design fields are different and the finite element displacements control the accuracy of the stochastic or sensitivity solutions, it is interesting to investigate the sensitivity of the density of the finite element mesh to the stochastic and sensitivity solutions.

The stochastic formulation proposed is rather more conveniently employed to displacement-type analysis than to deal with stress-type analysis. If the number of the first two moments of stress or strain response required in the analysis is smaller than the number of random variables this direct formulation can be ineffective. The similar situation occurs in static sensitivity analysis when the number of design constraints is larger than the number of design variables. This suggests that an alternative formulation similar to the adjoint variable approach applicable to stochastic systems can be developed.

Depending on special numerical integration techniques the mass, damping and stiffness matrices and their derivatives with respect to random and design variables can be alternatively generated explicitly or implicitly. Computer procedures with implicitly generated finite elements, however, have not been fully investigated. To adapt sensitivity options to fit into existing codes with implicit finite elements, future work is definitely required due to the increasing use of these elements.

Bibliography

[1] A.H.S. Ang and W.K. Tang. *Probability Concepts in Engineering Planning and Design. Vol. I and II. Basic Principles.* Wiley, 1984.

[2] J.H. Argyris and S. Kelsey. *Energy Theorems and Structural Analysis.* Butterworth, 1960.

[3] J.H. Argyris and M. Kleiber. Incremental formulation in nonlinear mechanics and finite strain elasto-plasticity - Natural approach. Part 1. *Comput. Meth. Appl. Mech. Eng.*, 11:125–157, 1977.

[4] J.H. Argyris, M. Kleiber, and J.S. Doltsinis. Incremental formulation in nonlinear mechanics and finite strain elasto-plasticity - Natural approach. Part 2. *Comput. Meth. Appl. Mech. Eng.*, 14:259–292, 1978.

[5] J.S. Arora and J.E.B. Cardoso. A design sensitivity analysis principle and its implementation into ADINA. *Comput. Struct.*, 32(3-4):691–705, 1989.

[6] J.S. Arora and L.H. Tseng. Numerical verification of design sensitivity analysis. *AIAA J.*, 27(1):117–129, 1989.

[7] J.S. Arora and L.H. Tseng. Optimum design of systems for dynamics and controls using sequential quadratic programming. *AIAA J.*, 27(12):1793–1800, 1989.

[8] K.E. Atkinson. *An Introduction to Numerical Analysis.* Wiley, 1978.

[9] G. Augusti, A. Baratta, and F. Casciati. *Probabilistic Methods in Structural Engineering.* Chapman and Hall, 1984.

[10] K.J. Bathe. *Finite Element Procedures in Engineering Analysis.* Prentice-Hall, 1982.

[11] K.J. Bathe and E.L. Wilson. *Numerical Methods in Finite Element Analysis.* Prentice-Hall, 1976.

[12] K.J. Bathe, E.L. Wilson, and F.E. Peterson. *SAP IV - A Structural Analysis Program for Static and Dynamic Response of Linear Systems.* Technical Report, College of Engineering Univ. California, June 1973.

[13] J.S. Bendat and A.G. Piersol. *Engineering Applications of Correlation and Spectral Analysis.* Wiley-Interscience, 1980.

[14] J.S. Bendat and A.G. Piersol. *Random Data: Analysis and Measurement Procedures.* Wiley-Interscience, 1971.

[15] L. Berke and V.B. Venkayya. Review of optimality criteria approaches to structural optimization. In *Proc. ASME Winter Annual Meeting*, New York, 1974.

[16] N.M. Bogoliubov. *Asymptotic Methods in the Theory of Non-Linear Oscillators.* Gordon and Breach, 1961.

[17] A. Borkowski and K.A. Sikorski. Ultimate load analysis by stochastic programming. In M. Kleiber and J.A. König, editors, *Inelastic Solids and Structures*, pages 311–329, Pineridge Press, 1989.

[18] E.O. Brigham. *The Fast Fourier Transform.* Prentice-Hall, 1974.

[19] J.B. Cardoso and J.S. Arora. Variational method for design sensitivity analysis in nonlinear structural mechanics. *AIAA J.*, 26(5):595–603, 1988.

[20] P.G. Ciarlet. *The Finite Element Method for Elliptic Problems.* North-Holland, 1978.

[21] R.W. Clough and J. Penzien. *Dynamics of Structures.* McGraw-Hill, 1975.

[22] E.A. Coddington and N. Levinson. *Theory of Ordinary Differential Equations.* McGraw-Hill, 1955.

[23] J.D. Cole. *Perturbation Methods in Applied Mechanics.* Blaisdell Waltham, 1968.

[24] J.D. Collins and W.T. Thomson. The eigenvalue problem for structural systems with statistical properties. *AIAA J.*, 7(4):642, 1969.

[25] R.D. Cook. *Concepts and Applications of Finite Element Analysis.* Wiley, 1974.

[26] J.W. Cooley and J.W. Tukey. An algorithm for machine calculation of complex fourier series. *Math. Comput.*, 19(4):297–301, 1965.

[27] H. Crammer. *The Elements of Probability Theory.* Wiley, 1955.

[28] S.H. Crandall and W.D. Mark. *Random Vibration in Mechanical Systems.* Academic Press, 1963.

[29] G. Dahlquist and A. Björck. *Numerical Methods. Series in Automatic Computation*, Prentice-Hall, 1969. (translated by N. Anderson).

[30] W.B. Davenport and W.L. Root. *An Introduction to the Theory of Random Signals and Noise.* McGraw-Hill, 1958.

[31] P.J. Davis and P. Rabinowitz. *Methods of Numerical Integration. Series in Comput. Sci. Appl. Math.*, Academic Press, 1975.

[32] K. Dems and Z. Mroz. Variational approach by means of adjoint systems to structural optimization and sensitivity analysis. II. Structure shape variation. *Solids Struct.*, 20(6):527–552, 1984.

[33] K. Dems and Z. Mroz. Variational approach to first- and second-order sensitivity analysis. *Int. J. Num. Meth. Eng.*, 21(4):637–646, 1985.

[34] V.N. Faddeeva. *Computatonal Methods of Linear Algebra.* Dover, 1959.

[35] Y.S. Feng and F. Moses. A method of structural optimization based on structural system reliability. *Struct. Mech.*, 14(4):437–453, 1986.

[36] C. Fleury. A unified approach to structural weight optimization. *Comput. Meth. Appl. Mech. Eng.*, 20:17–38, 1979.

[37] G.E. Forsythe and C.B. Moler. *Computer Solution of Linear Algebraic Systems.* Prentice-Hall, Englewood Cliffs, 1967.

[38] R.L. Fox and M.P. Kapoor. Rate of change of eigenvalues and eigenvectors. *AIAA J.*, 6(12):2426, 1968.

[39] D.M. Frangopol. Sensitivity studies in reliability-based plastic design. *Eng. Computation*, 1(3):139–144, 1984.

[40] P.M. Frank. *Introduction to System Sensitivity Theory.* Academic Press, 1978.

[41] R.H. Gallagher. *Finite Element Analysis: Fundamentals.* Wiley, 1975.

[42] C. Goffman. *Calculus of Several Variables.* Harper-Row, 1965.

[43] H. Goldstein. *Classical Mechanics.* Addison-Wesley, 1953.

[44] W,H. Greene and R.T. Haftka. Computational aspects of sensitivity calculations in transient structural analysis. *Comput. Struct.*, 32(2):433–443, 1989.

[45] W. Gutkowski, J. Bauer, and Z. Iwanow. Discrete structural optimization. *Comput. Meth. Appl. Mech. Eng.*, 51:71–78, 1984.

[46] W. Gutkowski, J. Bauer, and Z. Iwanow. Explicit formulation of Kuhn-Tucker necessary conditions in structural optimization. *Comput. Struci.*, 1990. (accepted for publication).

[47] R.T. Haftka. Second order sensitivity derivatives in structural analysis. *AIAA J.*, 20:1765–1766, 1982.

[48] R.T. Haftka, Z.N. Martinovic, W.L. Hallarer, and G. Schamel. An analytical and experimental study of a control systems sensitivity to structural modifications. *AIAA J.*, 25(2):310–315, 1987.

[49] R.T. Haftka and Z. Mroz. First- and second-order sensitivity analysis of linear and nonlinear structures. *AIAA J.*, 24(7):1187–1192, 1986.

[50] M. Haririan, J.B. Cardoso, and J.S. Arora. Use of ADINA for design optimization of nonlinear structures. *Comput. Struct.*, 26(1-2):123–133, 1987.

[51] E.J. Haug. A review of distributed parameter structural optimization literature. In E.J. Haug and J. Cea, editors, *Optimization of Distributed Parameter Structures*, Sijthoff-Nordhoff, Alphen aan den Rijn, 1981.

[52] E.J. Haug and J.S. Arora. *Applied Optimal Design.* Wiley, 1979.

[53] E.J. Haug, K.K. Choi, and V. Komkov. *Design Sensitivity Analysis of Structural Systems. Series in Math. Sci. Eng.*, Academic Press, 1986.

[54] T.D. Hien. Computational aspects in analysis of axisymmetric solids and shells subjected to arbitrary loading. *J. Mech.*, TVIII(2):7–11, 1986. (in Vietnamese).

[55] T.D. Hien. Elastoplastic analysis of anisotropic solids with kinematic-anisotropic hardening by the finite element method. *J. Mech.*, TVII(1):8–13, 1985. (in Vietnamese).

[56] T.D. Hien. Large deformation analysis for dynamics of elastoplastic by the total Lagrangian approach. *J. Mech.*, TIX(4):9–16, 1987. (in Vietnamese).

[57] T.D. Hien. Large deformation analysis for dynamics of elastoplastic by the updated Lagrangian approach. *J. Mech.*, TX(2):8–15, 1988. (in Vietnamese).

[58] T.D. Hien. *Nonlinear Dynamics of Complex Axisymmetric Structures Subjected to Asymmetric Loads.* PhD thesis, IFTR Pol. Acad. Sci, 1981. (in Polish).

[59] T.D. Hien, H.X. Hung, and M. Kleiber. Stability analysis of structures and code POLSAP. *IFTR-Report Pol. Acad. Sci.*, No. 34, 1989. (in Polish).

[60] T.D. Hien and M. Kleiber. Computational aspects in structural design sensitivity analysis for statics and dynamics. *Comput. Struct.*, 33(4):939–950, 1989.

[61] T.D. Hien and M. Kleiber. Finite element analysis based on stochastic Hamilton variational principle. *Comput. Struct.*, 1990. (accepted for publication).

[62] T.D. Hien and M. Kleiber. Stochastic design sensitivity in structural dynamics. *Int. J. Num. Meth. Eng.*, 1990. (accepted for publication).

[63] T.D. Hien and M. Kleiber. Stochastic structural design sensitivity of static response. *Comput. Struct.*, 1990. (accepted for publication).

[64] E. Hinton and D.R. Owen. *An Introduction to Finite Element Computations.* Pineridge Press, 1979.

[65] T. Hisada and S. Nakagiri. Stochastic finite element analysis of uncertain structural systems. In *Proc. 4rd Int. Conf. in Australia on FEM*, page 133, 1982.

[66] T. Hisada and S. Nakagiri. Stochastic finite element method developed for structural safety and reliability. In *Proc. 3rd Int. Conf. Saf. Reliab.*, pages 395–402, 1981.

[67] H.X. Hung, T.D. Hien, and M. Kleiber. Dynamic analysis of fluid-structure interaction problems. *Mech. Komput.*, 1990. (in Polish, accepted for publication).

[68] N.X. Hung, N.T. Khiem, and T.D. Hien. On the quasi-stationary response of mechanic systems to random excitations. *J. Mech.*, TVII(4):20–24, 1985. (in Vietnamese).

[69] R.A. Ibrahim. Structural dynamics with parameter uncertainties. *Appl. Mech. Rev.*, 40(3):309–328, 1987.

[70] B. Irons and S. Ahmad. *Techniques of Finite Elements.* Wiley, 1980.

[71] M.S. Jankovic. Analytical solutions for the n-th derivatives of eigenvalues and eigenvectors for a nonlinear eigenvalue problem. *AIAA J.*, 26(2):204–205, 1988.

[72] T. Kato. *Perturbation Theory for Linear Operators.* Springer Verlag, 1976.

[73] P.V. Khoi and T.D. Hien. On the operating life and reliability analysis of steel structures. *J. Tech. Sci.*, XXIII(9-10):1–4, 1985. (in Vietnamese).

[74] N.S. Khot and M.P. Kamat. Minimum weight design of truss structures with geometric non-linear behaviour. *AIAA J.*, 23(1):139–144, 1985.

[75] M. Kleiber. 'Three-fields' variational theorems for the rate problems of finite strain elasto-plasticity with discontinuous fields. *ISD-Report Univ. Stuttgart*, No. 207, October 1976.

[76] M. Kleiber. *Incremental Finite Element Modelling in Non-Linear Solid Mechanics.* PWN – Ellis Horwood, 1989.

[77] M. Kleiber. Natural language estimates of nonlinear response structural sensitivity. *Comput. Mech.*, 4:373–385, 1989.

[78] M. Kleiber. Perturbation approach to the incremental equations of large deformation elasto-plasticity. *Bull. Pol. Acad. Sci. Sec. Sci. Tech.*, XXVIII(3-4):75–80, 1980.

[79] M. Kleiber. Variational formulation in finite deformation elasto-plasticity with large increments and discontinuous fields. In *Proc. IUTAM Conf. Var. Meth. Mech. Solids*, Chicago, September 1978.

[80] M. Kleiber and T.D. Hien. DYNAX – a code for dynamic analysis of axisymmetric structures under arbitrary loading by the finite element method. *IFTR-Report Pol. Acad. Sci.*, No. 25, 1980. (in Polish).

[81] M. Kleiber and T.D. Hien. Linear dynamic analysis of axisymmetric structures subjected to asymmetric loads by the finite element method. *Eng. Trans. Pol. Acad. Sci.*, 30(2), 1982. (in Polish).

[82] M. Kleiber and T.D. Hien. Nonlinear dynamic analysis of complex axisymmetric structures under arbitrary loads. *Comput. Meth. Appl. Mech. Eng.*, 37:93–107, 1983.

[83] V. Kumar, S.J. Lee, and M.D. German. Finite element design sensitivity analysis and its integration with numerical optimization techniques for structural design. *Comput. Struct.*, 32(3-4):883–897, 1989.

[84] B.M. Kwak and T.W. Lee. Sensitivity analysis for reliability-based optimization using an AFOSM method. *Comput. Struct.*, 27(3):399–406, 1987.

[85] C. Lanczos. *Applied Analysis.* Prentice-Hall, Englewood Cliffs, 1956.

[86] C. Lanczos. *The Variational Principles of Mechanics.* Univ. Toronto Press, 1964.

[87] M.A. Lawrence. A finite element solution technique for plates of random thickness. In T.J.R. Hughes and E. Hinton, editors, *Finite Element Method for Plate and Shell Structures. Vol. 2: Formulations and Algorithms*, pages 213–228, Pineridge Press, 1986.

[88] T. Lekszycki and Z. Mroz. On optimal support reaction in viscoelastic vibrating structures. *Struct. Mech.*, 11(1):67–80, 1983.

[89] Ç.C. Lin and I.W. Liu. Optimal design based on optimality criterion for frame structures including buckling constraint. *Comput. Struct.*, 31(4):535–544, 1989.

[90] Y.K. Lin. *Probabilistic Theory of Structural Dynamics.* McGraw-Hill, 1967.

[91] Y.K. Lin, F. Kozin, Y.K. Wen, F. Casciati, G.I. Schuëlle, A. Der Kiureghian, O. Ditlevsen, and E.H. Vanmarcke. Methods of stochastic structural dynamics. *Struct. Safety*, 3(3-4):167–194, 1986.

[92] H. Lippmann. *Extremum and Variational Principles in Mechanics.* Springer, 1972.

[93] W.K. Liu, T. Belytschko, and G.H. Besterfield. A variational principle for probabilistic mechanics. In T.J.R. Hughes and E. Hinton, editors, *Finite Element Method for Plate and Shell Structures. Vol. 2: Formulations and Algorithms*, pages 285–311, Pineridge Press, 1986.

[94] W.K. Liu, T. Belytschko, and A. Mani. Probabilistic finite elements for nonlinear structural dynamics. *Comput. Meth. Appl. Mech. Eng.*, 56:61–81, 1986.

[95] W.K. Liu, T. Belytschko, and A. Mani. Random field finite elements. *Int. J. Num. Meth. Eng.*, 23:1831–1845, 1986.

[96] W.K. Liu, Besterfield, and T. Belytschko. Transient probabilistic systems. *Comput. Meth. Appl. Mech. Eng.*, 67:27–54, 1988.

[97] W.K. Liu, Besterfield, and T. Belytschko. Variational approach to probabilistic finite elements. *Eng. Mech.*, 114(12):2115–2133, 1988.

[98] E. Livne. Accurate calculation of control-augmented structural eigenvalue sensitivities using reduced-order. *AIAA J.*, 27(7):947–954, 1989.

[99] H.O. Madsen. Omission sensitivity factors. *Struct. Safety*, 5:35–45, 1988.

[100] H.C. Martin and G.F. Carey. *Introduction to Finite Element Analysis.* McGraw-Hill, 1969.

[101] E.F. Masur and Z. Mroz. Singular solutions in structural optimization problems. In S. Nemat-Nasser, editor, *Variational Methods in Mechanics of Solids*, pages 337–343, Pergamon Press, 1986.

[102] L. Meirowitch. *Elements of Vibration Analysis.* McGraw-Hill, 1986.

[103] R.H. Meric. Shape design sensitivity analysis of dynamic structures. *AIAA J.*, 26(2):206–212, 1988.

[104] A. Myslinsky. Bimodal optimal design of vibrating plates using theory and methods of nondifferentiable optimization. *J.O.T.A.*, 46(2):187–203, 1985.

[105] A.H. Nayfeh. *Introduction to Perturbation Techniques.* Wiley, 1981.

[106] A.H. Nayfeh. *Perturbation Methods.* Wiley, 1973.

[107] B. Noble. *Applied Linear Algebra.* Prentice-Hall, Englewood Cliffs, 1969.

[108] J.T. Oden. *Finite Element of Nonlinear Continua.* McGraw-Hill, 1972.

[109] J.T. Oden and J.N. Reddy. *Variational Methods in Theoretical Mechanics.* Springer, 1976.

[110] N. Olhoff and S.H. Rasmussen. On single and bimodal optimum buckling loads of clamped columns. *Solids Struct.*, 13:605–614, 1977.

[111] A.V. Oppenheim and R.W. Schafer. *Digital Signal Processing.* Prentice-Hall, Englewood Cliffs, 1975.

[112] A.V. Oppenheim, A.S. Willsky, and I.T. Young. *Signals and Systems. Series in Signal Processing*, Prentice-Hall, 1983.

[113] G.G. Pope and L.A. Schmit, editors. *Structural Design Applications of Mathematical Programming Techniques.* Agardograph, 1971.

[114] S. Prager and W. Prager. A note on optimal design of columns. *Mech. Sci.*, 21:249–251, 1979.

[115] W. Prager. *Variational Principles of Linear Elastostatics for Discontinuous Displacements, Strains and Stresses.* Folk Odquist Volume, 1967.

[116] J.S. Przemieniecki. Matrix structural analysis of substructures. *AIAA J.*, 1:138–147, 1963.

[117] J.S. Przemieniecki. *Theory of Matrix Structural Analysis.* McGraw-Hill, 1968.

[118] L.R. Rabiner and B. Gold. *Theory and Application of Digital Signal Processing.* Prentice-Hall, Englewood Cliffs, 1975.

[119] K.K. Raju, G.V. Rao, and N. Venugopal. Use of design sensitivity coefficients for prediction of structural behaviour after design modification. *Comput. Struct.*, 33(5):1329–1331, 1989.

[120] B. Rousselet. *Quelques Resultats en Optimisation de Domain.* PhD thesis, Univ. de Nice, 1981.

[121] Y.S. Ryu, M. Haririan, C.C. Wu, and J.S. Arora. Structural design sensitivity analysis of nonlinear response. *Comput. Struct.*, 21(1-2):245–255, 1985.

[122] J.C.T. Santos, M.M. Goshe, and C.H. Chang. An interactive post-processor for structural design sensitivity analysis and optimization: sensitivity display and what-if study. *Comput. Struct.*, 35(1):1–13, 1990.

[123] L.A. Schmit. Structural design by systematic synthesis. In *Proc. 2nd Conf. Elect. Comput. ASCE*, New York, 1960.

[124] K.A. Sikorski and A. Borkowski. Application of stochastic programming to limit analysis. *IFTR-Report Pol. Acad. Sci.*, No. 51, 1985. (in Polish).

[125] T.A. Stone, J.L.T. Santos, and E.J. Haug. An interactive pre-processor for structural sensitivity analysis and optimization. *Comput. Struct.*, 34(3):375–385, 1990.

[126] J. Szmelter. The energy method of networks of arbitrary shape in problems of the theory of elasticity. In W. Olszak, editor, *Proc. IUTAM Symp. Non-Homog. Elast. Plast.*, 1959.

[127] J. Szopa. Application of stochastic sensitivity functions to chaotic systems. *Sound Vib.*, 104(1):176–178, 1986.

[128] J. Szopa. Sensitivity of stochastic systems to initial conditions. *Sound Vib.*, 97(4):645–649, 1984.

[129] I. Tadjbakhsh and J.B. Keller. Strongest columns and isoparametric inequalities for eigenvalues. *Appl. Mech.*, 29:159–164, 1977.

[130] A.E. Taylor. *Advanced Calculus.* Gin. Boston, 1955.

[131] P. Thoft-Christensen. Recent advances in structural systems reliability theory. In *Proc. IABSE Symp.*, pages 101–108, Tokyo, 1986.

[132] J.M.T. Thomson and G.W. Hunt. Dangers of structural optimization. *Eng. Optim.*, 2:99–110, 1974.

[133] K.D. Tocher. *The Art of Simulation.* McGraw-Hill, 1968.

[134] P. Tong and J.N. Rossettos. *Finite Element Method. Basic Technique and Implementation.* The MIT Press, 1978.

[135] E. Vanmarcke, M. Shinozuka, S. Nakagiri, G.I. Schuelle, and M. Grigoriu. Random fields and stochastic finite elements. *Struct. Safety*, 3(3-4):143–166, 1986.

[136] E.H. Vanmarcke. *Random Fields: Analysis and Synthesis.* The MIT Press, 1983.

[137] E.H. Vanmarcke. Stochastic finite element analysis. In M. Shinozuka and J.T.P. Yao, editors, *Probabilistic Methods in Structural Engineering*, pages 278–294, ASCE, 1981.

[138] E.H. Vanmarcke and M. Grigoriu. Stochastic finite element analysis of simple beams. *ASCE, J. Eng. Mech. Div.*, 109(5):1203–1214, 1983.

[139] K. Washizu. *Variational Methods in Elasticity and Plasticity.* Pergamon Press, 1975.

[140] E. L. Wilson. The static condensation algorithm. *Int. J. Num. Meth. Eng.*, 8:199–103, 1974.

[141] E. L. Wilson. Structural analysis of axisymmetric solids. *AIAA J.*, 3:2269–2274, 1965.

[142] C.C. Wu and J.S. Arora. Design sensitivity analysis of nonlinear buckling load. *Comput. Mech.*, 3(2):129–140, 1988.

[143] R.J. Yang and M.E. Botkin. Accuracy of the domain material derivative approach to shape design sensitivities. *AIAA J.*, 25(12):1606–1610, 1987.

[144] O.C. Zienkiewicz. *The Finite Element Method in Engineering Science.* McGraw-Hill, second edition, 1971.

[145] O.C. Zienkiewicz and J.S. Campbell. Shape optimization and sequential linear programming. In R.H. Gallagher and O.C. Zienkiewicz, editors, *Optimum Structural Design*, Wiley, 1973.

[146] O.C. Zienkiewicz and R.C. Taylor. *The Finite Element Method.* McGraw-Hill, forth edition, 1989.

List of Symbols

1_m	identification vector
$a_{\xi\alpha}$, $a_{\eta\beta}$	coordinate transformation matrix
a_r	cross-sectional area
a_z	1st integration constant of Duhamel's convolution
A_z	integration approximation operator
b_z	2nd integration constant of Duhamel's convolution
b, b^r, b^s	vector of random variables
b_o^r, b_o^s	expectation functions of random variables
$B_{ij\alpha}$	strain-displacement relating matrix in global coordinates
$B_{ij\xi}$	strain-displacement relating matrix in local coordinates
c^v	uncorrelated (transformed) random variable
C	number of constraints
C_{ijkl}	constitutive tensor
$C(b^r, b^s, b^t)$	3rd-order center moment function of random variables
$C(b^r, b^s, b^t, b^u)$	4th-order center moment function of random variables

$Cov(b^r, b^s)$	covariance function of random variables
D	diagonal matrix
D, $D_{\alpha\beta}$	system damping matrix
$\mathcal{D}$	Rayleigh's dissipation function
e_r	Young modulus in stochastic analysis
E	total number of design variables
	total number of finite elements
	Young modulus in deterministic analysis
$E(b^r)$	expectation function of random variables
f	cycle frequency
f_i	vector of body forces
f_α	vector of nodal forces
$g(b^r)$	probability density function
$g(b^r, b^s)$	joint probability density function
g_z	uncorrelated adjoint modal load
g_α	vector of uncorrelated adjoint loads
G	structural response functional
h, h^e, h^l	vector of design variables
I_o, I_x, I_y	moments of inertia
$\mathcal{J}$	potential energy
$k_{\xi\zeta}$	element stiffness matrix
K, $K_{\alpha\beta}$	system stiffness matrix
l, l_e	structural member length
L	length of complex-valued series
	number of load cases acting on a system
	lower triangular matrix of Gauss decomposition
$\tilde{L}$	lower triangular matrix of Cholesky decomposition
$\mathcal{L}$	Lagrange function
M, $M_{\alpha\beta}$	system mass matrix
n	number of time intervals
N	total number of system degrees of freedom
p	time complex-valued series
p_z	modal load operator
	uncorrelated structure modal load
p_α	vector of uncorrelated structural loads
P	frequency complex-valued series (discrete Fourier spectrum)
q_α, q_β	vector of nodal displacements in global coordinates
q^*	particular solution of displacement
$Q_{z\alpha}$, $Q_{z\beta}$	system eigenvector matrix
r	frequency range factor for secularity elimination
r_e	sensitivity residual
R	total number of random variables
$R(b^r, b^s)$	autocorrelation function of random variables
$s^{(1)}$, $s_e^{(2)}$	scale factors in the optimization problem
$\mathcal{S}$	Lagrange function in the optimization problem

t	element thickness
	forward time variable
	running time variable
$\hat{t}_i$	vector of boundary tractions
t^*	dummy (time) variable for integration
T	terminal time function
$\mathcal{T}$	kinetic energy
	terminal time condition function
u_i, u_k	displacement vector
$u_{i,j}$	spatial derivative of displacement
$u_\xi^{(n)}$	vector of nodal displacements in local coordinates
U, $U_{r\nu}$	fundamental matrix of standard eigenproblem
V	total number of transformed random variables used in analysis
$Var(b^r)$	variance function of random variables
$Var(c^\nu)$	variance function of uncorrelated random variables
$\mathcal{W}$	cost function
x	spatial variable
y_α	normal (modal) displacements
z_β	displacement vector in homogeneous systems
Z	number of mode shapes used in analysis
$Z_{\alpha\beta}$, $Z_{d\beta}$	stress-displacement relating matrix
α	variation coefficient of random variables
	1st interpolating coefficient of Newmark integration
	approximating damping coefficient (mass term)
α_z	approximating modal damping coefficient (mass term)
β	approximating damping coefficient (stiffness term)
β_z	approximating modal damping coefficient (stiffness term)
γ	accelerating iteration coefficient
	weight density
δ	2nd interpolating coefficient of Newmark integration
δ_{uz}	Kronecker delta
Δ	time domain of Dirac measure
ε_{ij}	strain tensor
ζ	damping factor
θ	extrapolating coefficient of Wilson-θ integration
	small parameter of perturbation
ϑ_z	modal adjoint coordinates
Θ_ν	diagonal matrix of transformed variances
λ_α, λ_β	vector of adjoint variables
$\lambda_\alpha^{(1)}$	Lagrange multipliers associated with equilibrium condition
$\lambda_\alpha^{(2)}$	Lagrange multipliers associated with displacement constraints
$\lambda_\alpha^{(3)}$	Lagrange multipliers associated with stress constraints
$\lambda_\alpha^{(4)}$	Lagrange multipliers associated with cross-section constraints

ν	Poisson ratio
	dummy (time) variable for integration
ξ_s	modal damping coefficient
$\bar{\xi}_1$, $\bar{\xi}_2$	averaged damping coefficient
ϱ	mass density
σ_{ij}	stress tensor
τ	backward time variable
	dummy (time) variable for integration
ϕ	constraint functional
$\varphi_{i\alpha}$	shape function in global coordinates
$\psi_{i\xi}$	shape function in local coordinates
ω_{nyq}	Nyquist cutoff (folding) frequency
ω_s	natural frequency
$\bar{\omega}_1$, $\bar{\omega}_2$	averaged frequency
Ω	continuum volume
$\partial\Omega$	continuum boundary
$\Omega_{(s)}$, $\Omega_{(\alpha)}$	diagonal matrix of system eigenvalues

$(.)_o$, $(.)^o$	deterministic quantity
$(.)^{-1}$	inverse matrix
$(.)^{(2)}$	unknown of 2nd-order perturbation equations
$(.)^A$	allowable value
$(.)_{\text{binary}}$	base-2 number representation
$(.)_{\text{decimal}}$	base-10 number representation
$(.)^{MIN}$	minimum value
$(.)^T$	transposed vector or matrix
$(.)^{\cdot_k}$, $(.)^{\cdot_l}$	1st derivative with respect to design variables
$(.)^{\cdot_r}$, $(.)^{\cdot_s}$	1st derivative with respect to random variables
$(.)^{\cdot_v}$	1st derivative with respect to transformed random variable
$(.)^{\cdot_{rs}}$	2nd derivative with respect to random variables
$(.)^{\cdot_{vv}}$	2nd derivative with respect to transformed random variable
$(.)_{,\alpha}$, $(.)_{,\beta}$	1st derivative with respect to displacements
$0(.)$	order estimate
$Cov[(.),(.)]$	output spatial covariance function
$E[(.)]$	output spatial expectation function
$\text{mod}[(.)/(.)]$	remainder in integer-division operation
$\dot{w}$	1st time derivative of function w
$\ddot{w}$	2nd time derivative of function w
$\delta(.)$	1st variation
$\delta\left((.)\right)$, $\delta_\Delta\left((.)\right)$	Dirac delta distribution
$\Delta(.)$	increment
a.t.i.	at-time-instant
o.t.d.	over-time-domain

APPENDIX

P O L S A P – A Finite Element Code for Deterministic and Stochastic Analyses of Large 3D Structures

U S E R ' S M A N U A L

The computer program POLSAP, a modified and considerably extended version of the package SAP-IV, is designed for research and application environments. In SAP-IV five analysis types are supported. POLSAP has been worked out to deal with fourteen analysis options; and all the advantages of SAP-IV related to its numerical features, model size limits, etc. are remained. The system of total length of about 40,000 commands[1] has been developed for IBM compatible personal computers which run under MS DOS 3.0 and its later versions. All developments have been made using Fortran 77; the MS Fortran Compiler 5.0 and its later versions are recommended. Minimum hardware requirements are: 640KB of operating memory, a hard disk drive of 10MB and a CGA, VGA, Color Graphics or Hercules Graphics card. The package has been written to be readily adapted to fit into other operating systems such as UNIX, XENIX with only small non-Fortran modifications.

For deterministic systems POLSAP includes a library of nine finite element types available to solve problems of statics, thermal effects, free and forced vibrations and response spectrum of 1D, 2D and 3D structures. Solutions can be obtained for minimum-weight optimization of trusses, buckling loads and design sensitivity in statics, eigenvalues and dynamics of truss-beam-shell structures. Displacement and stress functions may be involved in the response functionals for sensitivity analysis. Design variables considered are cross-sectional area, length, thickness, Young modulus and mass density of structural members.

In stochastic analysis uncertainties in geometry and material parameters has been incorporated through a combination of the stochastic finite element technique, the second-moment analysis and the adjoint variable approach. The probabilistic distributions (spatial expectations and covariances) of static and dynamic response of truss-beam-shell structures can be evaluated. A version for stochastic design sensitivity analysis in statics and dynamics, where design variables are random, has been implemented into POLSAP to compute the first two moments of the sensitivity gradients of truss-beam-shell structures.

The input data should have the following format.

[1] The original system length was about 26,000 Fortran lines

I. Heading Line (12a4).

columns	*variable*	*entry*
1–48	HED(12)	Alphanumeric heading information.

II. Problem Control Line (13i5).

note	*columns*	*variable*	*entry*
(1)	1–5	NUMNP	Total number of nodal points in the model.
(2)	6–10	NELTYP	Number of element groups.
(3)	11–15	LL	Number of static load cases.
(4)	16–20	NF	Number of required eigenpairs.
(4)	21–25	NDYN	Analysis type code, EQ.0, Deterministic statics, EQ.1, Structural eigenproblem, EQ.2, Deterministic forced vibration, mode superposition, EQ.3, Deterministic response spectrum, EQ.4, Deterministic forced vibration, Wilson-θ integration, EQ.5, Structural design sensitivity, deterministic statics, EQ.6, Eigenvalue sensitivity, EQ.7, Buckling load, EQ.8, Structural design sensitivity, deterministic dynamics, EQ.9, Minimum-weight optimization (truss only), EQ.10, Stochastic statics, EQ.11, Stochastic forced vibration, EQ.12, Structural design sensitivity, stochastic statics, EQ.13, Structural design sensitivity, stochastic dynamics.
(5)	26–30	MODEX	Execution mode, EQ.0, problem solution, EQ.1, data check.
(6)	31–35	NAD	Total number of vectors used in a subspace iteration solution for eigenproblem, EQ.0, set to MIN(2*NF,NF+8).
(7)	36–40	KEQB	Number of degrees of freedom (equations) per block of storage, EQ.0, automatically computed by program.

(8)	51–55	NC	Number of displacement constraints (NDYN.EQ.5 only).
(9)	56–60	ICURVE	Dynamic response display flag (NDYN.EQ.4 only).
(10)	61–65	ICONTYP	Response functional type (NDYN.EQ.5 only), EQ.0, displacement constraint type, EQ.1, stress constraint type.

Notes

(1) Nodes are labeled with integers ranging from one (1) to the total number of nodes NUMNP. POLSAP exits with no diagnostic message if NUMNP is zero.

(2) For each different element type a new element group need be defined. Elements within groups are assigned integer labels ranging from one (1) to the total number of elements in the group. Element groups are input in Section IV, below. Element numbering must begin with one (1) in each different group. It is possible to use more than one group for an element type. For example, all columns of a building may be considered one group and the girders may be considered another group.

(3) At least one load condition (LL.EQ.1) must be specified for a static analysis type (NDYN.EQ.0, 5, 7, 9, 10, 12); LL is automatically equal to one (1) if NDYN.EQ.7, 9, 10, 12. If the data case calls for one of the dynamic analysis type (NDYN.EQ.1, 2, 3, 4, 6, 8, 11, 13), LL is inactive and can be input as zero or default and the number of load case is set to one (1) by POLSAP. The program always processes Section V (concentrated load/mass data) and Section VI (element load multipliers) and expects to read some data. For the case of NDYN.EQ.1, 2, 3, 4, 6, 8, 11, 13 only mass coefficients can be input in Section V, and one (1) blank element load multiplier line is expected in Section VI.

(4) For NDYN.EQ.0, 4, set NF=0. If NDYN.EQ.1 the lowest NF eigenpairs are computed and printed. If NDYN.EQ.2, 3, 6, 8, 11, 13 POLSAP first solves for the NF eigenpairs and then performs the dynamic response solution; for the options NDYN.EQ.8, 11, 13 number of requested modes can not be larger than 48. Thus, POLSAP expects to read the control line governing the eigenproblem (Section X.A) before reading data in Sections X.B, C, D. If NDYN.EQ.6 the design sensitivity problem is solved for NF lowest eigenvalues. If NDYN.EQ.4 POLSAP performs the response solution by step-by-step direct integration and no eigenvalue solution control line should be provided.

(5) In the data-check mode (MODEX.EQ.1), POLSAP writes only one file, File8, and this file may be saved for use as input to special purpose programs such as mesh plotters, etc. File8 contains all data input in its completely generated form. If MODEX.EQ.1, most of the expensive calculations required during normal execution (MODEX.EQ.0) are skipped. File8, however, is used for other purposes during problem solution.

(6) Since POLSAP solves for eigenpairs using the subspace iteration algorithm, the entry in columns 31–35 can be used to change the total number of iteration vectors to be used from the default minimum of 2*NF or NF+8 (whichever is smaller) to the value NAD. The effect of increasing NAD over the default value is to accelerate convergence in the calculations for the lowest NF eigensystems. NAD is principally a program testing parameter and should normally be left blank.

(7) KEQB is a program testing parameter which allows the user to test multiple equation block solutions using small data cases which would otherwise be one block problems. KEQB is normally left blank.

(8) NC is number of displacement constraints in structural design sensitivity analysis for static response. This parameter is active for NDYN.EQ.5 and ICONTYP.EQ.0 only. POLSAP expects to read the data in Section V.

(9) During problem solution, the time response of the displacement at a nodal point in a prescribed direction can be shown on the screen. POLSAP expects to read the data related to the degree of freedom in Section X.

(10) Type of the response functional assumed in static sensitivity analysis is defined. For the case ICONTYP.EQ.0 the functionals are described with displacement constraints and allowable displacements are included. If ICONTYP.EQ.1 the functionals are described with stress constraints, i.e. allowable stresses are included and expected to be read in Section IV.

III. Nodal Point Data (2(a1, i4), 5i5, 3d10.0, i5, d10.0).

note	*columns*	*variable*	*entry*
(1)	1	CT	Symbol describing coordinates system, DEFAULT, cartesian (X,Y,Z). C, cylindrical (R,Y,θ), (upper case letter),
(2)	2–5	N	Node number.
	6	IPR	Flag for nodal data printing, DEFAULT, full printing, (input, generated and mapping data), EQ.A, suppress printing generated data, EQ.B, suppress printing mapping array, EQ.C, both A and B, (upper case letters).
(3)	7–10	IX(N,1)	X-translation boundary condition code,
	11–15	IX(N,2)	Y-translation boundary condition code,
	16–20	IX(N,3)	Z-translation boundary condition code,
	21–25	IX(N,4)	X-rotation boundary condition code,
	26–30	IX(N,5)	Y-rotation boundary condition code,

	31–35	IX(N,6)	Z-rotation boundary condition code, EQ.0, free, EQ.1, fixed (no load allowed), GT.1, master (beam only) node number.
(4)	36–45	X(N)	X (or R)– ordinate,
	46–55	Y(N)	Y – ordinate,
	56–65	Z(N)	Z (or θ) – ordinate (in degrees).
(5)	66–70	KN	Generating increment for node numbers.
(6)	71–80	T(N)	Nodal temperature.

Notes

(1) A cylindrical coordinate system is allowed for the global description of nodal point locations. If a character C (upper case letter) is entered in column 1 then the entries given in columns 36–65 are taken to be references to a global cylindrical (R,Y,θ) system rather than to the cartesian (X,Y,Z) system. POLSAP converts cylindrical coordinates to cartesian coordinates using the formulae

$$X = R\sin\theta, \qquad Y \equiv Y, \qquad Z = R\cos\theta.$$

Cylindrical coordinate input is merely a user convenience for locating nodes in the standard (X,Y,Z) system, and no other references to the cylindrical system are implied; i.e., boundary condition specifications, output displacement components, etc. are referenced to the (X,Y,Z) system.

(2) Nodal point data must be defined for all (NUMNP) nodes. Node data may be input directly (i.e., each node on its own individual line) or the generating option may be used if applicable, see note (5), below. Admissible nodal point numbers range from one (1) to the total number of nodes, NUMNP.

(3) Boundary condition codes can only be assigned the following values:

IX(N,M).EQ.0, unspecified (free) translation (rotation) component,
IX(N,M).EQ.1, deleted (fixed) translation (rotation) component,
IX(N,M).EQ.K, node number K ($1<K\leq$NUMNP, and $K\neq N$) is the master node to which the M-th d.o.f. at node N is a slave.
(M=1,...,6).

A unspecified d.o.f. (IX(N,M).EQ.0) is free to translate or rotate as the solution dictates. Concentrated forces (moments) may be applied (Section V, below) in this d.o.f. One (1) system equilibrium equation is required for each unspecified d.o.f. in the model. The maximum number of equilibrium equations is always less than six (6) times the total number of nodes in the model. Deleted d.o.f. (IX(N,M).EQ.1) is removed from the final set of equilibrium equations. Deleted d.o.f. is fixed (point of reaction), and any loads applied in these d.o.f. are ignored by POLSAP. Nodes that are used for geometric reference only (i.e., nodes not assigned to any element) must have all six (6) d.o.f. deleted. Nodal d.o.f. having undefined stiffness (such

as rotations in an all truss model, out-of-plane components in a 2D model, etc.) should be deleted. Deletions have the beneficial effect of reducing the size of the set of equations that must be solved. The table below lists the types of d.o.f. that are defined by each different element type. The table was prepared assuming that the element has general orientation in (X,Y,Z) space.

Active Degrees of Freedom						
element type	*translations – rotations*					
	q_x	q_y	q_z	ϑ_x	ϑ_y	ϑ_z
1. 3D Truss	•[a]	•	•			
2. 3D Beam	•	•	•	•	•	•
3. Membrane	•	•	•			
4. 2D Quadrilateral		•	•			
5. Brick	•	•	•			
6. Plate/Shell	•	•	•	•	•	•
7. Boundary	•	•	•	•	•	•
8. Thick Shell	•	•	•			
9. 3D Pipe	•	•	•	•	•	•

[a] active component

Hence, for an all 3D brick model, only the X,Y,Z translations are defined at the nodes, and the number of equations can be cut in half by deleting the three (3) rotational components at every node. If a node is common to two or more different element types, then the non-trivial d.o.f. are found by combination. For example, all six (6) components are possible at a node common to both beam and truss elements; i.e., the beam governs.

A master/slave option is allowed to model rigid links in the system. For this case, IX(N,M).EQ.K means that the M-th d.o.f. at node N is slave to (dependent on) the same (M-th) d.o.f. at node K; node K is said to be the master node to which node N is slave. Note that no actual beam need to run from node K to node N, however the following restrictions hold:

- node one (1) cannot be a master node; i.e. K≠1,
- nodes N and K must be beam-only nodes; i.e., no other element type may be connected to either node N or K,
- a node N can be slave to only one master node K; multiple nodes, however, can be slave to the same master,
- if the beam from N to K is to be a rigid link arbitrarily oriented in the (X,Y,Z) space, then all six (6) d.o.f. at node N must be made slaves to node K.

Translation/rotation components for slave d.o.f. at node N are not recovered for printing; i.e., zeros appear as output for slave d.o.f.

(4) When CT (column 1) is equal to the character C (upper case letter), the values input in columns 36–65 are interpreted as the cylindrical (R,Y,θ) coordinates of

node N. Y is the axis of symmetry. R is the distance of a point from the Y-axis. The angle θ is measured clockwise from the positive Z-axis when looking in the positive Y direction. The cylindrical coordinate values are printed as entered on the line, but immediately after printing the global cartesian values are computed from the input entries. Note that boundary condition codes always refer to the (X,Y,Z) system even if the node happens to be located with cylindrical coordinates.

(5) Nodal point lines need not be input in node-order sequence. However, all nodes in the integer set (1,NUMNP) must be defined. Joint data for a series of nodes (N1, N1+KN2, N1+2*KN2,..., N2–KN2) may be generated from information given on two lines in sequence

line 1	N1	IX(N1,1) ...	X(N1) ...	KN1	T(N1) ,
line 2	N2	IX(N2,1) ...	X(N2) ...	KN2	T(N2) .

The mesh generating parameter KN2 is given on the second line of a sequence. Note that the node difference N2–N1 must be divisible by KN2. Intermediate nodes between N1 and N2 are located at equal intervals along the straight line between the two points. Boundary condition codes for the generated data are set equal to the values given on the first line. Node temperatures are found by linear interpolation between T(N1) and T(N2). Coordinate generating is always performed in the (X,Y,Z) system, and no generating is performed if KN2 is zero (blank).

(6) Nodal temperatures describe the actual (physical) temperature distribution in the structure. Average element temperatures established from the nodal values are used to select material properties and to compute thermal strains in the model (static analysis only).

IV. Element Data

Only data input for the element types whose finite element procedures have been considerably modified (when compared against SAP-IV) to incorporate design characteristics and uncertainties in geometry and material parameters into analysis are specifed below, i.e. data for **3D Truss, 3D Beam, Plate/Shell** and **Boundary**. The data input for other elements (**Membrane, 2D Quadrilateral, Brick, Thick Shell** and **3D Pipe**) can be found in SAP-IV **User's Manual**.

Type 1 – 3D Truss elements

Truss elements are identified by the number 1. Axial forces and stress are calculated for each element. A uniform temperature change and inertia loads in three directions can be considered as the basic element load conditions. The truss elements are described by the following sequence of lines.

A. *Control line* (3i5, 15x, 2i5).

columns	1–5	The number 1.
	6–10	Number of truss elements in the group.
	11–15	Number of material property types.
	31–35	Flag for sensitivity and/or optimization or stochastic analysis (ISENS), EQ.0, no, EQ.1, yes.
	36–40	Design and/or stochastic variable type, Inactive if ISENS.EQ.0, EQ.1, Cross-sectional area, EQ.2, Young modulus, EQ.3, Mass density, EQ.4, Length.

B. *Material property lines* (i5, 5d10.0).

There need be as many of the following lines as are necessary to define the properties listed below for each element in the structure.

columns	1–5	Material identification number.
	6–15	Young modulus.
	16–25	Coefficient of thermal expansion.
	26–35	Mass density.
	36–45	Cross-sectional area (Initial cross-sectional area if NDYN.EQ.9).
	46–55	Weight density (used to calculate gravity loads).

C. *Element load factors* (4d10.0). Four lines.

Three lines specifying the fraction of gravity in each of the three global coordinate directions to be added to each element load case.

Line 1. Multipliers of gravity load in the global +X direction.

columns	1–10	Element load case A.
	11–20	Element load case B.
	21–30	Element load case C.
	31–40	Element load case D.

Line 2. As above for gravity load in the global +Y direction.

Line 3. As above for gravity load in the global +Z direction.

Line 4. This indicates the fraction of the thermal load to be added to each of the element load cases A, B, C, D.

D. *Element data lines* (4i5, d10.0, i5, d10.0).

One per element in increasing numerical order starting with one (1).

columns	1–5	Element number.
	6–10	Node number I.
	11–15	Node number J.
	16–20	Material property number.
	21–30	Reference temperature for zero stress.
	31–35	Generating parameter k.
	36–45	Allowable normal stress, (NDYN.EQ.5 and ICONTYP.EQ.1 only).

Remarks

◇ If a series of elements exist such that the element number N, is one greater than the previous element number (i.e. $N_i=N_{i-1}+1$) and the nodal point number can be given by $I_i=I_{i-1}+k$ and $J_i=J_{i-1}+k$ then only the first element in the series need be provided. The element identification number, the temperature and the admissible value of the normal stress for the generated elements are set equal to the values on the first line. If k (given on the first line) in input as zero it is set to 1 by POLSAP. The element data line for the last truss element must always be given.

◇ The element temperature increment ΔT used to calculate thermal loads is given by $\Delta T=(T_i+T_j)/2-T_r$ where symbols T_i and T_j) represent the nodal temperatures specified on the nodal point data lines for nodes I and J; and T_r is the zero stress reference temperature specified on the element line. For truss elements it is generally more convenient to set $T_i=T_j=0.0$ such that $\Delta T=-T_r$ (minus sign). Other types of element loadings can be specified using an equivalent ΔT. If a truss element has an initial imperfection by an amount d (positive if too long) then $\Delta T=d/(\alpha L)$. If an initial prestress force P (positive if tensile) is applied to the element ends that is released after the element is connected to the rest of the structure then $\Delta T=-P/(\alpha AE)$, where A – cross-sectional area, L – element length and α – the coefficient of thermal expansion.

Type 2 – 3D Beam elements

Beam elements are identified by the number 2. Forces (axial and shear) and moments (bending and torsion) are calculated for each beam in its local coordinate system (x,y,z). Gravity loadings in global coordinate directions and specified fixed-end forces in local coordinate directions form the basic element load conditions. The beams elements are described by the following sequence of lines.

A. *Control line* (5i5, 5x, 2i5).

columns		
	1–5	The number 2.
	6–10	Number of beam elements in the group.
	11–15	Number of geometric property types.
	16–20	Number of fixed-end force sets.
	21–25	Number of material property types.
	31–35	Flag for sensitivity and/or stochastic analysis (ISENS), EQ.0, no, EQ.1, yes.
	36–40	Design and/or stochastic variable type, Inactive if ISENS.EQ.0, EQ.1, Cross-sectional area, EQ.2, Young modulus, EQ.3, Mass density, EQ.4, Length.

B. *Material property lines* (i5, 5d10.0).

columns		
	1–5	Material identification number.
	6–15	Young modulus.
	16–25	Poisson ratio.
	26–35	Mass density.
	36–45	Weight density (used to calculate gravity loads).

C. *Geometry property lines* (i5, 6d10.0).

columns		
	1–5	Geometric property number.
	6–15	Axial (local x-direction) area.
	16–25	Shear area associated with shear forces in local y-direction.
	26–35	Shear area associated with shear forces in local z-direction.
	36–45	Torsional inertia (about local x-axis).
	46–55	Flexural inertia about local y-axis.
	56–65	Flexural inertia about local z-axis.

One line is required for each unique set of properties. Shear areas need be specified only if shear deformations are to be included in the analysis.

D. *Element load factors* (4d10.0). Three lines.

Nodal point loads (no moments) due to gravity are computed. Three lines need be supplied which specify the fraction of these loads in each of the three global coordinate directions to be added to each element load case.

Line 1. Multipliers of gravity load in the global +X direction.

columns		
	1–10	Element load case A.
	11–20	Element load case B.
	21–30	Element load case C.
	31–40	Element load case D.

Line 2. As above for gravity load in the global +Y direction.

Line 3. As above for gravity load in the global +Z direction.

E. *Fixed-end forces* (i5, 6d10.0 / 5x, 6d10.0).

Two lines are required for each unique set of fixed-end forces occurring in the analysis. Distributed loads and thermal loads can be specified using the fixed-end forces.

Line 1

columns		
	1–5	Fixed-end force number.
	6–15	Fixed-end force in local x-direction at node I.
	16–25	Fixed-end force in local y-direction at node I.
	26–35	Fixed-end force in local z-direction at node I.
	36–45	Fixed-end moment about local x-direction at node I.
	46–55	Fixed-end moment about local y-direction at node I.
	56–65	Fixed-end moment about local z-direction at node I.

Line 2

columns		
	1–5	(Left blank)
	6–15	Fixed-end force in local x-direction at node J.
	16–25	Fixed-end force in local y-direction at node J.
	26–35	Fixed-end force in local z-direction at node J.
	36–45	Fixed-end moment about local x-direction at node J.
	46–55	Fixed-end moment about local y-direction at node J.
	56–65	Fixed-end moment about local z-direction at node J.

Values input are literally fixed-end values. Corrections due to hinges and rollers are performed within POLSAP.

F. *Element data lines* (10i5, 2i6, i8)

columns		
	1–5	Element number.
	6–10	Node number I.
	11–15	Node number J.
	16–20	Node number K (used for orientation of local y-axis).
	21–25	Material property number.

26–30	Element property number.
31–35	Fixed-end force identification for element load case A.
36–40	Fixed-end force identification for element load case B.
41–45	Fixed-end force identification for element load case C.
46–50	Fixed-end force identification for element load case D.
51–56	End release code at node I.
57–62	End release code at node J.
63–70	Optional parameter k used for automatic generation of element data. This option is described below under a separate heading. If the option is not used, the field is left blank.

The end release code at each node is a six digit number of ones and/or zeros. The 1st,...,6th digits respectively correspond to the force components R_x, R_y, R_z, M_x, M_y, M_z at each node (local coordinates). If any one of the above element end forces is known to be zero (hinge or roller), the digit corresponding to that component is one (1).

Remarks

◇ If a series of elements occurs in which each element number N_i is one greater than the previous number N_{i-1}, i.e. $N_i=NE_{i-1}+1$, only the element data line for the first element in the series need be given as input, provided

- the end nodal point numbers are $NI_i=NI_{i-1}+k$ and $NJ_i=NJ_{i-1}+k$,

and

- material property number,
- element property number,
- fixed-end force identification numbers for each element load case,
- element release codes,
- orientation of local y-axis

are the same for each element in the series. The values of k, if left blank, is taken to be one. The element data line for the last beam element must always be given.

◇ When successive beam elements have the same stiffness, element orientation and loading, POLSAP automatically skips recomputation of the stiffness. Note this when numbering the beams to obtain maximum efficiency.

Type 3 – Plate/Shell elements

Only rectangular and triangular elements are possible. The rectangular elements should be used as much as possible in finite element modelling. The plate or shell elements are described by the following sequence of lines.

A. *Control line* (3i5, 15x, 2i5).

columns	1–5	The number 6.
	6–10	Number of plate/shell elements in the group.
	11–15	Number of material property types.
	31–35	Flag for sensitivity and/or stochastic analysis (ISENS), EQ.0, no, EQ.1, yes.
	36–40	Design and/or stochastic variable type, Inactive if ISENS.EQ.0, EQ.1, Thickness, EQ.2, Young modulus, EQ.3, Mass density.

B. *Material property lines*

Anisotropic material properties are possible. For each different material, two lines must be supplied.

Line 1. (i10,20x,4d10.0).

columns	1–10	Material identification number.
	31–40	Mass density.
	41–50	Thermal expansion coefficient α_x.
	51–60	Thermal expansion coefficient α_y.
	61–70	Thermal expansion coefficient α_{xy}.

Line 2. (6d10.0).

columns	1–10	Constitutive component C_{xx}.
	11–20	Constitutive component C_{xy}.
	21–30	Constitutive component C_{xs}.
	31–40	Constitutive component C_{yy}.
	41–50	Constitutive component C_{ys}.
	51–60	Constitutive component G_{xy}.

The components define a 3x3-dimensional constitutive matrix, where

$$\{\sigma\} = \{\ \sigma_{xx}\quad \sigma_{yy}\quad \tau_{xs}\ \},$$
$$\{\epsilon\} = \{\ \epsilon_{xx}\quad \epsilon_{yy}\quad \gamma_{xy}\ \}$$

are the stress and strain vectors in the plane-stress case.

C. *Element load multipliers.* Five lines.

Line 1. (4d10.0)

columns	1–10	Distributed lateral load multiplier for load case A.
	11–20	Distributed lateral load multiplier for load case B.
	21–30	Distributed lateral load multiplier for load case C.
	31–40	Distributed lateral load multiplier for load case D.

Line 2. (4d10.0)

columns	1–10	Temperature multiplier for load case A.
	11–20	Temperature multiplier for load case B.
	21–30	Temperature multiplier for load case C.
	31–40	Temperature multiplier for load case D.

Line 3. (4d10.0)

columns	1–10	x-direction acceleration for load case A.
	11–20	x-direction acceleration for load case B.
	21–30	x-direction acceleration for load case C.
	31–40	x-direction acceleration for load case D.

Line 4. Same as *Line 3* for y-direction.

Line 5. Same as *Line 3* for z-direction.

D. *Element data lines* (8i5, 4d10.0).

One line for each element.

columns	1–5	Element number.
	6–10	Node number I.
	11–15	Node number J.
	16–20	Node number K.
	21–25	Node number L.
	26–30	Node number O (mid-node).
	31–35	Material property number, DEFAULT set to one (1).
	36–40	Generating parameter k.
	41–50	Element thickness.
	51–60	Distributed lateral load (pressure).
	61–70	Mean temperature variation T from the reference level in initial configuration.
	71–80	Mean temperature gradient $\partial T/\partial z$ across the shell thickness (a positive temperature gradient produces a negative curvature).

Remarks

◇ Nodal point numbers I,J,K,L are in sequence in counter-clockwise direction around a rectangular element. The local element coordinate system (x,y,z) is defined as follows:

x defined by LI-JK, where LI and JK are mid-points of sides L-I and J-K,
z normal to x and to the line joining mid-points IJ and KL,
y normal to x and z to complete the right-handed system.

This system is used to express all physical and kinematic shell properties (stress, strain, material law, etc.), except that the body force is referred to the global coordinate system (X,Y,Z). For the analyses of shallow shells, rotational constraints normal to the surface may be imposed by the addition of boundary elements at the nodes (Element Type 4). If columns 26–30 are left blank, mid-node properties are computed by averaging the four nodes. Triangular element can be used when columns 21–30 are left blank; the element is connected by three nodes I,J,K. However, an element mesh with as many rectangular elements as possible is recommended.

◇ Element lines must be in element number sequence. If element lines are omitted, POLSAP automatically generates the omitted information as follows: the increment for element number is one, i.e. $N_{i+1}=N_i+1$, the corresponding increment for nodal numbers is k, i.e.

$$NI_{i+1}=NI_i+k\ ,\quad NJ_{i+1}=NJ_i+k\ ,\quad NK_{i+1}=NK_i+k\ ,\quad NL_{i+1}=NL_i+k\ .$$

Material identification, element thickness, distributed load, temperature and temperature gradient for generated elements are the same. Always include the complete last element line.

◇ Output are moments per unit length and membrane stresses.

Type 4 – Boundary elements

A. *Control line* (2i5).

columns	1–5	The number 6.
	6–10	Number of boundary elements in the group.

B. *Element load multiplier line* (4d10.0)

columns	1–10	Multiplier for element load case A.
	11–20	Multiplier for element load case B.

21–30	Multiplier for element load case C.
31–40	Multiplier for element load case D.

C. *Element data lines* (8i5, 3d10.0).

columns 1–5	Node N, at which the elements is placed.
6–10	Node I,
11–15	Node J,
16–20	Node K,
21–25	Node L,
	Leave columns 11–25 blank if only node I is needed.
26–30	Code for displacement.
31–35	Code for rotation.
36–40	Generating parameter k.
41–50	Prescribed displacement along element axis.
51–60	Prescribed rotation about element axis.
61–70	Spring stiffness K for both extension and rotation, DEFAULT set to 10^{10}.

Remarks

◇ This element type is applied to constrain nodal displacements to specified values, compute support reactions and provide linear elastic supports to nodes. The boundary element is essentially a spring which can have axial displacement stiffness and axial rotational stiffness. There is no limit to the number of boundary elements which can be applied to any joint to produce the described effects. Boundary elements have no effect on the size of the stiffness matrix.

◇ *Direction of boundary elements.*
The direction of the boundary element at node N is specified in one of two ways: 1) a second nodal point I defines the direction of the element from node N to node I, 2) four nodal points I,J,K,L specify the direction of the element as the normal to the plane defined by two intersecting straight lines IJ and KL. The four points I,J,K,L need not be unique. A useful application for the analysis of shallow thin shells employs the boundary element to approximate rotational constraint about the surface normal as shown above. The vector **n** is given by the cross product $\mathbf{n}=\mathrm{IJ}\times\mathrm{KL}$ and defines the direction of the boundary element. Note that node I in case 1) and nodes I,J,K,L in case 2) are used only to define the direction of the element and if convenient may be any nodes used to define other elements. However artificial nodes may be created to define direction of boundary elements. These artificial nodes are input on the nodal point data lines with their coordinates and with all the boundary condition codes specified as one (1). It should be noted that node N is the structure node to which the boundary element is attached. In case 1) a positive displacement moves node N towards node I. Correspondingly, a positive force in the element means compression in the element. In case 2) a positive displacement moves node N into the direction **n**.

◇ *Displacement and rotation codes.*

Displacement code = 1. When this code is used, the displacement δ, specified in columns 41–50, and the spring stiffness K, specified in columns 61–70, are used by POLSAP in the following way. The load P, evaluated from $P=K\delta$, is applied to node N in the direction node N to node I in case 1) and into direction n in case 2), if δ is positive. If K is much greater than the stiffness of structure at node N without the boundary element, then the effect is to produce a displacement very nearly equal to δ at node N. If $\delta=0$, then P=0 and the stiff spring approximates a rigid support. Note that the load P will contribute to the support reaction for nonzero δ. The boundary condition codes specified on the structure nodal point data lines must be consistent with the fact that a load P is being applied to node N to effect the desired displacement (even when this displacement is zero).

Rotation code = 1. This case is analogous to the situation described above. A torque T, evaluated from $T=K\vartheta$, is applied to node N about the axis (direction) of the element. The rotation ϑ is specified in columns 51–60.

◇ *Generating parameter k.*

One line is needed for each element (in ascending nodal point order) except where element generation is used. When a series of nodes are such that: all have identical boundary elements attached, all boundary elements have same direction, all specified displacements and rotations are identical, the nodal sequence forms an arithmetic sequence, i.e., N, N+k, N+2k etc., then only the first and last node in the sequence need be input. The generating increment k is input in columns 36–40 of the first line.

◇ *Element load multipliers.*

Each of the four possible element load cases A, B, C, D associated with the boundary elements consists of the complete set of displacements as specified on the boundary element lines multiplied by the element load multiplier for the corresponding load case. As an example, suppose that displacement of node N is specified as 1.0, spring stiffness as 10^{10} and no other boundary element displacements are specified. Let case A multiplier be 0.0 and case B multiplier be 2.0. For element load case A the specified displacement is 0.0 while that for B is $2.0\times1.0=2.0$. Linear combinations of element load cases A, B, C, D for all types of elements collectively for a particular problem are specified on the structure element load multiplier lines. As far as the boundary element is concerned, this device is useful when a particular node has a support displacement in one load case but is fixed in others.

◇ *Recommendations*

If a boundary element is aligned with a global displacement direction, only the corresponding diagonal element in the stiffness matrix is modified. Therefore, no stiffness matrix ill-conditioning results. However, when the boundary element couples degrees of freedom, large off-diagonal elements introduce ill-conditioning into the stiffness matrix which can cause solution difficulties. In the analysis of shallow shells boundary elements with stiffness a fraction of the element bending stiffness should be used (say less than or about 0.1). In dynamic analysis artificially stiff boundary elements should not be used. (See note (7), Section X.A).

V. Concentrated Load / Mass. Design Sensitivity Constraints

A. *Concentrated load/mass lines* (2i5, 6d10.0).

note	*columns*	*variable*	*entry*
(1)	1–5	N	Nodal point number.
(2)	6–10	L	Structure load case number, GE.1, static analysis type, EQ.0, dynamic analysis type.
	11–20	FX(N,L)	Global X-direction force or X-translational mass coefficient.
	21–30	FY(N,L)	Global Y-direction force or Y-translational mass coefficient.
	31–40	FZ(N,L)	Global Z-direction force or Z-translational mass coefficient.
	41–50	MX(N,L)	Global X-axis moment or X-rotational inertia.
	51–60	MY(N,L)	Global Y-axis moment or Y-rotational inertia.
	61–70	MZ(N,L)	Global Z-axis moment or Z-rotational inertia.

Note

(1) For a static analysis case (NDYN.EQ.0, 5, 7, 9, 10, 12), one line is required for a nodal point (N) having applied (non-zero) concentrated forces or moments. All structure load cases must be grouped together for node N before data is entered for the next (higher) node at which loads are applied. Only the structural load cases for which node N is loaded need be given, but the structure load case numbers (L) which are referenced must be supplied in ascending order. Node loadings must be defined (input) in increasing node number order, but again, only those nodes actually loaded are required as input. The static loads defined in this section act on the structure exactly as input and are not scaled, factored, etc. by the element load case (A,B,C,D) multipliers (Section VI, below). Nodal forces arising from element loadings are combined (additively) with any concentrated loads given in this section. Applied force/moment vectors act on the structure, positive in the positive global directions. Only one line is allowed per node per load case.

For a dynamic analysis case (NDYN.EQ.1, 2, 3, 4, 6, 8, 11, 13) structure load cases have no meaning, but POLSAP expects to read data in this section nonetheless. In place of concentrated loads, lumped mass coefficients for the nodal degrees of freedom may be input for any (or all) nodes. The mass matrix is automatically constructed by POLSAP from element geometry and associated material densities; the mass coefficients read in this section are combined (additively) with the existing element-based lumped mass matrix. For mass input, a node mass only be specified once, and the load case number (L) must be zero (default).

The program terminates reading loads (or mass) data when a zero (or blank) node number (N) is encountered; i.e., terminate this section of input with a blank line. For the special case of a static analysis with no concentrated loads applied, input only one (1) blank line in this section. Similarly, a dynamic analysis in which the mass matrix is not to be augmented by any entries in this section requires only one (1) blank line as input.

(2) For static analyses: if NDYN.EQ.0, 5, structure load case numbers range from one (1) to the total number of load cases requested on the Problem Control Line, i.e. $1 \leq L \leq LL$; if NDYN.EQ.7, 9, 10, 12, L=1 is automatically reset by POLSAP. For dynamic analyses (NDYN.EQ.1, 2, 3, 4, 6, 8, 11, 13) the entry L is inactive

B. *Displacement constraints for static analysis of design sensitivity* (2i5, 6d10.0).

Skip this line if NDYN.NE.5 *or* ICONTYP.NE.0.

note	*columns*	*variable*	*entry*
(1)	1–5	N	Nodal point number.
	6–10	L	Sensitivity constraint case number.
	11–20	QX(N,L)	Allowable X-translation.
	21–30	QY(N,L)	Allowable Y-translation.
	31–40	QZ(N,L)	Allowable Z-translation.
	41–50	QXX(N,L)	Allowable X-rotation.
	51–60	QYY(N,L)	Allowable Y-rotation.
	61–70	QZZ(N,L)	Allowable Z-rotation.

Note

(1) For deterministic analysis of static sensitivity (NDYN.EQ.5), one line is required for each degree of freedom constrained with an admissible value of displacement. Only the constrained degrees of freedom need to be entered. All the cases of the sensitivity constraints must be grouped together for node N before data are entered for the next (higher) node at which the displacement components are bounded. Nodes must be typed in increasing number order. The allowable displacements or rotations must be positive. POLSAP terminates reading constraint data when a blank line is encountered.

VI. Element Load Multipliers (4d10.0).

note	*columns*	*variable*	*entry*
(1)	1–10	EM(1)	Multiplier for element load case A.
	11–20	EM(2)	Multiplier for element load case B.
	21–30	EM(3)	Multiplier for element load case C.

31–40 EM(4) Multiplier for element load case D.

Notes

(1) One line must be given for each static (NDYN.EQ.0, 5, 7, 9, 10, 12) structure load case requested on the Problem Control Line (LL). The lines must reference load case numbers in ascending order. The four (4) element load sets (A,B,C,D), if created during the processing of element data (Section IV, above), are combined with any concentrated loads specified in Section V for the structure load cases. For example, suppose an analysis case calls for seven (7) static structure loading conditions (i.e., LL=7), then POLSAP expects to read seven (7) lines in this section. Further, suppose line number three (3) in this section contains the entries:

$$[\,EM(1)\quad EM(2)\quad EM(3)\quad EM(4)\,] \;=\; [\,-3.0\quad 0.0\quad 2.0\quad 0.0\,]\,.$$

Structure load case three (3) will then be constructed using any concentrated loads specified in Section V minus (-) three (3) times of the loads in element set A plus (+) two (2) times of the loads in element set C. Load sets B and D will not be applied in structure load case 3. Element load sets may be referenced any number of times in order to construct different structure loading conditions. Element-based loads (gravity, thermal, etc.) can only be applied to the structure by means of the data entries in this section.

If this case calls for one of the dynamic analysis options, supply only one blank line in this section.

Input data for deterministic analyses of static response and static sensitivity (NDYN.EQ.0, 5) *are complete with the foregoing section.*

VII. Buckling Load Analysis (i5, d10.0).

Skip this line if NDYN.NE.7.

columns			
1–5	NITER	Maximum number of iterations accepted to reach the convergence tolerance, EQ.0 or DEFAULT set to 16.
6–15	TOLER	Convergence tolerance for buckling factor, EQ.0.0 or DEFAULT set to 10^{-5}.

Remark

◇ The problem is solved for the first buckling load factor (critical load divided by current load) and the corresponding buckling shape. The convergence norm is assumed as relative difference of the factor between the two successive iterations.

Input data for deterministic analysis of the global stability problem (NDYN.EQ.7) *are complete with the foregoing section.*

VIII. Minimum-Weight Optimization

Skip this section if NDYN.NE.9.

A. *Control line* (7i5, 3d10.0).

note	*columns*	*variable*	*entry*
(1)	1–5	NDMAX	Number of displacement constraints.
	6–10	NSMAX	Number of stress constraints.
	11–15	NAMIN	Number of cross-sectional area constraints.
	16–20	NEWSTIFF	Flag for modification of stiffness in adjoint equations, EQ.0, no, EQ.1, yes.
	21–25	IPRINT	Flag for printout mode,
(2)			EQ.0, concise printing,
(3)			EQ.1, full printing.
	26–30	INTERVAL	Printing interval in concise mode.
	31–35	ITERMAX	Maximum number of iterations requested, DEFAULT set to 16.
	36–45	TOLER	Convergence tolerance, DEFAULT set to 10^{-5}.
	46–55	BETA	Accelerating iteration coefficient.

Notes

(1) This option has been worked out for truss systems only.

(2) In concise-printing mode the following data are output at requested iteration (parameter INTERVAL):

- displacement scale factor, constraint number, node number and degree of freedom of the active displacement constraint,
- stress scale factor, constraint number and element number of the active stress constraint,
- design variable scale factor,
- Lagrangian multiplier for adjoint equations,
- object function value,

- convergence norm (relative difference of the object function between the two successive iterations),
- modified cross-sectional areas at the iteration.

(3) In full-printing mode the following data are output at each iteration:

- nodal displacements,
- element normal stresses and forces,
- those as in concise-printing mode, (2),
- nodal adjoint variables,
- element residuals,
- time log of the current iteration process.

B. *Displacement constraint lines* (3i5, d15.0).

columns	1–5	N	Constraint number.
	6–10	NPD(1,N)	Nodal point number.
	11–15	NPD(2,N)	Degree-of-freedom number.
	16–30	DMAX(N)	Maximum-allowable displacement.

Remark

◇ Displacement constraint numbers must be input in increasing order; however, need not be in successive order. Joint data for a series of constraints can be generated from information given on two lines in sequence

line 1	N1	NPD(1,N1)	NPD(2,N1)	DMAX(N1) ,
line 2	N2	NPD(1,N2)	NPD(2,N2)	DMAX(N2) .

The data are generated as:

$$\text{NPD}(1,N1+I) = \text{NPD}(1,N1) + I*(\text{NPD}(1,N2) - \text{NPD}(1,N1))/(N2-N1),$$
$$\text{DMAX}(N1+I) = \text{DMAX}(N1) + I*(\text{DMAX}(N2)-\text{DMAX}(N1))/(N2-N1),$$
$$I = 1,\ldots, N2-N1-1 .$$

The node difference must be divisible by the constraint difference. Intermediate nodes and allowable displacements are generated by linear interpolation. The degree-of-freedom number is set equal to the value given on the second line.

C. *Stress constraint lines* (2i5, d15.0).

columns	1–5	N	Constraint number.
	6–10	NEL(N)	Element number.

11–25	SMAX(N)	Maximum-allowable stress.

Remark

◇ Stress constraint numbers must be input in increasing order; however, need not be in successive order. Joint data for a series of constraints can be generated from information given on two lines in sequence

line 1	N1	NEL(N1)	SMAX(N1) ,
line 2	N2	NEL(N2)	SMAX(N2) .

The data are generated as:

NEL(N1+I) = NEL(N1) + I*(NEL(N2) - NEL(N1))/(N2–N1) ,
SMAX(N1+I) = SMAX(N1)+ I*(SMAX(N2) - SMAX(N1))/(N2–N1) ,
I = 1,...,N2–N1–1 .

D. *Cross-sectional area constraint lines* (2i5, d15.0).

columns	1–5	N	Constraint number.
	6–10	NEL(N)	Element number.
	11–25	AMIN(N)	Minimum-allowable cross-sectional area.

Remark

◇ Cross-sectional area constraint numbers must be input in increasing order; however, need not be in successive order. Joint data for a series of constraints can be generated from information given on two lines in sequence

line 1	N1	NEL(N1)	AMIN(N1) ,
line 2	N2	NEL(N2)	AMIN(N2) .

The constraint data are generated as follows:

NEL(N1+I) = NEL(N1) + I*(NEL(N2) - NEL(N1))/(N2–N1) ,
AMIN(N1+I) = AMIN(N1)+ I*(AMIN(N2) - AMIN(N1))/(N2–N1) ,
I = 1,...,N2–N1–1 .

Input data for deterministic analysis of the minimum-weight optimization problem (NDYN.EQ.9) *are complete with the foregoing section.*

IX. Stochastic Analysis of Static Response and Static Design Sensitivity

Skip this section if NDYN.NE.10, 12.

A. *Control flags for data input and printout* (4i5).

columns	1–5	INTYPE	Flag for covariance input, EQ.0, from the common input data file, EQ.1, from a unformatted file.
	6–10	IODIS	Printing expectations of nodal displacements,
	11–15	IOCOV	Printing covariances of nodal displacements,
	16–20	IOSTR	Printing stresses at mean configuration, EQ.0, no, EQ.1, yes.

Remark

◇ There are two options for data input of the covariance matrix of random variables. If INTYPE.EQ.1, POLSAP expects to read the covariance matrix from a unformatted file, whose specification (file name) is named by the user. The user will answer to a prompt on the screen during solution process. Since the matrix is symmetric, only the part above and including the diagonal (upper triangle) is stored in compact form in a one-dimensional array A of length NRAND*(NRAND+1)/2 so that

A(1)=Cov(1,1),
A(2)=Cov(2,2), A(3)=Cov(1,2),
A(4)=Cov(3,3), ...
...
A(NRAND*(NRAND+1)/2-NRAND+1) = Cov(NRAND,NRAND),
...
A(NRAND*(NRAND+1)/2) = Cov(1,NRAND),

where NRAND denotes the number of random variables defined by POLSAP in the considered finite element model. The elements of matrix A must be declared in double precision format. If INTYPE.EQ.0 the data are entered as follows.

B. *Covariance matrix lines* (i5, 5(i5, d10.0)).

Skip these lines if INTYPE.EQ.1.

columns	1–5	N1	Row number (N1) of the random variable.
	6–10	M1	Column number (M1) of random variable.

11–20	Cov(N1,M1)	Covariance of the N1-th and M1-th variables.
26–30	M2	Column number (M2) of random variable.
31–35	Cov(N1,M2)	Covariance of the N1-th and M2-th variables.
...	...	...

Remarks

◇ Only non-zero elements of the upper triangle and including the diagonal of the covariance matrix, i.e. Cov(N,M) with M≥N, need to be entered.

◇ Input data for row-column indices must be entered in increasing order; but need not in successive order. If number of components of N-th row is larger than five (5), type them on new line(s) in format 5(i5,d10.0) from columns 6–10, not repeating row-index (columns 1–5 are left blank). Each row of the covariance matrix (initialized with the diagonal element Cov(N,N)) must be read from a new line.

◇ Data input for the covariance matrix is terminated with a blank line.

Input data for stochastic analyses of static response and static sensitivity (NDYN.EQ.10, 12) *are complete with the foregoing section.*

X. Deterministic and Stochastic Analysis of Dynamic Response

Eight (8) types of dynamic analysis can be performed by POLSAP:

NDYN.EQ.1,	Deterministic solution of structural eigenproblem (complete input in Section X.A, below),
NDYN.EQ.2,	Deterministic analysis of forced vibrations by mode superposition (complete input in Sections X.A,C, below),
NDYN.EQ.3,	Deterministic analysis of response spectra (complete input in Sections X.A,D, below),
NDYN.EQ.4,	Deterministic analysis of forced vibrations by step-by-step direct integration (complete input in Section X.C, below),
NDYN.EQ.6,	Deterministic analysis of design sensitivity of eigenvalues (complete input in Section X.A, below),
NDYN.EQ.8,	Deterministic analysis of time response of design sensitivity (complete input in Sections X.A,C, below),
NDYN.EQ.11,	Stochastic analysis of forced vibrations (complete input in Sections X.A,B,C, below),
NDYN.EQ.13,	Stochastic analysis of time response of design sensitivity (complete input in Sections X.A,B,C, below).

If NDYN.EQ.2, 3, 6, 8, 11, 13 POLSAP first solves the structural eigenproblem, then the control data for eigenpair extraction must be supplied in Section X.A. For the case of the step-by-step direct integration analysis (NDYN.EQ.4) do not provide the eigenproblem control line. The concept of structure loading conditions and element load case (A, B, C, D) are not defined for the dynamic case. A lumped mass matrix is formed automatically using element geometry and assigned material densities. Known rotational inertias must be input for the individual nodal degrees of freedom in Section V, above. Non-zero impressed displacements (rotations) input by means of the boundary elements are ignored.

A. Deterministic Analysis of Structural Eigenproblem and/or Design Sensitivity of Eigenvalues.

Skip this line if NDYN.EQ.4.

Control line (3i5, 2d10.0, i5).

note	*columns*	*variable*	*entry*
(1)	1–5	IFPR	Flag for intermediate printing, EQ.0, no, Eq.1, yes.
(2)	6–10	IFSS	Flag for performing the Sturm sequence check, EQ.0, yes, EQ.1, no.
(2)	11–15	NITEM	Maximum number of iterations allowed to reach the convergence tolerance, DEFAULT set to 16.
(3)	16–25	RTOL	Convergence tolerance (accuracy) for the highest (NF-th) requested eigenvalue, DEFAULT set to 10^{-5}.
(4)	26–35	COFQ	Cut-off frequency (cycles/unit time), DEFAULT, NF eigensystems will be extracted, GT.0, extract only those values below COFQ.
(1)	41–45	IPRINT	Flag for structural eigenvector printing, EQ.0, yes, EQ.1, no.

Notes

(1) Extra output, such as intermediate matrices, convergence norms, etc. calculated at each iteration can be requested. Normal output consists of a list of NF eigenvalues followed by corresponding eigenvectors for each mode. NF is given in columns 16–20 of the Problem Control Line. If IPRINT.EQ.1, printing the structural eigenvectors is suppressed.

(2) The Sturm sequence check can be applied to check if any eigenvalue were missed, i.e. to verify if the lowest NF eigenvalues have been obtained. The factorization of the system matrix is performed at a shift just to the right of the NF-th eigenvalue. If during the subspace iteration the NF-th eigenvalue fails to converge to a tolerance of RTOL within NITEM iterations, then POLSAP resets number one (1) to IFSS and the Sturm sequence check is ignored; and eigensystems are accepted at the NITEM-th iteration. If a rigid body mode occurs POLSAP stops with a message. Note that if artificially stiff boundary elements are used and the elements of the system matrix may be small in comparison, although no rigid body modes may be present POLSAP may stop. In a dynamic analysis it is recommended not to use very stiff boundary elements.

(3) This tolerance test applies to the NF-th eigenvalue, and all eigenvalues lower than the NF-th one will be more accurate than RTOL. The lowest mode is found most accurately with precision decreasing with increasing mode number until the highest requested mode (NF) is accurate to a tolerance of RTOL. Iteration is terminated after k-th iteration if the NF-th eigenvalue λ satisfies the inequality

$$\frac{abs(\lambda_k - \lambda_{k-1})}{\lambda_{k-1}} \leq \text{RTOL} .$$

(4) The cut-off frequency (COFQ) is used to terminate computations if all eigenvalues below the specified frequency have been found. If the solution determines N eigenvalues less than COFQ (N≤NF), the Sturm sequence check is performed using the N-th eigenvalue as a shift.

Input data for deterministic analyses of the structural eigenproblem and eigenvalue sensitivity (NDYN.EQ.1,6) *are complete with the foregoing section.*

B. Data for Covariances of Random Variables.

Skip this section if NDYN.NE.11, 13.

Control line (2i5).

note	*columns*	*variable*	*entry*
(1)	1–5	INTYPE	Flag for covariance input, EQ.0, from the common input data file, EQ.1, from a unformatted file.
	6–10	NVAR	Number of requested transformed (uncorrelated) random variables, NVAR.GT.0.

Covariance matrix lines (i5, 5(i5, d10.0)).

Skip this section if INTYPE.EQ.1, otherwise the input data are entered similarly to the case of NDYN.EQ.10, 12 (Section IX.B, above).

N o t e s

(1) For the cases NDYN.EQ.11, 13, POLSAP expects to read the covariances of random variables. Similarly to the static cases (NDYN.EQ.10, 12) there are two options for data input of the covariance matrix. If INTYPE.EQ.1, POLSAP reads the covariance matrix from a unformatted file, whose specification (filename and extension) is named by the user. The user will answer to a prompt on the screen during solution. The matrix must be positive definite. Since it is symmetric, only the part above and including the diagonal (upper triangle) is stored in compact form in a one-dimensional array A of length NRAND*(NRAND+1)/2 (cf. Section IX.A, above) where NRAND denotes the number of random variables defined by POLSAP in the problem to be solved. The elements of A must be declared in double precision format. If INTYPE.EQ.0 the data are input as for the stochastic analysis of static responses, i.e. for NDYN.EQ.10, 12 (Section IX.B).

(2) For the options NDYN.EQ.11, 13, in order to reduce the double summation to the single summation (the mixed derivatives reduce to second derivatives) during computation of the right hand sides of the 2nd-order equations and the sensitivity gradients POLSAP always performs the transformation of the set of NRAND correlated random variables to a set of NVAR uncorrelated random variables through a standard eigenproblem solution. Analogous to modal analysis only a few (but *highest*) modes are required to capture the major characteristics of the probabilistic distributions. The entry NVAR.EQ.0 is illegal.

C. Deterministic and Stochastic Analysis of Dynamic Responses by Mode Superposition or Step-by-step Direct Integration.

Dynamic response can be evaluated with two types of forcing functions: 1) ground acceleration input in any or all of the three (3) global (X,Y,Z) directions; and/or 2) time varying loads applied in any nodal degrees of freedom (except *slave* ones). Time forcing functions are described in two steps. First, a number of time functions are specified by a set of discrete points $[f(t_i),t_i]$, $i=1,\ldots,k$. Each time function may have a number of definition points (k), a scalar multiplier β and reference to one of the input time functions f(t). The actual force (or acceleration) at any time τ equals $\beta \times f(\tau)$; $f(\tau)$ is found by linear interpolation between two of the input time points (t_i, t_{i+1}), where $t_i \leq \tau \leq t_{i+1}$. Assuming that the solution begins at zero time, an independent arrival time $t_a \geq 0$ may be assigned to each forcing function. The forcing function is applied to the system at the solution time t_a.

1. *Two control lines.*

Line 1 (5i5, 2d10.0, 5x, 2i5, d10.0).

note	*columns*	*variable*	*entry*
(1)	1–5	NFN	Number of different time functions, GE.1.
(1)	6–10	NGM	Flag for ground motion, EQ.0, no, EQ.1, yes.
(2)	11–15	NAT	Number of different arrival times for the forcing functions, EQ.0 or DEFAULT set all times are zero.
(3)	16–20	NT	Total number of solution time steps.
(4)	21–25	NOT	Output print interval, GE.1 and LE.NT.
(3)	26–35	DT	Solution time step Δt.

For the cases NDYN.EQ.2, 8, 11, 13 (*Skip this section if* NDYN.EQ.4)

(5)	36–45	DAMP	Damping factor (fraction of critical) to be applied to all NF modes.
(3)	51–55	INTEGR	Flag for integration of uncoupled equations, EQ.0, Wilson-θ algorithm, EQ.1, Newmark algorithm.
(3)	56–60	ISECULAR	Flag for elimination of secularities, EQ.0, no, EQ.1, yes.
(3)	61–70	RANGE	Frequency range factor for secularity elimination.

For the cases NDYN.EQ.4 (*Skip this section if* NDYN.EQ.2, 8, 11, 13)

(5)	36–45	ALPHA	Mass damping factor α.
	46–55	BETA	Stiffness damping factor β.

Line 2. Flags for stochastic sensitivity solution output (2i5).

Skip this line if NDYN.NE.13.

note	*columns*	*variable*	*entry*
(4)	1–5	IODIS	Print expectations of displacement response, EQ.0, no, EQ.1, yes.
	6–10	IOCOV	Print covariances of displacement response, EQ.0, no, EQ.1, yes.

Notes

(1) At least one (1) time function must be input. If no ground acceleration acts on the structure, set NGM to zero (or DEFAULT) and skip Section X.C.3, below. Both ground acceleration and nodal force input are allowed.

(2) If no arrival time values are input, all forcing functions begin acting on the structure at time zero. The same arrival time value may be referenced by different forcing functions. NAT determines the number of non-zero entries that POLSAP expects to read in Section X.C.4, below.

(3) POLSAP performs a step-by-step (implicit) integration of the equations of motion in time domain over NT time steps Δt. In cases NDYN.EQ.2, 8, 11, 13 the modal uncoupled equations of motion can be solved optionally by the Wilson-θ algorithm with θ=1.4 or the Newmark algorithm with δ=0.5, α=0.25. In case NDYN.EQ.4 the coupled system equations are integrated by the Wilson-θ method. If T is the period of the highest numbered mode Δt should be chosen such that $\Delta t/T < 0.1$. A larger time step (i.e. $\Delta t \geq 0.1T$) will not cause failure (instability), but participation of the higher modes is filtered from the predicted response. For the options NDYN.EQ.11, 13 the set of NRAND correlated random variables are transformed to a set of NVAR uncorrelated variables by the standard eigensolution. An algorithm based on the Fast Fourier transform can be used (ISECULAR.EQ.1) to eliminate secularity terms appeared in the right hand sides due to the application of the second-order perturbation technique. For the case the frequency range factor RANGE must be specified. RANGE is active only if ISECULAR.EQ.1 and defined as a fraction of the first mode structure frequency. From the authors experience the range should be chosen between 0.10 and 0.15. The entry RANGE.EQ.0.0 is illegal. If NDYN.EQ.11, 13 and ISECULAR.EQ.1 the number of solution time steps NT should be chosen to be larger than or equal to 8 and to satisfy equality MOD(NT/4)=0 (NT is divisible by 4). Note that the Fast Fourier transform is most effectively applied if $NT=2^n$ with n is an integer ($n \geq 3$). The secular elimination option and NT being a power of two are strongly recommended, otherwise the computation cost would be high for large systems.

(4) History of 0th-, 1st-, 2nd-order structural and adjoint accelerations, velocities and displacements are computed at every time step, but printing of the nodal displacements, the coefficients of the sensitivity gradients (deterministic solutions) or their probability distributions (the first two moments – spatial expectations and covariances; stochastic solutions) and recovery of element stresses are performed only at solution step intervals of NOT. For the case of the stochastic analysis of the time response of structural design sensitivity (NDYN.EQ.13), printing expectations and covariances of the displacement history is optional.

(5) The damping factor (DAMP) is applied to all NF modes. The admissible range for DAMP is between 0.0 (undamped) and 1.0 (critical viscous damping). In case NDYN.EQ.4 the damping matrix is assumed as a linear combination of the structure mass and stiffness, i.e. $C=\alpha M+\beta K$, where α and β are constants.

2. *Time-varying load lines* (4i5, d10.0).

note	*columns*	*variable*	*entry*
(1)	1–5	NP	Nodal point number where the load component (force or moment) is applied, GE.1 and LE.NUMNP.
(1)	6–10	IDOF	Degrees of freedom number (GE.1 and LE.6), (q_x=1, q_y=2, q_z=3, ϑ_x=4, ϑ_y=5, ϑ_z=6).
(2)	11–15	IFN	Time function number, GE.1 and LE.NFN.
(3)	16–20	IAT	Arrival time number, EQ.0, load applied at solution start, GE.1, non-zero arrival time.
(4)	21–30	P	Scalar multiplier for the time function, Eq.0, no load applied.

Notes

(1) One line is required for each nodal degree of freedom having applied time varying loads. IDOF is arranged in ascending sequence at any given node. This sequence must be input in ascending node order and terminated with a blank line, which also must be supplied even if no loads are applied.

(2) The time functions are input tabularly in Section X.C.5, below. Function values at times between input time points are computed with linear interpolation.

(3) If IAT is zero (or blank), the forcing function is assumed to act at zero time. If 1≤IAT≤NAT the forcing function begins acting on the structure when the solution reaches the IAT-th arrival time (defined in Section X.C.4, below).

(4) The actual magnitude of force (or moment) acting on the model at time t equals the value of function number IFN at t multiplied by P.

3. *Ground motion control line* (6i5).

Skip this line if NGM.EQ.0.

note	*columns*	*variable*	*entry*
(1)	1–5	NFNX	Time function number describing the ground acceleration in the X-direction.
	6–10	NFNY	Time function number describing the ground acceleration in the Y-direction.
	11–15	NFNZ	Time function number describing the ground acceleration in the Z-direction.
(2)	16–20	NATX	Arrival time number, X-direction.
	21–25	NATY	Arrival time number, Y-direction.
	26–30	NATZ	Arrival time number, Z-direction.

Notes

(1) A zero time function number indicates that no ground motion is applied for that particular direction.

(2) Zero arrival time references mean that the ground acceleration begins acting on the structure at zero time.

4. *Arrival time lines.*

Skip these lines and left one blank line if NAT.EQ.0.

Line 1. (8d10.0).

note	*columns*	*variable*	*entry*
(1)	1–10	AT(1)	Arrival time number 1.
	11–20	AT(2)	Arrival time number 2.
	...	...	...
	71–80	AT(8)	Arrival time number 8.

Line(s) 2 (required if NAT.GT.8) (8d10.0).

note	*columns*	*variable*	*entry*
(1)	1–10	AT(9)	Arrival time number 9.
	...	...	...

Note

(1) Input as many lines as are required to define NAT different arrival times, eight entries per line. If no arrival times were requested (NAT.EQ.0), supply one (1) blank line in this section.

5. *Time function definition lines.*

Supply on set (*Line 1* and *Line(s) 2*, below) of input for each of the NFN time functions requested in columns 1–5 of the control line (Section X.C.1, above). At least one set of time function lines is expected in this section. The line set is input in ascending function number order.

Line 1. (i5, d10.0, 12a5).

note	*columns*	*variable*	*entry*
(1)	1–5	NLP	Number of function definition points, GE.2.
(2)	6–15	SFTR	Scale factor to be applied to f(t) values, EQ.0.0 or DEFAULT set to 1.0.
	16–75	HED(12)	Alphanumeric information describing this function table.

Notes

(1) At least two points,i.e., 2 pairs [f(t),t], must be specified to define each time function. Less than two points would preclude linear interpolation in the table for f(t).

(2) The scale factor SFTR is used to multiply function values only; input time values are not changed. If the scale factor is omitted, SFTR is reset by POLSAP to 1.0 thereby leaving input function values unchanged.

Line(s) 2. (8d10.0).

note	*columns*	*variable*	*entry*
(1)	1–10	T(1)	Time value at point 1, t_1,
	11–20	F(1)	Function value at t_1, $f(t_1)$.
	21–30	T(2)	Time value at point 2, t_2,
	31–40	F(2)	Function value at t_2, $f(t_2)$.
	...	...	...

Note

(1) Input as many *Lines 2* as are required to define NLP pairs [t_i, $f(t_i)$], four (4) pairs per line. Pairs must be input in order of ascending time value. Care must be taken to ensure that the highest input time value (t_{NLP}) is at least equal to the value of time at the end of solution.

6. *Output definition lines.*

To minimize the amount of output which would be produced by POLSAP if all solutions (time history of the displacements, stresses, sensitivity gradient coefficients, probabilistic distributions of the displacement and sensitivity etc.) were printed, output requests for selected components must be specified in this section.

6.1. *Displacement output requests.*

Screen control line (2i5).

Skip this line if NDYN.NE.4 *or* ICURVE.NE.1.

note	*columns*	*variable*	*entry*
(1)	1–5	INODE	Node number, GE.1 and LE.NUMNP.
	6–10	IDOF	Degree-of-freedom number, GE.1 and LE.6.
	11–15	JUMP	Drawing interval, DEFAULT set to 1.

(2)	16–20	IWINDOW	Screen scaling flag, DEFAULT set to use all the screen.

Notes

(1) This option is active in the deterministic analysis of forced vibrations using the step-by-step direct integration (Wilson-θ) technique, i.e. NDYN.EQ.4 and ICURVE.EQ.1, where NDYN and ICURVE are specified on the Problem Control Line in Section I. The time response of one (1) displacement component at a node can be shown on the screen during the integration solution. Drawing on the screen is performed at solution step intervals of JUMP. The number of solution time steps NT may be divisible by JUMP or not. The parameter JUMP should be selected in the range of 5 to 50. After completion of drawing the response curve (the node displacements were computed), the solution process will be temporarily terminated with the DOS-pause. The response curve on the screen now can be printed or plotted by the DOS-command PRINT SCREEN. The computation process can be continued by pressing ENTER key.

(2) There are three options for the screen window, IWINDOW=0,1,2. Depending on monitor's dimension an appropriate parameter can be selected. The default option denotes using all the screen.

Output control line (2i5).

note	*columns*	*variable*	*entry*
(1)	1–5	KKK	Flag for output printing, EQ.3, recover maxima only, NE.3, history and maxima.

Note

(1) The type of output to be produced by POLSAP applies to all requests of either deterministic or stochastic solutions.

Node displacement request lines (7i5).

note	*columns*	*variable*	*entry*
(1)	1–5	NP	Node number, GE.1 and LE.NUMNP.
(2)	6–10	IDOF(1)	Displacement component, request 1,
	11–15	IDOF(2)	Displacement component, request 2,
	16–20	IDOF(3)	Displacement component, request 3,
	21–25	IDOF(4)	Displacement component, request 4,
	26–30	IDOF(5)	Displacement component, request 5,
	31–35	IDOF(6)	Displacement component, request 6, GE.1 and .LE.6.

Notes

(1) Only those nodes at which output is to be produced are entered in this section. Lines must be input in ascending node number order. Node numbers may not be repeated. This section must be terminated with a blank line.

(2) Displacement (expectation) component requests IDOF(N) range from 1 to 6, where q_x=1, q_y=2, q_z=3, ϑ_x=4, ϑ_y=5, ϑ_z=6. The first zero (or blank) encountered while reading IDOF(1), IDOF(2),..., IDOF(6) terminates information for the line. Displacement components at a node may be requested in any order. As an example, suppose that q_y, ϑ_x and ϑ_z are to be output at node 1001. The line could be written as (1001, 2, 6, 4, 0), etc. but only four (4) fields would have non-zero entries. For the case of stochastic analysis (NDYN.EQ.11, 13), because of symmetry only the upper triangle (including the diagonal) of the displacement covariance matrix is computed and printed at the requested time intervals. That is, POLSAP calculates and prints N history tables of displacement expectations and N(N+1)/2 history tables of displacement covariances, where N denotes the total number of the requested displacement components.

6.2. *Sensitivity component time history request* (2i5, d10.0).

Skip this line if NDYN.NE.8 *and* NDYN.NE.13.

note	*columns*	*variable*	*entry*
(1)	1–5	NPSENS	Node number, GE.1 and LE.NUMNP.
	6–10	IDOF	Degree-of-freedom number, GE.1 and LE.6.
	11–20	QALLOW	Displacement constraint value.

Note

(1) Only one (1) displacement constraint component is permitted for the deterministic and stochastic analysis of sensitivity time response, i.e. with NDYN.EQ.8 and NDYN.EQ.13.

6.3. *Stress and sensitivity output requests.*

Output control line (2i5).

note	*columns*	*variable*	*entry*
(1)	1–5	KKK	Flag for output printing, EQ.3, recover maxima only, NE.3, history and maxima.

Note

(1) See Section X.C.6.1, above.

Stress and sensitivity request lines (13i5).

Requests are grouped by element types in the same order as originally input in the Element Data (Section IV, above); and terminated by a blank line. Elenent number references within an element group must be in ascending order. Elenent number references may be omitted but not repeated. If no output is to be produced for an element group, then enter a blank line for its group. For the case of the deterministic analysis of the time response of design sensitivity (NDYN.EQ.8) the request list is treated as either the list of requested elements for stress printing or the list of requested design variables for sensitivity output. In stochastic analysis of the time response of displacements (NDYN.EQ.11) stresses are evaluated at the mean-displacement configuration of the finite element model. In stochastic analysis of the time response of design sensitivity (NDYN.EQ.13) the stress field is not computed; and the request list is treated as the list of requested random design variables for printing of the time response of expectations and covariances of the sensitivity gradients. Note that in cases NDYN.EQ.8, 13 only the requested numbers of elements are active for sensitivity printing; the stress component numbers S(N) specified below are inactive and need not be entered (left blank) if NDYN.EQ13.

note	*columns*	*variable*	*entry*
(1)	1–5	NEL	Element number for output.
(2)	6–10	IS(1)	Stress component number, request 1.
	11–15	IS(1)	Stress component number, request 2.
	...	...	...
	61–65	IS(12)	Stress component number, request 12.

Notes

(1) Terminate each different element output group (type) with a blank line. Elenents within a group must be in ascending order. Element number repetitions are ilegal. For the case of stochastic sensitivity analysis (NDYN.EQ.13), because of symnetry only the upper triangle (including the diagonal) of the sensitivity covariance natrix is computed and printed. That is, POLSAP calculates and prints N history tables of sensitivity expectations and N(N+1)/2 history tables of sensitivity covariances, where N denotes the total number of the requested design random variables.

(2) The first zero (or blank) request encountered while reading IS(1), ..., S(12) terminates information for the line. Table below lists the stress component numbers and corresponding descriptions for the various element types. Only the stress component number listed in the table are legal references.

Element type	*Maximum number of components*	*Stress component number*	*Output symbol*	*Description*
Truss	(2)	(1)	P/A	axial stress,
		(2)	P	axial force.
Beam	(12)	(1)	P1(I)	x-force at end I,
		(2)	V1(I)	y-shear at end I,
		(3)	V1(I)	z-shear at end I,
		(4)	T1(I)	x-torque at end I,
		(5)	M2(I)	y-moment at end I,
		(6)	M3(I)	z-moment at end I,
		(7)	P1(J)	x-force at end J,
		(8)	V1(J)	y-shear at end J,
		(9)	V1(J)	z-shear at end J,
		(10)	T1(J)	x-torque at end J,
		(11)	M2(J)	y-moment at end J,
		(12)	M3(J)	z-moment at end J.
Plate/ Shell	(6)	(1)	XX-S/R	XX-stress,
		(2)	YY-S/R	YY-stress,
		(3)	XY-S/R	XY-stress,
		(4)	XX-M/R	XX-moment,
		(5)	XX-M/R	YY-moment,
		(6)	XX-M/R	XY-moment.
Boundary	(2)	(1)	BDRY-F	boundary force,
		(2)	BDRY-M	boundary moment.

Input data for deterministic and stochastic analyses of the time history of forced vibrations and design sensitivity (NDYN.EQ.2, 4, 8, 11, 13) *are complete with the foregoing section.*

D. Deterministic Analysis of Response Spectrum.

Skip this section if NDYN.NE.3.

This option combines all NF mode shapes and frequencies computed during the eigensolution to calculate the maximum response in each of the lowest modes, where the spectra (displacement or acceleration) into the global X,Y,Z directions are assumed to be proportional to each other. The total response for displacements and stresses is calculated as the square root of the sum of the square of the modal maximum responses. For the case of a non-zero cut-off frequency COFQ (Section X.A), only those modes whose frequencies are less than COFQ will be combined in the analysis.

1. *Control line* (3d10.0, i5).

note	*columns*	*variable*	*entry*
(1)	1–10	FX	Factor for X-direction input,
	11–20	FY	Factor for Y-direction input,
	21–30	FZ	Factor for Z-direction input, EQ.0.0, not acting.
(2)	31–35	IST	Input spectrum type, EQ.0, displacement versus period, EQ.1, acceleration versus period,

Notes

(1) All three (3) direction factors may be non-zero in which case the entries represent the X,Y,Z components of the input direction vectors.

(2) IST defines the type of spectrum table to be input immediately following. The spectral displacements S_q and accelerations S_a are assumed to be related as $S_a = 4\pi^2 f^2 S_q$, where f is frequency (cycle/unit time).

2. *Spectrum lines*

Heading line (12a6).

note	*columns*	*variable*	*entry*
	1–72	HED(12)	Alphanumeric information used to label spectrum table.

Control line (i5, d10.0).

note	*columns*	*variable*	*entry*
	1–5	NPTS	Number of definition points in the spectrum table (NPTS.GE.2).
	6–15	SFTR	Scale factor used to adjust the displacement (acceleration) ordinates in the spectrum table, EQ.1.0, no adjustment.

Spectrum data lines (2f10.0).

note	*columns*	*variable*	*entry*
(1)	1–10	T	Period (reciprocal of frequency).
(2)	11–20	S	Value of displacement (or acceleration if IST.EQ.1).

N o t e s

(1) Input one definition point per line, NPTS lines are required in this section. Lines must be arranged in ascending value of period.

(2) S is interpreted to be a displacement quantity if IST was input as zero. For IST.EQ.1, S is an acceleration value.

Input data for response spectrum analysis (NDYN.EQ.3) *are complete with the foregoing section.*

Contents